Extensions of Poisson Geometric Process Model with Applications

WAI-YIN WAN

A thesis submitted in fulfillment of
the requirements for the degree of
Doctor of Philosophy

School of Mathematics and Statistics
The University of Sydney

August 2010

Abstract

The modelling of longitudinal and panel count data has a rich history. Despite the well-established time series count models, we seek a new direction to study panel and multivariate longitudinal count data with different characteristics.

We extend the Poisson geometric process (PGP) model introduced by Wan (2006) in the modelling of non-monotone trend for time series of counts. The PGP model is developed from the geometric process (GP) model pioneered by Lam (1988a) and Lam (1988b) to study positive continuous data with monotone trend. Lam (1988a) and Lam (1988b) states that a stochastic process (SP) $\{X_t, t = 1, 2, \dots\}$ is a GP if there exists a positive real number $a > 0$ such that $\{Y_t = a^{t-1}X_t\}$ generates a renewal process (RP) with mean $E(Y_t) = \mu$ and variance $Var(Y_t) = \sigma^2$ where a is the ratio of the GP.

Under the GP framework, the PGP model assumes that the count $W_t, t = 1, \dots, n$ follows a Poisson distribution with mean X_t where $\{X_t, t = 1, \dots, n\}$ forms a latent GP and the corresponding SP $\{Y_t\}$ follows some lifetime distributions with $E(Y_t) = \mu_t$ and $Var(Y_t) = \sigma_t^2$. The PGP model focuses on the modelling of the latent stationary SP instead of the latent GP and separates the effects on trend movement from the effects on the underlying system (SP) that generates the GP by individually modelling the ratio and the mean of the SP. This merit of the model enhances its applicability

in analyzing longitudinal and panel count data with non-monotone trends, overdispersion and cluster effects.

In view of other prominent characteristics including presence of excess zeros or outliers, diverse degrees of dispersion and serial correlation between observations, we extend the PGP model to take into account all these problems in turn by adopting different distributions for $\{Y_t\}$, replacing the Poisson data distribution with generalized Poisson distribution with more flexible dispersion structure and incorporating some past observations as time-evolving covariates in the mean link function. Moreover, concerning the lack of literature in the modelling of multivariate longitudinal count data, we consider a multivariate version of the PGP model to cope with contemporaneous correlation and cross correlation between time series on top of the other characteristics.

For statistical inference, these extended models are implemented using Markov chain Monte Carlo (MCMC) algorithms to avoid the evaluation of complicated likelihood functions and their derivatives which may involve high-dimensional integration. To demonstrate the properties and applicabilities of these models, a series of simulation studies and real data analyses are conducted. All in all, the extended PGP models taken into account all the pronounced characteristics of time series of counts are shown to provide satisfactory performance in both simulation studies and real data analyses. They certainly can become competitive alternatives to the traditional time series count models in the future.

Declaration

I declare that this thesis represents my own work, except where due acknowledgement is made, and that it has not been previously included in a thesis, dissertation or report submitted to this University or to any other institution for a degree, diploma or other qualifications.

Signed _____

Wai Yin WAN

Acknowledgements

First and foremost, I owe my deepest and sincere gratitude to my primary supervisor, Dr. Jennifer S. K. Chan, at the School of Mathematics and Statistics, The University of Sydney. Her rich intellect, inspiration, enormous guidance and intimate encouragement have provided a good basis for the present thesis. She has been a role model in her diligence in research, enthusiasm in teaching and ingenuity of ideas, to a mediocre student who left her family to go abroad and sometimes loses the direction in midst of difficulties. Secondly, I would also like to thank my associate supervisor, Dr. Boris Choy who has perpetual energy and enthusiasm in research. His insights and innovative ideas motivate me and broadens my perspective on future career development. Moreover, it is a pleasure to thank Prof. Neville Weber, my second associate supervisor, who offers me the opportunity to start my research degree in this renowned University and all the friends and staff in the School for their cares and support. Without any of them, I would not have such wonderful experiences.

Above all, I am indebted to my family and boyfriend for always supporting me unceasingly and encouraging me to move on and I would also like to thank God to equip me with the mathematical ability to study statistics. Their endless love and support have been invaluable in helping me to focus on my academic pursuits. Without them, I would not have had the courage to complete this thesis.

CONTENTS

List of Figures

List of Tables

CHAPTER 1

Introduction

1.1. Background

Analysis of event count data which prevails in all walks of lives has a long and rich history. In epidemiology, we observe the daily number of deaths in an epidemic outbreak; in engineering, we record the number of failures of an operating system until it breaks down; in business, we count the number of mobile phones sold every week for different phone models or brands; in insurance, we report the claim frequencies for a compulsory third party insurance policy. The list of areas in which time series of counts are observed and analyzed is endless.

Event count can be classified into three main categories including cross-sectional, longitudinal and panel. Different from cross-sectional data which is collected from a number of individuals at the same time point, longitudinal data, also known as time series data, are observations repeatedly measured from one subject over a series of time. If there are multiple outcomes observed at the same time, the outcomes that are potentially correlated is called multivariate longitudinal data. Regarded as a more general case, panel data is a set of longitudinal data collected from a number of

subjects. In this thesis, we will focus on the analysis of multivariate longitudinal count data and panel count data.

Longitudinal or panel count data are frequently obtained in follow-up or prospective studies such as randomized clinical trials in which the recurrent number of events is usually recorded successively at uniform time intervals. Inevitably, the non-stationarity and serial correlation structure in the time series make the modelling of panel data distinct and more complicated than cross-sectional data. In non-stationary time series, an increasing (or decreasing) trend often coincides with an increasing (or decreasing) variability in the data over time. When the mean is larger (smaller) than the variance, we refer such situation as underdispersion (or overdispersion). Ignoring the dispersion problems may lead to poor model fit, unreliable estimates and hence misleading interpretations.

Besides, exogenous covariates which can be time-invariant, time-variant or period-variant, are commonly measured along with the outcomes. For instance, in a tobacco use study, the weekly number of cigarettes taken by smokers may be affected by sex and age to start smoking which are time-invariant, number of doctor visits and alcohol consumption which are time-variant, and lastly income and education level which are period-variant. Including these covariates into the mean of the data distribution helps to investigate their effects on the outcome or allow for their effects in the studies of other variables of interest. For example, in a randomized clinical trial

on the efficacy of a medication for hypertension, undoubtedly the difference between the control group and treatment group is of primary interest. Moreever, sex, age or other measures of health condition which may affect the treatment result are regarded as nuisance variables and should also be allowed for in the study of treatment effect.

Particularly for panel count data which involves multiple subjects with different characteristics, population heterogeneity will arise inevitably. Taking the previous example of the hypertension medication study, between-subject variation may exist across each group of patients as the treatment may work better on some patients or due to measurement errors. In the past decades, extensive literature can be found in analyzing longitudinal and panel data. In these researches, extensions have been made continuously to some existing traditional count models to address all the aforementioned properties in the data.

This thesis focuses on the development of models for longitudinal or panel count data that can handle various characteristics of the count data arisen in different situations. The following section will first summarize briefly a few benchmarking models for modelling longitudinal count data and how they are developed and modified to study multivariate longitudinal and panel count data. The next two Sections will describe the development and method of inference of geometric process (GP) model from which the Poisson geometric process (PGP) model is developed and is adopted as the

start-up model in this research due to its indispensable ability to allow trend movement.

1.2. Overview of longitudinal count models

Based on the theory of state-space models, Cox (1981) classified the longitudinal count models into two streams, namely the observation-driven (OD) and parameter-driven (PD) models. A good monograph on the classification can be found in Cameron & Trivedi (1998). Denote W_t be the outcome at time $t = 1, \ldots, n$ where n is the total number of observations. The state-space model consists of an observation equation which specifies the distribution of the outcome W_t given the state variable and a state equation which specifies the transition distribution of the state variable. For both OD and PD models, while the observation equations are tantamount as they assume W_t follows some discrete distributions $f(w_t)$ such as Poisson and negative binomial distributions given the mean $E(W_t)$ as the state variable, their difference lies in the specification of the state equation for $E(W_t)$.

The OD models express the mean of the outcome explicitly as a function of past observations in order to construct an autocorrelation structure which can account for serial correlation between observations. On the other hand, the PD models introduce serial dependence through a latent variable which evolves independently of the past observations in the state equation. In the following Sections, a few benchmarking OD and PD models with model structures and extensions to multivariate longitudinal or panel count data will be discussed.

1.2.1. Observation-driven models. The OD models are so called because they introduce past observations into the mean of the current observation. An important class of the OD models is the integer-valued autoregressive moving average (INARMA) model developed under the framework of Gaussian autoregressive moving average (ARMA) model. This model pioneered by Al-Osh & Alzaid (1987) has developed extensively and a recent survey can be found in McKenzie (2003).

Under the INARMA model the outcome W_t is expressed as

$$W_t = \sum_{i=1}^{p} \alpha_i \circ W_{t-i} + \sum_{j=1}^{q} \gamma_j \circ U_{t-j} + U_t$$

where $U_t, t = 1, \ldots, n$ are non-negative latent integer-valued variables that are independently and identically distributed and $\circ$ is a binomial thinning operator such that

$$\alpha_i \circ W_{t-i} = \begin{cases} Bin(W_{t-i}, \alpha_i), & W_{t-i} > 0 \\ 0, & W_{t-i} = 0 \end{cases} \quad \text{and} \quad \gamma_j \circ U_{t-j} = \begin{cases} Bin(U_{t-j}, \gamma_j), & U_{t-j} > 0 \\ 0, & U_{t-j} = 0 \end{cases}$$

In other words, $\alpha_i, \gamma_j \in [0, 1]$ denote the probability of success for the binomial distribution for W_{t-i} and U_{t-j} respectively. Let $\boldsymbol{x}_t$ and $\boldsymbol{\beta}$ be vectors of time-evolving covariates and regression coefficients respectively, then the mean of U_t can be log-linked to a function of covariates $\boldsymbol{x}_t$ so that $E(U_t) = \exp(\boldsymbol{x}_t^T \boldsymbol{\beta})$. The resultant model is denoted as INARMA(p, q) model where p represents the autoregressive (AR) order for the observations and q specifies the moving average (MA) order for the errors.

Taking INARMA(1,0) model as an example, the conditional mean and variance for W_t are given by

$$\begin{aligned} E(W_t|\, W_{t-1}, \dots) &= \alpha_1 W_{t-1} + \exp(\boldsymbol{x}_t^T \boldsymbol{\beta}) \\ Var(W_t|\, W_{t-1}, \dots) &= \alpha_1(1-\alpha_1) W_{t-1} + Var(U_t) \end{aligned}$$

and the autocorrelation function $Corr(W_t, W_{t-k}) = \alpha_1^k$ is always positive. So, this model is restricted to positively serially correlated data.

A multivariate extension of the INARMA model can be found in Quoreshi (2008). Denote the data vector $\boldsymbol{W}_t = \{W_{it}, ..., W_{mt}\}^T$ with dimension m, the extended model called the vector integer-valued moving average (VINMA) model has the following form:

$$\begin{aligned} \boldsymbol{W}_t &= \sum_{j=1}^{q} \boldsymbol{\gamma}_j \circ \boldsymbol{U}_{t-j} + \boldsymbol{U}_t \\ \begin{pmatrix} W_{1t} \\ W_{2t} \\ \vdots \\ W_{mt} \end{pmatrix} &= \sum_{j=1}^{q} \begin{pmatrix} \gamma_{11q} & \gamma_{12q} & \cdots & \gamma_{1mq} \\ \gamma_{21q} & \gamma_{22q} & \cdots & \gamma_{2mq} \\ \vdots & \dots & \ddots & \vdots \\ \gamma_{m1q} & \gamma_{m2q} & \cdots & \gamma_{mmq} \end{pmatrix} \circ \begin{pmatrix} U_{1,t-q} \\ U_{2,t-q} \\ \vdots \\ U_{m,t-q} \end{pmatrix} + \begin{pmatrix} U_{1t} \\ U_{2t} \\ \vdots \\ U_{mt} \end{pmatrix} \end{aligned}$$

where $\boldsymbol{U}_t = \{U_{1t}, ..., U_{mt}\}^T$ is an integer-valued innovation sequence which is independently and identically distributed with its mean log-linked to some time-variant covariates $\boldsymbol{x}_{it}$ such that $E(U_{it}) = \exp(\boldsymbol{x}_{it}^T \boldsymbol{\beta}_i), i = 1, \dots, m$ where $\boldsymbol{\beta}_i$ is vector of regression coefficients for W_{it}. Besides accommodating covariate effects, the VINMA model is capable of fitting multivariate longitudinal count data with both negative or positive correlation between

pairs of time series. See Quoreshi (2008) for more details. However, Heinen (2003) criticized that the INARMA model is not practically applicable due to its cumbersome estimation of the model parameters. Hence emphases were only put on the studies of their stochastic properties.

To tackle the estimation problem, Davis *et al.* (1999) and Davis *et al.* (2003) proposed the generalized linear autoregressive moving average (GLARMA) model where W_t given the past history $\mathbb{F}_{t-1}$ follows Poisson distribution with mean μ_t and is denoted by

$$W_t | \, \mathbb{F}_{t-1} \sim Poi(\mu_t)$$

and $\mu_t = \exp(\boldsymbol{x}_t^T \boldsymbol{\beta} + U_t)$. Furthermore,

$$U_t = \phi_1 U_{t-1} + \cdots + \phi_p U_{t-p} + \sum_{i=1}^{q} \theta_i e_{t-i}$$

where U_t is an ARMA(p, q) process with noise $\left\{ e_t = \dfrac{W_t - \mu_t}{\mu_t^{\lambda}} \right\}, \lambda \in (0, 1]$ and past errors e_{t-i} which describe the correlation structure of W_t. The GLARMA model can allow for serial correlation in the count data by specifying the log of the conditional mean process as a linear function of previous counts. The main advantage of the GLARMA model is the efficient model estimation using maximum likelihood (ML) method in contrast to the INARMA model. This greatly widens the applications of the model to time series of counts.

Another benchmarking OD model is the autoregressive conditional Poisson (ACP) model emerged in Heinen (2003). Given the past observations

$\mathbb{F}_{t-1}$, the outcome W_t follows a Poisson distribution with mean μ_t which is written as

$$E(W_t|\,\mathbb{F}_{t-1}) = \mu_t = (\omega + \sum_{i=1}^{p} \alpha_i W_{t-i} + \sum_{j=1}^{q} \gamma_j \mu_{t-j}) \exp(\boldsymbol{x}_t^T \boldsymbol{\beta})$$

where ω, α_i's and γ_j's > 0 and again $\boldsymbol{x}_t$ and $\boldsymbol{\beta}$ are vectors of time-variant covariates and regression coefficients. Hence, the resultant model, which is denoted by ACP(p, q) model, has an autoregressive structure introduced by a recursion on lagged observations. In the same paper, he further extended the ACP model by replacing the Poisson distribution with Double Poisson distribution which can fit underdispersed or overdispersed data and by adding a generalized autoregressive conditional heteroskedasticity (GARCH) component to allow a time-varying variance structure. The resulting generalized conditional autoregressive Double Poisson (GDACP) model can deal with data with underdispersion or overdispersion and positive serial correlation.

A multivariate extension of the GDACP (MDACP) model has recently been investigated by Heinen & Rengifo (2007) using copulas to introduce dependence among several time series. This MDACP model, having similar properties as the GDACP model, can also accommodate positive or negative correlation among time series. See Heinen & Rengifo (2007) for more details.

In summary, the appeals of the OD models include the straightforward derivation of likelihood function and prediction. On the other hand, being a conditional rather than marginal model over past observations, they have

a shortcoming in the interpretation of covariate effects as the mean depends on past observations. In the light of this, another class of count models, the PD models were proposed to alleviate these problems.

1.2.2. Parameter-driven models. The most prominent PD model in the literature is the Poisson regression model with stochastic autoregressive mean developed by Zeger (1988). This model is essentially a log linear model in the family of generalized linear model (GLM) formulated by Nelder & Wedderburn (1972). Conditional on a latent non-negative stochastic process $\{U_t\}$ and a vector of time-variant covariates $\boldsymbol{x}_t$, assume that the outcome W_t is independent and follows a Poisson distribution with mean μ_t, then the conditional mean and variance are specified as

$$E(W_t|U_t) = Var(W_t|U_t) = \mu_t U_t = \exp(\boldsymbol{x}_t^T \boldsymbol{\beta}) U_t$$

where $\boldsymbol{\beta}$ is a vector of regression coefficients. To introduce both serial correlation and extra variation to the model, suppose that the latent process U_t is stationary and serially correlated with mean $E(U_t) = 1$, variance $Var(U_t) = \sigma_u^2$ and covariance $Cov(U_t, U_{t-k}) = \sigma_u^2 \rho_k$ where ρ_k represents the correlation between U_t and U_{t-k}. The unconditional moments are then given by

$$\begin{aligned} E(W_t) &= \exp(\boldsymbol{x}_t^T \boldsymbol{\beta}) \\ Var(W_t) &= \mu_t + \sigma_u^2 \mu_t^2 \\ Cov(W_t, W_{t-k}) &= \mu_t \, \mu_{t-k} \, \sigma_u^2 \, \rho_k. \end{aligned}$$

Clearly the model is suitable for longitudinal count data with overdispersion since the variance is larger than the mean and allows both positive or negative serial correlation as $-1 \leq \rho_k \leq 1$. More importantly, the time-varying variance and covariance increase the flexibility of the model structure in fitting data with non-constant variance and serial correlation. Some applications of this model can be found in Chan & Ledolter (1995) and Jung & Liesenfeld (2001) by adopting a Gaussian first order autoregressive structure for U_t.

Noticing the increasing need of modelling panel count data in a variety of areas, Zeger *et al.* (1988) extended the aforementioned GLM to a generalized linear mixed model (GLMM) by adding random effects to account for subject-specific effects in the panel data. Assume W_{it} be the outcome of subject $i, i = 1, \ldots, m$ at time $t, t = 1, \ldots, n$, $\boldsymbol{x}_{it}$ and $\boldsymbol{z}_{it}$ be vectors of subject-specific time-variant covariates and $\boldsymbol{U} = \{\boldsymbol{U}_1^T, \ldots, \boldsymbol{U}_m^T\}^T$ be a $qm \times 1$ vector of random effects. Under the GLMM, the outcome W_{it} follows a Poisson distribution with mean μ_{it} which can be expressed as

$$\mu_{it} = \exp(\boldsymbol{x}_{it}^T \boldsymbol{\beta} + z_{it}^T \boldsymbol{U}_i)$$

where $\boldsymbol{U}_i$ is assumed to be a multivariate normal variable. Later Brännäs & Johansson (1996) relaxed the independent assumption such that $Cov(\boldsymbol{U}_i, \boldsymbol{U}_j) \neq \mathbf{0}$ in order to allow for correlation between different pairs of time series. Nevertheless, enormous literature emerged afterwards to modify the model structure such as allowing correlation between covariates and random effects (Windmeijer, 2000) and replacing the underlying Poisson distribution

with other discrete distributions. See Winkelmann (2008) for a up-to-date survey of statistical techniques for the analysis of count data.

In contrast to the OD models, the specification of a latent stochastic process in the PD models enables a straightforward interpretation of the covariate effects on the outcome because they are formulated independent of the past observations. Yet in general, there exists difficulties in forecasting since the model is built on a latent process and the estimation of parameters requires considerable computational effort as the likelihood function containing multiple integrals is difficult to evaluate (Jung & Liesenfeld, 2001).

1.3. Overview of geometric process models

Overall, the OD and PD models focus on modelling overdispersion and serial correlation in longitudinal and panel count data while leaving the trend of the time series unattended. Evaluating the trend movement is important since it provides invaluable information for 'long-term' policy assessment, evaluation, planning and development in many studies of longitudinal count data, for example, in public health where clinical trials are conducted to study the efficacy of a treatment with respect to the long-term improvements of certain health variables, or in socioeconomics where policies are made based on the consistent and prolonged change of certain economic indicators.

This research extends the Poisson geometric process (PGP) model in Wan (2006) to allow for various characteristics of longitudinal and panel count data especially the trend movements. The PGP model is developed

from the GP model proposed by Lam (1988a) and Lam (1988b) for monotone positive continuous data. This GP model offers a straightforward approach to extend the PGP model for analyzing longitudinal and panel count data with monotone as well as non-monotone trend. The next Section will give a detailed discussion of the development and applications of the GP models on different types of data.

1.3.1. Geometric process model. In system maintenance, due to accumulating deterioration, the failure rate of the system increases gradually resulting in a monotone decreasing trend in the consecutive operating times. Nonhomogeneous Poisson process has been used for trend data. If the successive inter-arrival times are monotone, the Cox-Lewis model and exponential process model are commonly used. Lam (1988a) and Lam (1988b) on the other hand introduced a more direct approach, the geometric process (GP) to analyze the trend in such monotone process. The GP model is defined as follows.

Definition. Given a sequence of random variables $\{X_t, t = 1, 2, \dots\}$, if for some $a > 0$, $\{Y_t = a^{t-1}X_t\}$ forms a renewal process (RP) (Feller, 1949), then $\{X_t\}$ is called a geometric process (GP), and the real number a is called the ratio of the GP.

The GP model asserts that if the ratio a discounts X_t geometrically by $t - 1$ times, the resulting process $\{Y_t\}$ becomes stationary and forms a RP, which may follow some parametric distributions $f(y_t)$ such as exponential, gamma, Weibull and lognormal distributions with $E(Y_t) = \mu$ and

$Var(Y_t) = \sigma^2$. Hence, the mean and variance of the GP model are:

$$E(X_t) = \frac{\mu}{a^{t-1}} \quad \text{and} \quad Var(X_t) = \frac{\sigma^2}{a^{2(t-1)}}$$

respectively. Clearly, the GP model allows the mean and variance of the outcome to change over time so that any non-stationarity and non-constant volatility in the data can be allowed for. The moments are controlled by three parameters μ, a, and σ^2. The inverse relationship of the ratio a with the mean $E(X_t)$ explains why the trend becomes monotonically increasing when $a < 1$ but decreasing when $a > 1$. When $a = 1$, it becomes a stationary RP which is independently and identically distributed with the same distribution $f(y_t)$.

The merits of the GP model are twofold: its geometric structure and a ratio parameter a to model non-stationarity. Firstly, the model assumes that the observed data at time t form a latent RP after discounted by a ratio parameter a for $t-1$ times. Such a geometric structure often exists in systems that generate time series. The GP model focuses on the modelling of the latent stationary RP instead of the observed GP. By individually modelling the ratio and the mean of the RP, the model separates the effects on trend movement from the effects on the underlying system (the latent RP) that generates the observed GP. This approach is natural and appealing. Moreover the latent RP forms the state parameter of a state space model and hence can adjust for model dispersion and achieve model robustness by suitably assigning some heavy-tailed distributions to the latent RP. Secondly, the additional ratio parameter a makes the two-component (mean

and ratio) GP model a different but simple modelling approach to capture various characteristics, particularly the trend movement in time series.

With these nice features and simple model structure, the GP models have been widely applied in modelling inter-arrival times with monotone trend for the reliability and maintenance problems in the optimal replacement or repairable models (Lam, 1988a,b, 1992a,b). For example, Lam (1992b) succeeded in fitting the GP model to the inter-arrival times of the unscheduled maintenance actions for the U.S.S. Halfbeak No.3 and No. 4 main propulsion diesel engines. Moreover Lam & Zhang (1996a) analyzed the successive operating times in a two-component system arranged in series while Lam (1995) and Lam & Zhang (1996b) studied the times in a two-component system emerged in parallel. More examples can be found in Lam (1997), Lam *et al.* (2002), Lam & Zhang (2003), Lam *et al.* (2004), Zhang (1999), Zhang *et al.* (2001), Zhang (2002) and Zhang *et al.* (2002).

In most cases, the inter arrival times exhibit time-variant or time-invariant covariate effects, for instances, the operating time of a system is possibly affected by the environmental factors like humidity and temperature of the working site. Hence, adopting a homogeneous mean μ will be too restrictive in reality. Similar to GLM, the GP model can accommodate covariate effects by log-linking a linear function of some time-evolving covariates to the mean μ of the lifetime distribution $f(y_t)$ such that μ becomes μ_t and is expressed as

$$\ln \mu_t = \beta_{\mu 0} + \beta_{\mu 1} z_{\mu 1 t} + \cdots + \beta_{\mu q_\mu} z_{\mu q_\mu t} \tag{1.1}$$

where $z_{\mu kt}, k = 1, \ldots, q_\mu$ are some time-evolving covariates. After accommodating the covariates effects, $\{Y_t\}$ is no longer a renewal process but becomes a stochastic process (SP) as Y_t is not identically distributed with a constant mean. Instead it evolves over time subject to different exogenous effects. For example, Wan (2006) applied the extended GP model to study the daily number of infected cases in an epidemic outbreak of Severe Acute Respiratory Syndrome (SARS) in Hong Kong in 2003 and found that the daily number of infected cases increased with the daily temperature since the viruses are nourished under a warm environment.

In addition to covariate effects, multiple trends are often detected in longitudinal data. In epidemiology, the number of infected cases will surge before the precautionary measures such as contact tracing, quarantine and travel advices are implemented, but it will die out after the virus is under control. In marketing, the number of sales of an innovative product mounts due to increasing popularity and demand but again will attenuate after the market is saturated. Therefore, Chan *et al.* (2006) proposed the threshold GP model which fits a separate GP to different stages of development, like the growing, stabilizing and declining stages for the SARS outbreak in 2003. Assume $T_\kappa, \kappa = 1, 2, \ldots, K$ be the turning points of the κ^{th} GPs where the κ^{th} GP with n_κ observations is defined as

$$GP_\kappa = \{X_t,\, T_\kappa \leq t < T_{\kappa+1}\},\ \ \kappa = 1, \ldots, K, \tag{1.2}$$

$T_1 = 1$ and $T_\kappa = 1 + \sum_{j=1}^{\kappa-1} n_j, \kappa = 2, \ldots, K$ are the turning points of the

GPs such that $\sum_{\kappa=1}^{K} n_\kappa = n$. Then, the corresponding stochastic process $\{Y_t\}$ is given by

$$SP_\kappa = \{a_\kappa^{t-T_\kappa} X_t, \;\; T_\kappa \leq t < T_{\kappa+1}\}$$

where $a_\kappa, \kappa = 1, \ldots, K$ is the ratio parameter of the κ^{th} GP. To estimate the turning points, Chan *et al.* (2006) used a moving window method to locate the turning points for the daily number of infected cases in different stages of development for the 2003 SARS outbreak. The threshold model successfully explained the strength and direction of the multiple trends in the data. Other methods of estimating the turning points include the grid search and Bayesian sampling method (Chan & Leung, 2010). However, if there are too few observations or the time series is still on-going, it would be difficult to locate the turning points and thus the estimation of other model parameters and the accuracy of prediction may be affected. In general, the number of turning points can be determined by running different models that condition on K where K can be selected based on some model selection criteria such as Akaike information criterion (AIC) or deviance information criterion (DIC). See Lam (2007) for an overview and further references for the GP model and its extensions.

1.3.2. Binary geometric process model. Despite the flourishing development of the GP models, the scope of applications is confined to positive continuous data. While binary longitudinal data arise in many real life contexts, Chan & Leung (2010) pioneered the binary GP (BGP) model by

assuming the observed binary outcome $W_t, t = 1, \ldots, n$ as an indicator of whether an underlying GP X_t is greater than a certain cut off level b.

Definition. Assume the binary outcome W_t indicates if the underlying GP X_t is greater than certain cut off level b. Without loss of generality, the observed binary outcome can be written as

$$W_t = I(X_t > b) = I\left(\frac{Y_t}{a^{t-1}} > b\right) = I(Y_t > a^{t-1}b)$$

where $I(E)$ is an indicator function for the event E and $\{Y_t = a^{t-1}X_t\}$ is the underlying stochastic process. Setting $b = 1$ for simplicity, the probability P_t for the occurrence of the event $(W_t = 1)$ is given by

$$P_t = P(W_t = 1) = P(X_t > 1) = P(Y_t > a^{t-1}) = 1 - P(Y_t < a^{t-1}) = 1 - F(a^{t-1})$$

where $F(\cdot)$ is the cumulative distribution function (cdf) of Y_t. By assigning some lifetime distributions such as Weibull distribution with $E(Y_t) = \mu_t = \dfrac{\Gamma(1+\alpha)}{\lambda}$ to the underlying stochastic process $\{Y_t\}$, the probability P_t becomes

$$P_t = P(W_t = 1) = 1 - F(a^{t-1}) = \exp[-(\lambda a^{t-1})^{\alpha}]$$

where $\alpha > 0$ and $\lambda \geq 0$ are the shape and scale parameters of the Weibull distribution respectively.

Besides allowing for the time-evolving covariates in (1.1) and multiple trends in (1.2) by a threshold model, the ratio a can be log-linked to a linear function of time-evolving covariates z_{akt}, not necessary the same as $z_{\mu kt}$, to

account for non-monotone trend. So, a becomes a_t and is written as

$$\ln a_t = \beta_{a0} + \beta_{a1} z_{a1t} + \cdots + \beta_{aq_a} z_{aq_at}. \tag{1.3}$$

See Chan & Leung (2010) for a detailed description on a variety of trend patterns for P_t.

For applications, Chan & Leung (2010) studied the quarterly occurrence of coal mining disasters in Great Britain during 1851 to 1962. In the same paper, they analyzed the results from the weekly urine drug screens (positive or negative) of heroin use for 136 patients in a methadone clinic at Western Sydney in 1986. Investigating the trend patterns of patients allows the administrators to better monitor the condition of patients so that prompt action can be made to patients with deteriorating responses. They also demonstrated that the threshold BGP model performed better than the conditional logistic regression model, a common model for fitting binary data. Nevertheless, the extension to model binary longitudinal data certainly increases the applicability of GP models.

1.3.3. Poisson geometric process model. The development of the GP model to binary data implies that other classes of data including discrete counts and multinomial data can also be considered. Chan *et al.* (2004) and Chan *et al.* (2006) analyzed the number of coal mining disasters and the number of infected cases of SARS using the GP model and have adjusted for a few zero observations as the GP model is designated to positive continuous data. This adjustment however would be inappropriate if the data

is skewed or contains many zero observations. Wan (2006) therefore proposed the Poisson geometric process (PGP) model to analyze longitudinal count data.

Definition. Assume the count $W_t, t = 1, \ldots, n$ follows a Poisson distribution $f_P(w_t|x_t)$ with mean X_t where X_t forms a latent GP. Following the framework of GP model, the stochastic process $\{Y_t = a_t^{t-1}X_t\}$ follows some lifetime distributions $f(y_t)$ with mean μ_t and variance σ_t^2. Then, the resultant model is called the Poisson geometric process (PGP) model with probability mass function (pmf) given by

$$\begin{aligned} f(w_t) &= \int_0^\infty f_P\left(w_t \left| \frac{y_t}{a_t^{t-1}}\right.\right) f(y_t)\, dy_t \\ &= \int_0^\infty \frac{\exp\left(-\frac{y_t}{a_t^{t-1}}\right)\left(\frac{y_t}{a_t^{t-1}}\right)^{w_t}}{w_t!} f(y_t)\, dy_t. \end{aligned} \tag{1.4}$$

The PGP model belonged to the family of the GLMM model can be classified as a state space model with state variable X_t where $\{X_t\}$ is the latent GP evolving independently of the past outcomes. Some literature refers this to Poisson mixed model, a special case of GLMM because the resultant pmf is a composite of Poisson distribution and a mixing distribution (Karlis & Xekalaki, 2005). The mean and variance of W_t can then be derived as

$$\begin{aligned} E(W_t) &= E_x[E_w(W_t|X_t)] = E_x(X_t) = \frac{\mu_t}{a_t^{t-1}} \\ Var(W_t) &= E_x[Var_w(W_t|X_t)] + Var_x[E_w(W_t|X_t)] \\ &= E(W_t) + Var_x(X_t) = \frac{\mu_t}{a_t^{t-1}} + \frac{\sigma_t}{a_t^{2(t-1)}} \end{aligned} \tag{1.5}$$

where μ_t and a_t refer to the mean and ratio functions of the PGP model which can accommodate the time-evolving effects and non-monotone trend and are given by (1.1) and (1.3) respectively. See Wan (2006) for a review of different trend patterns. In addition, from (1.5) extra variation is added to the model to accommodate overdispersion. These distinctive features make the PGP model suitable for fitting count data with trends and overdispersion.

In Wan (2006), the exponential distribution is adopted for Y_t with mean $E(Y_t) = \mu_t$ and variance $Var(Y_t) = \sigma_t^2 = \mu_t^2$. So the pmf in (1.4) becomes

$$f(w_t) = \frac{\mu_t^{-1} a_t^{t-1}}{(\mu_t^{-1} a_t^{t-1} + 1)^{w_t+1}}$$

with mean and variance of W_t given by

$$E(W_t) = \frac{\mu_t}{a_t^{t-1}} \quad \text{and} \quad Var(W_t) = \frac{\mu_t}{a_t^{t-1}} + \left(\frac{\mu_t}{a_t^{t-1}}\right)^2.$$

Moreover, Wan (2006) extended the PGP model to study longitudinal count data with multiple trends by adopting the threshold model approach as in the GP and BGP models.

In order to simplify the PGP model, Wan (2006) simply assumes that the mean X_t of the Poisson count data W_t equal to the mean of the latent GP. In order words, the mean of the outcome becomes

$$E(W_t) = Var(W_t) = E(X_t) = \frac{\mu_t}{a_t^{t-1}}$$

Although, theoretically, the simplified PGP model is equivalent to the standard Poisson regression model, the interpretation of model parameters is

quite different. In the Poisson regression model, the regressors have multiplicative effect on the mean. However, in the PGP model, the mean function which reveals the initial level of the trend and the ratio function which reveals the direction and progression of the trend are interpreted separately. In this way, we can study the progression of trend more explicitly. This simplified model, though cannot allow for overdispersion, is sometimes more preferred to the PGP model due to its simplicity in model structure leading to less computation time in parameter estimation.

Chan *et al.* (2010b) and Wan (2006) further extended the PGP model to study panel count data. Assume that there are G groups of individuals which demonstrate different trend patterns and each individual has a probability π_l of coming from group $l, l = 1, \ldots, G$. The resultant mixture PGP (MPGP) model is essentially a probability mixture of G PGP models for some mixing proportions $0 \leq \pi_l \leq 1$ where $\sum_{l=1}^{G} \pi_l = 1$. The model is used to study the annual donation frequency of the female and male donors in Hong Kong whose first time donation was made between January 2000 and May 2001. The MPGP model lucidly identified three groups of donors namely committed, drop-out and one-time which have distinct donation patterns and the study provided useful information for the Hong Kong Blood Transfusion Service to maintain a stable blood storage by targeting at those regular committed donors.

Furthermore, considering the problem of overdispersion due to zero-inflation, Wan (2006) developed the PGP model using the hurdle model

approach originated from Mullahy (1986). Suppose that there is a probability ϕ that the outcome W_t at time t is zero, the zero-altered PGP (ZPGP) model and the pmf $f_z(w_t)$ is given by

$$f_z(w_t) = \begin{cases} \phi, & w_t = 0 \\ (1-\phi)\dfrac{f(w_t)}{1-f(0)}, & w_t > 0 \end{cases}$$

where $f(\cdot)$ is given by (1.4). The ZPGP model has been applied to analyze the number of new tumours for 82 bladder cancer patients who were divided into control and treatment groups since an overwhelming percentage of observations (80%) in the data are zeros. However, the ZPGP model failed to account for the population heterogeneity existed in both control and treatment groups, and thus this gives us an insight to develop a zero-altered PGP model with mixture effect to deal with the cluster effect.

1.4. Statistical inference

Apart from the modelling methodology, another extension of the PGP model is the methodology of inference. For the statistical inference of GP models, three methodologies are widely adopted including non-parametric (NP) inference, frequentist inference and Bayesian inference. The following Sections will discuss the three distinct methodologies.

1.4.1. Non-parametric inference. Non-parametric (NP) inference was first considered for parameter estimation in the GP model by Lam (1992b) as it is a simple distribution-free method. Some of the NP methods used in the GP model include the least-square error (LSE) method and the log-LSE

method. Later on, the NP inference is also adopted for parameter estimation in GP model (Chan *et al.*, 2004, 2006; Lam, 1992b; Lam & Zhang, 1996b; Lam *et al.*, 2004), BGP model (Chan & Leung, 2010) and PGP model (Wan, 2006) due to its simplicity. In this methodology, a criterion, usually the sum of squared error (SSE) is defined to measure the goodness-of-fit of a model. The NP method is so called because the criterion is independent of the data distribution. The principle of this method is to estimate the model parameters by minimizing the SSE which is defined as:

$$\begin{aligned} SSE_1 &= \sum_{t=1}^{n} [\ln X_t - E(\ln X_t)]^2 \\ \text{and} \quad SSE_2 &= \sum_{t=1}^{n} [X_t - E(X_t)]^2 \end{aligned}$$

for the log-LSE and LSE methods respectively. Lam (1992b) proposed the log-LSE method for the GP model and Wan (2006) and Chan & Leung (2010) considered the LSE method respectively for the PGP and BGP models.

To minimize the $SSE_m, m = 1, 2$, the Newton Raphson (NR) iterative method is used to solve the score equation $SSE'_m = 0$ for the parameter estimates $\boldsymbol{\theta}$ where SSE'_m and SSE''_m are the first and second order derivatives of the SSE_m with respect to X_t. Denote the parameter estimates in the k^{th} iteration by $\boldsymbol{\theta}^{(k)}$, the updating procedure is given by:

$$\boldsymbol{\theta}^{(k+1)} = \boldsymbol{\theta}^{(k)} - [SSE''_m(\boldsymbol{\theta}^{(k)})]^{-1} SSE'_m(\boldsymbol{\theta}^{(k)}). \tag{1.6}$$

The iteration continues until $\| \boldsymbol{\theta}^{(k+1)} - \boldsymbol{\theta}^{(k)} \|$ becomes sufficiently small and the final LSE estimates $\hat{\boldsymbol{\theta}}_{LSE} = \boldsymbol{\theta}^{(k+1)}$.

1.4.2. Frequentist inference. The classical maximum likelihood (ML) method has long been a popular methodology in statistical inference. Lam & Chan (1998) and Chan *et al.* (2004) applied the ML method for the inference of the GP model and showed that the ML method performs better than the NP methods in parameter estimation. The ML method was also adopted by Chan & Leung (2010) and Wan (2006) for different GP models.

This method requires the derivation of likelihood function based on the data distribution. Let $f(x_t)$ be the density function of X_t and denote a vector of unknown model parameters by $\boldsymbol{\theta}$. The likelihood function $L(\boldsymbol{\theta}|\, \boldsymbol{x})$ is

$$L(\boldsymbol{\theta}|\, \boldsymbol{x}) = \prod_{t=1}^{n} f(x_t|\, \boldsymbol{\theta})$$

and the log-likelihood function $\ell(\boldsymbol{\theta}|\, \boldsymbol{x})$ is

$$\ell(\boldsymbol{\theta}|\, \boldsymbol{x}) = \ln L(\boldsymbol{\theta}|\, \boldsymbol{x}) = \sum_{t=1}^{n} \ln f(x_t|\, \boldsymbol{\theta}).$$

To estimate the parameters $\hat{\boldsymbol{\theta}}_{ML}$ which maximizes the log-likelihood function $\ell(\boldsymbol{\theta}|\boldsymbol{x})$, we adopt the Newton Raphson (NR) iterative method in (1.6) for the LSE method by replacing $SSE'_m(\boldsymbol{\theta}^{(k)})$ and $SSE''_m(\boldsymbol{\theta}^{(k)})$ with $\ell\,'(\boldsymbol{\theta}^{(k)})$ and $\ell''(\boldsymbol{\theta}^{(k)})$ respectively. The procedure is updated iteratively until $\boldsymbol{\theta}^{(k+1)}$ converges and the ML estimates are given by $\hat{\boldsymbol{\theta}}_{ML} = \boldsymbol{\theta}^{(k+1)}$.

We can also derive the large sample properties for the ML estimates $\hat{\boldsymbol{\theta}}_{ML}$ using the following theorem:

Theorem:

$$\sqrt{n}(\hat{\boldsymbol{\theta}}_{ML} - \boldsymbol{\theta}) \xrightarrow{D} N(\mathbf{0}, n\boldsymbol{\Sigma})$$

where $\xrightarrow{D}$ means convergence in distribution when n is large, $\boldsymbol{\Sigma}$ is the covariance matrix and $s_{uv} = -E\left[\frac{\partial \ell^2(\boldsymbol{\theta})}{\partial \theta_u \partial \theta_v}\right]^{-1}$ is the element in the u^{th} row and v^{th} column of $\boldsymbol{\Sigma}$. With these asymptotic distributions, we can construct confidence intervals and perform hypothesis testing on $\boldsymbol{\theta}$.

While the likelihood function involves high-dimensional integration in the presence of missing data or latent state variable, for example, the missing group memberships for individuals in a mixture model, Wan (2006) considered the expectation-maximization (EM) method proposed by Dempster *et al.* (1977). The EM method consists of two steps: E-step and M-step. In the E-step, the latent group memberships are estimated by taking conditional expectation using the observed data and current parameter estimates. In the M-step, the likelihood function conditioning on the latent parameters, also called the “complete-data" likelihood, no longer involves integration. Hence, parameter estimates can be easily evaluated using NR iterative method. The procedures iterate between the E-step and M-step until convergence is attained.

However, Wan (2006) reported that the EM method is sensitive to starting values of the parameter estimates and sometimes the convergence rate is relatively slow (Jamshidian & Jennrich, 1997). In light of this, this research adopts the Bayesian method which is a competitive approach with the frequentist inference and has become more popular in the recent years.

1.4.3. Bayesian inference. As a competitive approach to the frequentist, the Bayesian inference is applied in Chan & Leung (2010) and Wan (2006). The biggest advantage of the Bayesian method over the ML method is that the former replaces the evaluation of complicated likelihood functions and their derivatives which may involve high-dimensional integration by some sampling algorithms. It has had increasing popularity in the recent years due to the advancement of computational power and the development of efficient sampling techniques. Moreover, the emergence of the statistical software `WinBUGS` makes the implementation of the Bayesian methodology more straightforward and feasible (Lunn *et al.*, 2000). `WinBUGS` is an interactive Windows version of the **B**ayesian inference **u**sing **G**ibbs **s**ampling (BUGS) program for Bayesian analysis of complex statistical models using MCMC techniques. It is a stand-alone program and can be called from other software such as `R` statistical package, `Stata` and `SAS`. In this thesis, all the MCMC algorithms are implemented using `WinBUGS` (Version 1.4.3) and `R2WinBUGS` package in `R`. The latter is particularly useful in performing simulations with a large number of repeated data sets because `WinBUGS` can be called repeatedly using `R` and the results are returned to `R` for estimating the model parameters in the simulation study.

In the statistical inference for GP models, Chan *et al.* (2010a), Chan & Leung (2010), Chan *et al.* (2010b) and Wan (2006) have considered the Bayesian approach for the BGP and PGP models. The Bayes theorem asserts that the posterior distribution for the parameter $\boldsymbol{\theta}$ conditional on data

$\boldsymbol{x}$ is proportional to the data likelihood $f(\boldsymbol{x}|\,\boldsymbol{\theta})$ and the prior densities, in other words,

$$f(\boldsymbol{\theta}|\,\boldsymbol{x}) = \frac{f(\boldsymbol{x}|\,\boldsymbol{\theta})f(\boldsymbol{\theta})}{\int f(\boldsymbol{x}|\,\boldsymbol{\theta})f(\boldsymbol{\theta})d\boldsymbol{\theta}} \propto f(\boldsymbol{x}|\,\boldsymbol{\theta})f(\boldsymbol{\theta}).$$

With no specific prior information for $\boldsymbol{\theta}$, non-informative priors with large variances are adopted. For parameters in non-restricted continuous ranges of values, normal priors are usually used. Whereas, for those restricted to positive ranges of values, gamma or generalized gamma priors are some possible choices, and for those parameters which represent the probability of certain events, uniform or beta priors are adopted.

After that, the model parameters are sampled from the posterior distribution and the parameter estimates $\hat{\boldsymbol{\theta}}_{BAY}$ are given by the mean or median of the posterior samples. Very often, the posterior distribution has a non-standard form and hence the evaluation of the posterior mean or median will be analytically complicated. Therefore, sampling methods including Markov chain Monte Carlo (MCMC) method with Gibbs sampling (Smith & Roberts, 1993; Gilks *et al.*, 1996) and Metropolis Hastings algorithm (Hastings, 1970; Metropolis *et al.*, 1953) are used to draw samples from the posterior conditional distributions of model parameters.

The idea of the Gibbs sampling is described below. Assume that we have three model parameters $\boldsymbol{\theta} = \{\theta_1, \theta_2, \theta_3\}$. The joint posterior distribution is written as $f(\theta_1, \theta_2, \theta_3|\boldsymbol{x})$ and the conditional density of one parameter given the other two parameters are written as $f(\theta_1|\,\theta_2, \theta_3, \boldsymbol{x})$,

$f(\theta_2|\,\theta_1, \theta_3, \boldsymbol{x})$, and $f(\theta_3|\,\theta_1, \theta_2, \boldsymbol{x})$ respectively. The algorithm for the implementation is illustrated below:

1 Begin at starting values of $\theta_1^{(0)}$, $\theta_2^{(0)}$, and $\theta_3^{(0)}$.

2 Draw $\theta_1^{(1)}$ from the conditional distribution $f(\theta_1|\,\theta_2^{(0)}, \theta_3^{(0)}, \boldsymbol{x})$.

3 Draw $\theta_2^{(1)}$ from the conditional distribution $f(\theta_2|\,\theta_1^{(1)}, \theta_3^{(0)}, \boldsymbol{x})$ using $\theta_3^{(0)}$ and the newly simulated $\theta_1^{(1)}$.

4 Draw $\theta_3^{(1)}$ from the conditional distribution $f(\theta_3|\,\theta_1^{(1)}, \theta_2^{(1)}, \boldsymbol{x})$ using $\theta_1^{(1)}$ and $\theta_2^{(1)}$.

5 Repeat Step 2 to 4 until R iterations have completed with the simulated values converged to the joint posterior density function.

`WinBUGS` adopts Gibbs sampling to reduce the complexity of sampling from the high-dimensional posterior distribution but at the cost of slower convergence rate. For each parameter, a chain of simulated estimates is obtained with its empirical distribution converges towards the posterior distribution. The posterior distribution $f(\boldsymbol{\theta}|\,\boldsymbol{x})$ can thus be approximated on the basis of these simulated values.

From the chain of R simulated values, we discard the first B iterations as the burn-in period to ensure that convergence has reached. From the remaining $(R - B)$ iterations, parameters are sub-sampled or thinned from every H^{th} iteration to reduce the autocorrelation in the samples. Resulting samples will consist of $M = \dfrac{R - B}{H}$ realizations with their mean or median taken to be the parameter estimates. In particular, when the posterior distributions of the parameters are skewed, which is usually the case for the

scale parameters, the sample median is adopted. To ensure the convergence and independence of the posterior sample, the history and autocorrelation function (ACF) plots have to be checked. A narrow horizontal band of the posterior sample running from left to right in the history plots and a sharp cut-off in the ACF plots indicate the convergence and independence of the posterior sample respectively. Throughout the thesis, we set the values $R = 55000$, $B = 5000$ and $H = 50$ for different extended PGP models unless otherwise specified.

In the data analysis, we sometimes need to test for the significance of certain parameters that are of primary interest. Some examples include the treatment effect of the medication in clinical trials and the effectiveness of the regulation in policy making. In Bayesian analysis, the signficiance of a parameter is based on a credible interval which is a posterior probability interval for interval estimation in contrast to point estimation. Credible intervals are used for purposes similar to those of confidence intervals in frequentist statistics. However credible intervals incorporate problem-specific contextual information from the prior distribution whereas confidence intervals are based only on the data. A parameter estimate is not significantly differ from zero if the credibility interval does not contain zero. For all the analyses in this thesis, the 95% credibility interval will be obtained from `WinBUGS` for some parameters of interest and Şthe parameter is significant" indicates that the 95% credibility interval does not contain zero and

hence the true value of the parameter of interest is significantly different from zero.

1.5. Objective and structure of thesis

Undoubtedly, the emergence of the PGP model has marked a milestone in the development of the GP models. However, so far only little work has been done on modelling panel count data and the use of exponential distribution as the lifetime distribution for Y_t is rather restrictive. Moreover, contemporary models for Poisson count time series discussed in Section 1.2 look specifically into the problem of overdispersion and serial correlation. Hence in this thesis, we will focus on incorporating the merits of both GP model and contemporary OD and PD models to yield a more flexible model that can allow for trend movements in particular and overdispersion and serial correlation in general. We will examine the trend movement of the panel and multivariate longitudinal count data while at the same time allowing for serial correlation using the OD approach whenever necessary.

Therefore, with respect to degrees of dispersion, a more general lifetime distribution such as the gamma distribution can be used as the mixing distribution of the PGP model to allow for overdispersion which may be caused by the presence of excess zeros or outliers. For zero-inflation, zero-inflated model or alternative models with a higher probability of zero may be considered. For model robustness, heavy-tailed distribution, such as log-t and log-exponential power (log-EP) distributions is a favorable choice for the

mixing distribution. Using a mixing distribution with more inclusive properties will lead to a more general structure in the PGP model for handling data with different degrees of overdispersion.

In addition, majority of literature focus on modelling count data with overdispersion, yet the opposite side, underdispersion has not received much attention. Under the PGP model, as extra variation is introduced by the mixing distribution, the only method to reduce the variation is to replace the Poisson distribution by another discrete distribution which can handle underdispersion. In the past decades, a few discrete distributions such as generalized Poisson and double Poisson distributions have emerged to fit underdispersed count data. They can be considered as a substitute for the Poisson distribution in the PGP model.

Furthermore, the existing aforementioned GP model and its extension have not accounted for serial correlation which may be prominent in longitudinal or panel count data. Hence, the PGP model will be extended to take into account this problem. Recently, Chan *et al.* (2010a) introduced the conditional autoregressive geometric process range (CARGPR) model, an extension of GP model using the approach of conditional autoregressive range (CARR) model in Chou (2005). By incorporating past observations in the mean function of the outcome, the CARGPR model can accommodate some AR structures which are prominent in financial data. Chan *et al.* (2010a) showed that there is substantial improvement of CARGPR model over CARR model in the in-sample estimation and out-sample forecast for

the 50 days movement of the daily price range of the All Ordinaries Index of Australia. This extension gives us insight that our subsequent proposed models can incorporate an AR structure using past observations in the mean of the latent GP in a similar way to the OD models.

However, as mentioned at the end of Section 1.2.1, using an OD model approach leads to difficulty in parameter interpretation. To cope with such problem, Diggle (1988) posited that the examination of the trend movements, covariate and cluster effects should precede the investigation of the serial correlation structure since the inference of the mean response with respect to trends, covariates and clustering is usually of primary interest. Hence in the first stage of the analysis, the specification of the mean of the outcome needs to be sufficiently flexible to accommodate all the trend movements, covariate effects and population heterogeneity and after that the remaining unexplained errors are assumed to be stationary and are used as a form of diagnostic to assess the preliminary serial correlation structure. Whereas, in the second stage, a flexible but economical covariance structure should be specified to allow for autocorrelation (Diggle, 1988).

Considering this modelling approach, our proposed models will first investigate the mean response such that the unexplained variation becomes non-stationary after accounting for various effects. Afterwards, a test of serial correlation for the Pearson residuals which are the standardized differences between the observations and predicted values from the model will be performed. In case of the presence of serial correlation, an appropriate

AR structure will be introduced by incorporating past observations into the mean function of the latent GP, the mean of the outcome. The suitability of the AR structure can be validated by examining the significance of the model parameters in the AR structure and by using some model selection criteria such as DIC.

Last but not least, the modelling of multivariate longitudinal data using GP model is an area that has not been explored. As multivariate longitudinal count data with non-monotone trends arise in many contexts, the extension of PGP model to study the trend patterns as well as the contemporaneous and cross correlations between multiple time series is definitely a new area that is worth of investigation.

The remaining thesis is structured as follows. Extensions of the PGP model under different situations will be investigated in Chapters 2 to 5. These situations include the zero-inflation caused by excess zero observations in Chapter 2, serious overdispersion due to extreme observations in Chapter 3, underdispersion in Chapter 4 and multivariate outcomes in Chapter 5. Lastly, Chapter 6 will summarize this research with some concluding remarks and implications for future developments.

CHAPTER 2

Mixture Poisson geometric process model

This Chapter extends the PGP model in (1.4) to fit longitudinal count data with zero-inflation.

2.1. Background

Repeated measurements of count data are common in many fields of research. One important characteristic of these data is the presence of excess zeros contributing to substantial population heterogeneity and overdispersion. We aim to develop models that accommodate these effects and to derive valid outcome measurement out of the proposed models. More specifically, we focus on models that do not only handle zero-inflated data but also provide useful information on treatment outcomes, say the identification of distinct treatment patterns and their group memberships resulting in better interpretation of the data.

The term “excess zeros" implies that the incidence of zero counts is greater than that expected from the Poisson distribution. Excess zeros may come from different sources and hence have different interpretations for the research outcome. For instances, the number of tumours recorded and removed from a patient in each visit may contain many zeros, either because he/she has recovered or the tumours have not yet grown to an observable

size by chance. Hence, it is important to treat the excess zeros carefully so that they would not dominate in the trend and give misleading information on treatment outcomes.

Researches on zero-inflated count data are extensive in areas like ecology (Welsh *et al.*, 1996), dental epidemiology (Bohning *et al.*, 1999), occupational health (Wang *et al.*, 2003; Yau & Lee, 2001), road safety (Miaou, 1994), medical and public health researches (Lam *et al.*, 2006), econometrics (Freund *et al.*, 1999), etc. There are different techniques to handle zero-inflated count data. The use of hurdle model (Mullahy, 1986) is one and zero-inflated models (Lambert, 1992) are another. For the former, the zero-altered hurdle models have received considerable attention in recent years.

While the studies of cross-sectional zero-inflated count data are enormous, models that address longitudinal zero-inflated count data, particularly time series of clustered and correlated observations, have not been well developed. Due to the hierarchical study design or the data collection procedure, inherent correlated structure within subject and underlying heterogeneity or clustering across subjects are often resulted simultaneously in the longitudinal data. This situation, particularly prevalent in medical research (Lee *et al.*, 2006), must be remedied as the ignorance leads to incorrect conclusions (Hur *et al.*, 2002).

Moreover, although most studies focus on the identification of significant covariates that affect the probability of the outcome, the overall time

trend of the outcome and the clustered pattern have seldom been addressed. The investigation of trend pattern is important as it provides insight about the progression of the outcome, and thus the appropriate remedial measures offered to different patients.

Considering the clustering and trends in the panel data, Chan & Leung (2010) applied the mixture Poisson geometric process (MPGP) model with exponential distribution to study the trends of the donation frequencies for some female and male donors in a blood service center and a simplified MPGP model was also considered. Results showed that the latter simplified MPGP model with a better model fit and mean squared error outperformed the MPGP model. On the other hand, to handle zero-inflation, Wan (2006) fitted a zero-altered Poisson geometric process (ZPGP) model using a hurdle model approach in Mullahy (1986) to the panel data in the bladder cancer study. The ZPGP model successfully coped with the problem of zero-inflation however has not accounted for the cluster effect within different treatment groups.

In order to deal with the population heterogeneity in the bladder cancer data, we propose two new models by extending the simplified MPGP model in Chan & Leung (2010) in two directions. First of all, we propose the zero-altered mixture Poisson geometric process (ZMPGP) model by adopting the hurdle model approach in the simplified MPGP model. Secondly, instead of using exponential distribution, we adopt a more general lifetime distribution for the stochastic process $\{Y_t = a_t^{t-1} X_t\}$ namely the gamma

distribution which contains an extra parameter to control the shape of the distribution. The resultant model is named as the mixture Poisson-gamma geometric process (MPGP-Ga) model. These models are compared with the simplified MPGP model from which they are extended.

To demonstrate the characteristics and applicability of our proposed models, the remaining Chapter is structured as follows. Firstly, the bladder cancer data will be described in Section 2.2. Then Section 2.3 will give a brief review of the simplified MPGP model on how it includes mixture effects to handle the population heterogeneity and to identify subgroups with distinct trend patterns, and follow by that is the introduction of the ZMPGP model using the hurdle model approach and MPGP-Ga model. After that, Section 2.4 will discuss the methodology for parameter estimation and some model selection criteria for the best model. The applicability of the proposed models will then be demonstrated through the bladder cancer data with model comparison in Section 2.5 followed by a conclusion in Section 2.6.

2.2. Bladder cancer data

In this research, we model the longitudinal count data obtained from a bladder cancer study conducted by the Veterans Administration Cooperative Urological Research Group (Hand *et al.*, 1994). In the study, a group of 82 patients who had superficial bladder tumours were selected to enter the trial. After removing the tumours inside their bodies, the patients were

assigned to one of the treatment groups with 46 taking placebo, an inactive substance having no therapeutic value, and 36 receiving thiotepa, an anti-cancer chemotherapy drug. The treatments were made quarterly for 36 months. At each visit, count of new tumours W_{it}, the outcome of the study, was recorded and new tumours were removed, thereafter the treatment continued. Since there are some outlying observations in the last two visits, we excluded these observations and the reduced dataset is given in Appendix 2.1. As the patients may not return for treatments at every quarter or may drop out of the clinical trial completely, there are 37% of missing appointments resulting in $n = 517$ observed data, amongst which 80% ($n_0 = 413$) are zero. Because of the high proportion of missing observations, the serial correlation in this panel data is not taken into consideration.

Over the visiting period, the overwhelming proportion of zero contributes to an overdispersion in the data which cannot be neglected. In this study, while treatment effect, placebo or thiopeta, on the new tumour counts is the main interest, the distinctive trend patterns displayed in the outcomes of the patients are also worthy of investigation. Therefore we extend the simplified MPGP model in Chan & Leung (2010) to include mixture effects, stochastic means for Poisson distribution and zero-inflated modelling in order to handle population heterogeneity and excess zeros.

2.3. MPGP model and its extension

2.3.1. Simplified MPGP model. Population heterogeneity and overdispersion are obvious in the bladder cancer data as some patients had very

high new tumour counts while the majority of other patients had zero counts throughout the visiting period. One way to accommodate population heterogeneity is to incorporate mixture effect into the mean and ratio functions. For the bladder cancer data, denote W_{it} as the count of new tumours for patient i at time t, $i = 1, \ldots m;\ t = 1, \ldots, n_i$ and $n = \sum_{i=1}^{m} n_i$. Assume that there are G groups of patients who have different trend patterns and each patient has a probability π_l of coming from group $l, l = 1, \ldots, G$. Under the framework of PGP model and conditional on group l, W_{it} is assumed to follow a Poisson distribution with mean X_{itl}. The simplified MPGP model set X_{itl} to be the mean of the latent GP for patient i directly. Then the mean of W_{it} is given by

$$E_l(W_{it}) = Var_l(W_{it}) = E(X_{itl}) = \frac{\mu_{itl}}{a_{itl}^{t-1}}. \tag{2.1}$$

To study the treatment effect while allowing different trend patterns, we accommodate covariate effect into the mean and ratio functions. Let the parameters $\boldsymbol{\beta}_{jl} = (\beta_{j0l}, \beta_{j1l}, \ldots, \beta_{jq_jl})^T$ be a vector of regression parameters β_{jkl}, where $j = \mu, a,\ k = 0, \ldots, q_j$ and $l = 1, \ldots, G$. The mean and ratio functions μ_{itl} and a_{itl} are given correspondingly by:

$$\mu_{itl} = \exp(\beta_{\mu 0l} + \beta_{\mu 1l} z_{\mu 1it} + \cdots + \beta_{\mu q_\mu l} z_{\mu q_\mu it}) \tag{2.2}$$

$$a_{itl} = \exp(\beta_{a0l} + \beta_{a1l} z_{a1it} + \cdots + \beta_{aq_a l} z_{aq_a it}) \tag{2.3}$$

where $z_{j0it} = 1$ and $z_{jkit},\ j = \mu, a; k = 1, \ldots, q_j$ are some time-evolving covariates. The non-constant ratio function allows a non-monotone trend. For instance, considering $z_{a1it} = t$, the time of visits of the bladder cancer

patients, an insignificant β_{a1l} reveals a monotone trend in group l and vice versa. Moreover, a significant positive estimate of β_{a0l} implies a decreasing trend whilst a significant negative estimate represents an increasing trend of new tumour counts throughout the visiting period. In case of a non-monotone trend, different values for β_{a0l} and β_{a1l} can describe a variety of trend patterns including U-shaped, bell shaped, exponential growth and decay with different rates, Gompertz curve, etc. Refer to Wan (2006) for more details.

The resultant model is essentially a probability mixture of G simplified PGP models such that the l^{th} PGP is associated with probability π_l subject to $\sum_{l=1}^{G} \pi_l = 1$ and a special case of this would be the simplified PGP model when $G = 1$. In the sequel to this Chapter, we will use PGP and MPGP models to refer to the simplified PGP ($G = 1$) and simplified MPGP models respectively. The pmf for W_{it} in the condition that patient i comes from group l can be expressed as:

$$f_{itl}(w_{it}) \quad = \quad L_{itl} = \frac{\exp\left(-\frac{\mu_{itl}}{{a_{itl}}^{t-1}}\right)\left(\frac{\mu_{itl}}{{a_{itl}}^{t-1}}\right)^{w_{it}}}{w_{it}!} \tag{2.4}$$

Since there are some missing observations in the bladder cancer data, we denote $I^*_{it} = 1$ as the indicator of a non-missing observation i at time t and 0 otherwise. The likelihood $L_c(\boldsymbol{\theta})$ and log-likelihood $\ell_c(\boldsymbol{\theta})$ functions for the complete data $\{W_{it}, I_{il}\}$ are then derived as

$$L_c(\boldsymbol{\theta}) = \prod_{i=1}^{m}\prod_{l=1}^{G}\left(\pi_l \prod_{t=1}^{n_i} L_{itl}^{I^*_{it}}\right)^{I_{il}} \text{ and } \ell_c(\boldsymbol{\theta}) = \sum_{i=1}^{m}\sum_{l=1}^{G} I_{il}(\ln \pi_l + \sum_{t=1}^{n_i} I^*_{it} \ln L_{itl}) \tag{2.5}$$

where L_{itl} is given by (2.4) and I_{il} is the group membership indicator for patient i such that $I_{il} = 1$ if patient i comes from group l and zero otherwise. The vector of model parameters is $\boldsymbol{\theta} = (\boldsymbol{\theta}_1^T, \ldots, \boldsymbol{\theta}_G^T, \pi_1, \ldots, \pi_G)^T$ where $\boldsymbol{\theta}_l$ is a vector of parameters $(\boldsymbol{\beta}_{\mu 0\, l}, \ldots, \boldsymbol{\beta}_{\mu q_\mu l}, \boldsymbol{\beta}_{a0l}, \ldots, \boldsymbol{\beta}_{aq_a l})^T$.

2.3.2. Zero-altered MPGP model. The hurdle model was originally proposed by Mullahy (1986) in the econometric study. The model is essentially a two-part model in which one part is a binary model for measuring whether the outcome overcomes the hurdle (say zero for zero-inflated data), while another part is a truncated model explaining those outcomes which pass the hurdle. A discrete distribution, like the Poisson distribution or negative binomial distribution which is suitable for overdispersed data, is usually assigned to the truncated model. As an effective technique to handle zero-inflated count data, we adopt the hurdle model approach and extend the MPGP model into the two-part zero-altered mixture PGP (ZMPGP) model.

Suppose there is a probability ϕ_t that the observed count W_{it} of patient i at time t is zero, we denote the indicator of the non-missing event '$W_{it} = 0$' by $I^*_{it0} = I(W_{it} = 0)$ and '$W_{it} > 0$' by I^*_{it1} respectively. Then the pmf for W_{it} conditional on group l in the ZMPGP model is given by:

$$f_{z,itl}(w_{it}) \;=\; \begin{cases} \phi_t, & w_{it} = 0 \\ (1-\phi_t)\,\dfrac{L_{itl}}{1 - L_{itl0}}, & w_{it} > 0 \end{cases}$$

where $L_{itl0} = f_{itl}(0)$, $L_{itl} = f_{itl}(w_{it})$, $f_{itl}(\cdot)$ are given by (2.4) and the mean function μ_{itl} and ratio function a_{itl} in (2.4) are given by (2.2) and

(2.3) respectively. The subscript z in $f_{z,itl}(w_{it})$ represents the model is zero-altered. Then, the means $E(W_{it})$ and variances $Var(W_{it})$ are expressed as:

$$E(W_{it}) = (1-\phi_t)\sum_{l=1}^{G}\pi_l\, E_l(W_{it}) = (1-\phi_t)\sum_{l=1}^{G}\pi_l\left(\sum_{s=1}^{\infty}\frac{s f_{itl}(s)}{1-f_{itl}(0)}\right) \quad (2.6)$$

$$\begin{aligned} Var(W_{it}) &= (1-\phi_t)\sum_{l=1}^{G}\pi_l\left(\sum_{s=1}^{\infty}\frac{[s-E_l(W_{it})]^2 f_{itl}(s)}{1-f_{itl}(0)}\right) \\ &\quad +(1-\phi_t)^2\left[\sum_{l=1}^{G}\pi_l\left(\sum_{s=1}^{\infty}\frac{s f_{itl}(s)}{1-f_{itl}(0)}\right)^2 - \left(\sum_{l=1}^{G}\pi_l\, E_l(W_{it})\right)^2\right] \end{aligned} \quad (2.7)$$

respectively where $E_l(W_{it})$ are the conditional means conditional on group l and given $W_{it} > 0$. Thereafter, we can derive the likelihood function $L(\boldsymbol{\theta})$ for the complete data $\{W_{it}, I_{il}\}$ as:

$$L(\boldsymbol{\theta}) = \prod_{i=1}^{m}\left\{\left(\prod_{t=1}^{n_i}\phi_t^{I^*_{it0}}\right)\prod_{l=1}^{G}\left[\pi_l\prod_{t=1}^{n_i}\left((1-\phi_t)\frac{L_{itl}}{1-L_{itl0}}\right)^{I^*_{it1}}\right]^{I_{il}}\right\} \quad (2.8)$$

and the log-likelihood function $\ell(\boldsymbol{\theta})$ as:

$$\begin{aligned} \ell(\boldsymbol{\theta}) &= \sum_{i=1}^{m}\sum_{t=1}^{n_i} I^*_{it0}\ln\phi_t + \sum_{i=1}^{m}\sum_{t=1}^{n_i} I^*_{it1}\ln(1-\phi_t) + \\ &\quad \sum_{i=1}^{m}\sum_{l=1}^{G} I_{il}\left\{\ln\pi_l + \sum_{t=1}^{n_i}\left[I^*_{it1}\ln\left(\frac{L_{itl}}{1-L_{itl0}}\right)\right]\right\}. \end{aligned}$$

where $\boldsymbol{\theta} = (\boldsymbol{\theta}_1^T, \ldots, \boldsymbol{\theta}_G^T, \pi_1, \ldots, \pi_G, \phi_1, \ldots, \phi_{\max_i(n_i)})^T$ is a vector of model parameters.

2.3.3. MPGP model with gamma distribution. An alternative way to handle zero-inflation is to add extra variability into the Poisson distribution so that the new distribution can allow for overdispersion. With a more flexible variance structure, the probability of zero can be adjusted to allow for

zero-inflation in the data. Therefore, we extend the MPGP model in the following way.

Conditional on group l, we assume that the mean of W_{it} forms a latent GP X_{itl} and the stochastic process $\{Y_{itl} = a_{itl}^{t-1} X_{itl}\}$ follows gamma distribution denoted by $f_G\left(y_{itl} \,\middle|\, r_l, \frac{1}{\mu_{itl}}\right)$ with mean $E(Y_{itl}) = r_l \mu_{itl}$ and variance $Var(W_{it}) = r_l \mu_{itl}^2$. Then the unobserved $\{X_{itl}\}$ can be integrated out to obtain the marginal pmf for W_{it}:

$$\begin{aligned} f_{g,itl}(w_{it}) &= \int_0^\infty \frac{\exp(-x_{itl}) {x_{itl}}^{w_{it}}}{w_{it}!} \frac{(a_{itl}^{t-1} x_{itl})^{r_l - 1} \exp(-a_{itl}^{t-1} x_{itl}/\mu_{itl})}{\mu_{itl}^{r_l} \Gamma(r_l)} \, a_{itl} \, dx_{itl} \\ &= \frac{\Gamma(r_l + w_{it})}{w_{it}! \, \Gamma(r_l)} \frac{\left(\frac{\mu_{itl}}{a_{itl}^{t-1}}\right)^{w_{it}}}{\left(1 + \frac{\mu_{itl}}{a_{itl}^{t-1}}\right)^{r_l + w_{it}}} \end{aligned} \tag{2.9}$$

which is the pmf for the well-known negative binomial (NB) distribution and the subscript g in $f_{g,it}(w_{it})$ represents the use of gamma distribution. Again the mean μ_{itl} and ratio a_{itl} functions are given by (2.2) and (2.3) respectively.

Conditional on group l, the resultant MPGP-Ga model has mean and variance for W_{it} given by

$$E_l(W_{it}) = r_l \frac{\mu_{itl}}{a_{itl}^{t-1}} \quad \text{and} \quad Var_l(W_{it}) = r_l \left[\frac{\mu_{itl}}{a_{itl}^{t-1}} + \left(\frac{\mu_{itl}}{a_{itl}^{t-1}}\right)^2\right]. \tag{2.10}$$

Clearly, the NB distribution shows overdispersion as $Var_l(W_{it}) = E_l(W_{it}) + \frac{E_l(W_{it})^2}{r_l}$. Moreover, the additional parameter r_l in the gamma distribution provides more flexibility to the distribution in handling overdispersion and makes the pmf in (2.9) capable of describing a number of shapes ranging

from exponential decay to normal. These distinctive features of the MPGP-Ga model make it suitable for modelling the new tumour counts in the bladder cancer data with substantial overdispersion, population heterogeneity and excess zeros.

The likelihood $L(\boldsymbol{\theta})$ and log-likelihood $\ell(\boldsymbol{\theta})$ functions for the complete data $\{W_{it}, I_{il}\}$ are the same as (2.5) with L_{itl} replaced by $f_{g,itl}(w_{it})$ in (2.9) and $\boldsymbol{\theta} = (\boldsymbol{\theta}_1^T, \ldots, \boldsymbol{\theta}_G^T, r_1, \ldots, r_G, \pi_1, \ldots, \pi_G)^T$ is a vector of model parameters. Analytically since gamma distribution can be reduced to exponential distribution when $r_l = 1$ and the NB distribution converges to the Poisson distribution when r_l approaches to infinity, the MPGP-Ga model can be reduced to the simplified MPGP model proposed in Wan (2006) and further reduced to the simplified PGP model with $G = 1$.

The following Section will discuss the Bayesian inference of different PGP models.

2.4. Bayesian Inference

For parameter estimation of the PGP, MPGP, ZMPGP and MPGP-Ga models, we adopt the Bayesian method using MCMC algorithms. The Bayesian framework, posterior and prior distributions and the full conditional posterior densities for the unknown model parameters will be derived in the next Section. While for model assessment, the best model is selected based on the a model selection criterion named as deviance information criterion (DIC). This will be discussed after the discussion of the MCMC algorithms.

2.4.1. MCMC algorithms. To implement the Bayesian method, different Bayesian hierarchies are established for different PGP models. Without loss of generality, the algorithms are given as follows:

$$
\begin{aligned}
&w_{it} \sim f_{it}(w_{it}) \\
&f_{it}(w_{it}) = I_{i1} f_{it1}(w_{it}) + \cdots + I_{iG} f_{itG}(w_{it}) \\
&f_{itl}(w_{it}) = L_{itl} \qquad \text{for PGP, MPGP, MPGP-Ga models} \\
&f_{itl}(w_{it}) = \phi_t^{I^*_{it0}} \left[(1-\phi_t) \frac{L_{itl}}{1 - L_{itl0}} \right]^{I^*_{it1}} \qquad \text{for ZMPGP model}
\end{aligned}
\tag{2.11}
$$

where I^*_{it0} and I^*_{it1} are the indicators of $W_{it} = 0$ and $W_{it} > 0$ respectively. Since the PGP model is a special case of the MPGP model when $G = 1$, therefore L_{itl} in (2.11) are given by (2.4) for the PGP and MPGP models and (2.9) for the MPGP-Ga model. For the ZMPGP model, $L_{itl0} = f_{itl}(0)$, $L_{itl} = f_{itl}(w_{it})$ and $f_{itl}(\cdot)$ refer to (2.4). The PGP, MPGP and MPGP-Ga models can be specified directly using the Poisson and NB data distributions while the truncated Poisson data distribution in the ZMPGP model requires the use of "ones trick" technique in `WinBUGS`. This technique allows the specification of any non-standard distributions, especially truncated distributions, that are not included in the list of standard distributions in `WinBUGS`. By creating an artificial data set with all data equal to one and same sample size as the observed data, and furthermore by assuming the artificial data follows a Bernoulli distribution with probability p_{it}, the required non-standard likelihood function can be attained by specifying

$p_{it} = f_{it}(w_{it})/C$ in `WinBUGS` where C is a scaling constant to ensure all $p_{it} < 1$.

In order to construct the posterior density, some prior distributions are assigned to the model parameters $\boldsymbol{\theta}$ as follows:

$$\beta_{jkl} \sim N(0, \tau^2_{jkl}),\ j = \mu, a;\ k = 0, 1, \ldots, q_j;\ l = 1, \ldots, G \quad (2.12)$$

$$\phi_t \sim \text{Uniform}(0, 1) \text{ for ZMPGP model} \quad (2.13)$$

$$r_l \sim \text{Gamma}(a_l, b_l) \text{ for MPGP-Ga model} \quad (2.14)$$

$$\pi_1 \sim \text{Uniform}(0, 1) \text{ for MPGP, ZMPGP \& MPGP-Ga models} \quad (2.15)$$

The prior specifications are mostly non-informative. For example, we set the hyperparameter $\tau^2_{jkl} = 1000$. For the gamma distribution of the MPGP-Ga model in (2.14), we set $a_1 = 7.5$, $a_2 = 0.1$ and $b_l = 10$ based on the information from the MPGP model that one group shows overdispersion whilst another shows underdispersion in the new tumour counts. In case of a G-group ($G > 2$) mixture model, the prior for $\boldsymbol{\pi} = (\pi_1, \ldots, \pi_G)$ can be replaced by the Dirichlet distribution $Dir(\alpha_1, \ldots, \alpha_G)$ where α_l is set to be $1/G$. Note that $\boldsymbol{I}_i = (I_{i1}, \ldots, I_{iG})$ are not observed, thus a Bernoulli distribution is assigned to $I_{i1} \sim Bern(\pi_1)$ or a multinomial distribution $\boldsymbol{I}_i \sim$ multinomial$(1, \pi_1, \ldots, \pi_G)$ is assigned if $G > 2$. With the posterior means $\bar{I}_{il}$ of the group membership indicators I_{il}, patient i is classified to group l' if $\bar{I}_{il'} = \max_l \bar{I}_{il}$.

To implement the MCMC algorithms, we derive the conditional posterior densities from which parameters are sampled. The conditional posterior densities are proportional to the joint posterior density of complete data likelihood and prior densities. Taking a 2-group ZMPGP model as an example, the complete data likelihood is given by (2.8) and the priors are given by (2.12), (2.13) and (2.15), hence treating I_{il} as missing observations, the joint posterior density is

$$f(\boldsymbol{\beta},\boldsymbol{\pi},\boldsymbol{\phi}|\boldsymbol{w},\boldsymbol{I}) \propto \left(\prod_{i=1}^{m}\left\{\left(\prod_{t=1}^{n_i}\phi_t^{I^*_{it0}}\right)\prod_{l=1}^{G}\left\{\pi_l\prod_{t=1}^{n_i}\left[(1-\phi_t)\frac{\exp(-\hat{w}_{itl})(\hat{w}_{itl})^{w_{it}}}{w_{it}!(1-\exp(-\hat{w}_{itl}))}\right]^{I^*_{it1}}\right\}^{I_{il}}\right\}\right)$$
$$\left(\prod_{j=\mu,a}\prod_{k=0}^{1}\prod_{l=1}^{G} f_N(\beta_{jkl}|\,0,\tau^2_{jkl})\right)\left(\prod_{t=1}^{10} f_U(\phi_t|\,0,1)\right) f_U(\pi_1|\,0,1)$$

where $f_N(\cdot|\,0,\tau^2_{jkl})$ represents a normal distribution with mean 0 and variance τ^2_{jkl}, $f_U(\cdot|\,0,1)$ denotes a uniform distribution on the interval $[0,1]$, $\boldsymbol{w}$ is a vector of the data w_{it}, $\boldsymbol{I}$ is a vector of I_{il}, $\boldsymbol{\beta}$ is a vector of β_{jkl} and $\boldsymbol{\phi}$ is a vector ϕ_t. The univariate full conditional posterior densities for each of the unknown model parameters $\boldsymbol{\theta} = (\boldsymbol{\beta}, \pi_1, \boldsymbol{\phi})$ and the latent group indicator I_{i1} are therefore given by:

$$f(\beta_{jkl}|\boldsymbol{w},\boldsymbol{I},\boldsymbol{\beta}^{-},\pi_1,\boldsymbol{\phi}) \;\propto\; \left\{\prod_{i=1}^{m}\prod_{t=1}^{n_i}\left[\frac{\exp(-\hat{w}_{itl}+\beta_{jkl}z_{jkit}w_{it})}{1-\exp(-\hat{w}_{itl})}\right]^{I^*_{it1}(I_{il})}\right\}\exp\left(-\frac{\beta^2_{jkl}}{2\tau^2_{jkl}}\right),$$
$$j=\mu,a; k=0,1; l=1,2$$

$$f(I_{i1}|\boldsymbol{w},\boldsymbol{\beta},\pi_1,\boldsymbol{\phi}) \;\propto\; \prod_{l=1}^{G}\left[\frac{\pi_l\prod_{t=1}^{n_i}\left(\frac{\exp(-\hat{w}_{itl})\hat{w}_{itl}^{w_{it}}}{1-\exp(-\hat{w}_{itl})}\right)^{I^*_{it1}}}{\sum_{l'=1}^{G}\left[\pi_{l'}\prod_{t=1}^{n_i}\left(\frac{\exp(-\hat{w}_{itl'})\hat{w}_{itl'}^{w_{it}}}{1-\exp(-\hat{w}_{itl'})}\right)^{I^*_{it1}}\right]}\right]^{I_{il}} = \text{Bernoulli}(\pi_1')$$

$$\text{where} \quad \pi_1' = \frac{\pi_1 \prod_{t=1}^{n_i} \left(\frac{\exp(-\hat{w}_{it1}) \hat{w}_{it1}^{w_{it}}}{1-\exp(-\hat{w}_{it1})} \right)^{I^*_{it1}}}{\sum_{l'=1}^{G} \left[\pi_{l'} \prod_{t=1}^{n_i} \left(\frac{\exp(-\hat{w}_{itl'}) \hat{w}_{itl'}^{w_{it}}}{1-\exp(-\hat{w}_{itl'})} \right)^{I^*_{it1}} \right]}$$

$$f(\pi_1|\boldsymbol{w}, \boldsymbol{I}, \boldsymbol{\beta}, \boldsymbol{\phi}) \propto \prod_{i=1}^{m} \prod_{l=1}^{G} \pi_l^{I_{il}} = \pi_1^{m_1} (1-\pi_1)^{m_2}$$

$$f(\phi_t|\boldsymbol{w}, \boldsymbol{I}, \boldsymbol{\beta}, \boldsymbol{\pi}, \boldsymbol{\phi}^-) \propto \prod_{i=1}^{m} \phi_t^{I^*_{it0}} (1-\phi_t)^{I^*_{it1}} = \phi_t^{n_{0t}} (1-\phi_t)^{n_{1t}}$$

where $\boldsymbol{\beta}^-$ and $\boldsymbol{\phi}^-$ are vectors $\boldsymbol{\beta}$ and $\boldsymbol{\phi}$ excluding β_{jkl} and ϕ_t, $m_l = \sum_{i=1}^{m} I_{il}$ is the number of patients classified to group l, $n_{0t} = \sum_{i=1}^{m} I^*_{it0}$ and $n_{1t} = \sum_{i=1}^{m} I^*_{it1}$ are the number of zero and non-zero observations at visit t respectively, and $\hat{w}_{itl} = E_l(W_{it})$ is given by (2.6).

The MCMC algorithms can be derived for the MPGP and MPGP-Ga models in a similar way. Nevertheless, the MCMC algorithms are implemented using the user-friendly software `WinBUGS` where the sampling scheme based on the conditional posterior densities is outlined in this Section and the Gibbs sampling procedures are described in Section 1.4.3. The posterior sample means are adopted as parameter estimates since the posterior densities of most model parameters are highly symmetric and the posterior sample mean is close to the posterior sample median.

2.4.2. Model selection criterion. For model assessment and comparison, a common measure, namely deviance information criteria (DIC) is

adopted. DIC originated by Spiegelhalter *et al.* (2002) is a Bayesian analogue of Akaike's Information Criterion (AIC) (Akaike, 1974). It is a measure of model fit and model complexity and has an advantage over the traditional AIC as it is not only applicable to nested models. DIC is composed of the posterior mean deviance $\overline{D(\boldsymbol{\theta})}$ which accounts for the fit of the model and the effective dimension p_D which assesses the complexity of the model. For the PGP model, DIC is given by

$$\begin{aligned} DIC_{M1} &= \overline{D(\boldsymbol{\theta})} + p_D \\ &= -\frac{4}{M}\sum_{j=1}^{M}\sum_{i=1}^{m}\sum_{t=1}^{n_i}[I_{it}^{*}\ln f_{it}(w_{it}|\,\boldsymbol{\theta}^{(j)})] + 2\sum_{i=1}^{m}\sum_{t=1}^{n_i} I_{it}^{*}\ln f_{it}(w_{it}|\,\overline{\boldsymbol{\theta}}) \end{aligned}$$

where M is the number of realizations in the MCMC sampling algorithms, $\boldsymbol{\theta}^{(j)}$ represents the vector of model parameter estimates under the j^{th} simulation in the posterior sample, $\overline{\boldsymbol{\theta}}$ is the vector of posterior means and $f_{it}(w_{it})$ is a density function given by (2.4) with $G = 1$. DIC_{M1} is output in `WinBUGS` as it supports the calculation of DIC of the PGP model. Unfortunately the computation of DIC is infeasible for mixture models like the MPGP (Model 2), ZMPGP (Model 3) and MPGP-Ga (Model 4) models. Applying the idea of Celeux *et al.* (2006), by considering I_{il} as missing data, the complete DIC are defined for Model 2 to 4 respectively as follows:

For the MPGP and MPGP-Ga models,

$$DIC_{M2,4} = -\frac{4}{M}\sum_{j=1}^{M}\sum_{i=1}^{m}\sum_{l=1}^{G} I'_{il}(\boldsymbol{\theta}^{(j)})\left[\ln \pi_l^{(j)} + \sum_{t=1}^{n_i} I^*_{it} \ln f_{itl}(w_{it}|\,\boldsymbol{\theta}^{(j)})\right] + 2\sum_{i=1}^{m}\sum_{l=1}^{G} I'_{il}(\overline{\boldsymbol{\theta}})\left[\ln \overline{\pi}_l + \sum_{t=1}^{n_i} I^*_{it} \ln f_{itl}(w_{it}|\,\overline{\boldsymbol{\theta}})\right] \quad (2.16)$$

$$\text{where} \quad I'_{il}(\boldsymbol{\theta}^{(j)}) = \frac{\pi_l^{(j)} \prod_{t=1}^{n_i} f_{itl}(w_{it}|\,\boldsymbol{\theta}^{(j)})^{I^*_{it}}}{\sum_{l'=1}^{G} \pi_{l'}^{(j)} \prod_{t=1}^{n_i} f_{itl'}(w_{it}|\,\boldsymbol{\theta}^{(j)})^{I^*_{it}}}$$

and $f_{itl}(w_{it})$ are given by (2.4) and (2.9) for the MPGP and MPGP-Ga respectively. For the ZMPGP model, DIC_{M3} is calculated below in a similar way as in (2.16) but with a different log-likelihood $\ln L(\boldsymbol{\theta}^{(j)})$ given by (2.8) to account for the different likelihoods for the zero and non-zero observations. So, we have

$$DIC_{M3} = -\frac{4}{M}\sum_{j=1}^{M}\sum_{i=1}^{m}\left\{\sum_{t=1}^{n_i} I^*_{it0} \ln \phi_t^{(j)} + \sum_{t=1}^{n_i} I^*_{it1} \ln(1-\phi_t^{(j)}) + \sum_{l=1}^{G} I'_{il}(\boldsymbol{\theta}^{(j)})\left[\ln \pi_l^{(j)} + \sum_{t=1}^{n_i} I^*_{it1} \ln\left(\frac{f_{itl}(w_{it}|\,\boldsymbol{\theta}^{(j)})}{1-f_{itl}(0|\,\boldsymbol{\theta}^{(j)})}\right)\right]\right\} + 2\sum_{i=1}^{m}\left\{\sum_{t=1}^{n_i} I^*_{it0} \ln \overline{\phi}_t + \sum_{t=1}^{n_i} I^*_{it1} \ln(1-\overline{\phi}_t) + \sum_{l=1}^{G} I'_{il}(\overline{\boldsymbol{\theta}})\left[\ln \overline{\pi}_l + \sum_{t=1}^{n_i} I^*_{it1} \ln\left(\frac{f_{itl}(w_{it}|\,\overline{\boldsymbol{\theta}})}{1-f_{itl}(0|\,\overline{\boldsymbol{\theta}})}\right)\right]\right\}. \quad (2.17)$$

$$\text{where} \quad I'_{il}(\boldsymbol{\theta}^{(j)}) = \frac{\pi_l^{(j)} \prod_{t=1}^{n_i} \left(\frac{f_{itl}(w_{it}|\,\boldsymbol{\theta}^{(j)})}{1-f_{itl}(0|\,\boldsymbol{\theta}^{(j)})}\right)^{I^*_{it1}}}{\sum_{l'=1}^{G} \pi_{l'}^{(j)} \prod_{t=1}^{n_i} \left(\frac{f_{itl'}(w_{it}|\,\boldsymbol{\theta}^{(j)})}{1-f_{itl'}(0|\,\boldsymbol{\theta}^{(j)})}\right)^{I^*_{it1}}}$$

and $f_{itl}(w_{it})$ is given by (2.4). Equations (2.16)-(2.17) correspond to DIC_6 for mixture distributions in Celeux *et al.* (2006) and as suggested there,

$I'_{il}(\boldsymbol{\theta}^{(j)})$ is used in place of $I_{il}^{(j)}$ to save computing storage space. A model with the smallest DIC is preferred as it indicates the chosen model has the best fit of the data accounting for its complexity.

2.5. Real data analysis

In the bladder cancer study, we are interested in investigating the treatment effect as well as the trend patterns of the patients' tumour counts while allowing for the population heterogeneity and excess zeros in the data. Table 2.1 in Appendix 2.2 summarizes the parameter estimates and their standard errors (SE) (in *italics*) and model assessment measures for all fitted models.

==========

Table 2.1 about here

==========

Starting from the simplest model, we first fitted the PGP model (Model 1). The mean function $\mu_{it} = \exp(\beta_{\mu 0} + \beta_{\mu 1} b)$ adopts 'treatment' ($z_{\mu 1it} = b = 1, 2$ to indicate 'thiotepa' and 'placebo' respectively) as a covariate and the ratio function $a_{it} = \exp(\beta_{a0} + \beta_{a1}\, t)$ adopts 'time' ($z_{a1it} = t = 1, \ldots, 10$) as a time-evolving covariate. The time effect in the ratio function measures the change in trend direction, increasing or decreasing, over time. As both the treatment and time effects are significant, they imply that thiotepa treatment is associated with a decrease in new tumour count (95%

CI for $\beta_{\mu 1}$:$[-1.196, -0.6807]$) and the new tumour count shows a decreasing and then a slightly increasing trend (95% CI for β_{a0}:$[0.0368, 0.3075]$; β_{a1}:$[-0.0298, -0.0020]$).

Not surprisingly, patients with thiotepa treatment have lower tumour counts in general. However within the treatment group, some of these patients had much higher counts (up to 9) while others had only zero counts throughout the visiting period. To handle the population heterogeneity, we postulate that there are two clusters of patients who responded differently to the placebo treatment and the thiotepa treatment. We fitted the MPGP model (Model 2) with the same set of covariates in the mean and ratio functions. We have considered the quadratic effect of time and interaction effect of time and treatment effect in the ratio function separately, but the parameter estimates were found to be insignificant (95% CI contains zero) and were discarded. Two clusters, namely the high-level and the low-level tumour groups, are identified in which patient i is classified to group l, $l = 1, 2$ if the posterior mean $\bar{I}_{il} = \max_{l'} \bar{I}_{il'}$. The low-level ($l = 1$) group mainly consists of patients with less than four tumour counts throughout the visiting period whereas the high-level ($l = 1$) group contains patients with relatively more tumours. Hence, the overdispersion in tumour counts amongst patients is captured by the mixture effect. The time effects (β_{a1l}) in both ratio functions are insignificant (95% CI contains zero) and hence are discarded. After refitting the model, the low-level groups show a monotone decreasing trend (95% CI for β_{a0l}:$[0.0392, 1.0350]$) in new tumour counts over the

period of visits. Whereas the trend for the high-level group is stationary (β_{a02}:$[-0.0143, 0.0658]$). Moreover the treatment effect is significant (95% CI for $\beta_{\mu 12}$:$[-0.8609, -0.2646]$) only in the high-level group. These indicate that the thiotepa treatment is 'effective' mainly for those patients with higher level of new tumours.

Comparing the observed (80%) and the expected (67%) proportions of zeros averaged over time, we find that the expected proportion is still much lower than the observed one. This signifies that the MPGP model is inadequate in modelling the zero-inflation in the data. These zeros contribute substantial noise in the detection of trends leading to insignificant time effects in both ratio functions. Hence despite the accommodation of population heterogeneity by incorporating the mixture effect, the DIC for the MPGP model does not show a great improvement.

To allow for zero-inflation, two models are considered, namely the ZMPGP model (Model 3) and the MPGP-Ga model (Model 4) as the distribution of both models give higher probabilities of zero counts than the Poisson distribution. Fitting a ZMPGP model using the hurdle approach is essentially equivalent to remove all zero observations and model the non-zero observations using a zero-truncated distribution. Equivalently, the model is a combination of a binary model to model the zero observations over the visiting period and a MPGP model for the non-zero observations. Hence, this model yields different results and interpretations from the MPGP model.

Under the ZMPGP model, after ignoring the zero observations, a majority of 72 (88%) patients are classified to the low-level group, amongst them 34 (47%) patients received treatment. In this model, the treatment effect is only significant in the low-level group (95% CI for $\beta_{\mu 11}$:$[-1.0870, -0.2996]$). The time effect in the ratio functions of both groups indicates the non-monotone trends of new tumour counts prevail. In Appendix 2.3, Figure 2.1(a) shows the trends of new tumour counts given by $(1-\phi_t)\widehat{W}_{itl}$ where $\widehat{W}_{itl} = E_l(W_{it})$ in (2.6) for respectively the three groups, namely the high-level ($l = 2$), the low-level without treatment ($l = 1, b = 1$) and the low-level with treatment ($l = 1, b = 1$) groups, and Figure 2.1(b) reveals the trends of individuals within each group. The predicted new tumour count for patient i at time t is given by $\widehat{W}_{it} = (1-\phi_t)\left(\bar{I}_{i1}\widehat{W}_{it1} + \bar{I}_{i2}\widehat{W}_{it2}\right)$. Note that the PGP model applies to discrete-time time series. However as we aim to generalize the model to a continuous-time one, smoothing curves are thus used to demonstrate the trend movements over a continuous time frame.

==========

Figures 2.1(a) and 2.1(b) about here

==========

Due to the fluctuating zero proportion over time, the expected new tumour counts are fluctuating but the fluctuation is much less rigorous for the low-level groups. In general, the new tumour counts for the high-level group decline but rebound nearly to the starting level whereas those for the low-level groups rise gently throughout but drop slightly near the end. The

wide gap of the new tumour counts between patients with and without treatment shows that there is treatment effect in the low-level group. Trends in both low- and high-level groups reveal that the condition of patients in the high-level group deteriorates in the later half of the visiting period whereas the treatment effect in the low-level groups starts with a lag. Since the ZMPGP model performs much better in handling the zero-inflated data, the DIC calculated using (2.17) decreases dramatically.

For the MPGP-Ga model, as it is capable of modelling overdispersed count data, the low-level group ($l = 1$) shrinks to accommodate patients essentially with zero observations throughout the study period. On the other hand, the high-level group ($l = 2$) contains mainly patients with fluctuating observations and hence accounts for most of the overdispersion in the new tumour counts. Compared to the MPGP model, the MPGP-Ga model has more distinct low-level and high-level groups. Overall, 46 patients (56%) are classified into the high-level group with 16 of them (35%) receiving treatment. Again in Appendix 2.3, Figure 2.2(a) reveals the predicted trends of new tumour counts for respectively the three groups, namely the low-level ($l = 1$), the high-level without treatment ($l = 2, b = 1$) and the high-level with treatment ($l = 1, b = 2$) groups, and Figure 2.2(b) shows the trends of individuals within each group. The predicted new tumour count for patient i at time t is given by $\widehat{W}_{it} = \bar{I}_{i1}\widehat{W}_{it1} + \bar{I}_{i2}\widehat{W}_{it2}$ where $\widehat{W}_{itl} = E_l(W_{it})$ is given by (2.10).

==========

Figures 2.2(a) and 2.2(b) about here

==========

Including zeros, differences across the three groups get wider for both observed and expected levels of new tumour counts when compared to those of the ZMPGP model. The low-level group contains patients with essentially zero new tumour counts throughout the visiting period and hence the treatment effect is insignificant in this group and is dropped thereafter. On the contrary, for the high-level groups, the time effect ($\hat{\beta}_{a12} = -0.0137$) in the ratio function demonstrates a U-shaped trend pattern and represents that the new tumour counts increase again after a gradual decline in the first five visits. Again the wide gap in the levels between new tumour counts in the high-level with and without treatment groups shows that there is significant treatment effect in this group (95% CI for $\beta_{\mu 12}$:$[-0.8318, -0.1357]$). These distinct trend patterns from the MPGP-Ga and ZMPGP models can probably be explained by their different modelling approaches and resultant classification.

Comparing to the ZMPGP model, there is an authentic decrease in the DIC calculated using (2.16) for the MPGP-Ga model, despite the fact that the expected proportion of zeros does not fit the observed one as good as in the ZMPGP model. The better DIC can be explained by the brevity and flexibility in the pmf of the MPGP-Ga model to handle overdispersion and thus it gives a better fit to the data.

Finally we conclude the performances of the proposed models to handle excess zero and overdispersion by plotting the expected proportions of zeros p_{0t} and expected variances v_t, over time with the observed proportions of zeros P_{0t} and observed variances V_t in Figures 2.3(a) and 2.3(b) in Appendix 2.3. The observed proportions of zeros and variances are simply calculated based on the observed data for each time t and are constant across models. The expected proportions of zeros p_{0t} are expressed as a weighted average of the probability of getting zero based on different densities over each treatment and mixture subgroup, where the weights are the sum of the mixture group indicators of the patients $\sum_i I_{il}$ in the subgroups. The expected variances v_t are also computed as weighted averages of the variance of each treatment and mixture groups. In particular, if there are two mixture groups in Model 2 to 4, the variance v_t comprises of the variance of expectation and the expectation of variance conditional on the mixture group l, that is we get the weighted average within the mixture group using π_l before calculating the overall expected variances. In other words,

$$v_t = \frac{1}{m}\left[\sum_{i=1}^{m} I(z_{\mu 1i}=1)v_{1t} + \sum_{i=1}^{m} I(z_{\mu 1i}=2)v_{2t}\right] \tag{2.18}$$

$$v_{bt} = \sum_{l=1}^{G} \pi_l \left[Var_l(W_{it}) + E_l(W_{it}^2)\right] - \left[\sum_{l=1}^{G} \pi_l E_l(W_{it})\right]^2, b = 1, 2 \tag{2.19}$$

where the mean $E_l(W_{it})$ and variance $Var_l(W_{it})$ conditional on group l are given by (2.1) and (2.10) for the MPGP and MPGP-Ga models respectively. For the ZMPGP model, $v_{bt} = Var(W_{it})$ is given by (2.7) when $z_{\mu 1i} = b$.

==========

Figures 2.3(a) and 2.3(b) about here

==========

Figure 2.3(a) shows that, across Model 1 to Model 4, the expected proportions of zeros p_{0t} increase in general and approach those of the observed proportions P_{0t}, with those of ZMPGP model being the best because ϕ_t is indeed estimated by P_{0t} at each time t. Hence the models are becoming more and more capable of handling excess zero which is the first focus of this Chapter. The second focus concerns the overdispersion of the data. Figure 2.3(b) shows that the observed and expected variances under different models are more deviated. While Model 1 and 2 are still inefficient to handle overdispersion, the performance of the MPGP-Ga model and ZMPGP model are much more satisfactory.

2.6. Discussion

Motivated by the bladder cancer data and the limited literature in modelling zero-inflated and overdispersed longitudinal time series of counts, we extend, in this Chapter, the MPGP model of Chan & Leung (2010) which cannot cope with excess zeros and substantial overdispersion. As the bladder cancer data from longitudinal measurements have substantial population heterogeneity, we first extend the PGP model to incorporate mixture effect and the resultant MPGP model is capable of distinguishing two groups of patients with very different trends of new tumour counts. At the same time,

zero-inflation is another problem in the data which seriously affects the prediction of trend patterns in the data. Hence, we develop two distinct models, namely the ZMPGP model and MPGP-Ga model to handle such problem. The ZMPGP model is essentially a mixture of zero-degenerated model and a zero-truncated MPGP model via the hurdle approach, while the MPGP-Ga model is a state space model with state variable $E_l(W_{it}) = X_{itl}$ where X_{itl} follows a gamma distribution.

It should be noted that while both ZMPGP and MPGP-Ga models are suitable for modelling data with overdispersion and excess zeros, they are not built to cater for serial correlation in the time series. This is because the data contains too many missing observations such that the autoregressive terms cannot be defined for a substantial portion of time points in the time series of most patients. Hence the OD and PD approaches of the popular panel count models reviewed in Chapter 1 are not considered here.

For model implementation, we adopt the Bayesian method with MCMC techniques by using `WinBUGS`. The models are assessed and compared through a popular criterion DIC which measures the fit of the model taking into account the model complexity. Results show that the ZMPGP model, though gives a substantial drop in DIC when compared with the MPGP model, is not as good as the MPGP-Ga model after model complexity is also taken into consideration.

In conclusion, the two target models, MPGP-Ga and ZMPGP have different performance and interpretation. The MPGP-Ga model has largest

variances in general because of the extra variability from the stochastic GP in the mean of Poisson distribution. The ZMPGP model also has relatively large variances due to the zero-truncated Poisson distribution. While other models still have relatively smaller variances, the MPGP-Ga model and ZMPGP model are more suitable for data with overdispersion. For zero-inflation, the two models handle the problem in a different way and therefore are suitable under different situations. In a medical context, the ZMPGP model recognizes the development of new tumours as a two-stage disease progression. The binary model decides whether the patients are at carcinogenic risk of recurrence of tumours. If they suffer from recurrence $(W_{it} > 0)$, the truncated Poisson model describes the subsequent trends which is usually of more clinical interest. On the contrary, if the zero observations reveal important information for treatment outcomes, the MPGP-Ga model is perhaps more appropriate.

Our study also gives us insight on the existence of non-monotone trend of new tumour counts. Both ZMPGP and MPGP-Ga models suggest that there is a possibility of resurgence of tumours across the visiting period despite the use of thiotepa. Therefore, clinicians should exercise some precautionary measures, such as dosage increment, to inhibit the resurrection of the tumours.

Lastly, there are 37% of missing data and they are simply ignored in the models by implicitly assuming that the missing are completely random. This assumption may be invalid as experiences in clinical trials show that

such dropouts are often nonignorable. Hence one possible remedy in this data analysis is to set up a dropout model to allow for the dropout effect on the treatment outcomes.

Appendix 2.1

Number of new tumours found in 82 patients taking placebo and thiotepa treatments in the bladder cancer study

Placebo:

	Visit (months)									
Patient	3	6	9	12	15	18	21	24	27	30
1	0	-	-	-	-	-	-	-	-	-
2	-	0	-	-	-	-	-	-	-	-
3	0	-	0	-	-	-	-	-	-	-
4	0	1	0	-	-	-	-	-	-	-
5	0	-	0	-	0	-	-	-	-	-
6	0	-	0	2	3	0	-	-	-	-
7	0	-	-	-	0	0	-	-	-	-
8	-	2	0	0	-	0	-	-	-	-
9	0	0	6	-	3	0	-	0	-	-
10	8	-	0	0	8	0	-	8	-	-
11	1	0	1	0	0	0	8	0	-	-
12	0	0	0	0	0	0	-	0	-	-
13	0	8	7	0	5	-	-	7	-	-
14	1	0	0	0	1	0	0	3	-	-
15	8	0	-	0	0	0	0	0	0	-
16	4	0	-	-	-	-	-	-	8	-
17	0	0	-	0	0	-	0	0	0	-
18	-	0	-	-	-	-	-	3	0	-
19	-	0	0	-	-	0	-	-	-	0
20	0	0	-	-	0	-	-	-	-	0
21	0	0	0	0	-	0	-	0	-	0
22	4	-	0	-	-	2	4	0	0	0
23	1	3	3	3	0	0	0	0	3	0
24	0	0	0	0	-	-	0	-	2	1
25	0	0	0	2	3	0	-	1	0	0
26	0	0	0	0	0	0	0	-	0	-
27	0	-	0	-	0	-	0	-	-	0
28	0	0	0	0	0	0	0	0	-	0
29	-	-	0	-	-	-	0	-	-	8
30	0	-	0	-	-	0	-	0	-	0
31	0	-	8	-	0	2	5	1	0	0
32	0	0	0	0	0	9	-	1	0	2
33	0	0	0	0	0	0	0	0	0	0
34	3	0	0	-	0	-	0	-	0	0
35	0	1	0	0	0	0	0	0	-	-
36	5	3	4	-	0	0	0	0	0	0
37	0	0	1	3	-	0	1	0	4	3
38	0	0	0	0	0	1	0	0	0	0
39	-	0	0	0	-	0	-	0	-	0
40	0	0	-	0	-	0	-	0	-	0
41	0	-	0	0	0	1	0	0	0	0
42	7	-	-	0	2	-	-	-	0	0
43	0	0	0	0	0	0	0	-	0	-
44	1	0	0	0	3	0	-	4	0	3
45	0	3	0	0	4	0	2	0	5	0
46	1	0	3	6	-	4	1	0	0	0

Thiotepa:

	Visit (months)									
Patient	3	6	9	12	15	18	21	24	27	30
47	-	8	-	-	-	-	-	-	-	-
48	0	0	0	-	-	-	-	-	-	-
49	-	0	0	-	-	-	-	-	-	-
50	0	-	-	0	-	-	-	-	-	-
51	1	0	0	0	0	-	-	-	-	-
52	7	7	2	0	0	0	-	-	-	-
53	-	0	-	0	-	2	-	-	-	-
54	-	-	-	-	-	0	-	-	-	-
55	2	-	-	-	-	0	-	-	-	-
56	0	0	0	0	0	2	0	-	-	-
57	0	0	0	-	0	0	0	-	-	-
58	0	-	0	0	-	0	0	0	-	-
59	-	-	0	0	-	0	-	0	-	-
60	0	0	0	0	0	0	0	0	-	-
61	0	2	0	3	-	-	1	0	0	-
62	0	1	0	0	0	-	0	-	0	-
63	2	-	-	-	-	-	-	-	-	0
64	0	0	0	-	-	-	0	0	3	0
65	0	0	0	0	0	0	0	0	0	-
66	0	1	0	0	3	0	0	3	3	0
67	0	0	0	0	0	0	2	1	2	-
68	-	0	-	-	0	0	-	3	2	1
69	0	0	0	0	0	0	0	0	0	0
70	0	0	0	0	0	0	0	0	0	0
71	1	0	-	0	-	0	0	0	1	0
72	-	-	0	-	-	-	-	0	-	-
73	2	0	0	0	0	0	1	2	1	0
74	0	0	0	0	0	-	0	0	0	-
75	1	0	0	0	0	0	0	0	0	-
76	0	0	0	0	0	0	0	0	0	0
77	-	-	-	0	0	-	-	0	-	0
78	1	-	0	0	-	-	0	1	-	0
79	0	-	-	-	-	-	0	0	-	-
80	0	0	0	0	0	0	0	0	0	0
81	0	0	0	0	0	0	0	0	0	0
82	0	0	0	0	0	0	0	0	0	0

Appendix 2.2

Tables

Table 2.1: Parameter estimates, SE (in *italics*) and DIC in different PGP models for the bladder cancer data

	Shape parameter	Group proportion		Mean parameter		Ratio parameter		GOF measure
		zero	mixture	intercept	treatment	intercept	time	
	r_l	$\phi^\dagger$	π_l	$\beta_{\mu 0l}$	$\beta_{\mu 1l}$	β_{a0l}	β_{a1l}	DIC
Model 1				1.0110	-0.9390	0.1707	-0.0158	1446.22
				0.1895	*0.1311*	*0.0694*	*0.0071*	
Model 2								
low-level			0.5439	-2.0640		0.5134		1204.83
$l = 1$			*0.0579*	*0.5126*		*0.4406*		
high-level			0.4561	1.1000	-0.5717	0.0266		
$l = 2$			*0.0579*	*0.2110*	*0.1558*	*0.0204*		
Model 3								
low-level		0.7882	0.7366	1.053	-0.7118	-0.3398	0.02979	1012.98
$l = 1$		*0.0554*	*0.0857*	*0.3857*	*0.1935*	*0.1578*	*0.0158*	
high-level		0.7882	0.2634	1.897		0.2113	-0.02212	
$l = 2$		*0.0554*	*0.0857*	*0.1492*		*0.1531*	*0.0172*	
Model 4								
low-level	76.37		0.3823	-6.9760		3.5120		**889.09**
$l = 1$	*15.34*		*0.0634*	*0.4293*		*0.4819*		
high-level	0.2943		0.6177	2.0900	-0.5064	0.1443	-0.0137	
$l = 2$	*0.0484*		*0.0634*	*0.2267*	*0.1751*	*0.1186*	*0.0131*	

$\dagger\phi$ is the average of $\phi_t, t = 1, \ldots, 10$ with average standard error.

Appendix 2.3

Figures

Figure 2.1: Trends of new tumour counts using ZMPGP model (Model 3)

(a) Overall trends

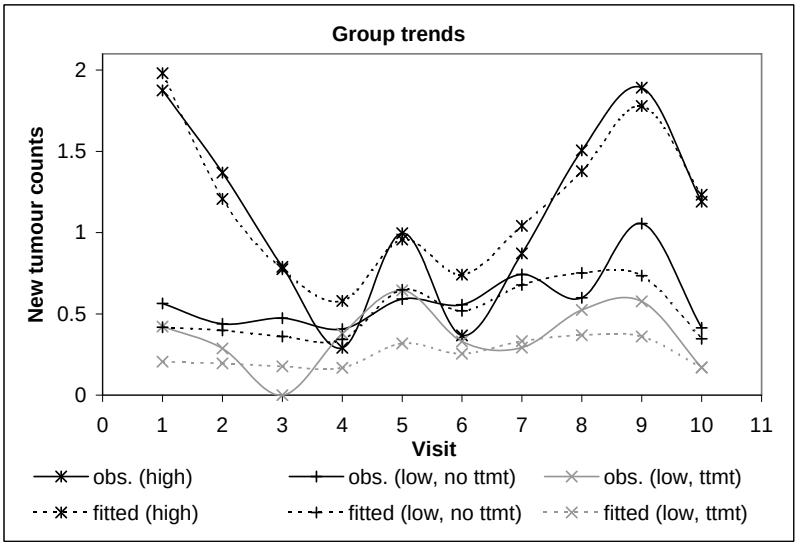

(b) Individual trends

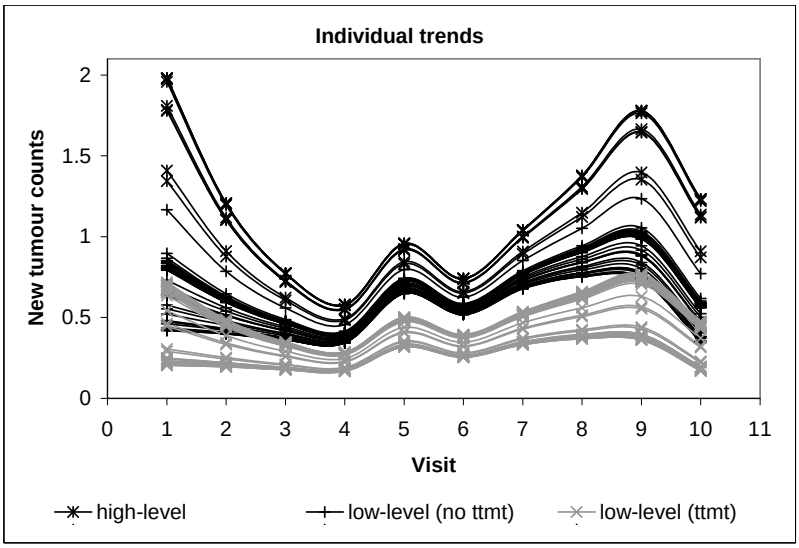

Figure 2.2: Trends of new tumour counts using MPGP-Ga model (Model 4)

(a) Overall trends

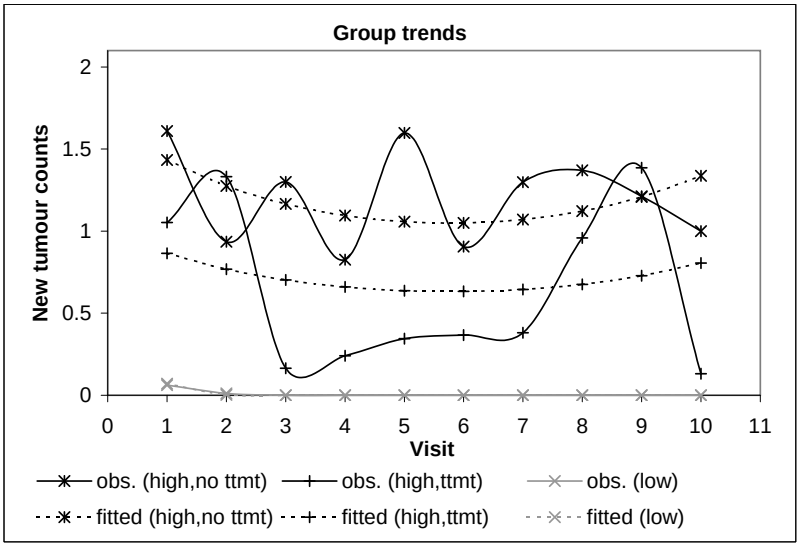

(b) Individual trends

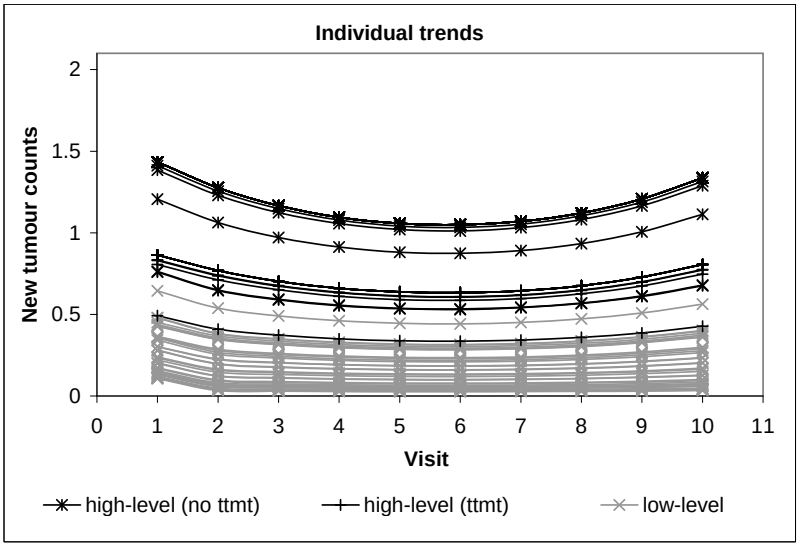

Figure 2.3: Proportions of zeros and variances of new tumour counts for Model 1 to 4

(a) proportions of zeros across time

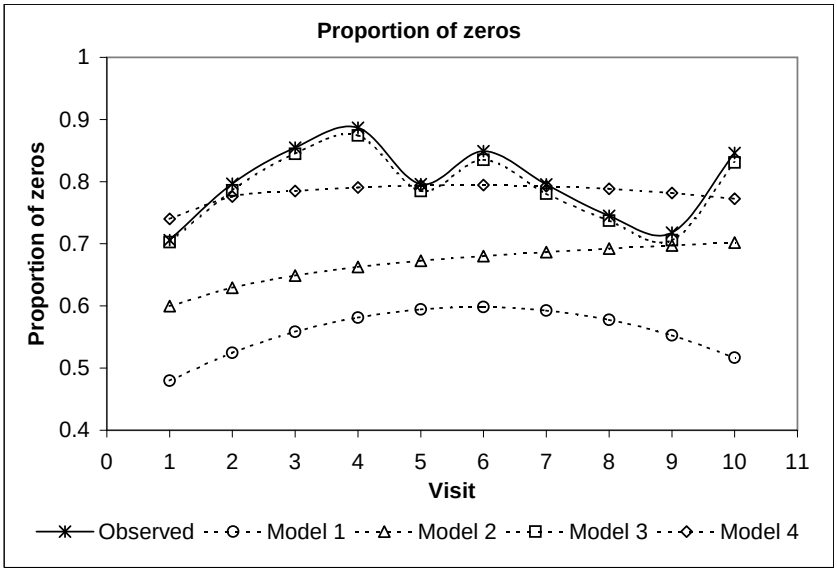

(b) variances across time

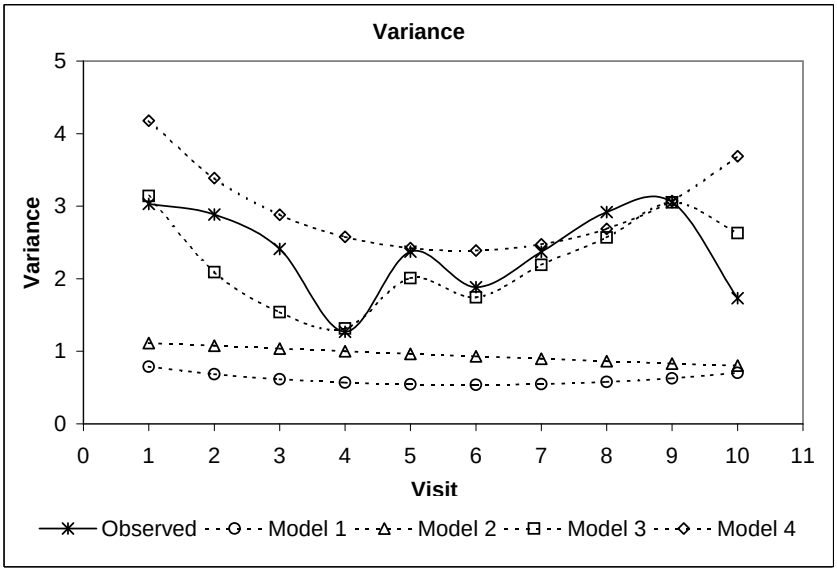

CHAPTER 3

Robust Poisson geometric process model

Continued from the development of PGP models to allow for overdispersion due to zero-inflation by the ZMPGP model in (2.4) and MPGP-Ga model (2.9), this Chapter focuses on accommodating overdispersion due to outlying observations.

3.1. Background

Most time series measured over continuous range assume a normal error distribution. These traditional time series models are however vulnerable to outliers. Outliers in time series have been realized as an influential factor in model fitting and forecasting. Failure to downweigh the outlying effects may lead to a poor model fit, an overestimation of variance, an inappropriate interpretation and an inaccurate prediction. This issue has received a great deal of attention, therefore several approaches have been developed to reduce the influence of outliers and the distributional deviation in the data analysis. In the past, two main approaches have been considered to cope with the overdispersion caused by the outliers. The first approach simply incorporates mixture effects to account for the heterogeneity in the distribution of the data. This can be viewed as a missing data problem assuming that the membership of the data from one of the distributions is unknown

and has to be estimated. The mixture model is usually implemented using expectation-maximization (EM) algorithm or Markov chain Monte Carlo (MCMC) sampling algorithm.

The second approach is to adopt a heavy-tailed distribution instead of the commonly used Gaussian distribution as the error distribution of the data. Some popular choices of heavy-tailed distributions include the Student's t-distribution and a more general class of distributions is the Pearson Type IV distribution (Johnson *et al.*, 1995). Alternatively, the exponential power (EP) distribution which can describe a leptokurtic (positive excess kurtosis) or platykurtic (negative excess kurtosis) shape is another good choice. However, in the context of Bayesian analysis, the implementation of these distributions is troublesome because the marginal posterior distributions of the parameters are difficult to derive using conventional numerical and analytic approximations (Choy & Smith, 1997). To overcome this problem, Box & Tiao (1973) proposed a new exponential power family of normal scale mixtures (SMN) and later Qin *et al.* (1998) pioneered the scale mixtures of uniforms (SMU) which replaces the normal distribution in the SMN form by uniform distribution. Theoretically, any distribution that can be expressed by SMN form, also has a SMU representation.

The hierarchical structure of the SMN or SMU representation possesses two prominent advantages: (1) the resulting density contains a mixing parameter which can accommodate the extra-Poisson variation and help to

identify the extreme values in outlier diagnosis and (2) the parameter estimation can be simplified by sampling from normal or uniform distribution using MCMC algorithms such as Gibbs sampling. The recent emergence of the software `WinBUGS` which performs Bayesian statistical inferences using MCMC algorithms also facilitates the implementation of these representations, thus enhancing their popularity in the context of Bayesian modelling. This hierarchical structure is very practical in insurance applications because it is well known that the normal error distribution falls short of allowing for irregular and extreme claims and hence contaminates the estimation procedure and leads to poor estimation. For instances, Choy & Chan (2003) applied the Student's t- and EP distributions in scale mixtures (SM) representations to predict the insurance premiums to be charged on the policyholders in credibility analysis and Chan *et al.* (2008) predicted and projected the loss reserves data with various heavy-tailed distributions under the generalized-t distribution family expressed in SMU representation.

So far, the techniques of using scale mixtures representation apply solely to continuous time series. Yet, discrete count time series is observed in many occasions especially in a medical context. In clinical trials where the measurements are usually longitudinal, sometimes the appearance of outlying observations may inflate the mean and variance of the data distribution and have an adverse effect on both the parameter estimation and prediction. Despite overdispersion caused by outlying observations, trend, cluster

effect and serial correlation are often detected in longitudinal count time series. Examining the trend patterns is particularly important as it provides useful information on the movement of outcomes over time.

To cope with overdispersion, clustering as well as serial correlation, Thall & Vail (1990) proposed adding subject-specific and time-specific random effects into the mean link function to give extra Poisson-variation to the outcomes. Assume that the outcome W_{it} follows a Poisson distribution, $\boldsymbol{x}_{it}$ and $\boldsymbol{\beta}$ are vectors of time-evolving covariates and regression coefficients, $\{\gamma_i, i = 1, ;m\}$ are positive-valued subject-specific random effects which are independently distributed and $\{u_t, t = 1, \ldots, n\}$ are positive-valued time-specific random effects which are independently and identically distributed. Under the GLMM framework, Thall & Vail (1990) showed that the marginal moments for W_{it} are given by

$$\begin{aligned} E(W_{it}) &= \exp(\boldsymbol{x}_{it}^T\boldsymbol{\beta}E[\ln(\gamma_i u_t)]) \\ Var(W_{it}) &= \exp(\boldsymbol{x}_{it}^T\boldsymbol{\beta}) + \left\{\frac{Var(\gamma_i)}{[E(\gamma_i)]^2} + \frac{Var(u_t)}{[E(u_t)]^2}\right\}[\exp(\boldsymbol{x}_{it}^T\boldsymbol{\beta})]^2 \\ Cov(W_{it}, W_{i,t-k}) &= \frac{Var(\gamma_i)}{[E(\gamma_i)]^2}\exp(\boldsymbol{x}_{it}^T\boldsymbol{\beta})\exp(\boldsymbol{x}_{i,t-k}^T\boldsymbol{\beta}). \end{aligned}$$

However, Jowaheer & Sutradhar (2002) pointed out that the above model is unable to accommodate autocorrelation structures such as the first-order autoregressive (AR(1)) structure. Therefore he considered a Poisson-gamma mixed model to allow for overdispersion and incorporated an autoregressive (AR) structure to the outcome to accommodate serial correlation. His model is essentially a negative binomial model and can be classified as a

OD model as the current outcome depends on past observations. Nevertheless, their models have not put much emphasis on investigating the trend movements and the mixed model approach which assumes the mean of the Poisson distribution follows gamma or log-normal distribution may be inadequate to cast light on the outlying effect caused by the extreme observations. To tackle this pitfall, plenty of studies considered various mixing distributions. Some useful ones include generalized inverse Gaussian, generalized gamma, generalized exponential, inverse gamma, etc. Refer to (Gupta & Ong, 2005) for more details.

In this Chapter, we seek a new direction to model overdispersed longitudinal time series of counts due to the presence of outliers while allowing for non-monotone trends, cluster effect and serial correlation. Our proposed model is an extension of the mixture Poisson geometric process (MPGP) model introduced by Chan *et al.* (2010b) and Wan (2006) and a modification of the MPGP-Ga model in the last Chapter by replacing the gamma distribution with some heavy-tailed distributions in SM representation. The resultant model is named as the robust mixture Poisson geometric process (RMPGP) model. In the RMPGP model, we assume that the outcome variable has a Poisson distribution with a stochastic mean which forms a latent GP, and the mean of the GP after geometrically discounted by the ratio follows a heavy-tailed distribution such as log-t distribution or log-exponential power (log-EP) distribution represented in SMN and SMU forms respectively. Under the SM representation, the model parameters can be simulated

using MCMC algorithms and the mixing parameters help to identify the extreme values in outlier diagnosis. To our knowledge, this is a pioneering work in adopting Student's t- and EP distributions as mixing distributions for time series of counts. Moreover, our proposed GP models have a trend component (ratio function) which enables the study of trend movements and can accommodate cluster effect using a mixture of robust Poisson geometric process (RPGP) models. These make the RPGP models more advantageous than many existing time series models for count data.

To demonstrate the characteristics and application of our models, the rest of the Chapter is presented as follows. First, the development of RPGP and RMPGP models using Student's t- and EP distributions from the PGP model will be described in Section 3.2. Section 3.3 will introduce the SM representation of the two heavy-tailed distributions and their implementation in the RMPGP model. Besides, the hierarchical structure and MCMC algorithms of the models will be given followed by the introduction of the model assessment criterion and a test for serial correlation. Furthermore, Section 3.4 will investigate the properties of the RMPGP models through a simulation study and Section 3.5 will demonstrate an application of the proposed models using the epilepsy data studied by Leppik *et al.* (1985) with discussion. Lastly, a brief summary will be given in Section 3.6.

3.2. Model specification

This Section first introduces the general framework of the RPGP model. Then the proposed model using two commonly used heavy-tailed distributions will be discussed with an examination of the model distributions. After that, the incorporation of mixture effect will be described briefly.

3.2.1. RPGP Model. Let W_{it} denotes the outcome for subject i at time t where $i = 1, \ldots m,\ t = 1, \ldots, n_i$ and $n = \sum_{i=1}^{m} n_i$. Assume that W_{it} follows a Poisson distribution $f_P(w_{it}|x_{it})$ with mean X_{it} which forms a latent GP. Furthermore, the stochastic process $\{Y_{it} = a_{it}^{t-1} X_{it}, t = 1, \ldots, n_i\}$ follows some lifetime distributions $f(y_{it})$, such as exponential distribution in Wan (2006) and gamma distribution in Chapter 2, with mean $E(Y_{it}) = \mu_{it}$, the resultant model is called Poisson geometric process (PGP) model.

Without loss of generality, we assume that the logarithm of Y_{it}, i.e. $Y_{it}^* = \ln Y_{it}$ follows a heavy-tailed distribution $f(y_{it}^*)$ with mean $E(Y_{it}^*) = \mu_{it}^*$. Then, the marginal pmf for W_{it} is

$$\begin{aligned} f(w_{it}) &= \int_0^\infty f_P\left(w_{it} \left| \frac{e^{y_{it}^*}}{a_{it}^{t-1}} \right.\right) f(y_{it}^*)\, dy_{it}^* \\ &= \int_0^\infty \frac{\exp\left(-\frac{e^{y_{it}^*}}{a_{it}^{t-1}}\right)\left(\frac{e^{y_{it}^*}}{a_{it}^{t-1}}\right)^{w_{it}}}{w_{it}!}\, f(y_{it}^*)\, dy_{it}^*. \end{aligned} \tag{3.1}$$

The resultant model is named as the robust Poisson GP (RPGP) model. The RPGP model is essentially a state space model with state variables X_{it} and has time-evolving mean and ratio functions to accommodate exogenous effects and non-monotone trends. The mean function μ_{it}^* which is

identity-linked and ratio function a_{it} which is log-linked to linear functions of covariates are defined as:

$$\mu_{it}^* = \beta_{\mu 0} + \beta_{\mu 1} z_{\mu 1 it} + \cdots + \beta_{\mu q_\mu} z_{\mu q_\mu it} \tag{3.2}$$

$$\ln a_{it} = \beta_{a0} + \beta_{a1} z_{a1it} + \cdots + \beta_{aq_a} z_{aq_a it} \tag{3.3}$$

where $z_{jkit},\ j = \mu, a; k = 1, \ldots, q_j$ are some time-evolving covariates.

By mixing the Poisson distribution with some heavy-tailed distributions, extra variability is added to the Poisson distribution which enables the model to accommodate the inflated variance caused by some extreme observations. In this Chapter, we consider the Student's t- and EP distributions because they have different shapes including heavier-than-normal to normal tails in the former as well as platykurtic shape and leptokurtic shape with a kink in the latter. The various shapes allow the model to be more flexible to capture different kurtoses in the data.

3.2.1.1. *RPGP model with Student's t-distribution.* If Y_{it}^* has a Student's t-distribution with mean μ_{it}^* and variance $\dfrac{\nu}{\nu-2}\sigma^2$, the probability density function of Student's t-distribution $f_T(y_{it}^*)$ is given by

$$f_T(y_{it}^*) = \frac{\Gamma(\frac{\nu+1}{2})}{\sqrt{\nu\pi}\sigma\Gamma(\frac{\nu}{2})}\left[1 + \frac{(y_{it}^* - \mu_{it}^*)^2}{\nu\sigma^2}\right]^{-\frac{(\nu+1)}{2}} \tag{3.4}$$

where μ_{it}^* is given by (3.2) and $\nu > 2$ is the degrees of freedom which controls the tailedness. A small ν gives a heavier tail and Student's t-distribution converges to normal distribution when $\nu \to \infty$. The kurtosis is $\dfrac{6}{\nu-4} + 3$ for $\nu > 4$ which is greater than 3, the kurtosis of the normal distribution.

To study the pmf of the proposed RPGP-t model, we assume $q_\mu = q_a = 1$, $z_{\mu 1} = b = 0, 1$ as the covariate effect and $z_{a1t} = t$ as the time-evolving effect in (3.2) and (3.3). Hence the mean function $\mu_t = \exp(\beta_{\mu 0} + \beta_{\mu 1} b)$ and ratio function $a_t = \exp(\beta_{a0} + \beta_{a1} t)$. Fixing $b = 1$ and $t = 2$, we change the values of one of the scale σ, shape ν or location parameters β_{a0} and $\beta_{\mu 0}$ each time while keeping the other parameters constant and approximate the pmf in (3.1) using Monte Carlo (MC) integration as described below. Conditional on covariate $z_{\mu 1} = b$ and time t, the marginal pmf estimator $\hat{f}_{bt}(w)$, in general, can be obtained by:

$$\hat{f}_{bt}(w) = \sum_{j=1}^{M_s} f_P\left(w \,\middle|\, \frac{e^{\hat{y}_{bt}^{*(j)}}}{a_t^{t-1}}\right) = \sum_{j=1}^{M_s} \frac{\exp\left(-\frac{e^{\hat{y}_{bt}^{*(j)}}}{a_t^{t-1}}\right)\left(\frac{e^{\hat{y}_{bt}^{*(j)}}}{a_t^{t-1}}\right)^w}{w!},\ w = 0, 1, \ldots, \infty;\ \text{and}$$

$$\hat{y}_{bt}^{*(j)} \sim f_T(y_{bt}^{*(j)} |\, \mu_t^*, \sigma, \nu),\ j = 1, \ldots, M_s \tag{3.5}$$

where $M_s = 10000$ is the number of simulations and the latent $\hat{y}_{bt}^{*(j)}$ are simulated from the Student's t-distribution in (3.4) given the parameters μ_{it}^*, σ and ν. Besides examining the mean and variance, we also study the kurtosis of the approximated pmf using the method in Gupta & Ong (2005) for a discrete distribution. The relative long-tailedness of the distribution is defined as $\lim_{w\to\infty} \dfrac{\hat{f}_{bt}(w+1)}{\hat{f}_{bt}(w)}$ where the limit is zero for Poisson distribution. By fixing the parameters at $\nu = 10, \sigma = 0.5, \beta_{\mu 0} = 3.0, \beta_{\mu 1} = -0.2, \beta_{a0} = 0.5$ and $\beta_{a1} = -0.1$ but leaving one floating, the marginal pmfs are displayed in Figures 3.1(a) to 3.1(d) in Appendix 3.3 with their means, variances and kurtoses summarized in Table 3.1 in Appendix 3.2. Note that since different

pmfs are drawn on the same graph for comparison, we use curves instead of bars to represent the marginal pmfs for better visualization.

==========

Figures 3.1(a) to 3.1(d) and Table 3.1 about here

==========

Results from Figures 3.1(a) to 3.1(d) reveal that in general the location, variability and tailedness of the marginal pmf depend on parameters $\boldsymbol{\beta}_{jk}, j = \mu, a; k = 0, 1$, in which a larger $\beta_{\mu 0}$ and a smaller β_{a0} lead to larger mean, variance and kurtosis. Whereas, ν and σ control the spread and the tail behaviour of the distribution without altering its mean. A smaller ν and a larger σ contribute to a larger variability and a heavier tail and thus the model can accommodate the outlying effect due to extreme values while keeping the mean unchanged. Since the variance of each distribution in Table 3.1 is substantially larger than the mean, the RPGP-t model is capable of fitting data with overdispersion due to outliers as well as data with equidispersion when σ is small.

3.2.1.2. *RPGP model with EP distribution.* If Y_{it}^* has an exponential power (EP) distribution, also known as generalized error distribution, with mean μ_{it}^* and variance σ^2, it has a probability density function

$$f_{EP}(y_{it}^*) = \frac{c_1}{\sigma} \exp\left[-\left| \frac{c_0^{1/2}(y_{it}^* - \mu_{it}^*)}{\sigma} \right|^{2/\nu} \right] \tag{3.6}$$

where $c_0 = \dfrac{\Gamma(3\nu/2)}{\Gamma(\nu/2)}$, $c_1 = \dfrac{c_0^{1/2}}{(\nu\Gamma(\nu/2))}$ and $\nu \in (0, 2]$ is a shape parameter which controls the kurtosis. This family subsumes a range of symmetric

distributions such as uniform ($\nu \to 0$) with kurtosis equal to 1.8, normal ($\nu = 1$) with kurtosis equal to 3 and double exponential ($\nu = 2$) with a kurtosis of 6. Its tails can be more platykurtic when $\nu < 1$ or more leptokurtic when $\nu > 1$ compared with the normal tail ($\nu = 1$).

By fixing the parameters at $\nu = 1, \sigma = 0.5, \beta_{\mu 0} = 3.0, \beta_{\mu 1} = -0.5, \beta_{a0} = 0.5$ and $\beta_{a1} = -0.1$ but leaving one floating, the marginal pmfs are again approximated using MC integration specified in (3.5) but replacing $f_T(y_{bt}^{*(j)} | \, \mu_t^*, \sigma, \nu)$ with $f_{EP}(y_{bt}^{*(j)} | \, \mu_t^*, \sigma, \nu)$ in (3.6). The effects of different parameters on the resulting pmfs are illustrated in Table 3.2 in Appendix 3.2 and Figures 3.2(a) to 3.2(d) in Appendix 3.3. Clearly, the tail of the distribution depends on all the parameters and the behaviours of the parameters σ, $\beta_{\mu 0}$ and β_{a0} on the resultant pmf are quite close to that of RPGP-t model. However, comparing Figure 3.2(a) with Figure 3.1(a), the shape parameter ν in the RPGP-EP model allows a wider range of shapes than that of the RPGP-t model as the EP distribution includes both leptokurtic and platykurtic shapes. Hence the RPGP-EP model can accommodate different degrees of tailedness due to moderate to adverse outlying effects.

==========

Figures 3.2(a) to 3.2(d) and Table 3.2 about here

==========

3.2.2. Incorporation of mixture effects. Overdispersion may arise due to cluster effect, hence an alternative way to tackle overdispersion is to add mixture effects into the mean and ratio functions. Suppose that there are G

groups of subjects who have different trend patterns and each subject has a probability π_l of coming from group $l, l = 1, \ldots, G$. Conditional on group l, the marginal pmf for W_{it} is given by:

$$f_{Dl}(w_{it}) = \int_{-\infty}^{\infty} \frac{\exp\left(-\frac{e^{y^*_{itl}}}{a_{itl}^{t-1}}\right)\left(\frac{e^{y^*_{itl}}}{a_{itl}^{t-1}}\right)^{w_{it}}}{w_{it}!} f_D(y^*_{itl})\, dy^*_{itl} \qquad (3.7)$$

where $D = T, EP$ denotes the Student's t- and EP distributions respectively and the group-specific mean μ_{itl} and ratio a_{itl} functions become

$$\mu^*_{itl} = \beta_{\mu 0l} + \beta_{\mu 1l} z_{\mu 1it} + \cdots + \beta_{\mu q_\mu l} z_{\mu q_\mu it}, \text{ and} \qquad (3.8)$$

$$\ln a_{itl} = \beta_{a0l} + \beta_{a1l} z_{a1it} + \cdots + \beta_{aq_a l} z_{aq_a it} \qquad (3.9)$$

respectively. The resultant model is named as robust mixture Poisson geometric process (RMPGP) model in which $f_D(y^*_{itl})$ is given by $f_T(y^*_{itl})$ in (3.4) or $f_{EP}(y^*_{itl})$ in (3.6) for the RMPGP-t or RMPGP-EP model. To illustrate the distribution of a 2-group RMPGP-EP model, its pmf ($\pi_1 f_1(w_{it}) + (1-\pi_1) f_2(w_{it})$) where $f_l(w_{it}), l = 1, 2$ is given by (3.7) is plotted in Figure 3.3 by assuming $G = 2, q_\mu = q_a = 1$, $t = 1$, $z_{\mu 1i} = 1$ and $z_{a1it} = t$. For $l = 1$, we set $\pi_1 = 0.8, \beta_{a01} = -0.1, \beta_{a11} = 0.05, \beta_{\mu 01} = 3, \beta_{\mu 11} = -0.2, \nu_1 = 0.2$ and $\sigma_1 = 0.2$ while for $l = 2$, we use $\beta_{a02} = 0.1, \beta_{a12} = -0.01, \beta_{\mu 02} = 5, \beta_{\mu 12} = -0.4, \nu_2 = 1.9$ and $\sigma_2 = 0.01$. Figure 3.3 clearly displays the two distinct modes in the distribution with a larger mode ($l = 1$) at smaller values of W and a smaller one ($l = 2$) at larger values of W representing the outliers. This explains how the incorporation of mixture effects

in the RMPGP-EP model can accommodate overdispersion due to cluster effects.

==========

Figure 3.3 about here

==========

3.3. Bayesian inference

Performing statistical inference using classical methods like maximum likelihood approach is cumbersome when the data distribution has no closed-form because the likelihood function involving high-dimensional integration is intractable. To avoid such numerical difficulties, we use a Bayesian approach via MCMC algorithms to convert the optimization problem to a sampling problem. Since the non-conjugate structure in the posterior distribution for both RMPGP models and the absolute term in the density function of the EP distribution complicate the sampling algorithms, representing the heavy-tailed distributions in a scale mixtures form produces a simpler set of full conditional posterior distributions for the parameters and alleviates the computational burden of the Gibbs sampler in the MCMC algorithms.

3.3.1. Scale mixtures representation of heavy-tailed distributions.

Choy & Smith (1997) has shown that Student's t- and EP distributions can be expressed in scale mixtures representation to facilitate the simulation in the MCMC algorithms via a Bayesian hierarchical structure. However, the

ways they handle outliers are different. Choy & Walker (2003) revealed that the former downweighs the extreme values, whereas the latter merely downweighs or bounds the influence of the outliers. Thus, it will be interesting to study their performances in outlier diagnosis. In the following, the Student's t-distribution expressed in SMN form and the EP distribution represented in SMU form will be discussed in detail.

3.3.1.1. *Student's t-distribution in SMN representation.* Assume that a continuous random variable Y has a Student's t-distribution $f_T(y)$ with location μ, scale σ^2 and degrees of freedom ν. The probability density function of Y is said to have a SMN representation if it can be expressed as

$$f_T(y|\,\mu,\sigma,\nu) = \int_0^\infty f_N\Big(y\,\Big|\,\mu,\frac{\sigma^2}{u}\Big)\, f_G\Big(u\,\Big|\frac{\nu}{2},\frac{\nu}{2}\Big)\,du \tag{3.10}$$

where $f_N(\cdot|\,c,d)$ represents a normal distribution with mean c and variance d, $f_G(\cdot|\,c,d)$ refers to a gamma distribution with mean $\frac{c}{d}$ and variance $\frac{c}{d^2}$, ν is a shape parameter and u is a mixing parameter which can be used to identify outlier. An outlier is indicated if u is substantially small since small value implies that the normal distribution in (3.10) has an inflated variance. When the variance $\frac{\sigma^2}{u}$ is inflated by a small u, the effect of the outlier on the parameter σ^2 will be downweighed.

Substituting the SMN form in (3.10) for (3.4) in the RMPGP-t model, the marginal pmf for W_{it} in (3.7), conditional on group l, becomes:

$$\int_{-\infty}^{\infty} \frac{\exp\left(-\frac{e^{y^*_{itl}}}{a^{t-1}_{itl}}\right)\left(\frac{e^{y^*_{itl}}}{a^{t-1}_{itl}}\right)^{w_{it}}}{w_{it}!} \int_0^\infty f_N\Big(y^*_{itl}\,\Big|\,\mu^*_{itl},\frac{\sigma^2_l}{u_{itl}}\Big)\, f_G\Big(u_{itl}\,\Big|\frac{\nu_l}{2},\frac{\nu_l}{2}\Big)\,du_{itl}\,dy^*_{itl}.$$

3.3.1.2. *Exponential power distribution in SMU representation.* Theoretically, any distribution that can be expressed in SMN form, also has a SMU representation (Qin *et al.*, 1998). To simplify the implementation of the MCMC sampling algorithm, Walker & Gutiérrez-Peña (1999) first proposed to express the EP distribution in SMU representation. In a slightly different form, Chan *et al.* (2008) wrote the EP distribution in SMU form as follows:

$$f_{EP}(y|\,\mu,\sigma) = \int_0^\infty f_U\big(y|\,\mu-\sigma u^{\nu/2},\mu+\sigma u^{\nu/2}\big)\, f_G\bigg(u\,\bigg|\,1+\frac{\nu}{2},\frac{1}{2}\bigg)\,du \quad (3.11)$$

where $f_U(\cdot|\,c,d)$ is a uniform distribution on the interval $[c,d]$ and again u is a mixing parameter. Different from the Student's t-distribution, the larger the u, the wider is the range of the uniform distribution to accommodate a possible outlier.

In the RMPGP-EP model, if we replace (3.6) with (3.11), the marginal pmf for W_{it} in (3.7), conditional on group l becomes:

$$\int_{-\infty}^{\infty} \frac{\exp\left(-\frac{e^{y^*_{itl}}}{a_{itl}^{t-1}}\right)\left(\frac{e^{y^*_{itl}}}{a_{itl}^{t-1}}\right)^{w_{it}}}{w_{it}!} \int_0^\infty f_U\Big(\mu^*_{itl}-\sigma_l u_{itl}^{\nu_l/2},\mu^*_{itl}+\sigma_l u_{itl}^{\nu_l/2}\Big)\, f_G\bigg(u_{itl}\,\bigg|\,1+\frac{\nu_l}{2},\frac{1}{2}\bigg)\,du_{itl}\,dy^*_{itl}. \quad (3.12)$$

3.3.2. MCMC algorithms. `WinBUGS` described in Section 1.4.3 is used to implement the MCMC algorithms. For the RMPGP-t and RMPGP-EP models, the hierarchical structure under the Bayesian framework is outlined as follows:

$$w_{it} \sim I_{i1} f_P\left(\frac{e^{y^*_{it1}}}{a^{t-1}_{it1}}\right) + \cdots + I_{iG} f_P\left(\frac{e^{y^*_{itG}}}{a^{t-1}_{itG}}\right)$$

$$y^*_{itl} \sim \begin{cases} f_N\left(\mu^*_{itl}, \frac{\sigma^2_l}{u_{itl}}\right) \text{ and } u_{itl} \sim f_G\left(\frac{\nu_l}{2}, \frac{\nu_l}{2}\right), & \text{for RMPGP-t model} \\ f_U\left(\mu^*_{itl} - \sigma_l u^{\nu_l/2}_{itl}, \mu^*_{itl} + \sigma_l u^{\nu_l/2}_{itl}\right) \text{ and } u_{itl} \sim f_G\left(1 + \frac{\nu_l}{2}, \frac{1}{2}\right), & \text{for RMPGP-EP model} \end{cases}$$

where μ^*_{itl} and a_{itl} are given by (3.8) and (3.9) and I_{il} is the group membership indicator for subject i such that $I_{il} = 1$ if he/she comes from group l and zero otherwise. In order to construct the posterior density, some prior distributions are assigned to the model parameters as follows:

$$\begin{aligned} \beta_{jkl} &\sim N(0, \tau^2_{jkl}), \qquad (3.13) \\ &\qquad j = \mu, a;\ k = 0, 1, \ldots, q_j;\ l = 1, \ldots, G \\ \sigma^2_l &\sim IG(c_l, d_l) \qquad (3.14) \end{aligned}$$

$$\nu_l \sim \begin{cases} \text{Uniform}(0.01, e_l), & \text{for RMPGP-t model} \\ \text{Uniform}(0, 2), & \text{for RMPGP-EP model} \end{cases} \qquad (3.15)$$

$$\begin{aligned} (I_{i1}, \ldots, I_{iG})^T &\sim \text{Multinomial}(1, \pi_1, \ldots, \pi_G) \qquad (3.16) \\ (\pi_1, \ldots, \pi_G)^T &\sim Dir(\alpha_1, \ldots, \alpha_G) \qquad (3.17) \end{aligned}$$

where c_l, d_l, e_l are some positive constants, $IG(c_l, d_l)$ denotes the inverse gamma distribution with density given by

$$f_{IG}(x|\, c_l, d_l) = \frac{d_l^{c_l}}{\Gamma(c_l)}\, x^{-(c_l+1)} \exp\left(-\frac{d_l}{x}\right)$$

and $Dir(\boldsymbol{\alpha})$ represents a Dirichlet distribution, a conjugate to multinomial distribution, with parameters $\boldsymbol{\alpha} = (\alpha_1, \ldots, \alpha_G)$ where α_l is set to be $1/G$.

In case of a 2-group ($G = 2$) mixture model, (3.16) can be simplified to $I_{i1} \sim$ Bernoulli(π_1), $I_{i2} = 1 - I_{i1}$ and (3.17) becomes a uniform prior Uniform$(0, 1)$ for π_1 with $\pi_2 = 1 - \pi_1$. With the posterior means $\bar{I}_{il}$ of the group membership indicators I_{il}, patient i is classified to group l' if $\bar{I}_{il'} = \max_l \bar{I}_{il}$.

According to Bayes' theorem, the posterior density is proportional to the joint densities of complete data likelihood and prior distributions. For the RMPGP-t and RMPGP-EP models, the complete data likelihood functions $L_T(\boldsymbol{\theta})$ and $L_{EP}(\boldsymbol{\theta})$ for the observed data w_{it} and missing data $\{y^*_{itl}, u_{itl}, I_{il}\}$ are:

$$L_T(\boldsymbol{\theta}) = \prod_{i=1}^{m}\prod_{l=1}^{G}\left[\pi_l \prod_{t=1}^{n_i} f_P(w_{it}|\,\boldsymbol{\beta}_{al}, y^*_{itl}) f_N(y^*_{itl}|\,\boldsymbol{\beta}_{\mu l}, \sigma_l, u_{itl}) f_G(u_{itl}|\,\nu_l)\right]^{I_{il}} \text{ and}$$

$$L_{EP}(\boldsymbol{\theta}) = \prod_{i=1}^{m}\prod_{l=1}^{G}\left[\pi_l \prod_{t=1}^{n_i} f_P(w_{it}|\,\boldsymbol{\beta}_{al}, y^*_{itl}) f_U(y^*_{itl}|\,\boldsymbol{\beta}_{\mu l}, \sigma_l, \nu_l, u_{itl}) f_G(u_{itl}|\,\nu_l)\right]^{I_{il}}. \quad (3.18)$$

The vector of model parameters $\boldsymbol{\theta} = (\boldsymbol{\beta}^T, \boldsymbol{\sigma}^T, \boldsymbol{\nu}^T, \boldsymbol{\pi}^T)^T$ where $\boldsymbol{\beta} = (\boldsymbol{\beta}^T_{\mu 1}, ..., \boldsymbol{\beta}^T_{\mu G}, \boldsymbol{\beta}^T_{a1}, ..., \boldsymbol{\beta}^T_{aG})^T = (\beta_{\mu 01}, ..., \beta_{\mu q_\mu G}, \beta_{a01}, ..., \beta_{a q_a G})^T$, $\boldsymbol{\sigma} = (\sigma_1, ..., \sigma_G)^T$, $\boldsymbol{\nu} = (\nu_1, ..., \nu_G)^T$ and $\boldsymbol{\pi} = (\pi_1, ..., \pi_G)^T$.

Treating $\{y^*_{itl}, u_{itl}, I_{il}\}$ as missing observations, the joint posterior density of the RMPGP-EP model is expressed as follows:

$$f(\boldsymbol{\beta}, \boldsymbol{\sigma}, \boldsymbol{\nu}, \boldsymbol{\pi}|\,\boldsymbol{w}, \boldsymbol{I}, \boldsymbol{y}^*, \boldsymbol{u}) \propto L_{EP}(\boldsymbol{\theta}) \left(\prod_{j=\mu,a}\prod_{k=0}^{q_j}\prod_{l=1}^{G} f_N(\beta_{jkl}|\,0, \tau^2_{jkl})\right)\left(\prod_{l=1}^{G} f_{IG}(\sigma^2_l|\,c_l, d_l)\right)$$
$$\left(\prod_{l=1}^{G} f_U(\nu_l|\,0, 2)\right) f_{Dir}(\boldsymbol{\pi}|\,\boldsymbol{\alpha})$$

where $\boldsymbol{w} = (w_{11}, w_{12}, ..., w_{mn_m})^T$, $\boldsymbol{I} = (I_{11}, I_{12}, ..., I_{mG})^T$, $\boldsymbol{y}^* = (y^*_{111}, y^*_{121}, ..., y^*_{mn_mG})^T$ and $\boldsymbol{u} = (u_{111}, u_{121}, ..., u_{mn_mG})^T$. The complete data likelihood $L_{EP}(\boldsymbol{\theta})$ of the RMPGP-EP model is given by (3.18) and the priors are given by (3.13)-(3.17). In Gibbs sampling, the unknown parameters are simulated iteratively from their univariate conditional posterior distributions which are proportional to the joint posterior density of complete data likelihood and prior densities.

The univariate full conditional posterior densities for each of the unknown model parameters in $\boldsymbol{\theta}$ and missing observations in $\{\boldsymbol{y}^*, \boldsymbol{u}, \boldsymbol{I}\}$ are given by:

$$f(\beta_{\mu kl}|\, \boldsymbol{w}, \boldsymbol{I}, \boldsymbol{y}^*, \boldsymbol{u}, \boldsymbol{\beta}^-, \boldsymbol{\sigma}, \boldsymbol{\nu}, \boldsymbol{\pi}) \;\propto\; \exp\left(-\frac{\beta^2_{\mu kl}}{2\tau^2_{\mu kl}}\right) \text{ restricted to}$$

$$\beta_{\mu kl} \in \left[z^{-1}_{\mu kit} \max_{i,\,t}(y^*_{itl} - \sigma_l u^{\nu_l/2}_{itl} - \sum_{\kappa \neq k} \beta_{\mu\kappa l} z_{\mu\kappa it}),\; z^{-1}_{\mu kit} \min_{i,\,t}(y^*_{itl} + \sigma_l u^{\nu_l/2}_{itl} - \sum_{\kappa \neq k} \beta_{\mu\kappa l} z_{\mu\kappa it}) \right],$$

if $z_{\mu kit} \neq 0$

$$f(\beta_{akl}|\, \boldsymbol{w}, \boldsymbol{I}, \boldsymbol{y}^*, \boldsymbol{u}, \boldsymbol{\beta}^-, \boldsymbol{\sigma}, \boldsymbol{\nu}, \boldsymbol{\pi}) \propto \exp\left\{ -\sum_{i=1}^{m} I_{il} \sum_{t=1}^{n_i} \left[\frac{e^{y^*_{itl}}}{a^{t-1}_{itl}} + \beta_{akl} z_{akit}(t-1) w_{it} \right] - \frac{\beta^2_{akl}}{2\tau^2_{akl}} \right\}$$

$$f(y^*_{itl}|\, \boldsymbol{w}, \boldsymbol{I}, \boldsymbol{y}^{*-}, \boldsymbol{u}, \boldsymbol{\beta}, \boldsymbol{\sigma}, \boldsymbol{\nu}, \boldsymbol{\pi}) \;\propto\; \exp\left(-\frac{e^{y^*_{itl}}}{a^{t-1}_{itl}} + y^*_{itl} w_{it}\right)$$

restricted to $y^*_{itl} \in (\mu^*_{itl} - \sigma_l u^{\nu_l/2}_{itl},\; \mu^*_{itl} + \sigma_l u^{\nu_l/2}_{itl})$

$$f(\sigma^2_l|\, \boldsymbol{w}, \boldsymbol{I}, \boldsymbol{y}^*, \boldsymbol{u}, \boldsymbol{\beta}, \boldsymbol{\sigma}^-, \boldsymbol{\nu}, \boldsymbol{\pi}) \;\propto\; \sigma_l^{-(\sum_{i=1}^{m} n_i I_{il} + 2c_l + 2)} \exp\left(-\frac{d_l}{\sigma^2_l}\right)$$

restricted to $\sigma^2_l > \max_{i,\,t}\left[\frac{(y^*_{itl} - \mu^*_{itl})^2}{u^{\nu_l}_{itl}}\right]$

$$f(u_{itl}|\, \boldsymbol{w}, \boldsymbol{I}, \boldsymbol{y}^*, \boldsymbol{u}^-, \boldsymbol{\beta}, \boldsymbol{\sigma}, \boldsymbol{\nu}, \boldsymbol{\pi}) \;\propto\; \exp\left(-\frac{u_{itl}}{2}\right) \text{ restricted to } u_{itl} > \left(\frac{y^*_{itl} - \mu^*_{itl}}{\sigma_l}\right)^{2/\nu_l}$$

$$
\begin{aligned}
f(\nu_l|\,\boldsymbol{w},\boldsymbol{I},\boldsymbol{y}^*,\boldsymbol{u},\boldsymbol{\beta},\boldsymbol{\sigma},\boldsymbol{\nu}^-,\boldsymbol{\pi}) &\propto \left[\Gamma\left(\frac{\nu_l}{2}+1\right)2^{\frac{\nu_l}{2}}\right]^{-\sum_{i=1}^{m} n_i I_{il}} \\
&\quad \text{restricted to } \nu_l > \max_{i,t} \frac{\ln\left(\frac{y^*_{itl}-\mu^*_{itl}}{\sigma_l}\right)^2}{\ln u_{itl}} \\
f(\boldsymbol{I}_i|\,\boldsymbol{w},\boldsymbol{I}^-,\boldsymbol{y}^*,\boldsymbol{u},\boldsymbol{\beta},\boldsymbol{\sigma},\boldsymbol{\nu},\boldsymbol{\pi}) &\propto \prod_{l=1}^{G}\left\{\frac{\pi_l \prod_{t=1}^{n_i} \frac{\exp\left(-\frac{e^{y^*_{itl}}}{a_{itl}^{t-1}}-\frac{u_{itl}}{2}\right)\left(\frac{e^{y^*_{itl}}}{a_{itl}^{t-1}}\right)^{w_{it}}}{\sigma_l\Gamma(\frac{\nu_l}{2}+1)2^{\frac{\nu_l}{2}}}}{\sum_{l'=1}^{G}\left[\pi_{l'}\prod_{t=1}^{n_i}\frac{\exp\left(-\frac{e^{y^*_{itl'}}}{a_{itl'}^{t-1}}-\frac{u_{itl'}}{2}\right)\left(\frac{e^{y^*_{itl'}}}{a_{itl'}^{t-1}}\right)^{w_{it}}}{\sigma_{l'}\Gamma(\frac{\nu_{l'}}{2}+1)2^{\frac{\nu_{l'}}{2}}}\right]}\right\}^{I_{il}} \\
&= \prod_{i=1}^{G}\pi_{il}'^{I_{il}} = \text{Multinomial}(1,\pi'_{i1},\ldots,\pi'_{iG}) \\
f(\pi_l|\,\boldsymbol{w},\boldsymbol{I},\boldsymbol{y}^*,\boldsymbol{u},\boldsymbol{\beta},\boldsymbol{\sigma},\boldsymbol{\nu},\boldsymbol{\pi}^-) &\propto \pi_l^{\sum_{i=1}^{m} I_{il}+\alpha_l-1}
\end{aligned}
$$

where $\boldsymbol{\beta}^-, \boldsymbol{y}^{*-}, \boldsymbol{u}^-, \boldsymbol{\sigma}^-, \boldsymbol{\nu}^-, \boldsymbol{\pi}^-$ and $\boldsymbol{I}^-$ and are vectors of $\boldsymbol{\beta}, \boldsymbol{y}^*, \boldsymbol{u}, \boldsymbol{\sigma}, \boldsymbol{\nu}, \boldsymbol{\pi}$ and $\boldsymbol{I}$ excluding $\beta_{jkl}, y^*_{itl}, u_{itl}, \sigma_l, \nu_l, \pi_l$ and $\boldsymbol{I}_i = (I_{i1},\ldots,I_{iG})^T$ respectively. The MCMC algorithms can be derived for the RMPGP-t model in a similar way. Nevertheless, the MCMC algorithms are implemented using the user-friendly software `WinBUGS` where the sampling scheme based on the conditional posterior densities is outlined in this Section and the Gibbs sampling procedures are described in Section 1.4.3.

3.3.3. Model selection criterion. For the simulation experiment in Section 3.4 and data analysis in Section 3.5, we adopt the deviance information criterion (DIC), originated by Spiegelhalter *et al.* (2002), as the model selection criterion. Deviance information criterion (DIC) is a sum of the posterior mean deviance $\overline{D(\boldsymbol{\theta})}$ measuring the model fit and the effective

dimension p_D which accounts for the model complexity. For the RMPGP model, the DIC is defined as

$$
\begin{aligned}
DIC &= \overline{D(\boldsymbol{\theta})} + p_D \\
&= -\frac{4}{M}\sum_{j=1}^{M}\sum_{i=1}^{m}\sum_{l=1}^{G} I_{il}^{'(j)}\left[\ln \pi_l^{(j)} + \sum_{t=1}^{n_i}\ln\left\{f_P(w_{it}|\, y_{itl}^{*(j)}, \boldsymbol{\beta}_{al}^{(j)}) f_D(y_{itl}^{*(j)}|\, \boldsymbol{\beta}_{\mu l}^{(j)}, \sigma_l^{(j)}, \nu_l^{(j)})\right\}\right] \\
&\quad +2\sum_{i=1}^{m}\sum_{l=1}^{G} \bar{I}_{il}'\left[\ln \bar{\pi}_l + \sum_{t=1}^{n_i}\ln\left\{f_P(w_{it}|\, \bar{y}_{itl}^{*}, \bar{\boldsymbol{\beta}}_{al}) f_D(\bar{y}_{itl}^{*}|\, \bar{\boldsymbol{\beta}}_{\mu l}, \bar{\sigma}_l, \bar{\nu}_l)\right\}\right] \qquad (3.19)
\end{aligned}
$$

where M is the number of realizations in the MCMC sampling algorithms, $f_D(\cdot), D = T$ or EP are densities given by (3.4) and (3.6) for the RMPGP-t and RMPGP-EP models respectively, $\boldsymbol{\beta}_{al} = (\beta_{a0l}, ..., \beta_{aq_al})^T$, $\boldsymbol{\beta}_{\mu l} = (\beta_{\mu 0l}, ..., \beta_{\mu q_\mu l})^T$, and $\theta^{(j)}$ and $\bar{\theta}$ represent the j^{th} posterior sample and posterior mean of parameter θ respectively,

$$
I_{il}^{'(j)} = \frac{\pi_l^{(j)}\prod_{t=1}^{n_i}\left\{f_P(w_{it}|\, y_{itl}^{*(j)}, \boldsymbol{\beta}_{al}^{(j)}) f_D(y_{itl}^{*(j)}|\, \boldsymbol{\beta}_{\mu l}^{(j)}, \sigma_l^{(j)}, \nu_l^{(j)})\right\}}{\sum_{l'=1}^{G}\pi_{l'}^{(j)}\prod_{t=1}^{n_i}\left\{f_P(w_{it}|\, y_{itl'}^{*(j)}, \boldsymbol{\beta}_{al'}^{(j)}) f_D(y_{itl'}^{*(j)}|\, \boldsymbol{\beta}_{\mu l'}^{(j)}, \sigma_{l'}^{(j)}, \nu_{l'}^{(j)})\right\}},
$$

and $\bar{I}_{il}'$ is defined in a similar way by replacing $y_{itl}^{*(j)}$ and $\boldsymbol{\theta}^{(j)}$ with $\bar{y}_{itl}^{*}$ and $\bar{\boldsymbol{\theta}}$. The rule of thumb is that the smaller the DIC, the better is the model.

3.3.4. Test for serial correlation. Parameter interpretation and prediction are made based on the best model. After investigating the trend, cluster and covariate effects, the remaining unexplained variation is used to test for serial correlation. In order to calculate the Pearson's residuals, the marginal mean and variance of the outcome W_{it} are needed. Denote the conditional mean and variance on the group being analyzed by $E_l(W_{it})$ and $Var_l(W_{it})$

respectively which are estimated using the approximated pmfs from the MC integration in (3.5) with the group-specific model parameters, the marginal predicted mean $\widehat{E}(W_{it})$ and variance $\widehat{V}ar(W_{it})$ are given by

$$\begin{aligned}\widehat{E}(W_{it}) &= \sum_{l=1}^{G} \bar{I}_{il} E_l(W_{it}) \\ \widehat{V}ar(W_{it}) &= \sum_{l=1}^{G} \bar{I}_{il} \left[Var_l(W_{it}) + E_l(W_{it})\right] - \left[\sum_{l=1}^{G} \bar{I}_{il} E_l(W_{it})\right]^2\end{aligned}$$

where $\bar{I}_{il}$ is the posterior mean of the group l membership indicator I_{il} for subject i. The Pearson residual is then defined as

$$\epsilon_{it} = \frac{w_{it} - \widehat{E}(W_{it})}{\sqrt{\widehat{V}ar(W_{it})}}.$$

The test statistic T_L under the null hypothesis that the Pearson residuals are not autocorrelated up to lag L is given by

$$T_L = \sum_{k=1}^{L} \sum_{i=1}^{m} n_i \left(\frac{\sum_{t=k+1}^{n_i} \epsilon_{it}\epsilon_{i,t-k}}{\sum_{t=1}^{n_i} \epsilon_{it}^2} \right)^2$$

and is asymptotically distributed as chi-square $\chi^2(mL)$ with degrees of freedom mL. See Brännäs & Johansson (1996) for more details.

If significant serial correlation is detected up to lag L, an appropriate autocorrelation structure is introduced in the model. To accomplish the autocorrelation, a L-order autoregressive structure (AR(L)) structure will be introduced to the model by adding L autoregressive (AR) terms $(W_{t-1}, \ldots, W_{t-L})$ as covariates into the mean function μ^*_{itl} in (3.8) and the chosen model will be refitted. The performance of the resultant model will

be evaluated based on the significance of the model parameters in the AR structure and the model selection criterion DIC .

3.4. Simulation study

To investigate the properties of the RPGP-t and RPGP-EP models, we conducted a simulation study in which $h = 100$ data sets are simulated from each of the RPGP models based on a set of true parameters. For simplicity, we set $G = 1$, $q_\mu = q_a = 1$ and each data set contains $m = 80$ time series of length $n_i = 8$ from $m_0 = 40$ subjects in the control group ($b = 0$) and another $m_1 = 40$ subjects in the treatment group ($b = 1$) with $z_{\mu 1it} = b$ in the mean function in (3.2). The degrees of freedom ν is set to include heavy ($\nu = 2.5$) and light ($\nu = 50$) tails for Student's t-distribution and platykurtic ($\nu = 0.1$) and leptokurtic ($\nu = 1.8$) shapes for EP distribution. The parameter β_{a1} in the ratio function in (3.3) with $z_{a1it} = t$ is also set to include different trend patterns by varying the sign and magnitude of the true value.

Afterwards both models are fitted to each data set using the Bayesian approach implemented by `WinBUGS` and `R2WinBUGS` which are described in Section 1.4.3. For the hyperparameters in the prior distributions (dropping the subscript 'l' since $G = 1$), we assign $\tau_{jk}^2 = 1000$ in (3.13), $c = d = 0.01$ in (3.14) and $e = 150$ in (3.15). The parameter estimate $\hat{\theta}$ is given by the average of $h = 100$ posterior medians $\hat{\theta}_j$. To examine the precision of the MCMC algorithms, the standard deviation (SD) of $\hat{\theta}_j$ over $h = 100$ simulated data sets for each parameter θ is reported. In addition, to assess the

accuracy of parameter estimates when the data set is simulated and fitted to the same model, we calculate the mean squared error (MSE) for each parameter θ which is defined as:

$$MSE = \frac{1}{h}\sum_{j=1}^{h}(\hat{\theta}_j - \theta)^2.$$

For model selection, the average DIC and average squared error (ASE) proposed by Wegman (1972) are used to assess the quality of the density estimator on the true pmf. Denote the true pmf of the RMPGP model by $f_{bt}(w)$ at time t with covariate b, the ASE is used to compare the performance of the two models fitted to the same simulated data set and is defined as

$$ASE = \sum_{b=0,1}\psi_b\sum_{t=1}^{n_i}\sum_{j=1}^{h}\sum_{w=0}^{\infty}\left\{\hat{f}_{bt}^{(j)}(w) - f_{bt}(w)\right\}^2$$

where $\hat{f}_{bt}^{(j)}(w)$ is the pmf estimator of (3.1) using MC integration described in (3.5) for counts w in the j^{th} simulated set at time t with treatment effect b and $\psi_b = \dfrac{m_b}{m}$ is the weight associated with the control ($b = 0$) or treatment group ($b = 1$). Clearly, the smaller the ASE, the closer is the estimated pmf to the true one and thus the better is the model performance.

Table 3.3 in Appendix 3.2 summarizes the results of the four sets of simulation experiments with the first two data sets simulated from the RPGP-t model and the next two simulated from the RPGP-EP model. In general, the MCMC algorithms give unbiased and precise estimates as both MSE and SD of most parameters are reasonably small. Moreover, the values of the shape parameter ν of the two models match with each other in terms of the

tailedness. For example, the small $\hat{\nu} = 5.286$ in the Student's t-distribution in data set 1 agrees with $\hat{\nu} = 1.8234$ which is close to 2 in the EP distribution. However, it is noticed that ν of the RPGP-t model has relatively lower precision and higher bias reflecting the higher level of difficulty in estimating the tailedness of the heavy-tailed Student's t-distribution.

==========

Table 3.3 about here

==========

In model comparison, although the RPGP-t model has a slightly smaller ASE (0.04504 versus 0.04817 averaged over the four simulated data sets), the RPGP-EP model outperforms the RPGP-t model with smaller DIC (1968.4 versus 1979.48). All in all, these simulation experiments show that the performance of the MCMC algorithms for the two models is satisfactory and the estimated pmfs $\hat{f}_{bt}^{(j)}(w)$ approximate the true pmfs $f_{bt}(w)$ reasonably well. While EP distribution can be platykurtic or leptokurtic with a kink and Student's t-distribution can give a very heavy tail when the outlying effect is tremendous, the two RPGP models are suitable under different circumstances.

3.5. Real data analysis

3.5.1. Data and model fitting. We illustrate the usefulness of our proposed models through the epilepsy data which can be found in Thall & Vail (1990) and given in Appendix 3.1. The data were collected from a clinical trial of 59 epileptics by Leppik *et al.* (1985). In the randomized controlled

trial, $m = 59$ patients suffering from simple or complex partial seizures were assigned to either the antiepileptic drug progabide ($z_{\mu 1i} = 1$) or the placebo ($z_{\mu 1i} = 0$) with no intrinsic therapeutic value. The seizure counts were recorded at a two-week interval for an eight-week period ($n_i = 4$) with no dropout or missing cases. As shown in Table 3.4 in Appendix 3.2, the seizure counts exhibit a prominent extra-Poisson variation with large variance to mean ratios at all time t due to some outlying observations as displayed in Figures 3.4(a) and 3.4(b) in Appendix 3.3. To assess the overdispersion in the data, we fitted a simple Poisson regression model using a mean link function $\eta_{it} = \exp(\beta_0 + \beta_1 z_{\mu 1i} + \beta_2 t)$ and a simplified PGP model in Wan (2006) using a mean function $\mu_{it} = \exp(\beta_{\mu 0} + \beta_{\mu 1} z_{\mu 1i})$ and a ratio function $a_{it} = \exp(\beta_{a0} + \beta_{a1} t)$. The mean and variance under both models are equivalent (indicated by '*' in Table 3.4) and are given by η_{it} and $\frac{\mu_{it}}{a_{it}^{t-1}}$ respectively. Obviously, neither of the two simple models, as restricted by their equidispersed property, can capture the overdispersion. Besides, the higher mean seizure counts of the placebo group indicate that 'treatment group' is a feasible covariate. Moreover, the gradually decreasing seizure counts over time for both placebo and progabide groups suggest that time t maybe a possible time-evolving covariate. In addition, population heterogeneity in terms of trend pattern and count level is detected intuitively. In consideration of these and the clinical interest of examining the trend patterns, we adopt the RMPGP models to analyze the epilepsy data.

==========

Figures 3.4(a) and 3.4(b) and Table 3.4 about here

==========

Referring to the MCMC algorithms detailed in Section 3.3.2, our prior specifications are mostly non-informative except for ν_l in the RMPGP-t model. In both RMPGP models, we assign $\tau^2_{jkl} = 1000$ in (3.13), $c_l = d_l = 0.001$ in (3.14) and $\alpha_l = 1/G$ in (3.17) for a G-group ($G \geq 2$) model. For ν_l in the RMPGP-t model, we take $e_l = 20$ since there is a high degree of overdispersion in the seizure counts. After implementing the MCMC algorithms in `WinBUGS`, the posterior sample means are adopted as parameter estimates since the posterior densities of most model parameters are highly symmetric such that the posterior sample mean is close to the posterior sample median.

We first fitted a simple RPGP model with treatment group ($z_{\mu 1it} = 0, 1$) as the covariate in the mean function μ_{itl} in (3.8) and two-week interval ($z_{a1it} = t = 1, 2, 3, 4$) as the time-evolving effect in the ratio function a_{itl} in (3.9). The insignificant $\beta_{\mu 1}$'s in both RPGP models indicate that the progabide treatment effect is insignificant (95% CIs for $\beta_{\mu 1}$ in RPGP-t model and RPGP-EP model include zero). However, within the treatment group, it is explicit that some of these patients have abnormally high seizure counts. Simply fitting a simple RPGP model may fail to allow for the cluster effect among patients receiving the same treatment. We therefore fitted the 2-group and 3-group RMPGP models using both Student's t- and EP

distributions but the results indicate that one of the groups in the 3-group RMPGP models degenerated and hence the models are discarded. Table 3.5 in Appendix 3.2 summarizes the parameter estimates, standard errors (SE) and model selection criterion DIC of the 1-group and 2-group RMPGP models.

==========

Table 3.5 about here

==========

3.5.2. Results. Not surprisingly, both RMPGP models give parallel results as they share some common model properties except the shape of the distribution of y^*_{itl}. In the RMPGP-t model, two distinct groups of patients are identified with the first group of patients having generally higher seizure counts and is named as the high-level group ($l = 1$). Within this group, 54% of the patients are receiving progabide and they have lower seizure counts in general ($\hat{\beta}_{\mu 11} < 0$) than those receiving placebo. However, the difference is insignificant since the 95% CI for $\beta_{\mu 11}$ is $[-0.7197, 0.0426]$ which includes zero. Whereas in the low-level ($l = 2$) group, 49% of the patients belong to the progabide group and again they generally have less epileptic seizures during the studying period ($\hat{\beta}_{\mu 12} < 0$, 95% CI:$[-0.5992, -0.0921]$). Moreover, the ratio function a_{it1} in (3.9) reveals that there is a slightly decreasing trend in the seizure counts in the high-level group while a_{it2} indicates that no obvious trend is detected in the low-level group. In addition, comparing with the low-level group, the relatively smaller $\hat{\nu}_1$ shows that the high-level

group has a higher degree of overdispersion in the seizure counts due to the existence of some abnormally large observations as revealed in Figures 3.4(a) and 3.4(b).

As expected, the RMPGP-EP model gives consistent results in terms of trend pattern and treatment effect. Moreover, the group membership of the patients has a close affinity with that of RMPGP-t model and two diverse groups, high-level and low-level groups, are recognized as well. But for the high-level group, despite the comparable mean level, the difference between the two treatment effects becomes significant (95% CI for $\beta_{\mu 11}$: $[-0.5992, -0.0921]$). Furthermore, the ratio function a_{it1} shows that the seizure count increases until the second 2-week interval ($t = 2$) before it drops in the next two 2-week intervals. Consistently, the estimate $\hat{\nu}_1 = 1.49$ (leptokurtic shape in the EP distribution) agrees with the small $\hat{\nu}_1 = 7.21$ (heavier-than-normal tail in the Student's t-distribution) in the RMPGP-t model indicating that the distribution of the seizure counts in the high-level group has a heavier tail to account for the higher degree of overdispersion. On the other hand, the smaller $\hat{\nu}_2 = 0.24$ (platykurtic in the EP distribution) indicates the model distribution is more uniform in the low-level group.

For model selection, the smaller DIC given by (3.19) as shown in Table 3.5 for the RMPGP-EP model manifests its better model fit on the epileptic seizure counts after accounting for the model complexity. A plausible explanation is that the EP distribution has a more flexible tail behaviour and thus provides a better fit to the data. To further investigate this, their

observed and fitted pmfs for the low-level group are illustrated in Figures 3.5(a) to 3.5(d) in Appendix 3.3 at different time points in Appendix 3.3. The observed pmf $f_{tl}(w)$ for group l at time t is generally given by

$$f_{tl}(w) = \sum_{b=0,1} \psi_b \left\{ \frac{\sum_{i=1}^{m} \bar{I}_{il} I(W_{it} = w) I(z_{\mu 1i} = b)}{\sum_{w'=0}^{\infty} \sum_{i=1}^{m} \bar{I}_{il} I(W_{it} = w') I(z_{\mu 1i} = b)} \right\}, \ w = 0, 1, 2, \ldots \quad (3.20)$$

where $I(W_{it} = w)$ is an indicator which returns 1 when $W_{it} = w$ for patient i at time t in group l and 0 otherwise, $I(z_{\mu 1i} = b)$ indicates the treatment group b of patient i, $\bar{I}_{il}$ is the posterior mean of the group membership indicator and ψ_b is the weight associated with the placebo ($b = 0$) or progabide group ($b = 1$). On the other hand, the fitted pmf $\hat{f}_{tl}(w)$ is obtained similarly by

$$f_{tl}(w) = \sum_{b=0,1} \psi_b \hat{f}_{btl}(w), \ w = 0, 1, 2, \ldots$$

where $\hat{f}_{btl}(w)$ is approximated by MC integration in (3.5) based on the parameter estimates $\boldsymbol{\theta}_l = (\boldsymbol{\beta}_{\mu l}^T, \boldsymbol{\beta}_{al}^T, \sigma_l, \nu_l)^T$. According to Figures 3.5(a) to 3.5(d), both models imitate the observed pmfs reasonably well. However, the predicted trend in the low-level group cannot accommodate the upsurge in the observation $w = 4$ at $t = 2$ resulting in a discrepancy between the observed and fitted pmfs as shown in Figure 3.5(b). It is not surprising to find that the two RMPGP models give similar pmfs as both have the capability of modelling highly overdispersed data. Nevertheless, despite the affinity, the slightly heavier tail in the distribution of the RMPGP-EP model possibly gives rise to the lower DIC.

In the best model (RMPGP-EP model), extra variation is added to the mean of the Poisson distribution through the mixing distribution. Therefore, the variances of the estimated pmf $\hat{f}_{tl}(w)$ of each treatment group given by (2.19) and the overall variances which comprises the variance of expectation and the expectation of variance conditional on the mixture group given by (2.18) show a dramatic improvement. For example, when $t = 1$, the overall variance of the RMPGP-EP model (137.23) is closer to the observed variance (220.08) than that of the PGP model (8.8729). These two variances are reported in Table 3.4 in Appendix 3.2.

==========

Figures 3.5(a) to 3.5(d) about here

==========

Advantageously, implementing the model using Bayesian approach enables us to study the latent stochastic process $\{y^*_{itl}\}$ and the mixing parameters u_{itl}. These unobserved parameters can be output by using the **Co**nvergence **D**iagnostic and Output **A**nalysis (`CODA`) software in `WinBUGS`. The `CODA` is a menu-driven set of `S-Plus` functions which produces an output file storing the posterior samples of all model parameters with their corresponding iteration numbers. For the RMPGP-EP model, to examine the density of the unobserved y^*_{itl} which are simulated from an EP distribution with location parameter μ^*_{itl}, scale parameter σ_l and shape parameter ν_l, we compare the densities of the posterior samples of y^*_{itl} with the normal

distribution which has the same mean and standard deviation as the posterior samples and the EP distribution also with same mean and standard deviation and a shape parameter $\hat{\nu}_l$. Four selected y^*_{itl} from each mixture group l and treatment group $z_{\mu 1i} = b = 0, 1$ are illustrated in Figure 3.6 in Appendix 3.3. Obviously, the y^*_{it1}'s have a leptokurtic shape whereas y^*_{it2}'s appear to be more uniform than the normal distribution. These agree with the results in Table 3.5 that the shape parameter of the high-level group is larger than that of the low-level group ($\hat{\nu}_1 > \hat{\nu}_2$) and explain how the EP distribution can downweigh the outlying effect.

==========

Figure 3.6 about here

==========

Furthermore, the outlier diagnosis is performed using the mixing parameter estimates $\hat{u}_{itl}$ in the RMPGP-EP model. An unusually large $\hat{u}_{itl}$ indicates that the observation w_{it} is possibly an outlier under group l. For fair comparison, we calculate the standardized observations $w'_{itl} = \dfrac{|w_{it} - \hat{w}_{itl}|}{\hat{\sigma}_{w_{itl}}}$ for patient i where $\hat{w}_{itl}$ and $\hat{\sigma}_{w_{itl}}$ are respectively the mean and standard deviation of the observed pmf $f_{tl}(w)$ in (3.20) at time t under group l. Both mixing parameters u_{itl} and standardized seizure counts w'_{itl} are sorted by groups ($l = 1, 2$) for better visualization and are then plotted in Figure 3.7 in Appendix 3.3.

==========

Figure 3.7 about here

==========

Clearly, all the top 10 (5%) outlying counts with the first 10 largest u_{itl} locate in the high-level group ($l = 1$) due to the presence of some extreme observations. They are highlighted in Figure 3.7 with the corresponding rank and observation w_{it} in parentheses. Not surprisingly, the correlation between u_{it1} and w'_{it1} is high ($r_{uw} = 0.9731$) which signifies the appropriateness of using the mixing parameters in outlier diagnosis. While the outlying effect is not substantial in the low-level group ($l = 2$), u_{it2} appears to be relatively smaller.

The top four outlying values come from the same patient with ID 49 who has abnormally high seizure counts at each 2-week interval. Besides, two large observations are identified from patients with ID 8 ($w_{8,1} = 40$) and 25 ($w_{25,3} = 76$) in Figure 3.7. In spite of large observation, four small seizure counts are also classified as outlier from patients with ID 10, 24, 39 and 56. Knowing which patients are associated with abnormal seizure counts, specialists can pay more attention to their abnormalities and alternative treatments may be considered accordingly. Besides the detection of outliers using the mixing parameters, the RMPGP-EP model also down-weighs the outlying effect and thus the general trend pattern is not distorted by the extreme observations.

Last but not least, we tested for the serial correlation in the best model by using the procedures described in Section 3.3.4. Starting from some lower lags, the large p-values of the chi-square tests for autocorrelation up to lag 1 (0.837) and lag 2 (0.999) affirm that there is no evidence of the presence of autocorrelation up to lag 2. Hence the tests for higher lags are not considered and the RMPGP-EP model is validated.

3.6. Discussion

In this Chapter, we extend the Poisson geometric process (PGP) model in Wan (2006) to allow for extra-Poisson variation when extreme observations appear in the data. Ignoring the outlying effects may lead to overestimated mean and variance resulting in invalid interpretation and prediction. As remedies, two methods are suggested to account for overdispersion which include adopting a heavy-tailed distribution and incorporating mixture effect. The latter can handle cluster effect in the data and overdispersion arisen from that may also be captured.

As a new direction to account for extreme observations leading to overdispersion and population heterogeneity, we apply the heavy-tailed distributions in the modelling of longitudinal count data and pioneer the robust Poisson geometric process (RPGP) model. This model allows the mean X_{it} of the Poisson distribution to follow a GP and the logarithm of the underlying stochastic process $\{Y_{it} = a_{it}^{t-1} X_{it}\}$ follows a heavy-tailed distribution. The resultant model is called the RPGP model. By varying a set of model parameters, the moments of the RPGP models are reported in Tables 3.1 and

3.2 in Appendix 3.2 and their pmfs are revealed in Figures 3.1 and 3.2 in Appendix 3.3. Although the marginal pmfs do not have closed-form, Monte Carlo (MC) integration in (3.5) can be used to approximate the pmfs, and hence the mean as well as the variance. Tables 3.1 and 3.2 in Appendix 3.2 show that the model can accommodate both equidispersed and overdispersed data with varying kurtoses.

The RPGP models and the RMPGP models which can allow for cluster effects are implemented using a Bayesian approach. Expressing the heavy-tailed distribution in a scale mixtures form facilitates the model implementation using MCMC algorithms and the mixing parameter enables us to perform outlier diagnosis as shown in the real data analysis. Here, the Student's t-distribution in scale mixtures of normals (SMN) and exponential power (EP) distribution in scale mixtures of uniforms (SMU) are adopted. Regarding serial correlation, a test is described in Section 3.3.4 for detecting an up-to-lag-L autocorrelation and some lagged observations can be easily incorporated into the mean function μ^*_{itl} in (3.8) as covariates if needed. The resultant models can be efficiently implemented via the user-friendly software, `WinBUGS`.

In addition, the simulation study shows that the performances of the two RPGP models are comparable and satisfactory. In the case of data with a very long tail, the RMPGP-t model seems to fit better since the tail of the Student's t-distribution is much heavier than that of the normal distribution. On the other hand, the RMPGP-EP model gives a better fit in the analysis

of epilepsy data with more diverse degrees of overdispersion across mixture groups as EP distribution has a more flexible shape which can be either leptokurtic or platykurtic.

Lastly, one pitfall of the RMPGP model is that taking log-transformation of the latent stochastic process $\{Y_{it}\}$ inevitably causes those data associated with close-to-zero means being identified as outliers. Hence when zero is dominant in the data, the proposed RMPGP models can be extended to include a zero-altered component as in the zero-altered MPGP model introduced in Chapter 2.

Appendix 3.1

Successive two-week seizure counts W_{it} for 59 epileptics in two treatment groups (0=placebo, 1=progabide)

patient	w_{i1}	w_{i2}	w_{i3}	w_{i4}	treatment
1	5	3	3	3	0
2	3	5	3	3	0
3	2	4	0	5	0
4	4	4	1	4	0
5	7	18	9	21	0
6	5	2	8	7	0
7	6	4	0	2	0
8	40	20	23	12	0
9	5	6	6	5	0
10	14	13	6	0	0
11	26	12	6	22	0
12	12	6	8	5	0
13	4	4	6	2	0
14	7	9	12	14	0
15	16	24	10	9	0
16	11	0	0	5	0
17	0	0	3	3	0
18	37	29	28	29	0
19	3	5	2	5	0
20	3	0	6	7	0
21	3	4	3	4	0
22	3	4	3	4	0
23	2	3	3	5	0
24	8	12	2	8	0
25	18	24	76	25	0
26	2	1	2	1	0
27	3	1	4	2	0
28	13	15	13	12	0
29	11	14	9	8	1
30	8	7	9	4	1
31	0	4	3	0	1
32	3	6	1	3	1
33	2	6	7	4	1
34	4	3	1	3	1
35	22	17	19	16	1
36	5	4	7	4	1
37	2	4	0	4	1
38	3	7	7	7	1
39	4	18	2	5	1
40	2	1	1	0	1
41	0	2	4	0	1
42	5	4	0	3	1
43	11	14	25	15	1
44	10	5	3	8	1
45	19	7	6	7	1
46	1	1	2	4	1
47	6	10	8	8	1
48	2	1	0	0	1
49	102	65	72	63	1
50	4	3	2	4	1
51	8	6	5	7	1
52	1	3	1	5	1
53	18	11	28	13	1
54	6	3	4	0	1
55	3	5	4	3	1
56	1	23	19	8	1
57	2	3	0	1	1
58	0	0	0	0	1
59	1	4	3	2	1

Appendix 3.2

Tables

Table 3.1: Moments of marginal pmfs for RPGP-t model under a set of floating parameters with fixed values of $\nu = 10, \sigma = 0.5, \beta_{\mu 0} = 3, \beta_{\mu 1} = -0.2, \beta_{a0} = 0.5, \beta_{a1} = -0.1$

floating parameter	**mean**	**variance**	**kurtosis**	**floating parameter**	**mean**	**variance**	**kurtosis**
$\nu = 1$	15.082	152.634	1.0017	$\sigma = 0.1$	12.279	14.110	0.1209
$\nu = 2$	14.381	110.855	1.0036	$\sigma = 0.5$	14.041	81.182	0.5579
$\nu = 5$	14.616	103.899	0.6568	$\sigma = 1.0$	16.143	230.454	0.9817
$\nu = 50$	13.985	69.826	0.3827	$\sigma = 2.0$	15.511	349.030	0.9832
$\beta_{\mu 0} = 1.0$	1.057	1.643	0.0411	$\beta_{a0} = -0.5$	34.452	262.605	0.9605
$\beta_{\mu 0} = 2.0$	2.891	6.827	0.2277	$\beta_{a0} = -0.01$	23.015	175.040	0.8652
$\beta_{\mu 0} = 3.0$	7.832	32.123	0.7399	$\beta_{a0} = 0.5$	14.460	95.392	0.7662
$\beta_{\mu 0} = 4.0$	20.814	153.217	1.1929	$\beta_{a0} = 1.5$	5.344	16.972	0.2819

Table 3.2: Moments of marginal pmfs for RPGP-EP model under a set of floating parameters with fixed values of $\nu = 1, \sigma = 0.5, \beta_{\mu 0} = 3, \beta_{\mu 1} = -0.5, \beta_{a0} = 0.5, \beta_{a1} = -0.1$

floating parameter	**mean**	**variance**	**kurtosis**	**floating parameter**	**mean**	**variance**	**kurtosis**
$\nu = 0.1$	9.379	16.987	0.0925	$\sigma = 0.1$	9.048	9.871	0.0782
$\nu = 0.5$	9.629	20.468	0.1312	$\sigma = 0.5$	10.331	42.865	0.2938
$\nu = 1.0$	10.174	39.574	0.3281	$\sigma = 1.0$	13.891	197.640	0.9747
$\nu = 2.0$	12.592	192.360	0.9835	$\sigma = 2.0$	14.627	327.645	0.9840
$\beta_{\mu 0} = 1.0$	1.382	1.956	0.0388	$\beta_{a0} = -0.5$	26.592	198.533	0.9605
$\beta_{\mu 0} = 2.0$	3.771	7.695	0.0982	$\beta_{a0} = -0.01$	16.845	104.392	0.8652
$\beta_{\mu 0} = 3.0$	10.386	46.856	0.3061	$\beta_{a0} = 0.5$	10.216	46.338	0.7662
$\beta_{\mu 0} = 4.0$	27.046	199.776	0.7261	$\beta_{a0} = 1.5$	3.788	10.512	0.2819

Table 3.3: Parameter estimates, SD, MSE, DIC and ASE in different RPGP models under 4 simulated data sets based on 4 sets of true parameters from different models

data	**model**	**parameter**	**true**	**estimate**	SD	MSE	DIC	ASE
1	RPGP-t	β_{a0}	-2.0	-1.9320	0.0379	0.0060	**2315.55**	**0.0371**
		β_{a1}	0.2	0.1960	0.0056	0.0000		
		$\beta_{\mu 0}$	-1.5	-1.6016	0.0307	0.0113		
		$\beta_{\mu 1}$	-0.5	-0.3232	0.0381	0.0327		
		ν	2.5	5.2860	1.3266	9.5040		
		σ	0.1	0.4244	0.0377	0.1066		
	RPGP-EP	β_{a0}		-1.8844	0.0382		2357.72	0.0592
		β_{a1}		0.1892	0.0052			
		$\beta_{\mu 0}$		-1.5034	0.0254			
		$\beta_{\mu 1}$		-0.3433	0.0416			
		ν		1.8234	0.1532			
		σ		0.1052	0.0132			
2	RPGP-t	β_{a0}	-1.0	-0.8651	0.0546	0.0211	1834.54	**0.0367**
		β_{a1}	0.2	0.1820	0.0110	0.0004		
		$\beta_{\mu 0}$	1.0	0.9794	0.0236	0.0010		
		$\beta_{\mu 1}$	-0.5	-0.4528	0.0329	0.0033		
		ν	50.0	50.9375	10.6352	112.86		
		σ	0.02	0.0203	0.0004	0.0000		
	RPGP-EP	β_{a0}		-0.8523	0.0540		**1816.94**	0.0377
		β_{a1}		0.1803	0.0108			
		$\beta_{\mu 0}$		0.9907	0.0178			
		$\beta_{\mu 1}$		-0.4541	0.0389			
		ν		1.0469	0.2979			
		σ		0.1014	0.0128			
3	RPGP-t	β_{a0}		-0.4852	0.0795		1883.96	**0.0543**
		β_{a1}		0.0987	0.0110			
		$\beta_{\mu 0}$		0.7384	0.0920			
		$\beta_{\mu 1}$		-0.2350	0.0454			
		ν		73.6282	18.1843			
		σ		0.3152	0.0654			
	RPGP-EP	β_{a0}	-0.5	-0.4289	0.0729	0.0103	**1860.39**	0.0550
		β_{a1}	0.1	0.0926	0.0105	0.0002		
		$\beta_{\mu 0}$	1.0	0.8287	0.0769	0.0352		
		$\beta_{\mu 1}$	-0.5	-0.2812	0.0656	0.0521		
		ν	0.1	0.2005	0.1178	0.0238		
		σ	0.5	0.6272	0.0701	0.0210		
4	RPGP-t	β_{a0}		0.9938	0.0694		1883.86	0.0521
		β_{a1}		-0.0996	0.0088			
		$\beta_{\mu 0}$		1.7407	0.0784			
		$\beta_{\mu 1}$		-0.2256	0.0549			
		ν		2.2267	1.1224			
		σ		0.1682	0.0028			
	RPGP-EP	β_{a0}	1.0	1.1048	0.0663	0.0153	**1838.56**	**0.0407**
		β_{a1}	-0.1	-0.1110	0.0087	0.0002		
		$\beta_{\mu 0}$	2.0	1.9388	0.0502	0.0062		
		$\beta_{\mu 1}$	-0.5	-0.3768	0.0743	0.0207		
		ν	1.8	1.8430	0.1174	0.0155		
		σ	0.2	0.1945	0.0225	0.0005		

Table 3.4: Mean and variance for the observed epilepsy data and of two simple fitted and RMPGP-EP models

		time				average
	model	$t = 1$	$t = 2$	$t = 3$	$t = 4$	**over time**
placebo						
mean	observed	9.3571	8.2857	8.7857	8.0000	8.6071
	Poisson*	9.3658	8.8385	8.3410	7.8714	8.6042
	PGP*	9.2073	8.9707	8.4645	7.7348	8.5943
	RMPGP-EP	10.047	10.4001	9.9565	8.7905	9.7984
variance	observed	102.76	66.656	215.29	57.926	107.93
	RMPGP-EP	187.19	214.02	198.25	141.92	185.34
progabide						
mean	observed	8.5806	8.4194	8.1290	6.7419	7.9677
	Poisson*	8.6700	8.1819	7.7214	7.2867	7.9557
	PGP*	8.5212	8.3023	7.8337	7.1584	7.9539
	RMPGP-EP	6.8235	7.2885	6.9278	5.9980	6.7595
variance	observed	332.72	140.65	193.05	126.66	193.97
	RMPGP-EP	92.114	124.37	107.44	77.371	100.32
overall						
mean	observed	8.9492	8.3559	8.4407	7.3390	8.2712
	Poisson*	8.9940	8.4920	8.0179	7.5704	8.2686
	PGP*	8.8729	8.6469	8.1573	7.4495	8.2816
	RMPGP-EP	8.3531	8.7652	8.3652	7.3233	8.2017
variance	observed	220.08	103.78	200.18	92.883	152.61
	RMPGP-EP	137.23	166.92	150.54	108.00	140.67

* indicates mean and variance are equivalent.

Table 3.5: Parameter estimates with SE and DIC in different RMPGP models for the epilepsy data

		RMPGP-t model			**RMPGP-EP model**		
	parameter	**estimate**	SE	DIC	**estimate**	SE	DIC
$G=1$	β_{a0}	-0.6435	0.1464	1923.08	0.0073	0.2780	1945.40
	β_{a1}	0.1218	0.0456		0.0089	0.0675	
	$\beta_{\mu 0}$	1.2970	0.1132		1.7460	0.1582	
	$\beta_{\mu 1}$	-0.2177	0.1393		-0.2637	0.1699	
	ν	73.2100	41.9200		1.1920	0.1883	
	σ	0.9826	0.0669		0.9036	0.1616	
$G=2$	β_{a01}	-0.0241	0.4366	1700.90	-0.2410	0.3122	**1660.66**
	β_{a11}	0.0192	0.1062		0.0739	0.0738	
	$\beta_{\mu 01}$	2.7070	0.1993		2.6700	0.1569	
high-level	$\beta_{\mu 11}$	-0.3544	0.1922		-0.3727	0.1342	
($l=1$)	ν_1	7.2110	4.7430		1.4860	0.2559	
	σ_1	0.5965	0.1029		0.4841	0.1304	
	π_1	0.4055	0.0738		0.4069	0.0688	
	β_{a02}	0.2058	0.2378		0.2169	0.2271	
	β_{a12}	-0.0464	0.0589		-0.0474	0.0581	
low-level	$\beta_{\mu 02}$	1.2750	0.1252		1.2750	0.0982	
($l=2$)	$\beta_{\mu 12}$	-0.3587	0.1656		-0.4193	0.1477	
	ν_2	10.9300	5.2690		0.2424	0.1813	
	σ_2	0.3286	0.1148		0.7327	0.1058	

Appendix 3.3

Figures

Figure 3.1: The pmfs of RPGP-t model with varying parameters

(a) ν

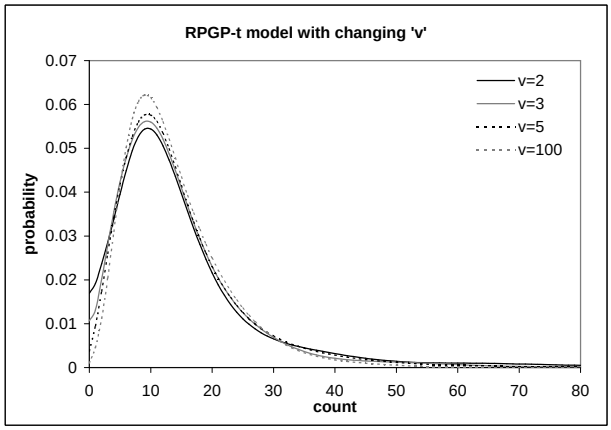

(b) σ

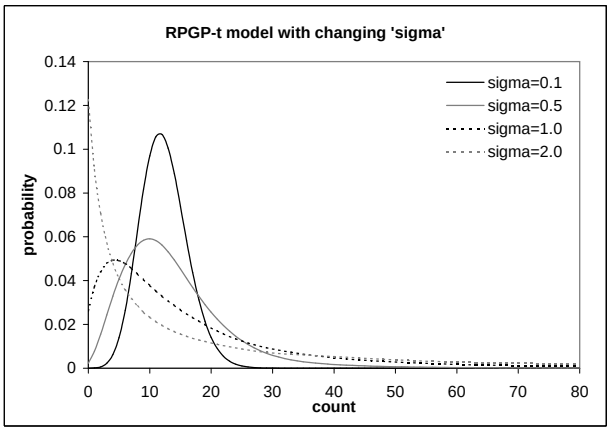

(c) $\beta_{\mu 0}$

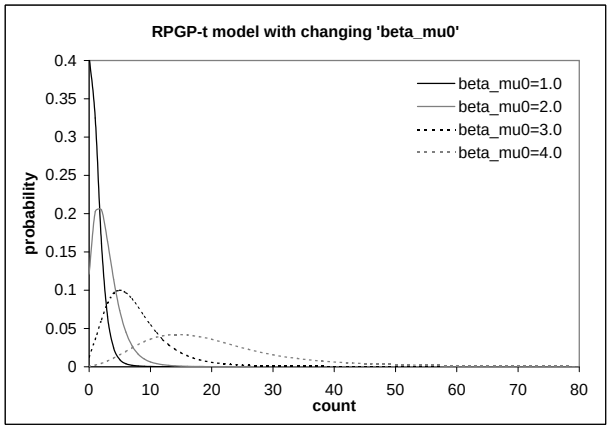

(d) β_{a0}

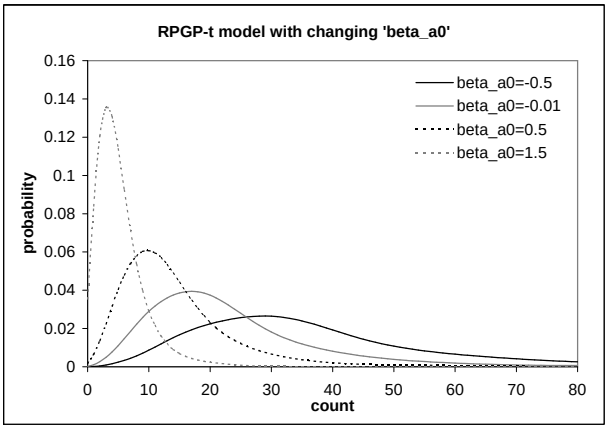

Figure 3.2: The pmfs of RPGP-EP model with varying parameters

(a) ν

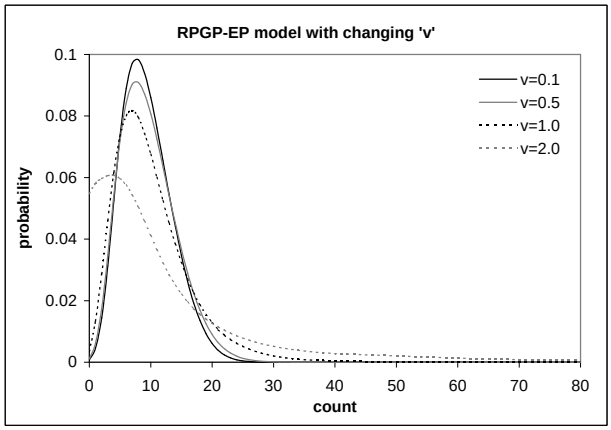

(b) σ

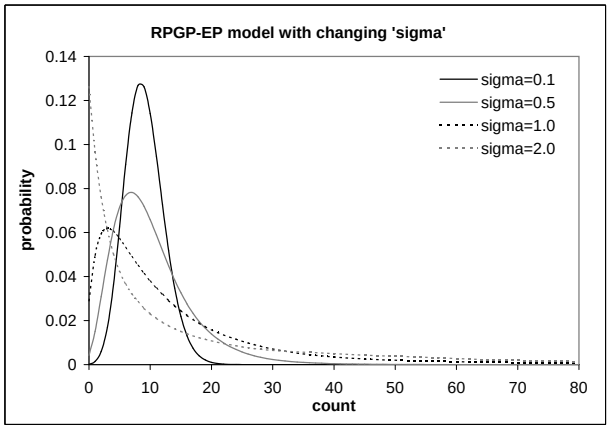

(c) $\beta_{\mu 0}$

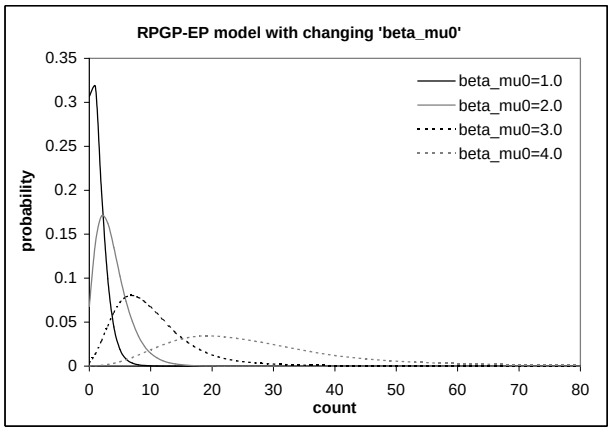

(d) β_{a0}

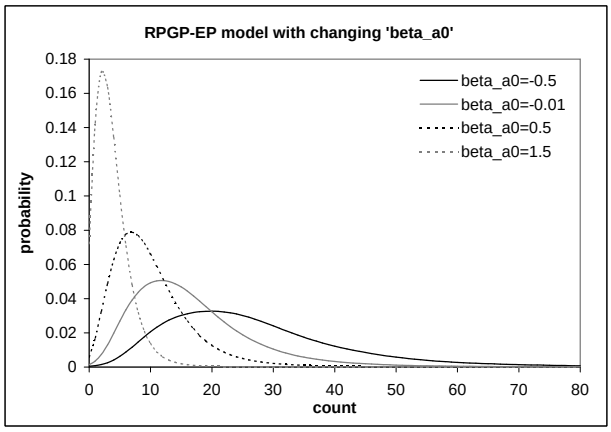

Figure 3.3: pmf of 2-group RMPGP-EP model at $t = 1$

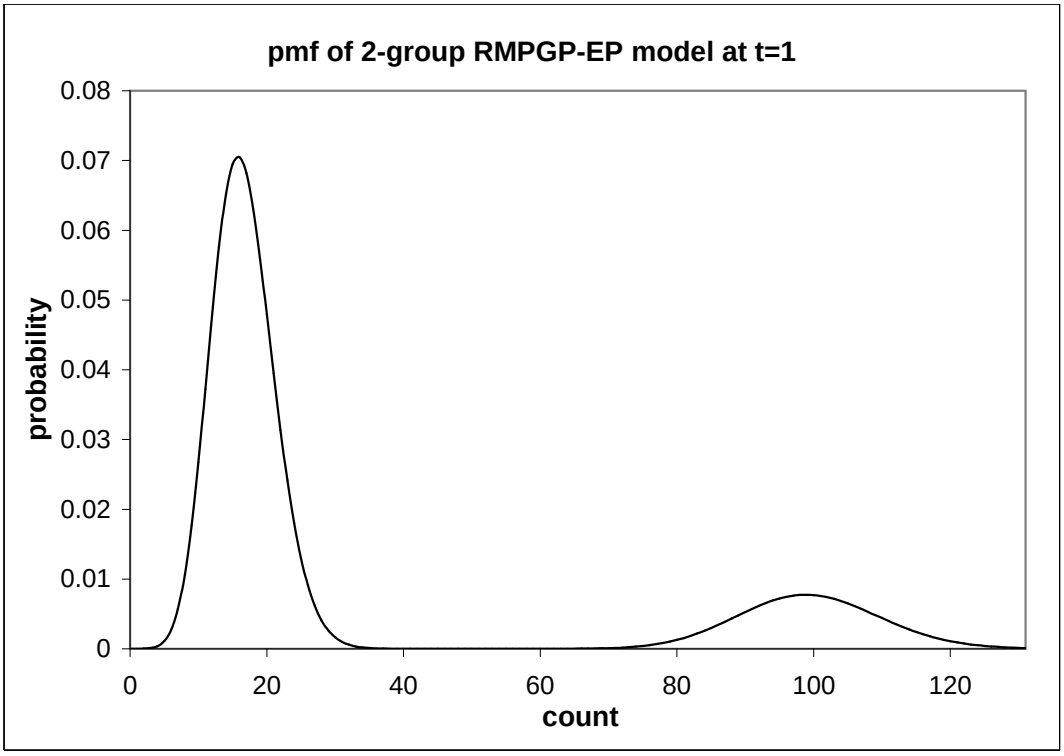

Figure 3.4: Dotplots of seizure counts across treatment group and time

(a) $t = 1$ and $t = 2$

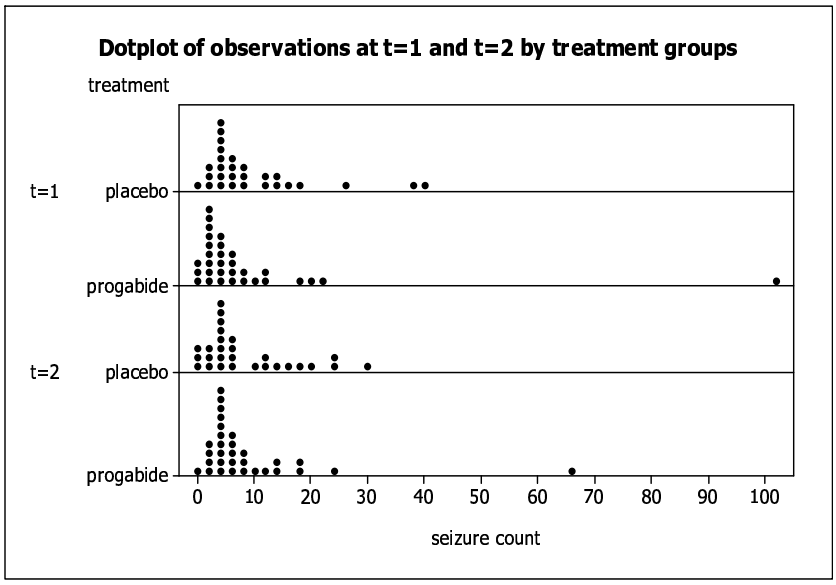

(b) $t = 3$ and $t = 4$

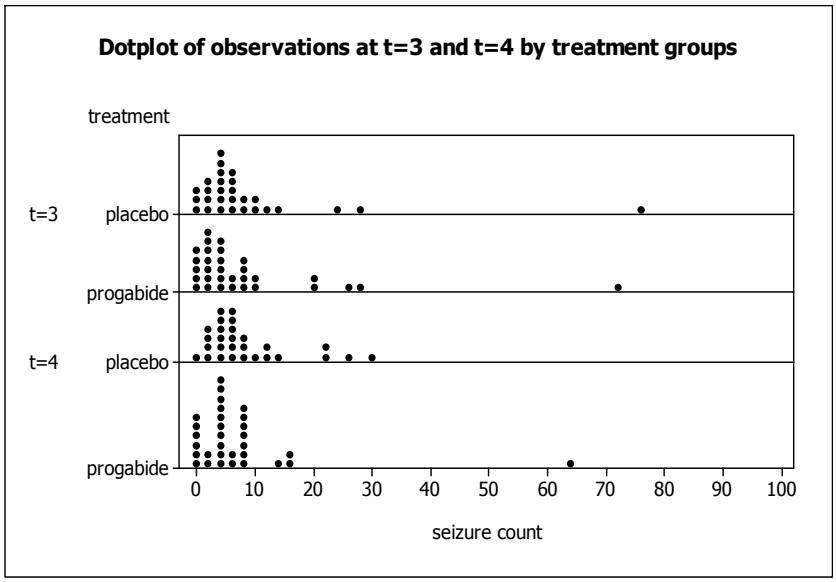

Figure 3.5: The pmfs of low-level group for RMPGP models at different times

(a) $t = 1$

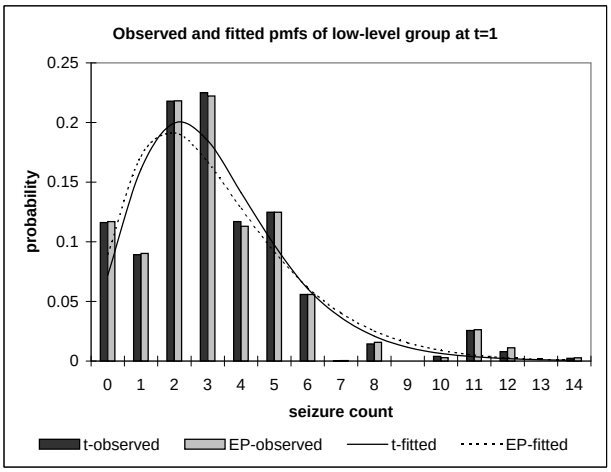

(b) $t = 2$

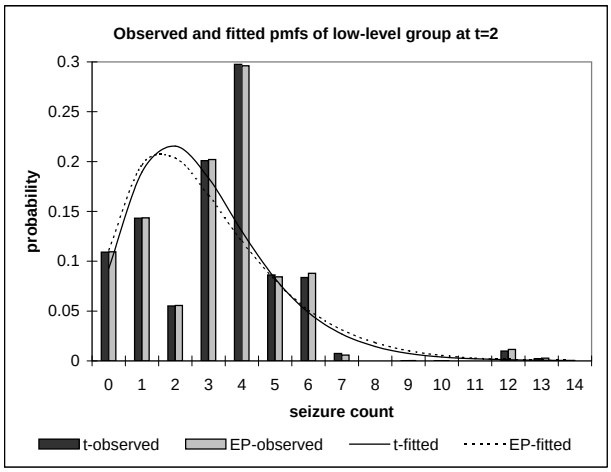

(c) $t = 3$

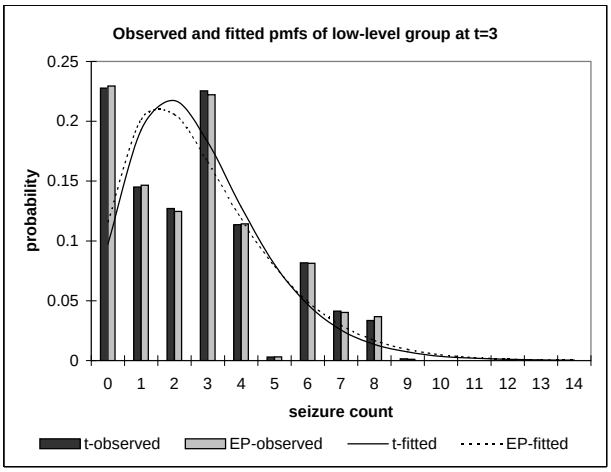

(d) $t = 4$

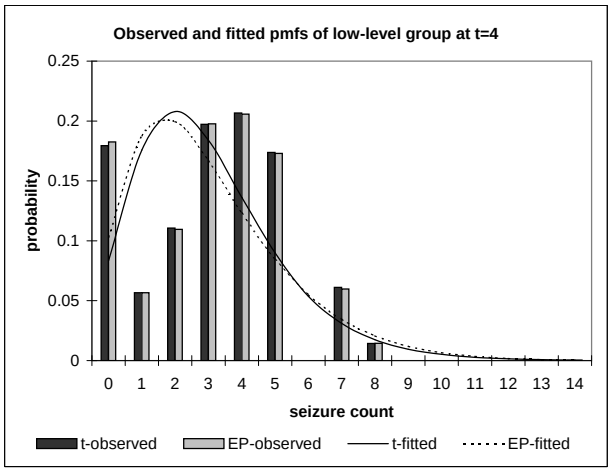

Figure 3.6: Comparison of densities of y_{itl}'s with normal and EP distributions

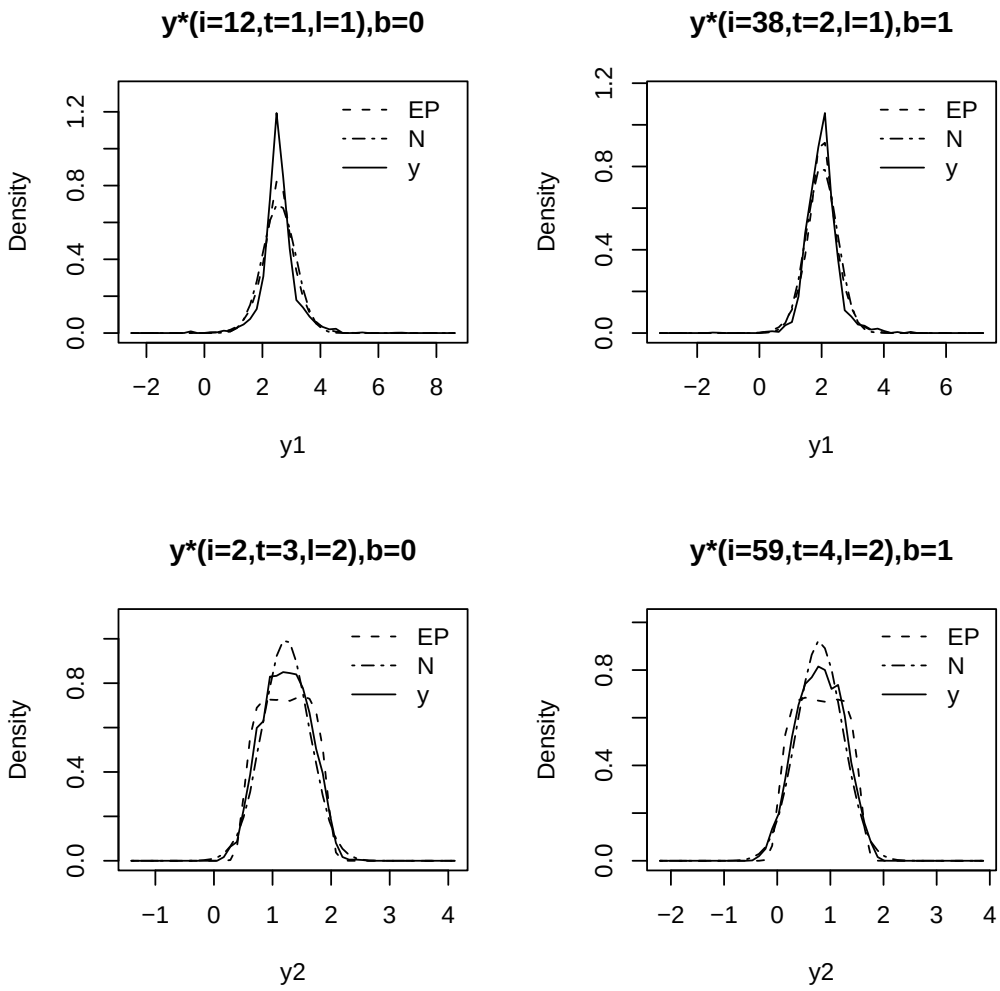

Figure 3.7: Outlier diagnosis using u_{itl} in the RMPGP-EP model

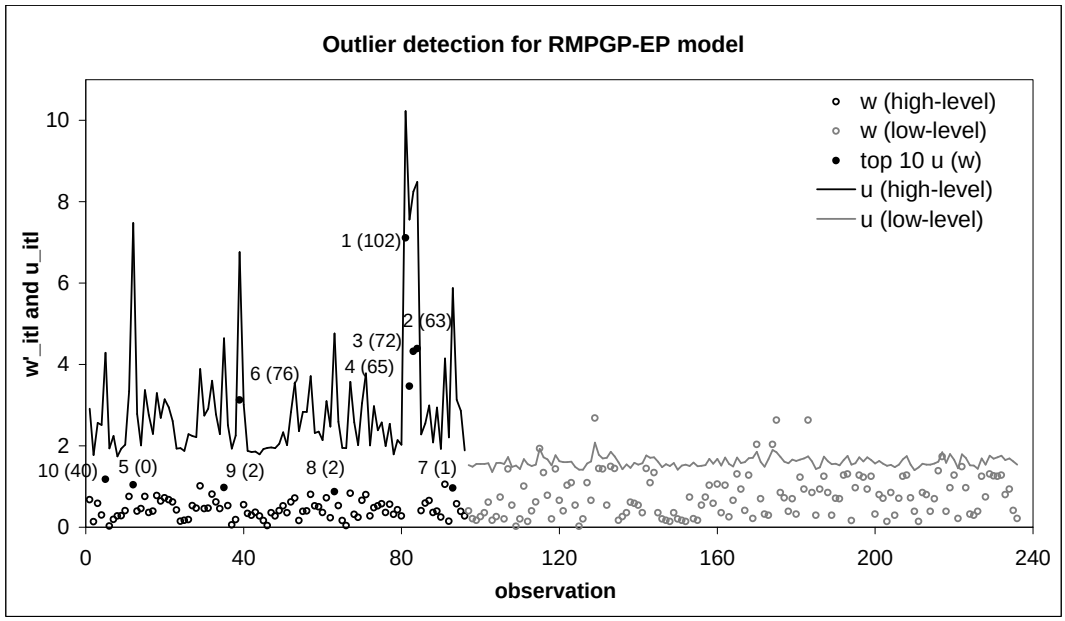

CHAPTER 4

Generalized Poisson geometric process model

PGP model has been extended to allow for overdispersion that is caused, in particular, by zero-inflation in Chapter 2 and extreme observations in Chapter 3. This Chapter extends the PGP model in (1.4) to fit longitudinal count data with more flexible degrees of dispersion ranging from underdispersion to overdispersion.

4.1. Background

Owing to the deficiency of the Poisson distribution that it can only handle equidispersed count data, our primary objective is to develop a unified model that can accommodate both overdispersion and underdispersion in longitudinal and panel count data. Besides considering the degree of dispersion, our proposed model should also take into account the trend movements, serial correlation between successive observations which is prominent in time series of counts and cluster effects which are often detected in repeated measures design. Throughout the history of count data modelling, since most count data exhibits overdispersion due to outliers, excess zero observations and population heterogeneity, enormous literature can be found to deal with overdispersion by using different methods to introduce extra-variation to the Poisson distribution.

One historic approach is to use the Poisson mixed distribution which assumes that the mean of the Poisson distribution follows a suitable mixing distribution. This mixed model approach was first considered by Greenwood & Yule (1920) which adopted a gamma distribution as the mixing distribution and resulted in the well-known negative binomial distribution. Since then, a large number of mixing distributions are considered and some benchmarking models include the Poisson-inverse Gaussian mixed model (Holla, 1966), Poisson-lognormal mixed model (Blumer, 1974) and Poisson-generalized gamma mixed model (Albrecht, 1984). See Karlis & Meligkotsidou (2005) for a detailed review.

Concerning overdispersion particularly due to zero-inflation, two strands of models, namely the hurdle model and the zero-inflated model prevail in the literature. The former class proposed by Mullahy (1986) first determines whether the outcome is zero or positive by a logistic model and then conditional on positive outcome, models the positive counts by a truncated discrete distribution, such as truncated Poisson or truncated negative binomial distribution. On the contrary, the latter class introduced by Lambert (1992) is regarded as a mixture of zero-truncated Poisson distribution and a component that degenerates at zero. These models, which are designed for cross-sectional count data, were later extended to fit longitudinal count data. Adopting the hurdle model, Dobbie & Welsh (2001) incorporated a serial dependence structure via a generalized estimating approach so that the marginal model structure can be preserved. On the other hand, Yau *et al.* (2003)

extended the zero-inflated Poisson model to zero-inflated negative binomial mixed regression model by introducing random effects to account for serial dependence between successive observations. Nevertheless, all these models have a component that adds extra variation to the Poisson distribution and therefore fail to deal with underdispersion.

Compared to overdispersion, the analogous problem of underdispersion relative to Poisson distribution has not received too much attention as it is less frequently observed in longitudinal and panel count data. But ignoring this problem will result in an overestimated variance and a misleading interpretation on the volatility of the data. Amongst the limited literature, Faddy (1997) proposed the birth process model based on a generalization of the Poisson process and stated that the rate of process (birth rate) at any time point is a function of time and depends on the current number of events. In the birth process model, overdispersion/underdispersion is attained when the rate of process is monotone increasing/decreasing with time. Besides the birth process model, other alternative distributions that can allow underdispersion include the Conway-Maxwell-Poisson distribution (Conway & Maxwell, 1962), generalized Poisson distribution Consul & Jain (1973), double Poisson distribution (Efron, 1986) and weighted Poisson distribution Ridout & Besbeas (2004).

Amongst all the aforementioned distributions for underdispersion, the generalized Poisson distribution (GPD) pioneered by Consul & Jain (1973) received considerably more attention. Relative to Poisson distribution, the

two-parameter GPD contains an additional parameter to control the shape of the distribution. The variance can be greater than, equal to or smaller than the mean when the parameter is positive, zero or negative respectively. Some extensions of the GPD distribution on cross-sectional count data include the generalized Poisson regression model (Consul & Famoye, 1992) to incorporate covariate effect, the zero-inflated generalized Poisson regression model (Angers & Biswas, 2003) to deal with excess zeros and the k-inflated generalized Poisson regression model (Bae *et al.*, 2005) to handle excessive k-valued observations. Until very recently, Xie *et al.* (2009) extended the zero-inflated generalized Poisson regression model to analyze correlated panel count data by incorporating a latent random effect to account for the serial dependence.

So far, the extension of the PGP models in the previous Chapters focuses only on overdispersion due to excess zeros in Chapter 2 and extreme observations in Chapter 3. To relax such restriction, we extend in this Chapter the PGP model to a more comprehensive model to handle longitudinal and panel count data with different degrees of dispersion by replacing the Poisson data distribution with GPD. The resultant model is named as the generalized Poisson geometric process (GPGP) model. Moreover, regarding our secondary objective, the GPGP model is further extended to the mixture generalized Poisson geometric process (GMPGP) model to incorporate cluster effects and serial dependence.

To demonstrate the model properties and applicability, the remainder of this Chapter is presented as follows. First, the GPGP and GMPGP models will be specified in Section 4.2 with a study of the model distribution. Next, Section 4.3 will discuss the implementation of the GMPGP model using MCMC algorithms followed by the introduction of the model assessment criterion. After that, the properties and practicability of the GMPGP model will be demonstrated through some simulation studies and real data analysis in Sections 4.4 and 4.5 respectively with comparison to the RMPGP-EP model (best model in Chapter 3). Lastly, Section 4.6 will give a summary of all the important findings.

4.2. Model specification

This Section first presents the GPD. Then, the GPGP model is introduced with a detailed examination of the model distribution.

4.2.1. Generalized Poisson distribution. The generalized Poisson distribution (GPD) was introduced by Consul & Jain (1973) and was investigated in detail by Consul (1989). If a random variable W has a GPD, then its probability mass function (pmf) denoted by $f_{GPD}(w|\,\lambda_1, \lambda_2)$ is given by:

$$f_{GPD}(w|\,\lambda_1, \lambda_2) = \begin{cases} \dfrac{\lambda_1(\lambda_1 + \lambda_2 w)^{w-1} \exp[-(\lambda_1 + \lambda_2 w)]}{w!}, & w = 0, 1, \ldots; \\ 0, & w > s \text{ when } \lambda_2 < 0 \end{cases} \tag{4.1}$$

where λ_1, $|\lambda_2| < 1$ and $s \geq 4$ is the largest natural number such that $\lambda_1 + \lambda_2 s > 0$ when $\lambda_2 < 0$. The two parameters λ_1 and λ_2 are subject to the following constraints:

1. $\lambda_1 \geq 0$
2. $max\{-1, -\frac{\lambda_1}{s}\} < \lambda_2 < 1.$

For the GPD, the mean and variance are given by:

$$E(W) = \frac{\lambda_1}{1-\lambda_2} \quad \text{and} \quad Var(W) = \frac{\lambda_1}{(1-\lambda_2)^3} = \frac{E(W)}{(1-\lambda_2)^2}.$$

Obviously, the shape of the GPD is controlled by the parameter λ_2. A negative λ_2 indicates underdispersion, the mean is less than the variance, whilst a positive λ_2 indicates overdispersion. The GPD reduces to the equidispersed Poisson distribution when $\lambda_2 = 0$. Moreover, the variance increases or decreases at a faster rate than the mean when λ_2 varies. Relative to the Poisson distribution, this two-parameter GPD demonstrates a wider range of shapes and thus can fit data with different degrees of dispersion.

4.2.2. Generalized Poisson geometric process model. Let W_{it} denotes the count for subject i at time t, $i = 1, \ldots, m,\ t = 1, \ldots, n_i$ and $n = \sum_{i=1}^{m} n_i$. Under the PGP framework, instead of using the Poisson distribution, we assume that the count W_{it} follows GPD with mean $E(W_{it}) = X_{it} = \frac{\lambda_{1it}}{(1-\lambda_2)}$. Without loss of generality, $\{X_{it} = \frac{Y_{it}}{a^{t-1}}, t = 1, \ldots, n_i\}$ forms a latent GP and Y_{it} follows gamma distribution $f_G(y_{it}|\, r, \frac{r}{\mu_i})$ with mean μ_i and variance $\frac{\mu_i^2}{r}$. So, conditional on $\lambda_2 > 0$, the marginal pmf for W_{it} becomes

$$f(w_{it}) = \int_0^\infty f_{GPD}(w_{it}|\, \lambda_{1it}, \lambda_2) f_G\left(y_{it} \,\middle|\, r, \frac{r}{\mu_i}\right) dy_{it}$$

$$= \int_0^\infty \frac{(1-\lambda_2) r^r y_{it}^r \left[\frac{(1-\lambda_2)y_{it}}{a^{t-1}} + \lambda_2 w_{it}\right]^{w_{it}-1} \exp\left\{-\left[\frac{(1-\lambda_2)y_{it}}{a^{t-1}} + \lambda_2 w_{it} + \frac{r y_{it}}{\mu_i}\right]\right\}}{a^{t-1}\mu_i^r\, \Gamma(r)\, w_{it}!}\, dy_{it} \quad (4.2)$$

where $\lambda_{1it} = \dfrac{(1-\lambda_2)y_{it}}{a^{t-1}}$. When $\lambda_2 < 0$, the marginal pmf for W_{it} is given by (4.2) when $w_{it} = 0, 1, \ldots, s_{it}$ and 0 when $w_{it} > s_{it}$. The resultant model is named as generalized Poisson geometric process (GPGP) model. Although there is no apparent simplification of the integral, its moment can be easily derived through conditional expectation and the law of total variance. In particular, the unconditional mean $E(W_{it})$ and variance $Var(W_{it})$ of the GPGP model are given by:

$$E(W_{it}) = E_x[E_w(W_{it}|X_{it})] = E_x(X_{it}) = E_y\left(\frac{Y_{it}}{a^{t-1}}\right) = \frac{\mu_i}{a^{t-1}} \tag{4.3}$$

$$\begin{aligned} Var(W_{it}) &= E_x[Var_w(W_{it}|X_{it})] + Var_x[E_w(W_{it}|X_{it})] \\ &= E_x\left[\frac{X_{it}}{(1-\lambda_2)^2}\right] + Var_x(X_{it}) \\ &= \frac{\mu_i}{a^{t-1}(1-\lambda_2)^2} + \frac{\mu_i^2}{a^{2(t-1)}r} = \frac{\mu_i}{a^{t-1}}\left[\frac{1}{(1-\lambda_2)^2} + \frac{\mu_i}{a^{t-1}r}\right] \end{aligned} \tag{4.4}$$

Clearly, μ_i and a control both the mean and variance while r and λ_2 act as the dispersion parameters as they only control the variance. Based on (4.4), the larger the r and the more negative the λ_2, the more underdispersed is the distribution of the GPGP model. Hence, by varying the model parameters, the GPGP model can be fitted to both overdispersed and underdispersed data.

4.2.3. Incorporation of mixture effects. Despite different degrees of dispersion, an adequate model for panel count data should account for population heterogeneity which often arises in repeated measures design, accommodate time-evolving covariate effects and address trend movements

which are usually detected in time series of counts. In light of these, we first extend the GPGP model to the mixture GPGP (GMPGP) model as follows.

To account for population heterogeneity, we postulate that there are G groups of subjects which have distinct trend patterns and each subject has a probability π_l of coming from group $l,\ l = 1, \ldots, G$. The resultant GMPGP model is essentially a mixture of G GPGP models in which each model is associated with a probability π_l. Secondly, concerning the covariate effects and trend movements, let $\boldsymbol{\beta}_{jl} = (\beta_{j0l}, \beta_{j1l}, \ldots, \beta_{jq_jl})^T$ to be a vector of regression parameters $\beta_{jkl}, j = \mu, a;\ k = 0, \ldots, q_j; l = 1, \ldots, G$. The mean μ_i and constant ratio a are extended to the mean function μ_{itl} and ratio function a_{itl} function respectively which can be log-linked to some time-evolving covariates $z_{jkit},\ i = 1, \ldots, m; t = 1, \ldots, n_i$ and they are given by:

$$\mu_{itl} = \exp(\beta_{\mu 0l} + \beta_{\mu 1l} z_{\mu 1it} + \cdots + \beta_{\mu q_\mu l} z_{\mu q_\mu it}) \tag{4.5}$$

$$a_{itl} = \exp(\beta_{a0l} + \beta_{a1l} z_{a1it} + \cdots + \beta_{aq_a l} z_{aq_a it}). \tag{4.6}$$

Then conditional on group l, the marginal pmf of the GMPGP model can be extended from (4.2) when $\lambda_{2l} > 0$ and becomes:

$$f_l(w_{it}) = \int_0^\infty \frac{(1-\lambda_{2l}) r_l^{r_l} y_{itl}^{r_l} \left[\frac{(1-\lambda_{2l}) y_{itl}}{a_{itl}^{t-1}} + \lambda_{2l} w_{it}\right]^{w_{it}-1} \exp\left\{-\left[\frac{(1-\lambda_{2l}) y_{itl}}{a_{itl}^{t-1}} + \lambda_{2l} w_{it} + \frac{r_l y_{itl}}{\mu_{itl}}\right]\right\}}{a_{itl}^{t-1} \mu_{itl}^{r_l} \Gamma(r_l)\, w_{it}!} dy_{itl}. \tag{4.7}$$

When $\lambda_{2l} < 0$, the marginal pmf for W_{it} is given by (4.7) for $w_{it} = 0, 1, \ldots, s_{it}$ and 0 for $w_{it} > s_{it}$. Based on (4.3) and (4.4), the mean $E_l(W_{it})$ and variance $Var_l(W_{it})$ conditional on group l become

$$E_l(W_{it}) = \frac{\mu_{itl}}{a_{itl}^{t-1}} \quad \text{and} \quad Var_l(W_{it}) = \frac{\mu_{itl}}{a_{itl}^{t-1}(1-\lambda_{2l})^2} + \frac{\mu_{itl}^2}{a_{itl}^{2(t-1)} r_l}. \quad (4.8)$$

4.2.4. Incorporation of serial correlation. As the outcome W_{it} in longitudinal and panel data is often serially correlated, an adequate count model should be able to incorporate a flexible serial dependence structure. To identify an appropriate serial dependence structure, we first fit a preliminary model and obtain the predicted value based on (4.8). Then the Pearson residuals and test statistic are derived in a similar way to the RMPGP models mentioned in Section 3.3.4 by using $E_l(W_{it})$ and $Var_l(W_{it})$ in (4.8).

If the residuals are serially correlated up to lag L, Dobbie & Welsh (2001) and Yau *et al.* (2003) adopted the PD approach, which is known as marginal model approach in Zeger *et al.* (1988), to incorporate serial dependence by adding random effects into the model. However we adopt the OD approach described in Section 1.2.1 by adding L lagged observations as autoregressive (AR) terms in the mean function μ_{itl} in (4.5). The model parameters will be re-estimated and the appropriateness of the assumed AR structure is evaluated through the significance of the parameters for the AR terms and the model selection criterion discussed in Section 4.3.2.

4.2.5. Approximation of distribution. Since the pmf in (4.7) does not have a closed-form, we approximate it using Monte Carlo (MC) integration

as described below. We hereafter drop the subscript i in the mean function μ_{itl} since only treatment-specific covariates are considered in the forthcoming simulation experiments and real data analysis. Conditional on covariates $z_{jkt} = z_{jkit}$ and time t, the pmf estimator $\hat{f}_{tl}(w)$ with mean function μ_{tl} and ratio function a_{tl} can be obtained by:

$$\hat{f}_{tl}(w) = \sum_{j=1}^{M_s} f_{GPD}\left(w \,\middle|\, \frac{\hat{y}_{tl}^{(j)}}{a_{tl}^{t-1}}, \lambda_{2l}\right)$$

$$= \sum_{j=1}^{M_s} \frac{(1-\lambda_{2l})\hat{y}_{tl}^{(j)} \left[\frac{(1-\lambda_{2l})\hat{y}_{tl}^{(j)}}{a_{tl}^{t-1}} + \lambda_{2l} w\right]^{w-1} \exp\left\{-\left[\frac{(1-\lambda_{2l})\hat{y}_{tl}^{(j)}}{a_{tl}^{t-1}} + \lambda_{2l} w\right]\right\}}{a_{tl}^{t-1} w!}, \; w = 0, 1, ..., \infty;$$

$$\hat{y}_{tl}^{(j)} \sim f_G\left(y_{tl}^{(j)} \,\middle|\, \mu_{tl}, \frac{r_l}{\mu_{tl}}\right), \; j = 1, \ldots, M_s \tag{4.9}$$

where M_s is the number of simulations and the latent $\hat{y}_{tl}^{(j)}$ are simulated from gamma distribution given the shape parameter r_l. The mean $\widehat{E}_l(W_t)$ and variance $\widehat{V}ar_l(W_t)$ of the approximated pmf $\hat{f}_{tl}(w)$ for group l and time t are calculated by:

$$\widehat{E}_l(W_t) = \sum_{w=0}^{\infty} w \hat{f}_{tl}(w) \;\text{ and }\; \widehat{V}ar_l(W_t) = \left[\sum_{w=0}^{\infty} w^2 \hat{f}_{tl}(w)\right] - [\widehat{E}_l(W_t)]^2 \tag{4.10}$$

and are compared with the values obtained in (4.8) to assess the performance of the MC integration.

To study the pmfs of the proposed GPGP model, we assume $G = 1$, $m = 1$, $q_\mu = q_a = 1$, $z_{\mu 1t} = b = 0, 1$ as the covariate effect in (4.5) and $z_{a1t} = t$ as the time-evolving covariate effect in (4.6). Hence dropping the subscript l in (4.9) since $G = 1$, the mean function is $\mu_t = \exp(\beta_{\mu 0} + \beta_{\mu 1} b)$ and the ratio function is $a_t = \exp(\beta_{a0} + \beta_{a1} t)$. Fixing $b = 1$ and $t = 2$,

we change the values of one of the model parameters at one time while keeping the other parameters constant and approximate the pmf in (4.2) using MC integration described in (4.9) with $M_s = 10000$. The marginal pmfs are displayed in Figures 4.1(a) to 4.1(d) in Appendix 4.3 with their means and variances summarized in Table 4.1 in Appendix 4.2. The mean and variance of the approximated pmf $\hat{f}_t(w)$ are calculated using (4.10) (dropping the subscript l) and are compared to the true values obtained from (4.3)-(4.4). Note that since different pmfs are drawn on the same graph for comparison, we use curves instead of bars to represent the marginal pmfs for better visualization.

==========

Figures 4.1(a) to 4.1(d) and Table 4.1 about here

==========

The close affinity between $E(W_t)$ & $\widehat{E}(W_t)$ and $Var(W_t)$ & $\widehat{V}ar(W_t)$ in Table 4.1 confirms that the MC integration gives a satisfactory approximation of the pmfs for the GPGP model in (4.2). Based on the Figures and results in Table 4.1, the parameters $\beta_{\mu 0}$ and β_{a0} control both the location and degree of dispersion of the distribution. A larger $\beta_{\mu 0}$ and a smaller β_{a0} lead to larger mean and variance of the resultant distribution. On the other hand, r serves as a dispersion parameter. Without altering the mean, a smaller r contributes to a larger variance for the distribution. Moreover, λ_2 is another important dispersion parameter which determines whether the distribution shows an underdispersion, equidispersion or overdispersion. Note

that since the gamma distribution of the underlying stochastic process $\{Y_t\}$ introduces extra variation to the GPD, a negative λ_2 does not necessarily reveal an underdispersion as shown in Table 4.1. For example, overdispersion ($E(W_t) < Var(W_t)$) is retained even when $\lambda_2 = -0.2$. But in fact, the variance is controlled by the factor $\frac{1}{(1-\lambda_2)^2} + \frac{\mu_t}{a_t^{t-1} r}$ based on (4.4). In general, the more negative the λ_2, the more underdispersed is the distribution. In summary, by varying the model parameters, the GPGP model can fit count data with different degrees of dispersion, ranging from underdispersion due to the concentration of observations over a small range of values to overdispersion due to some outlying observations.

4.3. Bayesian inference

For the statistical inference of generalized Poisson regression model, maximum likelihood (ML) method (Bae *et al.*, 2005) or moment method (Consul & Jain, 1973) are used since the model has tractable likelihood function. In the case when latent random effects are incorporated in the model, Yau *et al.* (2003) adopted the expectation-maximization (EM) method. However, since the likelihood function of the GMPGP model involves high-dimensional integration, we avoid the numerical difficulties in maximizing the intractable likelihood function by using the Bayesian approach via Markov chain Monte Carlo (MCMC) algorithms. Again, the MCMC algorithms are implemented using `WinBUGS`. The next Section derives the posterior distribution and univariate full conditional distributions followed by a description of the model selection criterion.

4.3.1. MCMC algorithms. Before implementing the MCMC algorithms, we outline the hierarchical structure of the GMPGP model under the Bayesian framework as follows:

$$\begin{aligned} w_{it} &\sim I_{i1} f_{GPD}\left(\frac{y_{it1}}{a_{it1}^{t-1}}, \lambda_{21}\right) + \cdots + I_{iG} f_{GPD}\left(\frac{y_{itG}}{a_{itG}^{t-1}}, \lambda_{2G}\right) \\ y_{itl} &\sim f_G\left(r_l, \frac{r_l}{\mu_{itl}}\right) \end{aligned}$$

where μ_{itl} and a_{itl} are given by (4.5) and (4.6) and I_{il} is the group membership indicator for subject i such that $I_{il} = 1$ if he/she comes from group l and zero otherwise. In order to construct the posterior density, some non-informative prior distributions are assigned to the model parameters as follows:

$$\beta_{jkl} \sim N(0, \tau_{jkl}^2), \quad j = \mu, a;\ k = 0, 1, \ldots, q_j;\ l = 1, \ldots, G \tag{4.11}$$

$$r_l \sim \text{Gamma}(c_l, d_l) \tag{4.12}$$

$$\lambda_{2l} \sim \text{Uniform}(-1, 1) \tag{4.13}$$

$$(I_{i1}, \ldots, I_{iG})^T \sim \text{Multinomial}(1, \pi_1, \ldots, \pi_G) \tag{4.14}$$

$$(\pi_1, \ldots, \pi_G)^T \sim Dir(\alpha_1, \ldots, \alpha_G) \tag{4.15}$$

where c_l, d_l are some positive constants and $Dir(\boldsymbol{\alpha})$ represents a Dirichlet distribution, a conjugate to multinomial distribution, with parameters $\boldsymbol{\alpha} = (\alpha_1, \ldots, \alpha_G)$. Without prior information, we assign $\tau_{jkl}^2 = 1000$ in (4.11), $c_l = d_l = 0.01$ in (4.12) and $\alpha_l = 1/G$ in (4.15) for a G-group

($G \geq 2$) model unless otherwise specified. In particular, for a 2-group ($G = 2$) GMPGP model, (4.14) is simplified to $I_{i1} \sim$ Bernoulli(π_1) with $I_{i2} = 1 - I_{i1}$ and (4.15) becomes $\pi_1 \sim$ Uniform$(0, 1)$ with $\pi_2 = 1 - \pi_1$. With the posterior means $\bar{I}_{il}$ of the group membership indicators I_{il}, patient i is classified to group l' if $\bar{I}_{il'} = \max_l \bar{I}_{il}$.

According to Bayes' theorem, the posterior density is proportional to the joint densities of complete data likelihood and prior probability distributions. For the GMPGP model, the complete data likelihood function $L(\boldsymbol{\theta})$ for the observed data w_{it} and missing data $\{y_{itl}, I_{il}\}$ is derived as:

$$L(\boldsymbol{\theta}) = \prod_{i=1}^{m} \prod_{l=1}^{G} \left\{ \pi_l \prod_{t=1}^{n_i} f_{GPD}(w_{it} | \, \boldsymbol{\beta}_{al}, \lambda_{2l}, y_{itl}) f_G(y_{itl} | \, \boldsymbol{\beta}_{\mu l}, r_l) \right\}^{I_{il}} . \quad (4.16)$$

The vector of model parameters $\boldsymbol{\theta} = (\boldsymbol{\beta}^T, \boldsymbol{\lambda}_2^T, \boldsymbol{r}^T, \boldsymbol{\pi}^T)^T$ where $\boldsymbol{\beta} = (\boldsymbol{\beta}_{\mu 1}^T, ..., \boldsymbol{\beta}_{\mu G}^T, \boldsymbol{\beta}_{a1}^T, ..., \boldsymbol{\beta}_{aG}^T)^T = (\beta_{\mu 01}, ..., \beta_{\mu q_\mu G}, \beta_{a01}, ..., \beta_{a q_a G})^T$, $\boldsymbol{\lambda}_2 = (\lambda_{21}, ..., \lambda_{2G})^T$, $\boldsymbol{r} = (r_1, ..., r_G)^T$ and $\boldsymbol{\pi} = (\pi_1, ..., \pi_G)^T$.

Treating $\{y_{itl}, I_{il}\}$ as missing observations, the joint posterior density of the GMPGP model is expressed as follows:

$$f(\boldsymbol{\beta}, \boldsymbol{\lambda}_2, \boldsymbol{r}, \boldsymbol{\pi} | \, \boldsymbol{w}, \boldsymbol{I}, \boldsymbol{y}) \propto L(\boldsymbol{\theta}) \left(\prod_{j=\mu,a} \prod_{k=0}^{q_j} \prod_{l=1}^{G} f_N(\beta_{jkl} | \, 0, \tau_{jkl}^2) \right) \left(\prod_{l=1}^{G} f_G(r_l | \, c_l, d_l) \right) \left(\prod_{l=1}^{G} f_U(\lambda_{2l} | \, -1, 1) \right) f_{Dir}(\boldsymbol{\pi} | \, \boldsymbol{\alpha})$$

where $\boldsymbol{w} = (w_{11}, w_{12}, ..., w_{mn_m})^T$, $\boldsymbol{I} = (I_{11}, I_{12}, ..., I_{mG})^T$ and $\boldsymbol{y} = (y_{111}, y_{121}, ..., y_{mn_mG})^T$. The complete data likelihood $L(\boldsymbol{\theta})$ of the GMPGP model is given by (4.16) and the priors are given by (4.11)-(4.15). In Gibbs sampling, the unknown

parameters are simulated iteratively from their univariate conditional posterior distributions which are proportional to the joint posterior density of complete data likelihood and prior densities.

The univariate full conditional posterior densities for each of the unknown model parameters $\boldsymbol{\theta}$ and missing observations $\boldsymbol{y}$ and $\boldsymbol{I}$ are given by:

$$f(\beta_{\mu kl}|\,\boldsymbol{w},\boldsymbol{I},\boldsymbol{y},\boldsymbol{\beta}^{-},\boldsymbol{\lambda}_2,\boldsymbol{r},\boldsymbol{\pi}) \propto \exp\left[-\sum_{i=1}^{m} I_{il} \sum_{t=1}^{n_i}\left(r_l \beta_{\mu kl} z_{\mu kit} + \frac{r_l y_{itl}}{\mu_{itl}}\right) - \frac{\beta_{\mu kl}^2}{2\tau_{\mu kl}^2}\right]$$

$$f(\beta_{akl}|\,\boldsymbol{w},\boldsymbol{I},\boldsymbol{y},\boldsymbol{\beta}^{-},\boldsymbol{\lambda}_2,\boldsymbol{r},\boldsymbol{\pi}) \propto$$

$$\prod_{i=1}^{m}\prod_{t=1}^{n_i}\left\{\left[\frac{y_{itl}(1-\lambda_{2l})}{a_{itl}^{t-1}} + \lambda_{2l} w_{it}\right]^{w_{it}-1} \exp\left[-\frac{y_{itl}(1-\lambda_{2l})}{a_{itl}^{t-1}} - \beta_{akl} z_{akit}(t-1)\right]\right\}^{I_{il}} \exp\left(-\frac{\beta_{akl}^2}{2\tau_{akl}^2}\right)$$

restricted to $a_{itl}^{t-1} < -\dfrac{y_{itl}(1-\lambda_{2l})}{s_{it}\lambda_{2l}}$ if $\lambda_{2l} < 0$

$$f(y_{itl}|\,\boldsymbol{w},\boldsymbol{I},\boldsymbol{y}^{-},\boldsymbol{\beta},\boldsymbol{\lambda}_{2l},\boldsymbol{r},\boldsymbol{\pi}) \propto$$

$$\left\{y_{itl}^{r_l}\left[\frac{y_{itl}(1-\lambda_{2l})}{a_{itl}^{t-1}} + \lambda_{2l} w_{it}\right]^{w_{it}-1} \exp\left[-\frac{y_{itl}(1-\lambda_{2l})}{a_{itl}^{t-1}} - \frac{r_l y_{itl}}{\mu_{itl}}\right]\right\}^{I_{il}}$$

restricted to $y_{itl} > -\dfrac{s_{it}\lambda_{2l} a_{itl}^{t-1}}{1-\lambda_{2l}}$ if $\lambda_{2l} < 0$

$$f(\lambda_{2l}|\,\boldsymbol{w},\boldsymbol{I},\boldsymbol{y},\boldsymbol{\beta},\boldsymbol{\lambda}_{2l}^{-},\boldsymbol{r},\boldsymbol{\pi}) \propto$$

$$\prod_{i=1}^{m}\prod_{t=1}^{n_i}\left\{(1-\lambda_{2l})\left[\frac{y_{itl}(1-\lambda_{2l})}{a_{itl}^{t-1}} + \lambda_{2l} w_{it}\right]^{w_{it}-1} \exp\left[-\frac{y_{itl}(1-\lambda_{2l})}{a_{itl}^{t-1}} - \lambda_{2l} w_{it}\right]\right\}^{I_{il}}$$

restricted to $\left(1 - \dfrac{s_{it} a_{itl}^{t-1}}{y_{itl}}\right)^{-1} < \lambda_{2l} < 1$

$$f(r_l|\,\boldsymbol{w},\boldsymbol{I},\boldsymbol{y},\boldsymbol{\beta},\boldsymbol{\lambda}_2,\boldsymbol{r}^{-},\boldsymbol{\pi}) \propto \prod_{i=1}^{m}\prod_{t=1}^{n_i}\left[\frac{r_l^{r_l} y_{itl}^{r_l}}{\mu_{itl}^{r_l}\Gamma(r_l)} \exp\left(-\frac{r_l y_{itl}}{\mu_{itl}}\right)\right]^{I_{il}} r_l^{c_l-1} \exp(-r_l\, d_l)$$

$$f(\pi_l|\,\boldsymbol{w},\boldsymbol{I},\boldsymbol{y},\boldsymbol{\beta},\boldsymbol{\lambda}_2,\boldsymbol{r},\boldsymbol{\pi}^{-}) \propto \pi_l^{\sum_{i=1}^{m} I_{il}+\alpha_l-1}$$

$$f(\boldsymbol{I}_i|\,\boldsymbol{w},\boldsymbol{I}^-,\boldsymbol{y},\boldsymbol{\beta},\boldsymbol{\lambda}_2,\boldsymbol{r},\boldsymbol{\pi}) \propto$$

$$\prod_{l=1}^{G}\left[\frac{\pi_l\prod_{t=1}^{n_i}\frac{(r_l y_{itl})^{r_l}(1-\lambda_{2l})}{\mu_{itl}^{r_l}\Gamma(r_l)a_{itl}^{t-1}}\left[\frac{y_{itl}(1-\lambda_{2l})}{a_{itl}^{t-1}}+\lambda_{2l}w_{it}\right]^{w_{it}-1}e^{-\left(\frac{y_{itl}(1-\lambda_{2l})}{a_{itl}^{t-1}}+\lambda_{2l}w_{it}+\frac{r_l y_{itl}}{\mu_{itl}}\right)}}{\sum_{l'=1}^{G}\left\{\pi_{l'}\prod_{t=1}^{n_i}\frac{(r_{l'}y_{itl'})^{r_{l'}}(1-\lambda_{2l'})}{\mu_{itl'}^{r_{l'}}\Gamma(r_{l'})a_{itl'}^{t-1}}\left[\frac{y_{itl'}(1-\lambda_{2l'})}{a_{itl'}^{t-1}}+\lambda_{2l'}w_{it}\right]^{w_{it}-1}e^{-\left(\frac{y_{itl'}(1-\lambda_{2l'})}{a_{itl'}^{t-1}}+\lambda_{2l'}w_{it}+\frac{r_{l'}y_{itl'}}{\mu_{itl'}}\right)}\right\}}\right]^{I_{il}}$$

$$=\prod_{i=1}^{G}\pi_{il}'^{I_{il}} = \text{Multinomial}(1,\pi_{i1}',\ldots,\pi_{iG}')$$

where $\boldsymbol{\beta}^-,\boldsymbol{y}^-,\boldsymbol{\lambda}_2^-,\boldsymbol{r}^-,\boldsymbol{\pi}^-$ and $\boldsymbol{I}^-$ are vectors of $\boldsymbol{\beta},\boldsymbol{y},\boldsymbol{\lambda}_2,\boldsymbol{r},\boldsymbol{\pi}$ and $\boldsymbol{I}$ excluding $\beta_{jkl},y_{itl},\lambda_{2l},r_l,\pi_l$ and $\boldsymbol{I}_i=(I_{i1},\ldots,I_{iG})^T$ respectively. Nevertheless, the MCMC algorithms are implemented using the user-friendly software `WinBUGS` where the sampling scheme based on the conditional posterior densities is outlined in this Section and the Gibbs sampling procedures are described in Section 1.4.3 and the posterior sample medians are adopted as parameter estimates.

4.3.2. Model selection criterion. In this analysis, we adopt the deviance information criterion (DIC), originated by Spiegelhalter *et al.* (2002), as the model selection criterion. For the GPGP model, the DIC is defined as

$$DIC=\overline{D(\boldsymbol{\theta})}+p_D$$

$$=-\frac{4}{M}\sum_{j=1}^{M}\sum_{i=1}^{m}\sum_{l=1}^{G}I_{il}'^{(j)}\left\{\ln\pi_l^{(j)}+\sum_{t=1}^{n_i}\ln\left[f_{GPD}(w_{it}|\,y_{itl}^{(j)},\boldsymbol{\beta}_{al}^{(j)},\lambda_{2l}^{(j)})f_G(y_{itl}^{(j)}|\,\boldsymbol{\beta}_{\mu l}^{(j)},r_l^{(j)})\right]\right\}$$

$$+2\sum_{i=1}^{m}\sum_{l=1}^{G}\bar{I}_{il}'\left\{\ln\bar{\pi}_l+\sum_{t=1}^{n_i}\ln\left[f_{GPD}(w_{it}|\,\bar{y}_{itl},\bar{\boldsymbol{\beta}}_{al},\bar{\lambda}_{2l})f_G(\bar{y}_{itl}|\,\bar{\boldsymbol{\beta}}_{\mu l},\bar{r}_l)\right]\right\} \quad (4.17)$$

where $\theta^{(j)}$ and $\bar{\theta}$ represent the j^{th} posterior sample and posterior mean of parameter θ respectively,

$$I_{il}^{'(j)} = \frac{\pi_l^{(j)} \prod_{t=1}^{n_i} \left\{ f_{GPD}(w_{it} | \, y_{itl}^{(j)}, \boldsymbol{\beta}_{al}^{(j)}, \lambda_{2l}^{(j)}) f_G(y_{itl}^{(j)} | \, \boldsymbol{\beta}_{\mu l}^{(j)}, r_l^{(j)}) \right\}}{\sum_{l'=1}^{G} \pi_{l'}^{(j)} \prod_{t=1}^{n_i} \left[f_{GPD}(w_{it} | \, y_{itl'}^{(j)}, \boldsymbol{\beta}_{al'}^{(j)}, \lambda_{2l'}^{(j)},) f_G(y_{itl'}^{(j)} | \, \boldsymbol{\beta}_{\mu l'}^{(j)}, r_{l'}^{(j)}) \right]},$$

and $\bar{I}'_{il}$ is defined in a similar way by replacing $y_{itl}^{(j)}$ and $\boldsymbol{\theta}^{(j)}$ with $\bar{y}_{itl}$ and $\bar{\boldsymbol{\theta}}$. For model selection, the best model should give the smallest DIC indicating it has the best fit after accounting for the model complexity.

4.4. Simulation studies

The objectives of the simulation studies are twofold: (1) to compare the similarities and differences in the properties of the GPGP model and the RPGP-EP model introduced in Chapter 3 and (2) to assess the competence of the two models under different levels of dispersion. Regarding the first objective, we performed a 'cross' simulation study. For the second objective, the two models were fitted to some data with different degrees of dispersion. The procedures and results of these studies are discussed in the next two Sections.

4.4.1. Comparisons between GPGP and RPGP models. We conducted some cross simulations in which data simulated from one model is 'cross'-fitted by both models. By setting $G = 1$ and $q_\mu = q_a = 1$, $h = 100$ data sets are simulated from each of the GPGP model in (4.7) or RPGP-EP model in (3.12) with the true parameters given in Table 4.2 in Appendix 4.2, and they are fitted using both GPGP and RPGP-EP models. Each data set contains

$m = 80$ time series of length $n_i = 8$ from $m_0 = 40$ subjects in the control group ($b = 0$) and another $m_1 = 40$ subjects in the treatment group ($b = 1$). In both GPGP and RPGP-EP models (dropping subscript l since $G = 1$), the treatment effect $z_{\mu 1it} = b$ is adopted in the mean functions in (4.5) and (3.2) and time ($z_{a1it} = t$) is incorporated as the time-evolving effect in and the ratio functions in (4.6) and (3.3). In addition, different values are assigned to $\beta_{\mu k}$ and $\beta_{ak}, k = 0, 1$ to give different trend patterns and baseline levels. Moreover, the dispersion parameter ν of the RPGP-EP model is set to be 0.1 to attain overdispersion in data set 1 and λ_2 of the GPGP model is set to be -0.99 to acquire underdispersion in data set 2.

Implemented using `WinBUGS` and `R2WinBUGS` with non-informative priors as described in Section 4.3.1 for the GPGP model and Section 3.4 for the RPGP-EP model, the parameter estimate $\hat{\theta}$ is calculated as the average of $h = 100$ posterior medians $\hat{\theta}^{(j)}$ in the j^{th} data set. To examine the precision of the MCMC sampling algorithms, the standard deviation (SD) of $\hat{\theta}^{(j)}$ over $h = 100$ simulated data sets for each parameter θ is evaluated. To assess the accuracy of parameter estimates when the data set is simulated from and fitted by the same model, we calculate the mean squared error (MSE) for each parameter θ which is given by:

$$MSE = \frac{1}{h}\sum_{j=1}^{h}(\hat{\theta}^{(j)} - \theta)^2.$$

For model assessment, the average DIC is used to measure the goodness-of-fit of the model while taking into account the model complexity. For

the GPGP model, DIC is computed using (4.17) while that of the RPGP-EP model is calculated by (3.19). Table 4.2 summarizes the results of this cross simulation study including the true parameters under different models and various model assessment criteria such as the SD, MSE and DIC. The reasonably small SD and MSE for all the parameters reflect that the MCMC algorithms give precise and unbiased estimates except for r which has a larger MSE due to its relatively larger magnitude of the estimate.

To demonstrate the level of dispersion in each data set, we approximated the pmfs $\hat{f}_t(w)$ based on the sets of true parameters (true model) and fitted parameters (GPGP and RPGP-EP models) using MC integration described in (4.9) for the GPGP model and in (3.5) for the RPGP-EP model. Based on $\hat{f}_t(w)$, the mean and variance of the true models, GPGP and RPGP-EP models are calculated and reported in Table 4.3 in Appendix 4.2. Note that unlike the GPGP model, the unconditional mean and variance of the RPGP-EP model cannot be expressed explicitly as in (4.3) and (4.4) because $\{Y_{it}\}$ follows log-uniform distribution. For fair comparison we therefore evaluate the mean $\widehat{E}(W_t)$ and variance $\widehat{V}ar(W_t)$ using (4.10) based on the approximated pmfs $\hat{f}_t(w)$ in the MC integration for both models in the sequel.

As indicated in Table 4.3, for data set 1, the overall variance of the true pmfs is 2.53 which is larger than the overall mean 2.05 showing overdispersion. Based on the estimates of $\boldsymbol{\beta}_a$ and $\boldsymbol{\beta}_\mu$, the true mean shows a gradually increasing trend till $t = 3$ and a substantially decreasing trend afterwards. This non-monotone trend is well captured by the GPGP and

RPGP-EP models. Besides, the two models give similar mean and variance across time and are comparable to those of the true model. These results reveal that both models can cope with overdispersed count data and therefore they have similar average DIC with the GPGP model slightly outperforming the RPGP-EP model (1828.3 versus 1860.4) in Table 4.2.

==========

Tables 4.2 and 4.3 about here

==========

On the other hand, in data set 2, the overall variance (1.31) of the true pmfs is less than the overall mean (3.5) showing underdispersion. This time the trend is generally increasing but turns downwards after $t = 5$. Although both models can describe the non-monotone trend pattern, the RPGP-EP model which cannot accommodate underdispersed data shows a poor model fit with a substantially larger average DIC than the GPGP model (1756.6 versus 2178.7) in Table 4.2. In addition, the variance of the RPGP-EP model is inevitably larger than that of the true model as the furthest degree of dispersion this model can attain is only equidispersion. This explains why the mean of the RPGP-EP model is underestimated across time. On the contrary, the GPGP model shows an overwhelming advantage over the RPGP-EP model in fitting underdispersed data as supported evidently by the affinity in the variance between the GPGP and true models in Table 4.3.

This simulation study highlights the fact that while the two models are competitive in dealing with overdispersed data, only the GPGP model which has a more flexible dispersion structure is suitable for analyzing underdispersed data.

4.4.2. Assessment of level of dispersion. In the second part of the simulation studies, one data set was selected from the data set 2 which is simulated from the GPGP model in the cross simulation study as described in the previous Section with true parameters given in Table 4.2. This data set which exhibits an underdispersion across time as revealed by the mean and variance in Table 4.4 in Appendix 4.2 was fitted to both GPGP and RPGP-EP models. Results in Table 4.5 show that the GPGP model consistently gives a better model fit since it can allow for underdispersion while the RPGP-EP model fails to do so.

Two more data sets were then generated by adding some outliers in order to make the data distribution become equidispersed and overdispered (see Table 4.4). More specifically, we add a constant to all observations of the last subject in both control group ($i = 40$) and treatment group ($i = 80$) to study the responses of model parameters to the presence of outlying values. Without altering the overall trend and with a slight increase in the overall mean across time, the data distribution becomes equidispersed by adding a constant nine and overdispersed by adding a constant fifteen.

In the case of equidispersion, for the RPGP-EP model, the parameters of the mean and ratio functions do not alter too much since the trend movement remains unchanged and the level of time series only increases slightly. As expected, the shape parameter ν for $\{Y_{it}^* = \ln Y_{it}\}$ has changed sharply from 0.15 to 0.88 and the scale parameter σ has increased moderately. These imply that the distribution of the underlying latent stochastic process $\{Y_{it}^*\}$ becomes more heavy-tailed and overdispersed to accommodate the outlying observations. While for the GPGP model, again the parameters in the mean and ratio functions remain nearly stagnant except for the shape parameter r of $\{Y_{it}\}$ which drops abruptly to allow for the inflated variance due to the enlarged observations. The dispersion parameter λ_2 in the GPGP model however does not increase but instead becomes slightly more negative, due to the fact that the variance of the distribution is controlled by the factor $\dfrac{1}{(1-\lambda_2)^2} + \dfrac{\mu_t}{a_t^{t-1} r}$, which involves both λ_2 and r as shown in (4.4). This reveals that the shape parameter r of the gamma distribution for $\{Y_{it}\}$ has a stronger effect than the dispersion parameter λ_2 in the GPD for the outcome $\{W_{it}\}$ on the level of dispersion and the decrease in r 'absorbs' the outlying effect by increasing the tailedness of the model distribution. On the contrary, the RPGP-EP model downweighs the outlying effect by increasing the shape parameter ν of the EP distribution for $\{Y_{it}^*\}$. Comparing the model fit with the first case of underdispersion, the DIC shows a substantially larger percentage change for the RPGP-EP

model (2.6% versus 10.4%) indicating that the GPGP model still performs better in the situation of equidispersion.

In the case of overdispersion, the parameters show similar movements with a dramatic increase in ν in the RPGP-EP model (0.88 to 1.98) and a further decrease in r in the GPGP model (6.11 to 4.09). However this time the percentage increase in the DIC compared with the situation of equidispersion for both models becomes closer because they both can handle overdispersed data by increasing the tailedness of the model distribution, in different ways. In the RPGP-EP model, the outlying effect is downweighed by widening the interval of the uniform distribution of the underlying latent stochastic process $\{Y_{it}^*\}$ whereas in the GPGP model, it is accommodated by magnifying the variance of $\{Y_{it}\}$.

Lastly we also investigate the case of zero-inflation, a common source of overdispersion. To compare the performance of the two models in modelling zero-inflated data with a high proportion of zeros, we simulated a data set with the same structure mentioned at the beginning of Section 4.4.1 from the zero-inflated GPGP model with the following pmf:

$$f_z(w_{it}) = \begin{cases} \phi + (1-\phi)f(w_{it}), & \text{when } w_{it} = 0 \\ (1-\phi)f(w_{it}), & \text{when } w_{it} > 0 \end{cases}$$

where $f(w_{it})$ is given by (4.2), $\phi = 0.5, \beta_{\mu 0} = 2.0, \beta_{\mu 1} = -0.5, \beta_{a0} = 0.8, \beta_{a1} = -0.1, \lambda_2 = 0.2$ and $r = 1.0$. The data set simulated from the zero-inflated GPGP model has a high percentage of zeros observations (78%) which leads to overdispersion and a U-shaped trend pattern as shown

in Table 4.4. Not surprisingly, since both models can cope with overdispersed data, the model fits of the two models indicated in Table 4.5 are close with the GPGP model marginally outperforms the RPGP-EP model. The dispersion parameter $\hat{\lambda}_2 = 0.39$ in the GPGP model and the shape parameter $\hat{\nu} = 1.95$ in the RPGP-EP model also agree with each other and confirm overdispersion.

==========

Tables 4.4 and 4.5 about here

==========

In sum, the two simulation studies manifest the pitfall of RPGP-EP model in modelling underdispersed data. On the contrary, GPGP model is more comprehensive as it can fit data with different degrees of dispersion by varying the two model parameters λ_2 and r. As the two simulation studies have revealed the satisfactory performance of the GPGP model, its practicability will be demonstrated in the following real data analysis.

4.5. Real data analysis

In this Section, the applicability of the GMPGP model is illustrated via a panel data analysis of the arrest for cannabis use in New South Wales (NSW), Australia. The background and the properties of the data are first described. Then the results of the analysis and model comparison are interpreted in detail.

4.5.1. Overview. Cannabis is a recreational drug with few toxic acute effects compared to other illicit drugs. The prevalence of canabbis use is high as it gives users a sense of mild euphoria and relaxation but also has some short-term side effects such as drowsiness and loss of coordination. An overdose of cannabis will exert deleterious effect on motor skills and reaction time causing road traumas (Jones *et al.*, 2005). Besides, the cannabis abusers and quitters will experience paranoia and other withdrawal symptoms which make them feel irritated or make them become aggressive. These may result in violent behaviours and assaults and consequently lead to mounting crime rates.

Unfortunately, the arrest of cannabis use was not effective as recognized by the NSW Drug Summit. To alleviate this problem, the NSW Police and Drug and Alcohol Coordination initiated the Cannabis Cautioning Scheme in April 2000 to assist offenders to consider the legal and health ramifications of their cannabis use and seek treatment and support (Baker & Goh, 2004). Under this scheme, first- and second-time offenders who are caught using or possessing of not more than 15g of dried cannabis would receive a formal police caution rather than facing criminal charges and court proceedings. The caution includes information about the consequence of cannabis use and access to treatment and support services. It was expected that the scheme could reduce the number of cannabis users throughout the state but this effect still remained skeptical (Baker & Goh, 2004).

The objective of this data analysis is to evaluate the effectiveness of the policy through the study of trend movement of the number of arrests for dealing and trafficking of cannabis in NSW during 2001 to 2008. The data is available on the official website of the NSW Bureau of Crime Statistics and Research (http://www.bocsar.nsw.gov.au/lawlink/bocsar/ll_bocsar.nsf/pages/bocsar_onlinequeries) and is described as follows.

4.5.2. Data and model fitting. The data set contains 344 yearly number W_{it} of arrests for cannabis dealing and trafficking from 2001 to 2008 in 43 local government areas (LGAs) within Sydney, the metropolitan region of NSW with the highest prevalence of drug dealing and trafficking amongst all NSW divisions. This results in $m = 43$ time series in which each consists of eight yearly counts ($n_i = 8$) as reported in Appendix 4.1.

Clearly, the data exhibits cluster effects and overdispersion due to the fact that some LGAs like Sydney, Bankstown, Blacktown, Campbelltown, have significantly higher number of arrests for cannabis dealing and trafficking throughout the studying period. Therefore, we incorporate mixture effects into the model as described in Section 4.2.3. We postulate that there exists G groups of LGAs in which each of the groups has distinct level of arrests and trend pattern. Without any prior information about the number of groups that can be classified from the data, we fit the model with $G = 1, 2, \ldots, m$ group(s) and determine the value of G by assessing the DIC and the significance of the model parameters. Moreover, the time series generally shows a decreasing trend during 2001 to 2004, stabilizes in

2004-2005 followed by a further drop in 2005-2007 but rebounds slightly in 2008. In view of these characteristics and the desire to examine the competence of the GMPGP model in handling overdispersed data by comparing with the RMPGP-EP model, we fitted both GMPGP and RMPGP-EP models to the data taken into account the non-monotone trend patterns, overdispersion and population heterogeneity.

Considering the non-monotone trends, we incorporate a time evolving effect $z_{a1it} = \ln t$ in the ratio function a_{itl} in (4.6). Since there is no measure of covariate effect on the trend level in the data, we simply set the mean function $\mu_{itl} = \beta_{\mu 0l}$. Regarding the cluster effects, as we have no prior information about the number of groups in the panel data, we fitted the GMPGP models with $G = 1, 2, 3, \ldots, m$ group(s) respectively using the MCMC algorithms described in Section 4.3.1. For the priors, we specify $c_l = 0.1$, $d_1 = 0.05$ and $d_2 = 0.1$ in (4.12) while other hyperparameters are specified as described in Section 4.3.1. The results of the analysis are elaborated in the following Section.

4.5.3. Results. The 1-group GMPGP model ($G = 1$) fails to explain the population heterogeneity leaving a large deviation between the observed and predicted counts for some LGAs with high occurrences of cannabis dealing and trafficking. This poor fit is revealed from the larger DIC (3788.36) of the 1-group GMPGP model when compared to that of the 2-group GMPGP model ($DIC = 3751.78$). However, a 3-group GMPGP model ($G = 3$) overfits the data with one cluster actually degenerating.

Therefore we stop the model fitting process at $G = 3$ and confirm that the 2-group GMPGP model ($G = 2$) is the most appropriate one to fit the data and further fit a 2-group RMPGP-EP model for model comparison. In addition, we find that the parameters $\beta_{a1l}, l = 1, 2$ in the ratio functions are insignificant (95% CI for β_{a1l} contains zero) for both models indicating that the trends are indeed monotone in both groups. Hence we drop the redundant time-evolving covariate $\ln t$ in the ratio functions and they become $a_{itl} = \exp(\beta_{a0l})$. In Appendix 4.2, Table 4.6 summarizes the parameter estimates, standard errors (SE) and model selection criterion DIC for the GMPGP and RMPGP-EP models.

==========

Table 4.6 about here

==========

In the two fitted models, two distinct groups of LGAs are identified, namely the high-level ($l = 1$) and low-level ($l = 2$) groups since the initial trend of the former group is higher across time ($\hat{\beta}_{\mu 01} > \hat{\beta}_{\mu 02}$). For the GMPGP model, the high-level group ($l = 1$) demonstrates a stationary trend since β_{a01} is not significantly different from zero (95% CI for β_{a01}:$[-0.0062, 0.1033]$) while the trend low-level group ($l = 2$) shows a monotone declining trend (95% CI for β_{a02}:$[0.0326, 0.1493]$). For the RMPGP-EP model, both high-level and low-level groups exhibit a monotone decreasing trend as the two parameters β_{a01} (95% CI:$[0.0095, 0.1344]$) and β_{a02} (95% CI:$[0.0401, 0.1528]$) are significantly greater than zero.

Concerning the classification, the LGA i is classified to group l, $l = 1, 2$ if the posterior mean $\bar{I}_{il} = \max_{l'} \bar{I}_{il'}$. With respect to the GMPGP model, 15 LGAs are categorized to the high-level group ($l = 1$) with $\bar{I}_{i1} = \max_{l'} \bar{I}_{il'}$ and as expected Sydney which is the central business district with a high concentration of pubs and night clubs belongs to this group. Most of the LGAs classified in this group, including Bankstown, Canterbury, Fairfield, Liverpool, Parramatta, Holroyd, Penrith and Blacktown, are located in the central or outer west of Sydney. While a few of them like Baulkham Hills, Gosford and Wyong are situated in northern Sydney, only two LGAs, Hurstville and Sutherland Shire are located in the south and one LGA, Campbelltown in the southwest. The categorization implies that the arrests for cannabis dealing and trafficking are concentrated in the inner and western part of Sydney. These results concur with the findings in Baker & Goh (2004) that the number of charges laid for minor cannabis use in April 2001 to March 2003 were significantly higher in the inner metropolitan area like Sydney and some western local area commands like Bankstown, Parramatta, Holroyd, Penrith and Blacktown.

The classification of the LGAs in the RMPGP-EP model are nearly identical except that 2 more LGAs, Marrickville in the inner Sydney area and Waverley in the eastern Sydney area are categorized in the high-level group. The affinity of the classification may possibly be due to the similar way that the two models capture the population heterogeneity by incorporating mixture effects. Since the LGAs with outlying observations are

classified into the high-level group ($l = 1$), this group thus exhibits a higher degree of overdispersion in contrast to the low-level group ($l = 2$) which comprises of LGAs with low incidence counts. To verify this, we compare the mean and variance over time of the two groups for both GMPGP and RMPGP-EP models. To begin with, we evaluate the approximated pmfs $\hat{f}_{tl}(w)$ of the two groups using MC integration described in (4.9) for the GMPGP model with $a_{tl} = \exp(\beta_{a0l})$ and $\mu_{tl} = \exp(\beta_{\mu 0l})$. For the RMPGP-EP model, $\hat{f}_{tl}(w)$ is obtained by

$$\hat{f}_{tl}(w) = \sum_{j=1}^{M_s} f_P\left(w \,\middle|\, \frac{e^{\hat{y}_{tl}^{*(j)}}}{a_{tl}^{t-1}}\right) = \sum_{j=1}^{M_s} \frac{\exp\left(-\frac{e^{\hat{y}_{tl}^{*(j)}}}{a_{tl}^{t-1}}\right)\left(\frac{e^{\hat{y}_{tl}^{*(j)}}}{a_{tl}^{t-1}}\right)^w}{w!},\ w = 0, 1, \ldots, \infty; \text{ and}$$

$$\hat{y}_{tl}^{*(j)} \sim f_{EP}(y_{tl}^{*(j)} |\, \mu_{tl}^*, \sigma_l, \nu_l),\ j = 1, \ldots, M_s$$

where $f_{EP}(\cdot)$ is given by (3.6) and $\mu_{tl}^* = \beta_{\mu 0l}$. Then we compute the observed pmfs under the two models at different time t by:

$$f_{tl}(w) = \frac{\sum_{i=1}^{m} \bar{I}_{il} I(W_{it} = w)}{\sum_{w'=0}^{\infty} \sum_{i=1}^{m} \bar{I}_{il} I_{itl}(W_{it} = w')}, w = 0, 1, \ldots$$

where $I(W_{it} = w) = 1$ if $W_{it} = w$ and 0 otherwise and $\bar{I}_{il}$ is the posterior mean of the membership indicator I_{il} for LGA i in group l. For both models, the predicted mean $\widehat{E}_l(W_t)$ and variance $\widehat{V}ar_l(W_t)$ are calculated using (4.10). Similarly, the observed mean $E_l(W_t)$ and variance $Var_l(W_t)$ are computed by replacing $\hat{f}_{tl}(w)$ with $f_{tl}(w)$. These means and variances are reported in Table 4.7 in Appendix 4.2. Noticeably, the degree of overdispersion is substantially higher in the high-level group since some extreme

observations ($w_{4,1} = 155, w_{4,2} = 114$) in Sydney, one of the LGAs in this group, inflate the variability of the counts dramatically. However, as both GMPGP and RMPGP-EP models are robust to outliers and can downweigh its influence in parameter estimation, the predicted variances of the high-level group are underestimated in the first two years but are getting close to the observed variances in the next six years for both models.

==========

Table 4.7 about here

==========

To investigate the trend movements, the distinct patterns for the two groups are illustrated in Figure 4.2 in Appendix 4.3 by plotting the observed mean $E_l(W_t)$ and predicted mean $\widehat{E}_l(W_t)$ under different models. The Figure shows a declining trend in both high-level and low-level groups with a relatively slower rate in the latter group. Moreover, the closeness between the observed and predicted trends justify the adequacy of the models to fit the panel data. Overall, these results give statistical evidence that the Cannabis Caution Scheme is associated with the drop in the number of arrests for cannabis dealing and trafficking in NSW. In other words, our results imply that the Cannabis Caution Scheme is effective in reducing the number of cannabis users within the Sydney metro area. This finding also agrees with the 2007 National Drug Strategy Household Survey (Australian Institute of Health and Welfare, 2008) that the proportion of the population aged 14 years and over who had used cannabis in the last 12 months has

fallen from 15.8% in 2001 to 14.4% in 2004 and further reduced to 11.6% in 2007.

==========

Figure 4.2 about here

==========

In the model comparison, after accounting for the model complexity, the GMPGP model with a smaller DIC outperforms the RMPGP-EP model and gives a better fit to the data. To explain this, we investigate the difference in model performance by comparing the observed pmf $f_{tl}(w)$ and fitted pmf $\hat{f}_{tl}(w)$ under the two models. Figures 4.3(a) and 4.3(b) in Appendix 4.3 display the observed and fitted pmfs of the high-level group in both models at two chosen times $t = 1$ and $t = 5$. They clearly show that the distribution of the GMPGP model has a heavier tail to accommodate the outlying observations. The case is similar for the low-level group as shown in Figures 4.4(a) and 4.4(b) in Appendix 4.3. Because of the heavier tail, relative to the RMPGP-EP model, the GMPGP model generally gives higher predicted counts and lower variances for both groups as revealed in Table 4.7.

==========

Figures 4.3(a), 4.3(b), 4.4(a) and 4.4(b) about here

==========

Lastly, for the GMPGP model, the best model, according to the DIC, we tested for the serial correlation using the procedures described in Section 4.2.4. Starting from some lower lags, the p-values of the chi-square test for autocorrelation up to lag 1,2 and 3 are 0.005, 0.015 and 0.124 respectively. These results confirm the presence of serial correlation in the data and therefore we refit the GMPGP model by including the AR(1) and AR(2) terms into the mean function μ_{itl}. However, the AR(2) term in the high-level group and all the AR terms in the low-level group are insignificant and thus are discarded. The final model is the 2-group GMPGP model with an AR(1) term incorporated into the mean function $\mu_{it1} = \exp(\beta_{\mu 01} + \beta_{\mu 11} w_{i,t-1})$ for the high-level group. The parameter estimates with SE for the final model abbreviated as GMPGP-AR(1) model are reported in Table 4.7. Not surprisingly, the parameter estimates are comparable to those of the GMPGP model and the GMPGP-AR(1) model has a better DIC indicating that the model fit has improved. Moreover, the significant positive $\beta_{\mu 11} = 0.0198$ implies that the current observation is positively correlated with the previous observation in the high-level group.

Last but not least, to illustrate their distinct trend movements and the categorization of the LGAs in the GMPGP-AR(1) model, we plot the predicted individual and group trends for both high-level ($l = 1$) and low-level ($l = 2$) groups in Figures 4.5(a) and 4.5(b) in Appendix 4.3. The predicted number of arrest for cannabis dealing and trafficking for an individual LGA i at time t is given by $\widehat{W}_{it} = \bar{I}_{i1}\widehat{E}_1(W_{it}) + \bar{I}_{i2}\widehat{E}_2(W_{it})$ where $E_l(W_{it})$ is

given by (4.8) and $\bar{I}_{il}$ is the posterior mean of the membership indicator for group l, while that for the predicted group trend is simply given by a weighted average of $E_l(W_{it})$ given by (4.10) with weight $\bar{I}_{il}$ for group l, that is, $\frac{\sum_i \bar{I}_{il} E_l(W_{it})}{\sum_i \bar{I}_{il}}$. Note that for clearer visualization, Figure 4.5(b) does not include the outlying predicted trend for the LGA, Sydney.

==========

Figures 4.5(a) and 4.5(b) about here

==========

Figure 4.5(a) vividly reveals that the LGA Sydney, though has a remarkably high number of arrests for cannabis dealing and trafficking, shows the greatest drop throughout the entire studying period. While compared to Sydney, other LGAs generally show a downward trend with a much slower decreasing rate. Furthermore, Figure 4.5(b) shows the clear classification of the LGAs by incorporating mixture effects into the model and the predicted group trend in the high-level group demonstrates the 'invulnerability' of the GMPGP-AR(1) model to extreme observations. In summary, the findings with respect to the trend movements certainly provide useful information for the allocation of police force to bring down the cannabis use especially in those LGAs with higher number of arrests for cannabis dealing and trafficking.

4.6. Discussion

In this Chapter, we propose the generalized Poisson geometric process (GPGP) model which relaxes the restriction of overdispersion in the previous PGP-Ga and RPGP models. The GPGP model adopts a more general data distribution, the generalized Poisson distribution (GPD), to account for both underdispersed and overdispersed data. Moreover, similar to RPGP models, it can accommodate non-monotone trends, serial correlation, covariate and cluster effects. By varying different model parameters, the mean and variance of the GPGP model are reported in Table 4.1 and their pmfs are illustrated in Figures 4.1(a) to 4.1(d). Although the marginal pmf of the GPGP model does not have a closed-form, Monte Carlo (MC) integration in (4.9) can be used to approximate the pmf, and hence the mean as well as the variance. Results in Table 4.1 show that the model can accommodate data with trends and different degrees of dispersion.

The GPGP model can be implemented through MCMC algorithms using `WinBUGS`. In order to assess the comprehensiveness of the proposed model, we perform a model comparison with the RPGP-EP model proposed in Chapter 3 because it can fit data ranging from equidispersion to heavy overdispersion. We investigate the suitability and performances of the two models by conducting two simulation studies. The first study is a cross simulation which assesses the similarities and differences of their model properties. The second study compares their competence under four situations: (1) underdispersion; (2) equidispersion; (3) overdispersion; and

(4) zero-inflation. Our findings highlight that while the performances of the two models are comparable and satisfactory in the case of overdispersion, the GPGP model has a much better performance in handling underdispersed data in which the RPGP-EP model falls short to do so.

Lastly, the analysis of cannabis data demonstrates the applicability of the GMPGP model to account for cluster effects, trend movements and serial correlation as well as compares its competence in handling overdispersion with the RMPGP-EP model. Results show that even the data is overdispersed, the GMPGP model still outperforms the RMPGP-EP model as it can accommodate outliers by the heavier tail of the model distribution. On the other hand, in the presence of outliers, the RMPGP-EP model downweighs the detrimental effect of outliers by allowing a leptokurtic distribution for the stochastic process $\{Y_{it}^{*}\}$. Nevertheless, the different degrees of emphasis on outlyling observations make the two models appropriate under panel studies with different objectives.

Appendix 4.1

Number of arrests for cannabis dealing and trafficking in Sydney during 2001-2008

Statistical Subdivision	LGA	year 2001	2002	2003	2004	2005	2006	2007	2008
Inner Sydney	Botany Bay	6	2	4	2	3	1	1	2
	Leichhardt	2	1	1	2	0	1	1	2
	Marrickville	7	5	6	4	7	8	5	5
	Sydney	143	114	88	85	69	44	46	57
Eastern Suburbs	Randwick	8	3	6	8	8	2	4	1
	Waverley	4	7	13	6	12	1	2	3
	Woollahra	2	0	0	1	0	0	0	4
St George-Sutherland	Hurstville	4	8	10	3	2	3	5	13
	Kogarah	4	2	5	4	4	3	2	1
	Rockdale	5	4	6	6	5	3	2	5
	Sutherland Shire	7	8	11	16	9	9	3	9
Canterbury-Bankstown	Bankstown	22	17	12	20	22	13	19	15
	Canterbury	18	9	13	16	17	22	17	26
Fairfield-Liverpool	Fairfield	18	13	5	17	24	12	9	6
	Liverpool	47	9	13	15	17	8	14	5
Outer South Western Sydney	Camden	1	2	2	2	1	2	1	3
	Campbelltown	18	22	13	16	34	35	5	16
	Wollondilly	5	3	0	2	1	0	0	1
Inner Western Sydney	Ashfield	4	5	6	2	2	1	1	2
	Burwood	1	2	2	5	2	1	2	4
	Canada Bay	3	2	0	5	1	0	2	2
	Strathfield	6	3	0	3	1	0	1	1
Central Western Sydney	Auburn	2	0	3	2	7	5	3	6
	Holroyd	6	11	3	9	5	9	3	7
	Parramatta	22	15	9	18	15	12	8	7
Outer Western Sydney	Blue Mountains	3	5	3	4	0	2	6	2
	Hawkesbury	9	6	4	2	7	3	2	3
	Penrith	30	5	13	10	18	5	3	8
Blacktown	Blacktown	30	25	26	19	14	16	13	5
Lower Northern Sydney	Hunters Hill	0	0	2	0	1	0	0	0
	Lane Cove	0	0	0	0	0	0	0	1
	Mosman	2	0	1	0	4	1	0	0
	North Sydney	4	5	1	2	2	2	1	1
	Ryde	10	11	3	3	1	4	0	1
	Willoughby	3	0	1	2	2	0	1	0
Central Northern Sydney	Baulkham Hills	11	2	2	2	5	14	12	3
	Hornsby	8	6	7	6	4	4	0	3
	Ku-ring-gai	2	0	3	0	2	3	1	0
Northern Beaches	Manly	3	0	1	3	1	4	0	5
	Pittwater	1	1	6	0	1	1	0	1
	Warringah	5	10	2	3	4	2	2	7
Gosford-Wyong	Gosford	9	11	7	26	6	5	3	4
	Wyong	5	4	21	5	13	7	6	4
mean		11.63	8.33	7.77	8.28	8.21	6.23	4.79	5.84
variance		512.9	306.9	190.2	187.7	148.2	81.4	63.7	88.9

Appendix 4.2

Tables

Table 4.1: Moments of marginal pmfs for GPGP model under a set of floating parameters with fixed values of $\lambda_2 = 0.2, r = 30, \beta_{\mu 0} = 3, \beta_{\mu 1} = -0.5, \beta_{a0} = -0.5, \beta_{a1} = 0.2$

floating	**Using (4.10)**		**Using (4.3)&(4.4)**		**floating**	**Using (4.10)**		**Using (4.3)&(4.4)**	
parameter	$\widehat{E}(W_t)$	$\widehat{V}ar(W_t)$	$E(W_t)$	$Var(W_t)$	**parameter**	$\widehat{E}(W_t)$	$\widehat{V}ar(W_t)$	$E(W_t)$	$Var(W_t)$
$\lambda_2 = -0.5$	13.413	11.924	13.464	12.026	$r = 1.2$	13.328	172.493	13.464	172.097
$\lambda_2 = -0.2$	13.468	15.544	13.464	15.392	$r = 2.0$	13.437	105.519	13.464	111.673
$\lambda_2 = 0.2$	13.476	27.207	13.464	27.079	$r = 8.0$	13.427	44.339	13.464	43.696
$\lambda_2 = 0.5$	13.476	60.041	13.464	59.897	$r = 40.0$	13.415	25.402	13.464	25.569
$\beta_{\mu 0} = 0.7$	1.361	2.191	1.350	2.170	$\beta_{a0} = -1.0$	22.013	50.025	22.198	51.109
$\beta_{\mu 0} = 1.5$	3.012	5.030	3.004	4.995	$\beta_{a0} = -0.4$	12.081	23.584	12.182	23.982
$\beta_{\mu 0} = 2.0$	4.968	8.611	4.953	8.557	$\beta_{a0} = 0.2$	6.630	11.777	6.686	11.937
$\beta_{\mu 0} = 3.0$	13.460	26.895	13.464	27.079	$\beta_{a0} = 0.8$	3.639	6.113	3.669	6.182

Table 4.2: Parameter estimates, SD, MSE and DIC for GPGP and RPGP-EP models in cross simulation (Study 1)

data	**model**	**parameter**	**true**	**estimate**	SD	MSE	DIC
1	GPGP	β_{a0}		-0.4948	0.0817		**1828.30**
		β_{a1}		0.0997	0.0114		
		$\beta_{\mu 0}$		0.7838	0.0872		
		$\beta_{\mu 1}$		-0.2379	0.0466		
		λ_2		-0.0386	0.0432		
		r		6.2626	1.1012		
	RPGP-EP	β_{a0}	-0.5	-0.4289	0.0729	0.0103	1860.39
		β_{a1}	0.1	0.0926	0.0105	0.0002	
		$\beta_{\mu 0}$	1.0	0.8287	0.0769	0.0352	
		$\beta_{\mu 1}$	-0.5	-0.2812	0.0656	0.0521	
		ν	0.1	0.2005	0.1178	0.0238	
		σ	0.5	0.6272	0.0701	0.0210	
2	GPGP	β_{a0}	-0.05	-0.0523	0.0334	0.0011	**1756.63**
		β_{a1}	0.005	0.0053	0.0040	0.00002	
		$\beta_{\mu 0}$	-2.0	-2.0857	0.3033	0.0984	
		$\beta_{\mu 1}$	-0.5	-0.2589	0.0225	0.0586	
		λ_2	-0.99	-0.7616	0.1207	0.0713	
		r	30	26.7556	8.2767	78.3453	
	RPGP-EP	β_{a0}		-0.1281	0.0400		2178.65
		β_{a1}		0.0128	0.0045		
		$\beta_{\mu 0}$		0.9573	0.0652		
		$\beta_{\mu 1}$		-0.1952	0.0464		
		ν		0.0875	0.0248		
		σ		0.3653	0.0286		

Table 4.3: Mean and variance of the true, GPGP and RPGP-EP models in cross simulation (Study 1)

			time								average
data	**model**		1	2	3	4	5	6	7	8	**over time**
1	true	mean	2.255	3.104	3.356	3.056	2.278	1.379	0.678	0.279	2.048
	GPGP		1.966	2.631	2.899	2.605	1.935	1.165	0.578	0.235	1.752
	RPGP-EP		2.177	2.739	2.923	2.557	1.900	1.137	0.573	0.243	1.781
	true	variance	2.731	3.964	4.362	3.924	2.737	1.550	0.719	0.285	2.534
	GPGP		2.439	3.548	4.032	3.519	2.389	1.307	0.590	0.227	2.256
	RPGP-EP		2.861	3.791	4.150	3.495	2.408	1.322	0.620	0.252	2.363
2	true	mean	3.262	3.391	3.499	3.571	3.610	3.606	3.566	3.495	3.500
	GPGP		2.943	3.066	3.168	3.235	3.271	3.265	3.229	3.160	3.167
	RPGP-EP		2.430	2.688	2.902	3.055	3.138	3.133	3.058	2.900	2.913
	true	variance	1.199	1.262	1.315	1.339	1.361	1.361	1.340	1.312	1.311
	GPGP		1.281	1.352	1.405	1.432	1.456	1.458	1.436	1.403	1.403
	RPGP-EP		2.695	3.024	3.289	3.487	3.584	3.579	3.485	3.282	3.303

Table 4.4: Mean and variance of four simulated data sets under different situations (Study 2)

		time								average
data		1	2	3	4	5	6	7	8	**over time**
underdispersion	mean	2.750	3.088	3.013	3.213	3.300	3.175	3.075	3.075	3.086
equidispersion		2.975	3.313	3.238	3.438	3.525	3.400	3.300	3.300	3.311
overdispersion		3.125	3.463	3.388	3.588	3.675	3.550	3.450	3.450	3.461
zero-inflation		3.025	1.425	0.613	0.238	0.713	0.525	1.350	2.138	1.253
underdispersion	variance	1.658	1.777	1.354	1.258	1.428	1.437	1.665	1.412	1.499
equidispersion		3.772	3.509	3.120	3.616	3.063	3.585	3.630	2.922	3.402
overdispersion		7.402	6.885	6.519	7.410	6.374	7.238	7.162	6.149	6.892
zero-inflation		26.860	5.463	2.620	0.639	2.992	1.822	8.306	14.171	7.859

Table 4.5: Parameter estimates, SE and DIC in GPGP and RPGP-EP models under different degrees of dispersion (Study 2)

model	**parameter**	**underdispersion**		**equidispersion**		**overdispersion**		**zero-inflation***	
		estimate	SE	**estimate**	SE	**estimate**	SE	**estimate**	SE
GPGP	β_{a0}	-0.0669	0.0194	-0.0389	0.0513	-0.0733	0.0283	1.1370	0.2042
	β_{a1}	0.0070	0.0024	0.0040	0.0062	0.0080	0.0033	-0.1398	0.0243
	$\beta_{\mu 0}$	1.1430	0.0368	1.2255	0.0606	1.2365	0.0516	1.1405	0.2459
	$\beta_{\mu 1}$	-0.2212	0.0312	-0.2037	0.0413	-0.1915	0.0451	-0.0919	0.1932
	λ_2	-0.8792	0.1019	-0.9651	0.0432	-0.9701	0.0422	0.3874	0.0644
	r	19.3500	8.4734	6.1110	0.4832	4.0845	0.2801	0.3012	0.0397
	DIC	1893.60		1943.31	(+2.6%)	1966.24	(+1.2%)	1312.66	NA
RPGP -EP	β_{a0}	-0.1809	0.0254	-0.1111	0.0228	-0.1244	0.0368	1.5320	0.1179
	β_{a1}	0.0188	0.0038	0.0115	0.0032	0.0127	0.0053	-0.1798	0.0162
	$\beta_{\mu 0}$	1.0380	0.0064	1.0950	0.0125	1.0880	0.0093	0.6003	0.0220
	$\beta_{\mu 1}$	-0.4143	0.0157	-0.1672	0.0242	-0.2892	0.0175	-0.6094	0.1260
	ν	0.1462	0.0731	0.8775	0.1264	1.9810	0.0161	1.9510	0.0344
	σ	0.1090	0.0059	0.2005	0.0067	0.1189	0.0039	0.6763	0.0679
	DIC	2206.33		2435.34	(+10.4%)	2449.17	(+0.6%)	1317.85	NA

* A new data set is simulated.

Table 4.6: Parameter estimates, SE and DIC in 2-group GMPGP and RMPGP-EP models for the cannabis data

	RMPGP-EP model			**GMPGP model**			**GMPGP-AR(1) model**	
group	**parameter**	**estimate**	SE	**parameter**	**estimate**	SE	**estimate**	SE
$l = 1$	β_{a01}	0.0798	0.0304	β_{a01}	0.0455	0.0273	0.0529	0.0268
high-level	$\beta_{\mu 01}$	2.6200	0.1183	$\beta_{\mu 01}$	2.9600	0.1378	2.4350	0.1433
				$\beta_{\mu 11}$			0.0198	0.0022
	σ_1	0.5512	0.0707	λ_{21}	0.7238	0.0260	0.6221	0.0327
	ν_1	1.4060	0.1617	r_1	29.600	21.340	25.280	18.840
	π_1	0.4034	0.0812	π_1	0.3530	0.0822	0.4694	0.0923
$l = 2$	β_{a02}	0.1039	0.0287	β_{a02}	0.0915	0.0296	0.0966	0.03272
low-level	$\beta_{\mu 02}$	1.0750	0.1308	$\beta_{\mu 02}$	1.2910	0.1273	1.084	0.1885
	σ_2	0.5208	0.0851	λ_{22}	0.1098	0.1581	0.0773	0.1459
	ν_2	1.1640	0.2368	r_2	2.7030	2.7870	3.0580	4.2560
	DIC	3812.77		DIC	3751.78		**3644.21**	

Table 4.7: Observed and predicted means and variances of GMPGP and RMPGP-EP models for the cannabis data

			time								average
model	**cluster**		*2001*	*2002*	*2003*	*2004*	*2005*	*2006*	*2007*	*2008*	**over time**
							mean				
GMPGP	high-level	observed	25.685	17.966	16.464	18.333	18.168	13.934	10.786	11.967	16.663
		predicted	19.280	18.408	17.599	16.829	16.084	15.365	14.681	14.020	16.533
	low-level	observed	3.940	3.053	3.011	2.780	2.763	2.021	1.512	2.484	2.695
		predicted	3.620	3.311	3.025	2.768	2.514	2.300	2.101	1.932	2.696
RMPGP -EP	high-level	observed	23.621	16.665	15.404	16.893	16.896	13.053	10.103	11.237	15.484
		predicted	18.094	16.791	15.816	14.735	13.807	12.804	11.844	10.807	14.337
	low-level	observed	3.751	2.848	2.752	2.621	2.504	1.753	1.301	2.291	2.478
		predicted	3.548	3.200	2.900	2.595	2.326	2.102	1.881	1.704	2.532
							variance				
GMPGP	high-level	observed	1097.8	686.88	394.73	354.11	243.30	124.71	114.44	178.24	399.28
		predicted	261.81	249.78	238.44	227.64	217.18	207.27	197.79	188.86	223.60
	low-level	observed	7.302	9.459	7.484	4.392	6.897	4.566	3.306	5.119	6.066
		predicted	9.490	8.278	7.180	6.309	5.498	4.897	4.303	3.799	6.219
RMPGP -EP	high-level	observed	1014.8	627.35	362.67	333.49	231.26	119.45	106.95	164.64	370.07
		predicted	281.01	259.66	230.47	216.08	200.66	170.60	148.89	149.79	207.14
	low-level	observed	6.938	8.997	6.120	3.942	5.785	2.605	2.197	4.076	5.083
		predicted	9.247	8.115	6.921	5.727	4.899	4.197	3.536	3.008	5.706

Appendix 4.3

Figures

Figure 4.1: The pmfs of GPGP model with varying parameters

(a) λ_2

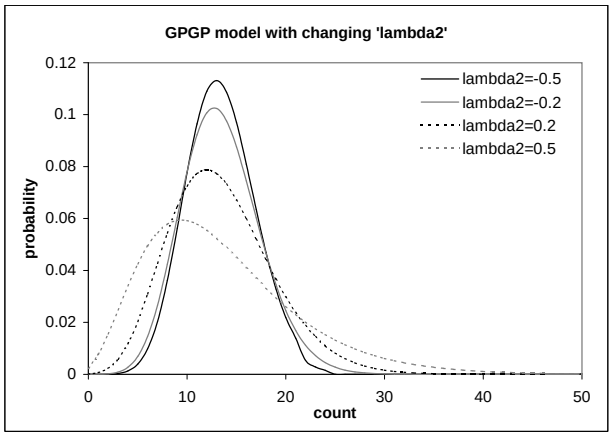

(b) r

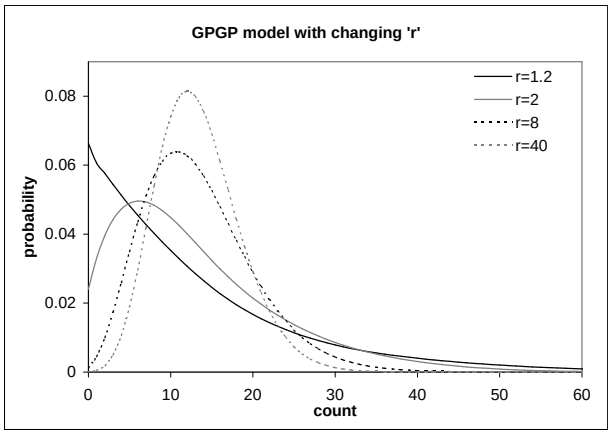

(c) $\beta_{\mu 0}$

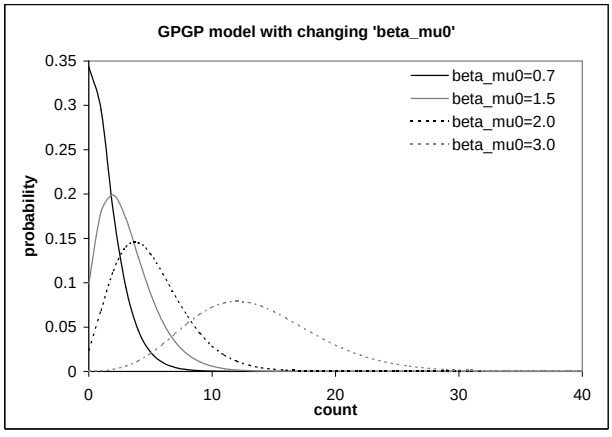

(d) β_{a0}

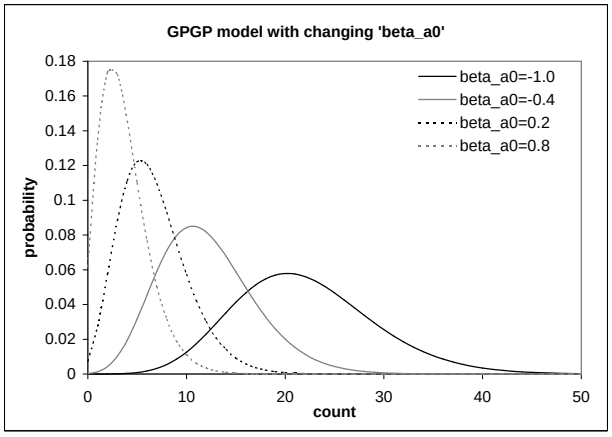

Figure 4.2: Observed and predicted trends of GMPGP and RMPGP-EP models

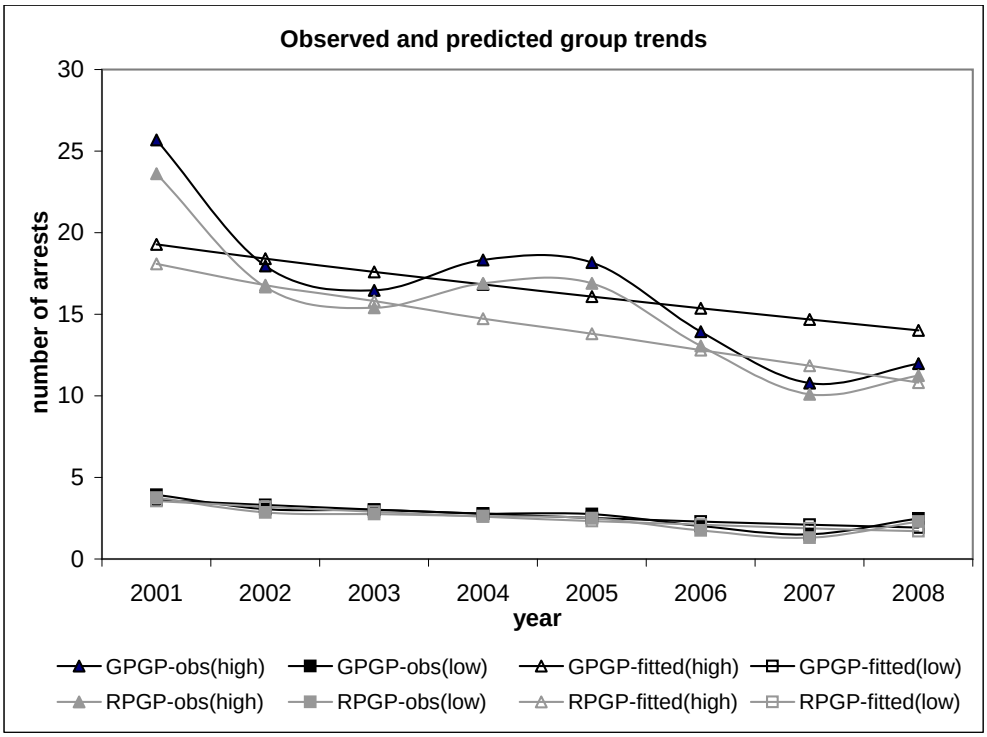

Figure 4.3: The pmfs of high-level group for GMPGP and RMPGP-EP models at different t

(a) $t = 1$ (b) $t = 5$

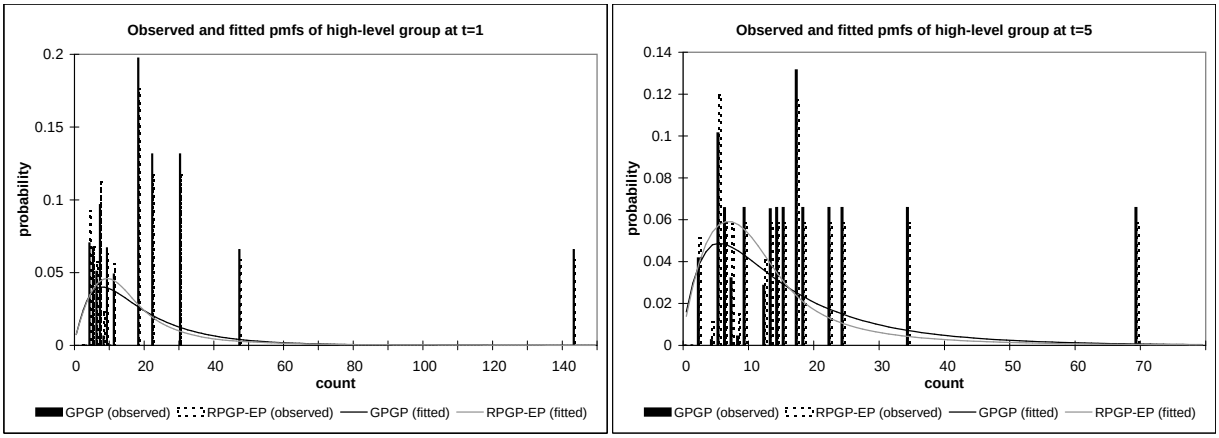

Figure 4.4: The pmfs of low-level group for GMPGP and RMPGP-EP models at different t

(a) $t = 1$ (b) $t = 5$

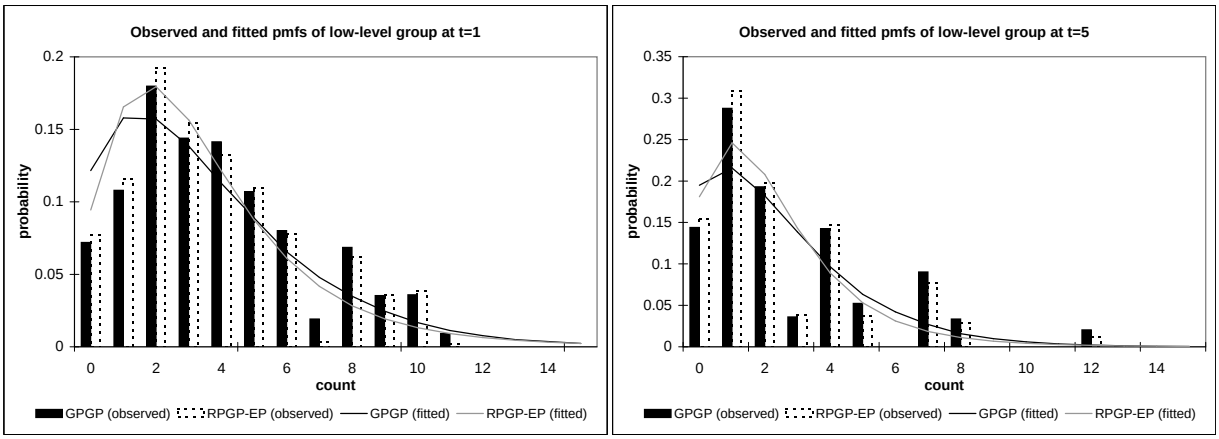

Figure 4.5: Predicted individual and group trends of GMPGP-AR(1) model

(a) with Sydney

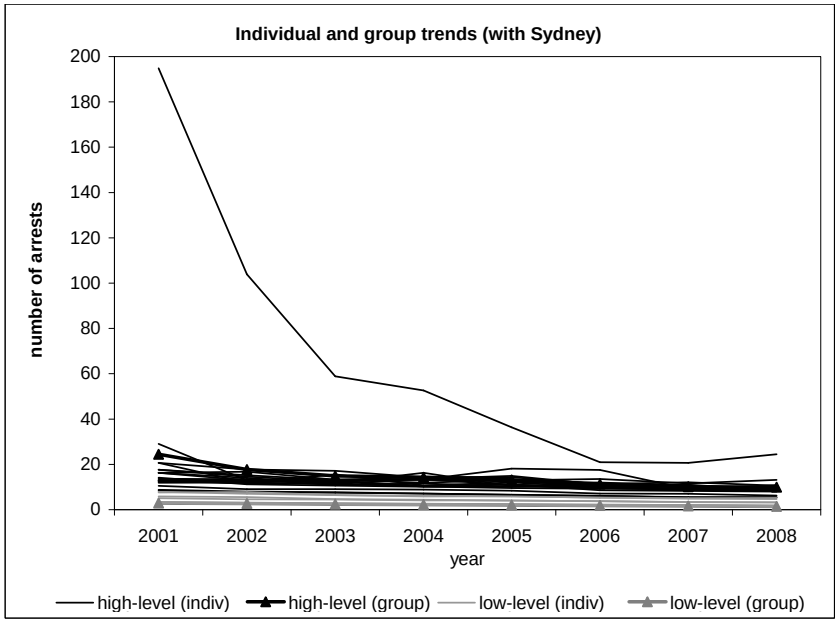

(b) without Sydney

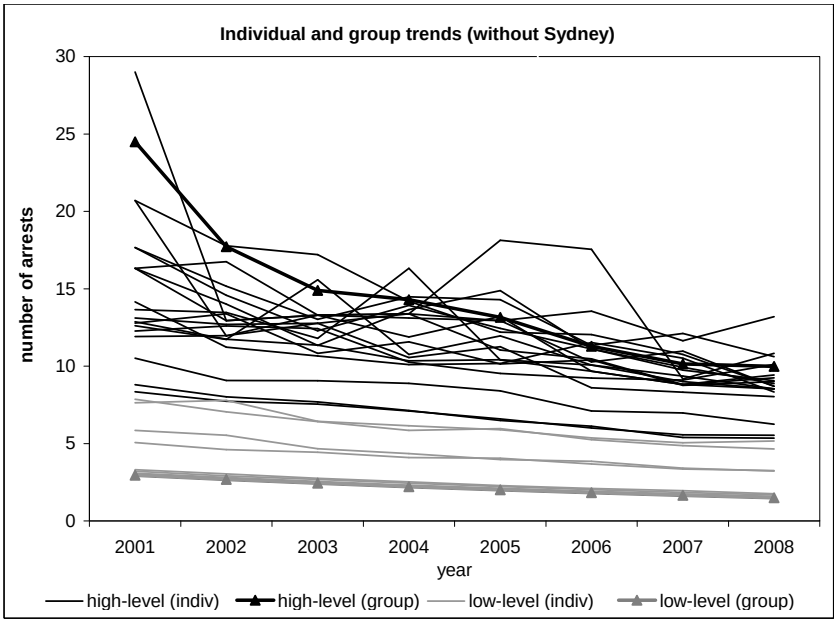

CHAPTER 5

Multivariate generalized Poisson log-t geometric process model

Chapters 2 to 4 extend the PGP models to analyze univariate longitudinal and panel count data with various characteristics (including zero-inflation, overdispersion and underdispersion while allowing for the serial correlation and cluster effects). This Chapter extends the generalized Poisson geometric process (GPGP) model described in (4.2) described in the previous Chapter to study multivariate longitudinal count data.

5.1. Background

The modelling of multivariate time series of counts has drawn attention increasingly as its application ranges widely in different areas. Data such as sales, crimes, car accidents, occupational injuries, industrial control and diseases are often measured in a multivariate manner with more than one outcome associated with the same subject and the outcomes are usually correlated. Let W_{it} be the count at time t from the i^{th} time series. The objective of this Chapter is to innovate an adequate count model for multivariate longitudinal count data in a geometric process (GP) framework to address the trend movements, covariate effects, serial correlation between observations $(W_{it}, W_{i,t-L})$ in individual time series and cross correlation

$(W_{it}, W_{i',t-L})$ and contemporaneous correlation $(W_{it}, W_{i't})$ between time series where $L, L = 1, \ldots, n-1$ denotes the lag of the observations.

While the literature for the multivariate distribution is extensive for continuous data, researches for discrete multivariate counts are relatively limited due to the computational difficulties in implementation. The multivariate normal distribution is commonly used as an alternative choice to model discrete data (Karlis, 2003). Unfortunately, it fails particularly when the count data is skewed due to the prevalence of small or zero observations.

In the multivariate time series of counts, different time series usually possess different properties such as dispersion, trend movement and serial correlation between observations. Moreover, cross correlation and contemporaneous correlation may exist between pairs of time series. This Chapter proposes a new model namely multivariate generalized Poisson log-t geometric process (MGPLTGP) model to allow for all these properties. The model is shown to have several advantages over some existing models in the literature.

The development of multivariate models starts from the consideration of cross-sectional count data. Amongst all the available multivariate models, models with the bivariate Poisson distribution proposed by Kocherlakota & Kocherlakota (1992) and the multivariate Poisson (MP) distribution by Johnson *et al.* (1997) are the most straightforward extensions of the univariate Poisson model. It is because they have closed-form joint probability

mass function (pmf). Each random variable of the MP distribution is expressed as a sum of two independent univariate Poisson random variables in which one variable is common in all the sums. In this way, the marginal distribution is essentially the simple Poisson distribution with mean equals to variance and the covariance between all pairs of variables would be the mean of the common Poisson variable (Refer to Section 5.2.1 for more details). However, the equal and positive correlation between all pairs of Poisson variables is very restrictive and the model is only applicable to equidispersed data.

Thereafter, Karlis & Meligkotsidou (2005) extended the covariance structure in the basic MP distribution by allowing a different covariance for each pair of variables. Nevertheless, the restriction on positive correlation and equidispersion still remained unsolved. Throughout the past decade, a number of researches have considered using a mixed model approach to deal with the overdispersed multivariate counts with negative correlation. A list of the mixed models can be found in Karlis & Xekalaki (2005). These MP mixed models can be classified into two types. The first type is generally a composite of MP distribution with a univariate mixing distribution as it assumes that the means of the MP random variables are proportional to a random variable following a univariate mixing distribution. Properties of this type of models are described in Kocherlakota (1988). Despite that the

mixing component adds extra variation to the resultant distribution to account for data with overdispersion, this model can apply only to positively correlated multivariate counts as the covariance function is always positive.

As a generalization of the first type, the second type imposes a multivariate mixing distribution on the mean vector of the MP distribution. Using this approach, the covariances of the unconditional MP variables are simply expressed in terms of the covariances of the mixing parameters. In this way, the unconditional variables may exhibit negative correlation as well as overdispersion. Nonetheless, the MP mixed model of the second type, though is suitable for modelling overdispersed count data with negative correlation, cannot cope with underdispersed data. Moreover, the resulting distribution is very complicated and in practice most models consider a special case in which the MP variables are assumed to be independent. See Karlis & Xekalaki (2005) for more details of the two types of mixed MP distributions.

In the context of time series analysis, some applications of these aforementioned models include Karlis (2003), Wang *et al.* (2003) and Lee *et al.* (2005). For instances, Karlis (2003) applied the MP model to analyze the number of road accidents on 24 central roads of Athens during 1987-1991. In the analysis, the time effect is investigated through the correlation structure which assumes all pairs of time series have equal and positive correlation. Wang *et al.* (2003) adopted a bivariate zero-inflated Poisson regression model to study the monthly musculoskeletal and non-musculoskeletal

injuries from November 1992 to October 1995. Their model belongs to the family of MP mixed models of the second kind and treats time as the exposure without taking into account the serial correlation. Later on, Lee *et al.* (2005) extended this model by incorporating multivariate normal random effects with an autoregressive (AR) structure to account for serial correlation for each individual time series but has not taken into account the cross correlation between time series. Nonetheless, all these applications have not addressed the trend movement and are limited to overdispersed data.

To simplify the modelling of covariances between pairs of time series while allowing for different degrees of dispersion, this Chapter adopts the approach in the MP mixed model of the second type but replaces the Poisson distribution with generalized Poisson distribution (GPD) for the outcomes to result in a multivariate generalized Poisson mixed model. To be specific, we extend the generalized Poisson geometric process (GPGP) model described in Chapter 4 which is so far the most comprehensive model amongst all existing PGP models to multivariate count data. In essence, this model with the multivariate mixing distribution not only can allow a flexible degree of dispersion, but also accommodate various contemporaneous correlation structures by adopting different covariance matrices. Moreover, as non-stationarity, serial and cross correlation are often prominent in time series, our proposed model describes the trend movement explicitly while taking into account the autocorrelation structure in individual time series and across time series.

In our proposed model, assume that the observed multivariate counts follow independent GPDs, the means of the GPDs after discounting geometrically $(t-1)$ times become stationary and form a latent stochastic process. We then assign the multivariate log-t (MLT) distribution as the mixing distribution to the latent variables such that its mean and covariance matrix can accommodate covariate effects and different correlation structures respectively. The MLT distribution is preferred to multivariate lognormal (MLN) distribution which was adopted by Aitchinson & Ho (1989) and Ma *et al.* (2008) as it provides more flexibility in the tail behavior for handling outlying observations. Besides, if appropriate, some serial and cross correlation structures can be accommodated by incorporating some lagged observations as time-evolving covariates into the log-linked mean function in individual time series or across time series. The resultant model is essentially a multivariate version of the RPGP model and GPGP models which have been investigated in Chapter 3 and 4 respectively.

For model implementation, the MP model and the MP mixed model adopt the expectation-maximization (EM) algorithm in the likelihood approach (Karlis, 2003; Karlis & Meligkotsidou, 2007). However such method becomes computational intensive due to the complexity of the joint pmf as the number of dimension increases. This shortcoming makes the model less favorable in real-life applications. On the other hand, Karlis & Xekalaki (2005) adopted a Bayesian approach for model implementation. In a Bayesian

perspective, the evaluation of the complex joint pmf can be avoided by constructing a simple Gibbs sampler to simulate the parameters from their full conditional posterior distributions. Similar to the approach in the RPGP model, the MLT distribution in our proposed model is expressed in scale mixtures of MLNs. Under the scale mixtures representation, the parameter estimation can be simplified by sampling from multivariate normal distribution using Markov chain Monte Carlo (MCMC) algorithms and the additional mixing parameters in the scale mixtures of MLNs help to identify the extreme observations in the outlier diagnosis. Refer to Chapter 3 for more details.

The rest of the Chapter is organized as follows. Section 5.2 will briefly review the well-established MP models and MP mixed models. Section 5.3 will introduce the proposed multivariate generalized Poisson log-t geometric process (MGPLTGP) model using scale mixtures of MLNs. In Section 5.4, we will discuss the implementation of MGPLTGP model using MCMC algorithms followed by the introduction of the model assessment criterion. After that, a real data analysis of the MGPLTGP model with model comparison will be given in Section 5.5. Lastly Section 5.6 will give some concluding remarks with plausible future extensions.

5.2. A review of multivariate Poisson models

5.2.1. Multivariate Poisson model. The multivariate Poisson (MP) model is derived through the multivariate reduction (Mardia, 1971). Suppose that $V_i, i = 0, \ldots, m$ are independent Poisson random variables with mean η_i.

Then the random variables $W_i = V_i + V_0, i = 1, \ldots, m$ follow jointly a multivariate Poisson (MP) distribution where m represents the dimension of the distribution. The joint pmf $f_{MP}(\boldsymbol{w}|\boldsymbol{\eta})$ is given by

$$f_{MP}(\boldsymbol{w}|\,\boldsymbol{\eta}) = f(w_1, w_2, \ldots, w_m|\,\eta_0, \eta_1, \ldots, \eta_m)$$

$$= \exp\left(-\sum_{i=0}^{m}\eta_i\right)\prod_{i=1}^{m}\frac{\eta_i^{w_i}}{w_i!}\sum_{i=0}^{\xi}\left[\prod_{j=1}^{m}\binom{w_j}{i}(i!)^{m-1}\left(\frac{\eta_0}{\prod_{k=1}^{m}\eta_k}\right)^{i}\right]$$

where $\boldsymbol{w} = \{w_1, w_2, \ldots, w_m\}$ and $\xi = \min(w_1, w_2, \ldots, w_m)$. Marginally, each W_i follows a Poisson distribution and its mean, variance and covariance are given by

$$E(W_i) = Var(W_i) = \eta_i + \eta_0 \quad \text{and} \quad Cov(W_i, W_j) = \eta_0 \ \text{ for all } \ i \neq j.$$

If $\eta_0 = 0$, then the joint distribution reduces to a product of m independent Poisson distributions. However, the use of the MP model is rather restricted due to the unrealistic assumption that all pairs of variables have the same covariance. See Johnson *et al.* (1997) for more details.

To allow a more flexible covariance structure, Karlis & Meligkotsidou (2005) proposed using a two-way covariance structure to improve the practicability of the MP model. Assume that $W_i = \sum_{k=1}^{i} V_{ki} + \sum_{k=i+1}^{m} V_{ik}$ for $i = 1, \ldots, m-1$ and $W_m = \sum_{k=1}^{m} V_{km}$, where $V_{ik}, i \leq k \leq m$ are independent Poisson random variables with mean η_{ik}, then the mean, variance and covariance become

$$\begin{aligned} E(W_i) = Var(W_i) &= \begin{cases} \sum_{k=1}^{i} \eta_{ki} + \sum_{k=i+1}^{m} \eta_{ik}, & \text{for } i < m \\ \sum_{k=1}^{m} \eta_{km}, & \text{for } i = m \end{cases} \\ Cov(W_i, W_j) &= \eta_{ij}, \text{ for } i < j. \end{aligned} \tag{5.1}$$

In addition, the applicability of the MP model can be enhanced by log-linking η_{ik} with some covariates such that $\ln \eta_{ik} = \boldsymbol{z}_{ik}^T \boldsymbol{\beta}_{ik}$ for $i \leq k \leq m$, where $\boldsymbol{z}_{ik} = \{z_{0ik}, z_{1ik}, \ldots, z_{q_{ik}ik}\}^T$ and $\boldsymbol{\beta}_{ik} = \{\beta_{0ik}, \beta_{1ik}, \ldots, \beta_{q_{ik}ik}\}^T$ are $(q_{ik}+1) \times 1$ vectors of covariates and regression coefficients respectively. Refer to Karlis & Meligkotsidou (2005) for more details. In the remainder of this Chapter, we will denote by $f_{MP}(\boldsymbol{w}|\,\boldsymbol{\eta})$ the joint pmf of the MP model with two-way covariance structure and parameter vector $\boldsymbol{\eta} = \{\eta_{11}, \eta_{12}, \ldots, \eta_{m-1,m}, \eta_{mm}\}^T$.

Although the extension enables the MP model to accommodate covariate effects and a more flexible covariance structure as it allows varying covariances across pairs of (W_i, W_j) in (5.1), clearly the MP model still fails to fit overdispered or negative correlated data which are commonly found in real life. Hence, the mixed model approach is considered to remedy these limitations.

5.2.2. Multivariate Poisson mixed model. A majority of the multivariate Poisson mixed models can be classified into two categories. Without loss of generality, assume that W_i follows a MP distribution with its mean

proportional to a univariate random variable α where α has a mixing density $g(\alpha|\,\mu,\sigma^2)$ with mean μ and variance σ^2. The probability function of the MP mixed distribution can be expressed as

$$f_{MPM1}(\boldsymbol{w}|\,\mu,\sigma^2)=\int_{\alpha} f_{MP}(\boldsymbol{w}|\,\alpha\boldsymbol{\eta})\;g(\alpha|\,\mu,\sigma^2)\;d\alpha.$$

Examples for the mixing densities include gamma and generalized inverse Gaussian distributions. The mean, variance and covariance of the first type of MP mixed model are given by

$$\begin{aligned}
E(W_i) &= E_\alpha[E_w(W_i|\,\alpha\eta_{1i},\ldots,\alpha\eta_{ii},\alpha\eta_{i,i+1},\ldots,\alpha\eta_{im})]\\
&= \begin{cases} E_\alpha\left[\alpha(\sum_{k=1}^{i}\eta_{ki}+\sum_{k=i+1}^{m}\eta_{ik})\right]=\mu\left(\sum_{k=1}^{i}\eta_{ki}+\sum_{k=i+1}^{m}\eta_{ik}\right), & \text{for } i<m\\ E_\alpha\left[\alpha(\sum_{k=1}^{m}\eta_{km})\right]=\mu\left(\sum_{k=1}^{m}\eta_{km}\right), & \text{for } i=m \end{cases}\\
Var(W_i) &= E_\alpha[Var_W(W_i|\,\alpha\eta_{1i},\ldots,\alpha\eta_{ii},\alpha\eta_{i,i+1},\ldots,\alpha\eta_{im})]+\\
&\qquad Var_\alpha[E_w(W_i|\,\alpha\eta_{1i},\ldots,\alpha\eta_{ii},\alpha\eta_{i,i+1},\ldots,\alpha\eta_{im})]\\
&= \begin{cases} \mu\left(\sum_{k=1}^{i}\eta_{ki}+\sum_{k=i+1}^{m}\eta_{ik}\right)+\sigma^2\left(\sum_{k=1}^{i}\eta_{ki}+\sum_{k=i+1}^{m}\eta_{ik}\right)^2, & \text{for } i<m\\ \mu\left(\sum_{k=1}^{m}\eta_{km}\right)+\sigma^2\left(\sum_{k=1}^{m}\eta_{km}\right)^2, & \text{for } i=m \end{cases}\\
Cov(W_i,W_j) &= E_\alpha[Cov_w(W_i,W_j|\,\alpha\eta_{1i},..,\alpha\eta_{ii},\alpha\eta_{i,i+1},..,\alpha\eta_{im},\alpha\eta_{1j},..,\alpha\eta_{jj},\alpha\eta_{j,j+1},..,\alpha\eta_{jm})]\\
&\quad +Cov_\alpha[E_w(W_i|\,\alpha\eta_{1i},..,\alpha\eta_{ii},\alpha\eta_{i,i+1},..,\alpha\eta_{im})\\
&\qquad E_w(W_j|\,\alpha\eta_{1j},..,\alpha\eta_{jj},\alpha\eta_{j,j+1},..,\alpha\eta_{jm})]\\
&= E_\alpha(\alpha\eta_{ij})+Cov_\alpha\left[\alpha\left(\sum_{k=1}^{i}\eta_{ki}+\sum_{k=i+1}^{m}\eta_{ik}\right),\alpha\left(\sum_{k=1}^{j}\eta_{kj}+\sum_{k=j+1}^{m}\eta_{jk}\right)\right]
\end{aligned}$$

$$= \begin{cases} \mu\eta_{ij} + \sigma^2 \left(\sum_{k=1}^{i} \eta_{ki} + \sum_{k=i+1}^{m} \eta_{ik} \right) \left(\sum_{k=1}^{j} \eta_{kj} + \sum_{k=j+1}^{m} \eta_{jk} \right), & \text{for } i < m \\ \mu\eta_{ij} + \sigma^2 \left(\sum_{k=1}^{m} \eta_{ik} \right) \left(\sum_{k=1}^{m} \eta_{jk} \right), & \text{for } i = m. \end{cases}$$

By mixing the MP distribution with different mixing densities, the MP mixed model can now account for overdispersion in the data as the mixing distribution $g(\alpha)$ adds extra variation to the model. This mixed model however only allows positive correlation between any pair of the multivariate Poisson random variables which constrains its applicability.

The second type of the MP mixed model acts as a remedial model and is a generalization of the first type. It imposes a multivariate mixing distribution $g(\boldsymbol{\eta}|\, \boldsymbol{\mu}, \boldsymbol{\Sigma})$ on the parameter vector $\boldsymbol{\eta} = \{\eta_{11}, \eta_{12}, \ldots, \eta_{m-1,m}, \eta_{mm}\}^T$ of the MP distribution. A model of this type is highly complicated and the implementation is computationally intensive. In practice, most models assume $\eta_{ij} = 0$ for $i < j$ which implies that the model starts with m independent Poisson distributions with mean η_{ii}. Hence the joint pmf can be expressed as

$$f_{MPM2}(\boldsymbol{w}|\, \boldsymbol{\mu}, \boldsymbol{\Sigma}) = \int_{\boldsymbol{\eta}} \left[\prod_{i=1}^{m} f_P(w_i|\, \eta_{ii}) \right] g(\boldsymbol{\eta}|\, \boldsymbol{\mu}, \boldsymbol{\Sigma})\, d\boldsymbol{\eta}$$

where $f_P(w_i|\, \eta_{ii})$ is a univariate Poisson distribution with mean η_{ii}, and the mean vector and covariance matrix of the multivariate mixing distribution are respectively

$$\boldsymbol{\mu} = \begin{pmatrix} \mu_1 \\ \mu_2 \\ \vdots \\ \mu_m \end{pmatrix} \quad \text{and} \quad \boldsymbol{\Sigma} = \begin{bmatrix} \sigma_1^2 & \sigma_{12} & \dots & \sigma_{1m} \\ \vdots & \sigma_2^2 & \dots & \sigma_{2m} \\ \vdots & \vdots & \ddots & \vdots \\ \sigma_{m1} & \sigma_{m2} & \dots & \sigma_m^2 \end{bmatrix}.$$

Hence, the mean, variance and covariance of the second type of MP mixed model are written as

$$\begin{aligned} E(W_i) &= E_\eta[E_w(W_i|\,\eta_{ii})] = \mu_i \\ Var(W_i) &= E_\eta[Var_W(W_i|\,\eta_{ii})] + Var_\eta[E_w(W_i|\,\eta_{ii})] = \mu_i + \sigma_i^2 \\ Cov(W_i, W_j) &= E_\eta[Cov_w(W_i, W_j|\,\eta_{ii}, \eta_{jj})] + Cov_\eta[E_w(W_i|\,\eta_{ii})E_w(W_j|\,\eta_{jj})] \\ &= Cov_\eta(\eta_{ii}, \eta_{jj}) = \sigma_{ij}. \end{aligned} \tag{5.2}$$

Explicitly, the covariances of the pairs of multivariate Poisson random variables are simply the covariances of the mixing distribution, thus this mixed model of the second type can fit multivariate count data with negative correlation if $\sigma_{ij} < 0$ as well as overdispersion as its variance is greater than its mean. Amongst all the multivariate mixed distribution, the multivariate log-normal distribution has been adopted most (Aitchinson & Ho, 1989; Karlis & Meligkotsidou, 2007; Ma *et al.*, 2008) due to its well-defined moments and well-established properties. References for the MP mixed models can be found in Karlis & Xekalaki (2005).

Despite the progressive extensions of the MP mixed models, they still lack the ability to model underdispersed multivariate count data and so this

motivates us to replace the Poisson distribution with the generalized Poisson distribution which can handle both underdispersed and overdispersed data. Using the MP mixed model approach of the second kind, we pioneer a new model called multivariate generalized Poisson log-t (MGPLTGP) model by extending the Poisson distribution to generalized Poisson distribution (GPD) within the GP modelling framework. In addition, we adopt multivariate log-t (MLT) distribution instead of multivariate lognormal (MLN) distribution in Aitchinson & Ho (1989) as the mixing distribution for the latent stochastic process (SP) of the GP as the former distribution has an adjustable heavier-than-normal tail to downweigh the effect of outliers on the parameter estimation. The MGPLTGP model is introduced in the following Section.

5.3. Multivariate generalized Poisson log-t geometric process model

Previous developments of GP model were confined to univariate data. In light of the need to study multivariate data which arises in various disciplines, we consider a multivariate extension of the PGP model combining the modelling approach of both GPGP and RPGP models as follows.

5.3.1. Model specification. Denote the vector of counts by $\boldsymbol{W}_t = \{W_{1t}, \ldots, W_{mt}\}^T$ at time $t, t = 1, \ldots, n$. Assume that W_{it} follows an independent GPD with mean X_{it}, then each $X_{it} = \dfrac{Y_{it}}{a_i^{t-1}} = \dfrac{\lambda_{1it}}{1-\lambda_{2i}}, t = 1, \ldots, n$ forms a latent GP where $\{Y_{it}\}$ is a latent SP and a_i is the ratio of the GP that describes the progression of the trend for W_{it}. Similar to the

RPGP model, we further assume that $\boldsymbol{Y}_t^* = \ln \boldsymbol{Y}_t = \{Y_{1t}^*, \ldots, Y_{mt}^*\}^T$ follows a multivariate Student's t- (MT) distribution $f_{MT}(\boldsymbol{y}_t^* | \, \boldsymbol{\mu}^*, \boldsymbol{\Sigma}, \nu)$ with mean vector and covariance matrix given respectively by

$$\boldsymbol{\mu} = \begin{pmatrix} \mu_1^* \\ \mu_2^* \\ \vdots \\ \mu_m^* \end{pmatrix} \quad \text{and} \quad \boldsymbol{\Sigma} = \begin{bmatrix} \sigma_1^2 & \sigma_{12} & \ldots & \sigma_{1m} \\ \vdots & \sigma_2^2 & \ldots & \sigma_{2m} \\ \vdots & \vdots & \ddots & \vdots \\ \sigma_{m1} & \sigma_{m2} & \ldots & \sigma_m^2 \end{bmatrix}$$

and degrees of freedom ν. The joint pmf $f_{_{GPMT}}(\boldsymbol{w}_t)$ can be written as

$$f_{_{GPMT}}(\boldsymbol{w}_t) = \int_{\mathbb{R}^m} \left[\prod_{i=1}^{m} f_{GPD}(w_{it} | \, \lambda_{1it}, \lambda_{2i}) \right] f_{MT}(\boldsymbol{y}_t^* | \, \boldsymbol{\mu}^*, \boldsymbol{\Sigma}, \nu) \, d\boldsymbol{y}_t^* \quad (5.3)$$

where $\mathbb{R}^m$ denotes the set of all real vectors in a m-dimensional space, $f_{GPD}(\cdot | \lambda_{1it}, \lambda_{2i})$ is the pmf of GPD given by (4.1) with mean $\dfrac{\lambda_{1it}}{1-\lambda_{2i}}$ and variance $\dfrac{\lambda_{1it}}{(1-\lambda_{2i})^3}$, $\lambda_{1it} = \dfrac{\exp(y_{it}^*)(1-\lambda_{2i})}{a_i^{t-1}}$ and $f_{MT}(\boldsymbol{y}_t^* | \, \boldsymbol{\mu}^*, \boldsymbol{\Sigma}, \nu)$ which acts as the mixing density is given by

$$f_{MT}(\boldsymbol{y}_t^* | \, \boldsymbol{\mu}^*, \boldsymbol{\Sigma}, \nu) = \frac{\Gamma(\frac{\nu+m}{2})}{\Gamma(\frac{\nu}{2}) \nu^{\frac{m}{2}} \pi^{\frac{m}{2}} |\boldsymbol{\Sigma}|^{\frac{1}{2}}} \left[1 + \frac{1}{\nu} (\boldsymbol{y}_t^* - \boldsymbol{\mu}^*)^T \boldsymbol{\Sigma}^{-1} (\boldsymbol{y}_t^* - \boldsymbol{\mu}^*) \right]^{-\frac{\nu+m}{2}} \quad (5.4)$$

The MGPLTGP model examines the trend effect before investigating the correlation between the pair of time series. Since the resultant MGPLTGP model does not have a closed-form joint pmf in (5.3), the parameter estimation can be undertaken via MCMC algorithms. Following the idea of the RPGP in Chapter 3, to enhance the efficiency of the sampling algorithms, Wakefield *et al.* (1994) proposed expressing the MT distribution in scale

mixtures of multivariate normals, so (5.4) becomes:

$$f_{MT}(\boldsymbol{y}_t^* | \, \boldsymbol{\mu}^*, \boldsymbol{\Sigma}, \nu) = \int_0^\infty f_{MN}\left(\boldsymbol{y}_t^* \,\middle|\, \boldsymbol{\mu}^*, \frac{\boldsymbol{\Sigma}}{u_t}\right) f_G\left(u_t \,\middle|\, \frac{\nu}{2}, \frac{\nu}{2}\right) \, du_t \quad (5.5)$$

where $f_{MN}\left(\boldsymbol{y}_t^* \,\middle|\, \boldsymbol{\mu}^*, \frac{\boldsymbol{\Sigma}}{u_t}\right)$ is a multivariate normal distribution with mean vector $\boldsymbol{\mu}^*$ and covariance matrix $\frac{\boldsymbol{\Sigma}}{u_t}$, and $f_G\left(u_t \,\middle|\, \frac{\nu}{2}, \frac{\nu}{2}\right)$ is a gamma distribution with mean 1 and variance $\frac{2}{\nu}$. Hence, the joint pmf in (5.3) using scale mixtures representation in (5.5) is rewritten as

$$f_{GPMT}(\boldsymbol{w}_t) = \int_{\mathbb{R}^m}\int_0^\infty \left[\prod_{i=1}^m f_{GPD}(w_{it} | \, \lambda_{1it}, \lambda_{2i})\right] f_{MN}\left(\boldsymbol{y}_t^* \,\middle|\, \boldsymbol{\mu}^*, \frac{\boldsymbol{\Sigma}}{u_t}\right) f_G\left(u_t \,\middle|\, \frac{\nu}{2}, \frac{\nu}{2}\right) du_t \, d\boldsymbol{y}_t^*$$

where $\lambda_{1it} = \dfrac{\exp(y_{it}^*)(1-\lambda_{2i})}{a_{it}^{t-1}}$.

Using scale mixtures representation simplifies the full conditional distributions and thus facilitates the MCMC algorithms such as Gibbs sampling. Another advantage of using scale mixtures representation is that the resulting density contains an extra mixing parameter u_t which helps to identify extreme observations in outlier diagnosis. The smaller the u_t, the more outlying is the vector of observations $\boldsymbol{w}_t$.

5.3.2. Covariate and period effects. To extend the practicability of the model, we accommodate some time-evolving or exogenous covariate effects into the mean μ_i^* and ratio a_i. Denote the covariates by z_{klit} and regression parameters by $\beta_{jki}, j = \mu, a; k = 1, \ldots, q_j; i = 1, \ldots, m; t = 1, \ldots, n$ for the mean μ_{it}^* and ratio a_{it} functions respectively, where $q_j, j =$

μ, a represents the number of covariates in μ_{it}^* and a_{it} correspondingly, then

$$\mu_{it}^* = \beta_{\mu 0i} + \beta_{\mu 1i} z_{\mu 1it} + \cdots + \beta_{\mu q_\mu i} z_{\mu q_\mu it} \tag{5.6}$$

$$\ln a_{it} = \beta_{a0i} + \beta_{a1i} z_{a1it} + \cdots + \beta_{aq_a i} z_{aq_a it}. \tag{5.7}$$

In addition, we assume that there are some piecewise constant time-varying effects called period effects which change the mean described β_{jki} and/or the shape of the distribution described by the dispersion parameter λ_{2i}, covariance matrix $\mathbf{\Sigma}$ and degrees of freedom ν across the intervention periods. Denote the p^{th} intervention period which starts at T_p and ends at $T_{p+1} - 1$ by $\{t, T_p \leq t \leq T_{p+1} - 1\}$ where P is the total number of periods. Then

$$\lambda_{2it} = \sum_{p=1}^{P} \lambda_{2ip}\, I(T_p \leq t \leq T_{p+1} - 1) \tag{5.8}$$

$$\nu_t = \sum_{p=1}^{P} \nu_p\, I(T_p \leq t \leq T_{p+1} - 1) \tag{5.9}$$

$$\mathbf{\Sigma}_t = \sum_{p=1}^{P} \mathbf{\Sigma}_p\, I(T_p \leq t \leq T_{p+1} - 1) \tag{5.10}$$

where $I(E)$ is an indicator function of the event E and λ_{2ip}, ν_p and

$$\mathbf{\Sigma}_p = \begin{bmatrix} \sigma_{1p}^2 & \sigma_{12p} & \dots & \sigma_{1mp} \\ \vdots & \sigma_{2p}^2 & \dots & \sigma_{2mp} \\ \vdots & \vdots & \ddots & \vdots \\ \sigma_{m1p} & \sigma_{m2p} & \dots & \sigma_{mp}^2 \end{bmatrix}$$

represent the dispersion parameter, degrees of freedom and covariance matrix in period p respectively. Note that period effects can be incorporated in

the mean μ_{it}^* and ratio a_{it} functions as covariates using indicator variables and interaction of indicator variables.

Hence, the joint pmf in (5.6) becomes

$$f_{GPMT}(\boldsymbol{w}_t) = \int_{\mathbb{R}^m}\int_0^{\infty}\left[\prod_{i=1}^{m} f_{GPD}(w_{it}|\,\lambda_{1it},\lambda_{2it})\right] f_{MN}\left(\boldsymbol{y}_t^* \,\middle|\, \boldsymbol{\mu}_t^*, \frac{\boldsymbol{\Sigma}_t}{u_t}\right) f_G\left(u_t \,\middle|\, \frac{\nu_t}{2}, \frac{\nu_t}{2}\right) du_t\, d\boldsymbol{y}_t^* \quad (5.11)$$

where $\lambda_{1it} = \dfrac{\exp(y_{it}^*)(1-\lambda_{2it})}{a_{it}^{t-1}}$ and the mean, variance and covariance for W_{it} conditional on period p are derived as follows:

$$\begin{aligned}
E(W_{it}) &= E_x[E_w(W_{it}|X_{it})] = E_x(X_{it}) = \frac{E_y(Y_{it})}{a_{it}^{t-1}} = \frac{E_u[E_y(Y_{it}|U_t)]}{a_{it}^{t-1}} \\
&= \frac{E_u[\exp(\mu_{it}^* + \frac{\sigma_{it}^2}{2U_t})]}{a_{it}^{t-1}} = \frac{\exp(\mu_{it}^*)}{a_{it}^{t-1}}\, E_u\left[\exp\left(\frac{\sigma_{it}^2}{2U_t}\right)\right] \\
Var(W_{it}) &= E_x[Var_w(W_{it}|X_{it})] + Var_x[E_w(W_{it}|X_{it})] = \frac{E_y(Y_{it})}{a_{it}^{t-1}(1-\lambda_{2it})^2} + \frac{Var_y(Y_{it})}{a_{it}^{2(t-1)}} \\
&= \frac{\exp(\mu_{it}^*)}{a_{it}^{t-1}(1-\lambda_{2it})^2}\, E_u\left[\exp\left(\frac{\sigma_{it}^2}{2U_t}\right)\right] + \frac{E_u[Var_y(Y_{it}|U_t)] + Var_u[E_y(Y_{it}|U_t)]}{a_{it}^{2(t-1)}} \\
&= \frac{\exp(\mu_{it}^*)}{a_{it}^{t-1}(1-\lambda_{2it})^2}\, E_u\left[\exp\left(\frac{\sigma_{it}^2}{2U_t}\right)\right] + \frac{E_u\left[\exp\left(2\mu_{it}^* + \frac{\sigma_{it}^2}{U_t}\right)[\exp(\frac{\sigma_{it}^2}{U_t}) - 1]\right]}{a_{it}^{2(t-1)}} \\
&\quad + \frac{Var_u\left[\exp\left(\mu_{it}^* + \frac{\sigma_{it}^2}{2U_t}\right)\right]}{a_{it}^{2(t-1)}} \\
&= \frac{\exp(\mu_{it}^*)}{a_{it}^{t-1}(1-\lambda_{2it})^2}\, E_u\left[\exp\left(\frac{\sigma_{it}^2}{2U_t}\right)\right] \\
&\quad + \frac{\exp(2\mu_{it}^*)}{a_{it}^{2(t-1)}}\left\{E_u\left[\exp\left(\frac{2\sigma_{it}^2}{U_t}\right)\right] - E_u\left[\exp\left(\frac{\sigma_{it}^2}{2U_t}\right)\right]^2\right\} \\
Cov(W_{it}, W_{jt}) &= Cov_x(X_{it}, X_{jt}) = \frac{1}{(a_{it}a_{jt})^{t-1}}\, Cov_y(Y_{it}, Y_{jt})
\end{aligned}$$

$$
\begin{aligned}
&= \frac{1}{(a_{it}a_{jt})^{t-1}}\left\{E_u[Cov_y(Y_{it},Y_{jt}|U_t)]+E_u[E_{y_i}(Y_{it}|U_t)E_{y_j}(Y_{jt}|U_t)]\right.\\
&\quad \left.-E_u[E_{y_i}(Y_{it}|U_t)]E_u[E_{y_j}(Y_{jt}|U_t)]\right\}\\
&= \frac{\exp(\mu_{it}^*+\mu_{jt}^*)}{(a_{it}a_{jt})^{t-1}}\left\{E_u\left[\exp\left(\frac{\sigma_{it}^2+\sigma_{jt}^2}{2U_t}\right)\left[\exp\left(\frac{\sigma_{ijt}}{U_t}\right)-1\right]\right]\right.\\
&\quad \left.+E_u\left[\exp\left(\frac{\sigma_{it}^2+\sigma_{jt}^2}{2U_t}\right)\right]-E_u\left[\exp\left(\frac{\sigma_{it}^2}{2U_t}\right)\right]E_u\left[\exp\left(\frac{\sigma_{jt}^2}{2U_t}\right)\right]\right\} \quad (5.12)
\end{aligned}
$$

Although the mean and variance cannot be evaluated explicitly, they can be approximated using Monte Carlo (MC) integration. By simulating $u_t^{(j)}, j = 1,\ldots,M_s$ from $f_G\left(u_t^{(j)} \,\middle|\, \frac{\nu_t}{2},\frac{\nu_t}{2}\right)$,

$$E[h(u_t)] = \int_0^\infty h(u_t) f_G\left(u_t \,\middle|\, \frac{\nu_t}{2},\frac{\nu_t}{2}\right) du_t$$

can be evaluated by $\frac{1}{M_s}\sum_{j=1}^{M_s} h(u_t^{(j)})$ where $h(u_t)$ is a function of u_t and $M_s = 10000$ is the number of simulations.

5.3.3. Approximation of joint probability mass function. To study the distribution in (5.3), we adopt the MC integration discussed below to approximate the intractable joint pmf. Given the mean vector $\boldsymbol{\mu}_t^*$, ratio function a_{it}, covariance matrix $\boldsymbol{\Sigma}_t$, degrees of freedom ν_t, and dispersion parameter λ_{2it}, the joint pmf estimator $\hat{f}_t(\boldsymbol{w})$ at time t in general, can be approximated by:

$$
\begin{aligned}
\hat{f}_t(\boldsymbol{w}) &= \sum_{j=1}^{M_s}\left[\prod_{i=1}^{m} f_{GPD}\left(w_i \,\middle|\, \frac{\exp(\hat{y}_{it}^{*(j)})(1-\lambda_{2it})}{a_{it}^{t-1}},\lambda_{2it}\right)\right],\\
&\qquad\qquad w_i = 0,\ldots,\infty; i = 1,\ldots,m \text{ and}\\
\hat{\boldsymbol{y}}_t^{*(j)} &\sim f_{MT}(\boldsymbol{y}_t^{*(j)}|\,\boldsymbol{\mu}_t^*,\boldsymbol{\Sigma}_t,\nu_t),\ j = 1,\ldots,M_s \qquad (5.13)
\end{aligned}
$$

where $M_s = 10000$ and the latent vector $\hat{\boldsymbol{y}}_t^{*(j)} = \{y_{1t}^{*(j)}, \ldots, y_{mt}^{*(j)}\}^T$ is simulated from the multivariate Student's t-distribution in (5.4) given the parameters $\boldsymbol{\mu}_t^*$, $\boldsymbol{\Sigma}_t$ and ν_t. Then, the marginal mean $\widehat{E}(W_{it})$, variance $\widehat{V}ar(W_{it})$ and covariance $\widehat{C}ov(W_{it})$ of the approximated joint pmf $\hat{f}_t(\boldsymbol{w})$ at time t are obtained by:

$$\widehat{E}(W_{it}) = \sum_{\boldsymbol{w}\in\mathbb{N}_0^m} w_i \hat{f}_t(\boldsymbol{w}), \;\; \widehat{V}ar(W_{it}) = \left[\sum_{\boldsymbol{w}\in\mathbb{N}_0^m} w_i^2 \hat{f}_t(\boldsymbol{w})\right] - [\widehat{E}(W_{it})]^2$$

$$\text{and } \widehat{C}ov(W_{it}, W_{jt}) = \left[\sum_{\boldsymbol{w}\in\mathbb{N}_0^m} w_i w_j \hat{f}_t(\boldsymbol{w})\right] - \widehat{E}(W_{it})\widehat{E}(W_{jt}) \qquad (5.14)$$

where $\mathbb{N}_0^m$ denotes the set of natural numbers including zero in a m-dimensional space and $\boldsymbol{w} = \{w_1, \ldots, w_m\}^T$.

To investigate the effects of different parameters on the joint pmf, we simulated the joint pmf in (5.3) of a bivariate generalized Poisson log-t geometric process (BGPLTGP) model ($m = 2$) using MC integration with $M_s = 10000$ as described in (5.13). For demonstrative purpose, the period effect is dropped and thus $P = 1$. Assuming $\mu_{it}^* = \beta_{\mu 0i}$, $\ln a_{it} = \beta_{a0i}$ and $t = 2$, we change the values of one of the model parameters each time while keeping the other parameters constant. The bivariate distributions are displayed in the contour plots in Figures 5.1(a) to 5.1(f) in Appendix 5.2 with contour lines drawn at the same level for fair comparison. Correspondingly, their means, variances, covariances and correlations are summarized in Table 5.1 in Appendix 5.2. Note that two set of means, variances, and

covariances using (5.12) and (5.14) are reported to assess the accuracy of the MC integration.

==========

Figures 5.1(a) to 5.1(f) and Table 5.1 about here

==========

The first four contour plots investigate the effect of the parameters in the mixing density, the multivariate log-t distribution. Starting with Figures 5.1(a) and 5.1(b), σ_{12} controls solely the covariance and thus the correlation of the bivariate counts (W_{1t}, W_{2t}) without altering the variances or means of the bivariate counts. A negative σ_{12} leads the major axis of the contour lines to make a negative angle with the vertical axis and a larger magnitude corresponds to a larger angle between the major axis and the vertical axis indicating stronger correlation. In other words, the strength of the correlation increases with the magnitude of σ_{12} while the direction of correlation aligns with the sign of σ_{12} as shown in Table 5.1. Meanwhile, σ_2^2 determines mainly the variance of W_{2t}. The larger the σ_2^2, the more dispersed is the count W_{2t} indicated by the more scattered pattern in Figure 5.1(b). As σ_2^2 has relatively less effects on the mean of W_{2t} and covariance, they only increase slightly with σ_2^2.

On the other hand, ν plays a more important role in the variances and covariance of the bivariate counts but a minor role in the means. The smaller the ν, the larger are the variances and covariance with a slight increase in the means. Lastly, Figure 5.1(d) reveals that the parameter $\beta_{\mu 02}$ in the

mean function μ_{2t}^* of W_{2t} controls its mean, variance and covariance and in general they all increase with $\beta_{\mu 02}$ as revealed in Table 5.1.

For the parameters in the GPD, β_{a02} in the ratio function a_{02} has similar effect on the distribution as $\beta_{\mu 02}$. This time the smaller the β_{a02}, the larger are the mean, variance and covariance of W_{2t}. Therefore, Figure 5.1(e) looks like an inverted mirror image of Figure 5.1(d). Whereas, another dispersion parameter λ_{22} in the GPD mainly controls the degree of dispersion of W_{2t} without altering much its mean and covariance as illustrated in Figure 5.1(f). Note that a negative λ_{22} does not necessarily reveal that W_{2t} is underdispersed. For example, in the first row the last section of Table 5.1 while W_{1t} is underdispersed when $\lambda_{21} = -0.8$, W_{2t} is overdispersed when $\lambda_{22} = -0.8$. But in general, the more negative the λ_{22}, the less overdispersed is W_{2t}.

Overall the performance of the MC integration is satisfactory as indicated by the close affinity of the approximated mean, variance and covariance using (5.12) and (5.14). To minimize the computational time, we therefore will adapt (5.12) in the sequel to estimate the three moments for the MGPLTGP model.

5.3.4. Test for serial and cross correlations. The above Sections have discussed how the MGPLTGP model can accommodate time-evolving covariate effects, trend movements, different degrees of dispersion for each

time series and the contemporaneous correlation between pair of time series. To achieve an adequate model, any serial correlation between the observations in each time series and cross correlation between time series need to be taken into account. For detecting the presence of serial correlation in each time series $\{W_{it}\}$ or cross correlation between two time series W_{it} and W_{jt}, we first compute the remaining unexplained variation known as the Pearson's residual $\epsilon_{it}, i = 1, \ldots, m; t = 1, \ldots, n$ using

$$\epsilon_{it} = \frac{w_{it} - \widehat{E}(W_{it})}{\sqrt{\widehat{V}ar(W_{it})}}.$$

Then, the test statistic T_{ijL} under the null hypothesis that the Pearson residuals are not autocorrelated ($i = j$) or cross-correlated ($i \neq j$) up to lag L is given by

$$T_{ijL} = n \sum_{k=1}^{L} \left(\frac{\sum_{t=k+1}^{n} \epsilon_{it}\epsilon_{j,t-k}}{\sum_{t=1}^{n} \epsilon_{it}^2} \right)^2$$

and is asymptotically distributed as chi-square $\chi^2(L)$ with degrees of freedom L. See Cameron & Trivedi (1998) for more details.

For the test of serial correlation in each time series $W_{it}, t = 1, \ldots, n$, if the p-values are significant up to lag L, an AR(L) structure will be introduced by adding L lagged observations ($W_{i,t-1}, \ldots, W_{i,t-L}$) into the mean function μ_{it}^* in (5.6). Whereas, for cross correlation between a pair of time series, L lagged observations ($W_{i,t-1}, \ldots, W_{i,t-L}$) of time series W_{it} will be incorporated into the mean function μ_{jt}^* of time series $W_{jt}, t = 1, \ldots, n$. Afterwards the model will be refitted and an appropriate AR structure is

selected if the resultant model has the smallest DIC with statistically significant AR coefficients.

In the next Section, the model implementation and assessment will be described in details.

5.4. Bayesian inference

For statistical inference, maximum likelihood (ML) method via expectation maximization (EM) algorithm is widely adopted in the MP model (Karlis, 2003; Wang *et al.*, 2003) or MP mixed model (Karlis & Meligkotsidou, 2005, 2007). Despite the pros of using EM algorithm, Karlis & Meligkotsidou (2005) has pinpointed that as the dimension m of the time series increases, the computation is more demanding as the complexity of the model increases. In particular for the MP mixed model, the increasing number of latent random effects in the mixing distribution will induce a heavy computational burden and reduce the efficiency of parameter estimation (Karlis & Meligkotsidou, 2007).

To avoid numerical difficulties in maximizing the intractable likelihood function involving high-dimensional integration, we adopt the Bayesian approach via Markov chain Monte Carlo (MCMC) algorithms to convert an optimization problem to a sampling problem. The following Section derives the posterior distribution and univariate full conditional distributions followed by a discussion of the model assessment measure.

5.4.1. MCMC algorithms. Before implementing the MCMC algorithms, we outline the hierarchical structure of the MGPLTGP model under the Bayesian framework as follows:

$$w_{it} \sim f_{GPD}\left(\frac{e^{y^*_{it}}(1-\lambda_{2it})}{a_{it}^{t-1}}, \lambda_{2it}\right), \;\; \boldsymbol{y}^*_t \sim f_{MN}\left(\boldsymbol{\mu}^*_t, \frac{\boldsymbol{\Sigma}_t}{u_t}\right) \;\text{ and }\; u_t \sim f_G\left(\frac{\nu_t}{2}, \frac{\nu_t}{2}\right)$$

where $\mu_{it}, a_{it}, \lambda_{2it}, \nu_t$ and $\boldsymbol{\Sigma}_t$ are given by (5.6)-(5.10). In order to construct the posterior density, some non-informative prior distributions are assigned to the model parameters as follows:

$$\beta_{jki} \;\sim\; N(0, \tau^2_{jki}),\; j = \mu, a;\; k = 0, 1, \ldots, q_j;\; i = 1, \ldots, m \tag{5.15}$$

$$\lambda_{2it} \;\sim\; \text{Uniform}(-1, 1) \tag{5.16}$$

$$\boldsymbol{\Sigma}_t \;\sim\; IW(\boldsymbol{\Psi}_t, r_t) \tag{5.17}$$

$$\nu_t \;\sim\; \text{Gamma}(c_t, d_t) \tag{5.18}$$

where

$$\boldsymbol{\Psi}_t \;=\; \sum_{p=1}^{P} \boldsymbol{\Psi}_p \, I(T_p \le t \le T_{p+1} - 1), r_t = \sum_{p=1}^{P} r_p \, I(T_p \le t \le T_{p+1} - 1),$$

$$c_t \;=\; \sum_{p=1}^{P} c_p \, I(T_p \le t \le T_{p+1} - 1), d_t = \sum_{p=1}^{P} d_p \, I(T_p \le t \le T_{p+1} - 1),$$

τ^2_{jki}, c_p, d_p are some positive constants, $IW(\boldsymbol{\Psi}_t, r_t)$ represents an inverse Wishart distribution $f_{IW}(\cdot|\boldsymbol{\Psi}, r)$ with mean $\dfrac{\boldsymbol{\Psi}}{r - m - 1}$, $\boldsymbol{\Psi}$ is a real-valued positive-definite matrix and $r > m - 1$ is the degrees of freedom. Inverse Wishart distribution is commonly used as a conjugate prior for the symmetric and positive-definite $m \times m$ covariance matrix $\boldsymbol{\Sigma}$ of the multivariate

normal distribution. Its probability density function $f_{IW}(\boldsymbol{\Sigma}|\boldsymbol{\Psi}, r)$ is given by

$$f_{IW}(\boldsymbol{\Sigma}|\boldsymbol{\Psi}, r) = \frac{|\boldsymbol{\Psi}|^{\frac{r}{2}}|\boldsymbol{\Sigma}|^{-\frac{(r+m+1)}{2}} \exp\left[-\frac{\text{tr}(\boldsymbol{\Psi}\boldsymbol{\Sigma}^{-1})}{2}\right]}{2^{\frac{rm}{2}}\Gamma_m(\frac{r}{2})}$$

where $\Gamma_m(\cdot)$ denotes a multivariate Gamma function with dimension m and tr($\boldsymbol{A}$) is the trace of matrix $\boldsymbol{A}$.

According to Bayes' theorem, the posterior density is proportional to the joint densities of complete data likelihood and prior probability distributions. For the MGPLTGP model, denote $\boldsymbol{w} = (\boldsymbol{w}_{1t}^T, \boldsymbol{w}_{2t}^T, ..., \boldsymbol{w}_{mt}^T)^T$ as the data vector, $\boldsymbol{y}^* = ({\boldsymbol{y}_{1t}^*}^T, {\boldsymbol{y}_{2t}^*}^T, ..., {\boldsymbol{y}_{mt}^*}^T)^T$ as the latent vector of the stochastic process and $\boldsymbol{u} = (u_1, u_2, ..., u_n)^T$ as a vector of mixing parameters, the complete data likelihood function $L(\boldsymbol{\theta})$ for the observed data $\boldsymbol{w}$ and missing data $\{\boldsymbol{y}^*, \boldsymbol{u}\}$ is derived as:

$$L(\boldsymbol{\theta}) = \prod_{t=1}^{n}\left\{\left[\prod_{i=1}^{m} f_{GPD}\left(\frac{e^{y_{it}^*}}{a_{it}^{t-1}}, \lambda_{2it}\right)\right] f_{MN}\left(\boldsymbol{y}_t^* \,\middle|\, \boldsymbol{\mu}_t^*, \frac{\boldsymbol{\Sigma}_t}{u_t}\right) f_G\left(u_t \,\middle|\, \frac{\nu_t}{2}, \frac{\nu_t}{2}\right)\right\} \quad (5.19)$$

where the vector of model parameters $\boldsymbol{\theta} = (\boldsymbol{\beta}_\mu, \boldsymbol{\beta}_a, \boldsymbol{\lambda}_2, \boldsymbol{\Sigma}, \boldsymbol{\nu})^T$ where $\boldsymbol{\beta}_j = (\beta_{j01}, ..., \beta_{jq_j1}, ..., \beta_{j0m}, ..., \beta_{jq_jm})^T, j = \mu, a; k = 0, \ldots, q_j$ are parameters in the mean function in (5.6) and ratio function in (5.7), $\boldsymbol{\lambda}_2 = (\lambda_{211}, \lambda_{212}, \ldots, \lambda_{2mP})^T$, $\boldsymbol{\Sigma} = (\boldsymbol{\Sigma}_1, \ldots, \boldsymbol{\Sigma}_p)^T$ and $\boldsymbol{\nu} = (\nu_1, \ldots, \nu_P)^T$.

Treating y_{it}^* and u_t as missing observations, the posterior density of the MGPLTGP model is derived as:

$$f(\boldsymbol{\theta}|\,\boldsymbol{w},\boldsymbol{y}^*,\boldsymbol{u}) \propto L(\boldsymbol{\theta}) \left[\prod_{i=1}^{m}\prod_{j=\mu,a}\prod_{k=0}^{q_j} f_N(\beta_{jki}|\,0,\tau_{jki}^2)\right] \prod_{i=1}^{m}\prod_{p=1}^{P} f_U(\lambda_{2ip}|\,-1,1) \left[\prod_{p=1}^{P} f_{IW}(\boldsymbol{\Sigma}_p|\,\boldsymbol{\Psi}_p,r_p) f_G(\nu_p|\,c_p,d_p)\right]$$

where $f_N(\cdot|\,c,d)$ represents a normal distribution with mean c and variance d, $f_U(\cdot|\,c,d)$ is a uniform distribution on the interval $[c,d]$, the complete data likelihood $L(\boldsymbol{\theta})$ is given by (5.19) and the priors are given by (5.15)-(5.18).

Knowing the joint posterior density, we can then formulate the set of conditional posterior densities for all the unknown model parameters which is essential for Gibbs sampling. The following shows the full conditional posterior densities for each of the model parameters in $\boldsymbol{\theta} = (\boldsymbol{\beta}_\mu, \boldsymbol{\beta}_a, \boldsymbol{\lambda}_2, \boldsymbol{\Sigma}, \boldsymbol{\nu})^T$ and the two sets of missing observations y_{it}^* and u_t:

$$f(\beta_{\mu ki}|\,\boldsymbol{w},\boldsymbol{y}^*,\boldsymbol{u},\boldsymbol{\beta}^-,\boldsymbol{\lambda}_2,\boldsymbol{\Sigma},\boldsymbol{\nu}) \propto \prod_{t=1}^{n} \exp\left[-\frac{(\boldsymbol{y}_t^*-\boldsymbol{\mu}_t^*)^T\boldsymbol{\Sigma}_t^{-1}(\boldsymbol{y}_t^*-\boldsymbol{\mu}_t^*)}{2u_t}\right] \exp\left(-\frac{\beta_{\mu ki}^2}{2\tau_{\mu ki}^2}\right)$$

$$f(\beta_{aki}|\,\boldsymbol{w},\boldsymbol{y}^*,\boldsymbol{u},\boldsymbol{\beta}^-,\boldsymbol{\lambda}_2,\boldsymbol{\Sigma},\boldsymbol{\nu}) \propto \prod_{t=1}^{n} \left\{ \left[\frac{\exp(y_{it}^*)(1-\lambda_{2it})}{a_{it}^{t-1}} + \lambda_{2it}w_{it}\right]^{w_{it}-1} \exp\left[-\frac{\exp(y_{it}^*)(1-\lambda_{2it})}{a_{it}^{t-1}} - \beta_{aki}z_{akit}(t-1)\right]\right\} \exp\left(-\frac{\beta_{aki}^2}{2\tau_{aki}^2}\right)$$

$$\text{restricted to } a_{it}^{t-1} < -\frac{\exp(y_{it}^*)(1-\lambda_{2it})}{s_{it}\lambda_{2it}} \text{ if } \lambda_{2it} < 0$$

$$f(\lambda_{2ip}|\,\boldsymbol{w},\boldsymbol{y}^*,\boldsymbol{u},\boldsymbol{\beta},\boldsymbol{\lambda}_2^-,\boldsymbol{\Sigma},\boldsymbol{\nu}) \propto \prod_{t=1}^{n} \left\{ (1-\lambda_{2it}) \left[\frac{\exp(y_{it}^*)(1-\lambda_{2it})}{a_{it}^{t-1}} + \lambda_{2it}w_{it}\right]^{w_{it}-1} \exp\left[-\frac{\exp(y_{it}^*)(1-\lambda_{2it})}{a_{it}^{t-1}} - \lambda_{2it}w_{it}\right]\right\}$$

$$\text{restricted to } \left[1-\frac{s_{it}a_{it}^{t-1}}{\exp(y_{it}^*)}\right]^{-1} < \lambda_{2it} < 1$$

$$f(\boldsymbol{\Sigma}_p|\,\boldsymbol{w},\boldsymbol{y}^*,\boldsymbol{u},\boldsymbol{\beta},\boldsymbol{\lambda}_2,\boldsymbol{\Sigma}^-,\boldsymbol{\nu}) \propto \prod_{t=1}^{n}\exp\left[-\frac{(\boldsymbol{y}_t^*-\boldsymbol{\mu}_t^*)^T\boldsymbol{\Sigma}_t^{-1}(\boldsymbol{y}_t^*-\boldsymbol{\mu}_t^*)}{2u_t}\right]|\boldsymbol{\Sigma}_p|^{-\frac{r_p+m+2}{2}}\exp\left[-\frac{\text{tr}(\boldsymbol{\Psi}_p\,\boldsymbol{\Sigma}_p^{-1})}{2}\right]$$

$$f(\nu_p\,|\,\boldsymbol{w},\boldsymbol{y}^*,\boldsymbol{u},\boldsymbol{\beta},\boldsymbol{\lambda}_2,\boldsymbol{\Sigma},\boldsymbol{\nu}^-) \propto \prod_{t=1}^{n}\prod_{i=1}^{m}\frac{\nu_t^{\frac{\nu_t}{2}+c_t-1}\left(\frac{u_t}{2}\right)^{\frac{\nu_t}{2}}\exp\left(-\frac{u_t\nu_t}{2}-d_t\nu_t\right)}{\Gamma\left(\frac{\nu_t}{2}\right)}$$

$$f(\boldsymbol{y}_t^*|\,\boldsymbol{w},\boldsymbol{u},\boldsymbol{\beta},\boldsymbol{\lambda}_2,\boldsymbol{\Sigma},\boldsymbol{\nu}) \propto \prod_{i=1}^{m}\left\{\left[\frac{\exp(y_{it}^*)(1-\lambda_{2it})}{a_{it}^{t-1}}+\lambda_{2it}w_{it}\right]^{w_{it}-1}\exp\left[y_{it}^*-\frac{\exp(y_{it}^*)(1-\lambda_{2it})}{a_{it}^{t-1}}\right]\right\}$$
$$\exp\left[-\frac{(\boldsymbol{y}_t^*-\boldsymbol{\mu}_t^*)^T\boldsymbol{\Sigma}_t^{-1}(\boldsymbol{y}_t^*-\boldsymbol{\mu}_t^*)}{2u_t}\right]$$
$$\text{restricted to } y_{it}^* > \ln\left(-\frac{s_{it}\lambda_{2it}a_{it}^{t-1}}{1-\lambda_{2it}}\right) \text{ if } \lambda_{2it}<0$$

$$f(\boldsymbol{u}_t|\,\boldsymbol{w},\boldsymbol{y}^*,\boldsymbol{u}^-,\boldsymbol{\beta},\boldsymbol{\lambda}_2,\boldsymbol{\Sigma},\boldsymbol{\nu}) \propto \exp\left[-\frac{(\boldsymbol{y}_t^*-\boldsymbol{\mu}_t^*)^T\boldsymbol{\Sigma}_t^{-1}(\boldsymbol{y}_t^*-\boldsymbol{\mu}_t^*)}{2u_t}\right]u_t^{\frac{\nu_t-1}{2}}\exp\left(-\frac{\nu_t u_t}{2}\right)$$

where $\boldsymbol{u}^-,\boldsymbol{\beta}^-,\boldsymbol{\lambda}_2^-,\boldsymbol{\Sigma}^-$ and $\boldsymbol{\nu}^-$ are vectors of $\boldsymbol{u},\boldsymbol{\beta},\boldsymbol{\lambda}_2,\boldsymbol{\Sigma}$ and $\boldsymbol{\nu}$ excluding $u_t,\beta_{jki},\lambda_{2ip},\boldsymbol{\Sigma}_p$ and ν_p respectively. The MCMC algorithms are implemented using `WinBUGS` where the sampling scheme based on the conditional posterior densities is outlined in this Section and the Gibbs sampling procedures are described in Section 1.4.3.

5.4.2. Model selection criterion. Under the Bayesian approach, we adopt a model comparison criterion namely the deviance information criterion (DIC) originated by Spiegelhalter *et al.* (2002) which measures the fit of the data to the model and at the same time account for the model complexity. DIC is defined as the sum of a classical measure of fit called

posterior mean deviance $\overline{D(\boldsymbol{\theta})}$ and twice the effective number of parameters p_D which accounts for the model complexity.

For the MGPLTGP model, the DIC output by `WinBUGS` is defined as

$$\begin{aligned} DIC &= \overline{D(\boldsymbol{\theta})} + p_D \\ &= -\frac{4}{M}\sum_{j=1}^{M}\sum_{t=1}^{n}\sum_{i=1}^{m}\ln\left[f_{GPD}\left(w_{it}\,\middle|\,\frac{\exp(y_{it}^{*(j)})(1-\lambda_{2it}^{(j)})}{a_{it}^{(j)(t-1)}},\lambda_{2it}^{(j)}\right)\right] \\ &\quad +2\sum_{t=1}^{n}\sum_{i=1}^{m}\ln\left[f_{GPD}\left(w_{it}\,\middle|\,\frac{\exp(\bar{y}_{it}^{*})(1-\bar{\lambda}_{2it})}{\bar{a}_{it}^{t-1}},\bar{\lambda}_{2it}\right)\right] \end{aligned}$$

where M is the number of realizations in the MCMC sampling algorithms, $\theta^{(j)}$ and $y_{it}^{*(j)}$ represent the j^{th} posterior sample of parameter θ and y_{it}^{*} respectively, and $\bar{\theta}$ and $\bar{y}_{it}^{*}$ are their posterior means. Model with a smaller DIC is chosen as the best model since it has a better fit to the data after accounting for the model complexity.

5.5. Real data Analysis

The practicability of our proposed MGPLTGP model is demonstrated through the study of the use of amphetamine and narcotics in New South Wales (NSW), Australia. The overview, data structure, model fitting procedures and lastly the results are discussed as follows.

5.5.1. Overview. Amphetamine is a psychostimulant drug that causes euphoria and decreased fatigue. An abusive use of this illicit drug makes user experience drug-induced psychosis which may lead to aggressive and violent behaviour (McKetin *et al.*, 2006). In the past decade, the prevalence of amphetamine type substances use in Australia stabilized during 1998 to

2002 after a substantial rise from 1993 to 1998, but has flared up again in late 2002 to 2007 as revealed by the figure that the emergency department admissions of amphetamine type substances use surged by 139% in NSW. This upsurge is believed to be caused by the heroin shortage in Australia which started at around late December in 2000 and prompted many heroin users to switch to amphetamine use (Weatherburn *et al.*, 2003). Elaborately, heroin shortage was the consequence of the dismantling of a major syndicate in mid-2000 which allegedly had been bringing in large shipments of heroin to Australia from traditional source countries on a very regular basis. Thereafter, the increasing risk in smuggling heroin into Australia together with more active street-level drug law enforcement led to the dramatic fall in heroin availability and drug purity and subsequently the mounting heroin price and difficulty in obtain heroin (Degenhardt *et al.*, 2005). Vividly the reduction in heroin use is ongoing after the onset of heroin shortage, however whether it is associated to an increase in amphetamine substance use remains debatable.

Treating use or possession of amphetamine and narcotics as a proxy of amphetamine type substances use and heroin use respectively in NSW, Snowball *et al.* (2008) examined the relationship between the monthly number of arrests for use or possession of the two illicit drugs during 1995 to 2008 using a tradition multivariate time series model and found no evidence to support the association between heroin shortage and increasing amphetamine type substances consumption. Their model has allowed for

the non-stationarity of the two time series yet does not have an explicit trend component to investigate the trend movement. To obtain a more clear picture on how heroin shortage affects the trend movement and detect any serial, contemporaneous and cross correlations in the arrests for use or possession of amphetamines and narcotics, we fitted a bivariate generalized Poisson log-t geometric process (BGPLTGP) model ($m = 2$) to the data described below.

5.5.2. Data and model fitting. The data in Appendix 5.1 consists of a bivariate time series on the monthly number of arrests for use or possession of amphetamine (W_{1t}) and narcotics (W_{2t}) in Sydney, one of the 153 local government areas (LGAs) in NSW from January 1995 to December 2008 ($n = 168$) and can be assessed on the official website of the NSW Bureau of Crime Statistics and Research (the link is given at the end of Section 4.5.1). Instead of using an aggregate number of arrests in a state level, we focus on the data from Sydney, one of the 153 LGAs in NSW because its trend pattern does not differ much from that of the aggregate data in the state level used in Snowball *et al.* (2008) as Sydney is the metropolis of NSW with the highest arrest rates of illicit drug use or possession. The bivariate time series of monthly number of arrests are plotted in Figure 5.2 in Appendix 5.3 with a vertical reference line indicating the onset of heroin shortage.

==========

Figure 5.2 about here

==========

In Figure 5.2, the numbers of arrests for use or possession of both drugs show an upward trend collectively before heroin shortage with the arrests for narcotics use outnumber that for amphetamine. Noticeably once heroin shortage began in late December 2000 ($t = 72$), the trend for narcotics levels off gradually with less variation while that for amphetamine continues to grow with inflating overdispersion. Besides, there are abrupt changes in the means of both time series after heroin shortage commenced. The mean monthly number of arrests surges from 9.31 cases to 24.98 cases for amphetamine use or possession while that of narcotics slumps from 21.58 cases to 15.28 cases. In addition, the contemporaneous correlation between the bivariate time series is although insignificant ($r_w = -0.09, p = 0.243$), the contemporaneous correlation in different periods are significantly positive ($r_{w1} = 0.370, p = 0.0007; r_{w2} = 0.269, p = 0.004$) with a higher correlation r_{w1} prior to heroin shortage.

Taking into account the trend movement in each time series and contemporaneous correlations between time series before and during heroin shortage, we fitted a BGPLTGP model to investigate whether heroin shortage exacerbates amphetamine use contemporaneously in Sydney. Since heroin shortage is expected to incur a change in the mean, trend movement and contemporaneous correlation structure of the bivariate time series, we define the time before shortage as the control period ($p = 1, T_1 = 1$) and those months after December 2000 as the intervention period ($p = 2, T_2 = 73$) and incorporate period effects into the dispersion parameter λ_{2t}, degrees

of freedom ν_t and covariance matrix $\mathbf{\Sigma}_t$ to allow varying contemporaneous correlation structures and degrees of dispersion in different periods. In addition, we incorporate the period effect as covariate effect $z_{\mu 1it} = z_{a2it} = b = 0, 1$ in the mean function in (5.6) and ratio function in (5.7) to detect any changes in the mean or trend of the monthly number of arrests for use or possession of the two illicit drugs due to heroin shortage. Furthermore, since non-monotone trend is observed in Figure 5.2, we accommodate the natural logarithm of time t as the time-evolving covariate ($z_{a1it} = \ln t$) and an interaction term of time and heroin shortage ($z_{a3it} = b \ln t = 0, \ln t$) in the ratio function to allow a change in trend movement across time and period. In other words, the mean function μ^*_{it}, ratio function a_{it}, dispersion parameter λ_{2it} in (5.8), degrees of freedom ν_t in (5.9) and covariance matrices $\mathbf{\Sigma}_t$ in (5.10) for $i = 1, 2$ and $t = 1, \ldots, 168$ are expressed as

$$\begin{aligned}
\mu^*_{it} &= \beta_{\mu 0i} + \beta_{\mu 1i} b && (5.20)\\
\ln a_{it} &= \beta_{a0i} + \beta_{a11} \ln t + \beta_{a2i} b + \beta_{a3i} b \ln t && (5.21)\\
\lambda_{2it} &= \lambda_{2i1}\, I(1 \le t \le 72) + \lambda_{2i2}\, I(73 \le t \le 168) \\
\nu_t &= \nu_1\, I(1 \le t \le 72) + \nu_2\, I(73 \le t \le 168) \\
\mathbf{\Sigma}_t &= \mathbf{\Sigma}_1\, I(1 \le t \le 72) + \mathbf{\Sigma}_2\, I(73 \le t \le 168) && (5.22)
\end{aligned}$$

Using the MCMC algorithms described in Section 5.4.1, we use non-informative priors by setting $\tau^2_{jki} = 1000$ in (5.15), $\mathbf{\Psi}_1 = \mathbf{\Psi}_2 = \begin{bmatrix} 0.1 & 0.005 \\ 0.005 & 0.1 \end{bmatrix}$,

$r_1 = r_2 = 2$ in (5.17) and $c_1 = c_2 = d_1 = d_2 = 0.01$ in (5.18). After implementing the MCMC algorithms using `WinBUGS`, the parameter estimates are given by the posterior medians of the samples.

To assess the competency of our proposed model, two competitive models are considered for model comparison. The first one is the bivariate Poisson (BP) model with two-way covariance structure described in Section 5.2.1 with $W_{it} = V_{iit} + V_{12t}, i = 1, 2$. The mean η_{iit} of V_{iit} in (5.1) is log-linked to the same set of covariates as in the BGPLTGP model such that

$$\ln \eta_{iit} = \beta_{0ii} + \beta_{1ii} b + \beta_{2ii} \ln t + \beta_{3ii} (\ln t)^2 + \beta_{4ii} b \ln t + \beta_{5ii} b (\ln t)^2$$

where $i = 1, 2$ refers to amphetamine and narcotics respectively and $b = 0, 1$ indicates the presence of heroin shortage. Besides, the contemporaneous correlation η_{12t} between the bivariate time series in (5.1) which is given by

$$\ln \eta_{12t} = \beta_{012} + \beta_{112} b \tag{5.23}$$

detects any change in the contemporaneous correlation structures.

Another competitive model is the bivariate Poisson mixed model of the second type mentioned in Section 5.2.2. In particular we adopt a multivariate log-normal distribution as the mixing density suggested by Aitchinson & Ho (1989) and the resultant model is named as BPLN model. In this model, the log-linked mean function μ_{it} in (5.2) is given by

$$\ln \mu_{it} = \beta_{0i} + \beta_{1i} b + \beta_{2i} \ln t + \beta_{3i} (\ln t)^2 + \beta_{4i} b \ln t + \beta_{5i} b (\ln t)^2 \tag{5.24}$$

and a period effect is incorporated into the covariance matrix $\mathbf{\Sigma}_t$ in the same way as (5.22) in the BGPLTGP model to allow for different contemporaneous correlation structures between the bivariate time series in different periods. The BP and BPLN models are considered as competitive because they incorporate the same exogenous effect b, similar time-evolving covariates $\ln t$ and $(\ln t)^2$ and their interactions $b \ln t$ and $b(\ln t)^2$ to allow for non-linear trend patterns in both time series. These assimilate with the time-evolving covariates in the ratio function a_{it} in (5.21) of the BGPLTGP model in which $\ln a_{it}^{t-1} = (t-1)\ln a_{it} = (t-1)(\beta_{a0i} + \beta_{a1i}\ln t + \beta_{a2i} b + \beta_{a3i} b \ln t)$ where $\beta_{aki}, k = 0, \ldots, 3$ can allow for a variety of trend patterns similar to β_{kii} and $\beta_{ki}, l = 2, \ldots, 5$ in (5.23) and (5.24) for the BP and BPLN models respectively.

Last but not least, we fitted a bivariate Poisson lognormal geometric process (BGPLNGP) model using bivariate lognormal distribution with the same mean and ratio functions as in the BGPLTGP model except that the bivariate Student's t-distribution is replaced by the bivariate normal distribution with the same covariance matrix $\mathbf{\Sigma}_t$ given by (5.22) for $\boldsymbol{y}_t^*$.

Overall, the four models assume Poisson distribution, Poisson distribution mixed with bivariate lognormal distribution, Poisson GP mixed with bivariate lognormal distribution and generalized Poisson GP mixed with bivariate log-t distribution for the bivariate time series, namely the BP, BPLN,

BPLNGP and BGPLTGP models. All models have allowed for heroin shortage effect in the means, non-monotone trends and contemporaneous correlation but in different ways due to different model structures and data distributions. The first three models are compared to the BGPLTGP model to investigate whether the GP approach versus the multivariate Poisson or mixed multivariate Poisson approach as well as whether the bivariate log-t mixing distribution versus bivariate lognormal distribution are more preferable and provide better model fit in analyzing multivariate longitudinal count data. The results of the analysis including parameter estimates, standard errors (SE) and DIC output in `WinBUGS` are summarized in the following Section.

5.5.3. Results. Table 5.2 in Appendix 5.2 reports the estimate and standard error (SE) of the parameters for the four fitted models. Using the parameter estimates, the expected value, variance and covariance of the monthly number of arrests for the two illicit drugs use or possession over time are calculated. For the BP and BGPLTGP models, (5.1) and (5.12) are used respectively. For the BPLN model, the mean, variance and covariance of the lognormal distribution are substituted in (5.2). Whereas for the BPLNGP model, the expected number, variance and covariance are derived in a similar way as (5.2) and are given by

$$E(W_{it}) = \frac{\exp(\mu^*_{it} + \frac{\sigma^2_{it}}{2})}{a^{t-1}_{it}}, \;\; Var(W_{it}) = \frac{\exp(\mu^*_{it} + \frac{\sigma^2_{it}}{2})}{a^{t-1}_{it}} + \frac{\exp(2\mu^*_{it} + \sigma^2_{it})[\exp(\sigma^2_{it}) - 1]}{a^{2(t-1)}_{it}}$$

and $Cov(W_{it}, W_{jt}) = \dfrac{\exp\left(\mu^*_{it} + \mu^*_{jt} + \frac{\sigma^2_{it}}{2} + \frac{\sigma^2_{jt}}{2}\right)[\exp(\sigma_{ijt}) - 1]}{(a_{it}a_{jt})^{t-1}}$

where μ^*_{it} and a_{it} are defined in (5.20) and (5.21) respectively as in the BGPLTGP model. To visualize the model performance and facilitate comparison, the expected monthly number of arrests for use or possession of amphetamine and narcotics are illustrated respectively in Figures 5.3(a) and 5.3(b) in Appendix 5.3 for all the models. Similarly, the SE of the monthly number of arrests for the two illicit drugs use or possession are plotted in Figures 5.4(a) and 5.4(b) in Appendix 5.3.

==========

Table 5.2 and Figures 5.3(a), 5.3(b), 5.4(a) and 5.4(b) about here

==========

Figures 5.3(a) and 5.3(b) indicate the consistent increasing trends for the bivariate time series. After allowing for the trends, the contemporary correlation between the two time series is still weakly positive but ceases to be significant both before and during the heroin shortage as shown by the insignificant covariance parameters (labelled as 'cov' in the third column 'type' in Table 5.2) in all fitted models (95% credibility intervals include zero) except for the BP model in Table 5.2. Amongst the four models, BP model gives the worst fit to the data as it has the largest DIC. The significant covariance parameters and the largest DIC can be explained by its inability to account for overdispersion in the bivariate counts as illustrated in Figures 5.4(a) and 5.4(b) that its SE is substantially lower than the other

three models. Due to the ability to account for overdispersion, the BPLN and BPLNGP models give substantially smaller $DICs$ than the BP model indicating an improvement in the model fit. Not surprisingly, their $DICs$ are close since the two models have similar model structures except that the latter adopts a GP approach. Their expected monthly numbers of arrests and SEs are also comparable as revealed in Figures 5.3 and 5.4. Nevertheless, the smaller DIC in the BPLNGP model supports the use of a GP approach with an explicit ratio function for the trend movement in modelling multivariate longitudinal count data.

Although both BPLN and BPLNGP models can account for overdispersion, the BGPLTGP model in which the GPD for the data and bivariate log-t distribution for the underlying stochastic process $\{\boldsymbol{Y}_t^*\}$ provide a wider range of dispersion, gives the best model fit (smallest DIC in Table 5.2) to the data and thus is chosen as the best model. With reference to Figure 5.3(a) which plots the expected monthly number of arrests for amphetamine use or possession, the upward trend of the BGPLTGP model continues throughout the period with a slightly higher rate of increase during the period of heroin shortage. On the contrary, as shown in Figure 5.3(b), the expected monthly number of arrests for narcotics use or possession is higher at the start and rises at a faster rate than that of amphetamine before heroin shortage. Followed by a rapid drop in the mean, the growth ceases after the onset of heroin shortage in late December 2000. Besides, as

revealed in Figures 5.4(a) and 5.4(b), the SE of the monthly number of arrests for amphetamine use or possession inflates with the mean throughout the entire period. On the other hand, the monthly number of arrests for narcotics use or possession becomes less overdispersed with a minor growth in variance after the onset of heroin shortage.

Lastly, we performed the tests for serial and cross correlations described in Section 5.3.4 for the best model, the BGPLTGP model. With respect to serial correlation, no significant serial correlation is found for amphetamine since the p-values of the chi-square test described in Section 5.3.4 for testing serial correlation up to lag 1,2,3,4 and 5 are 0.411, 0.509, 0.678, 0.416 and 0.555 respectively. However, significant serial correlations are detected for narcotics up to at least lag 5 with p-values equal to 6.36×10^{-6}, 1.41×10^{-8}, 5.81×10^{-11}, 7.68×10^{-13} and 2.49×10^{-13} for lag up to 1, 2, 3, 4 and 5 correspondingly. These suggest that adding some lagged observations $(W_{2,t-1},\ldots,W_{2,t-5})$ into the mean function μ^*_{2t} in (5.20) may help to reduce the serial dependency. For cross correlation, the monthly number of arrests for amphetamine use or possession has significant cross correlations (up to lag 6) with that for narcotics use or possession. The p-values for testing whether $Corr(W_{1t},W_{2,t-L})$ are significantly different from zero are 0.07, 0.04, 0.03, 0.02, 0.03, 0.01, 0.02, 0.10, 0.62, 0.37, 0.57 and 0.19 for $L=-7,\ldots,-1,0,1,\ldots,4$ respectively. To take into account this long-term association, we incorporated some lagged observations $(W_{1,t-1},\ldots,W_{1,t-6})$ from amphetamine into the mean function μ^*_{2t}

for narcotics and vice versa. Different AR structures were fitted and the final BGPLTGP model with the smallest DIC (1991.23) and significant AR terms is achieved with the mean functions for the bivariate time series given by

$$\begin{aligned}\mu^*_{1t} &= 1.908 + 1.692b + 0.0106w_{2,t-1}\\ \mu^*_{2t} &= 2.2 + 0.651b + 0.0142w_{2,t-1} + 0.01w_{2,t-2}.\end{aligned}$$

where all $\beta_{\mu k1}, k = 0, 1, 2$ and $\beta_{\mu k2}, k = 0, \ldots, 3$ in the mean functions are significant. Besides, all other model parameters are quantitatively similar to that of the BGPLTGP model without accounting for serial and cross correlations given in the last column of Table 5.2. The parameter estimates, SE and DIC of the final model are given in Table 5.3 in Appendix 5.2.

==========

Table 5.3 about here

==========

Regarding the objective of the study, the insignificant covariance parameters $\sigma_{12p}, p = 1, 2$ in the final model reveal that the weak positive contemporaneous correlation across the bivariate time series does not give any evidence of the instantaneous association between the growth in the monthly number of arrests for amphetamine use or possession and the decline in the monthly number of arrests for narcotics use or possession due to heroin shortage in Sydney. Unexpectedly, concerning the long-term association, the significant parameter $\hat{\beta}_{\mu 21} = 0.0106$ in the final model (95% CI

for $\beta_{\mu 21}$:$[0.0015, 0.0191]$) implies that after the trend movements have been accounted for, an increase in the number of arrests for use or possession of narcotics in a certain month is followed by an increase in the number of arrests for use or possession of amphetamine in the next month (lag 1). Our finding, though confined to Sydney LGA, on one hand agrees with Snowball *et al.* (2008) that the decline in the monthly number of arrests for narcotics use or possession is not accompanied by the growth in the monthly number of arrests for amphetamine use or possession at a state level for all 153 LGAs in NSW. On the other hand, another finding that the growth of the number of arrests for narcotics use or possession in the previous month is positively associated with the current growth of that for amphetamine disagrees with Snowball *et al.* (2008) which found no long-term association between the monthly numbers of arrests for narcotics and amphetamine use or possession.

5.6. Discussion

In this Chapter, we propose the multivariate generalized Poisson log-t geometric process (MGPLTGP) model which is essentially a generalized Poisson mixed model using multivariate log-t distribution as the mixing density in the GP modelling framework. The model has several outstanding properties over some traditional multivariate Poisson count models. First, it can handle negatively correlated multivariate counts which the multivariate

Poisson (MP) models fail to do so. Secondly, it fits multivariate longitudinal count data with different degree of dispersion ranging from overdispersion to underdispersion which is a shortcoming of the MP mixed models. Thirdly, the trend movement is analyzed explicitly using a ratio function that 'detrends' the latent GP $\{X_{it}, t = 1, \ldots, n\}$ geometrically to a stationary stochastic process $\{Y_{it}\}$ which is then fitted by a mixing distribution. Lastly, the mixing density, the multivariate log-t distribution has a heavier-than-lognormal tail which can handle serious overdispersion due to outlying observations.

The model is implemented through MCMC sampling algorithms using `WinBUGS`. By expressing the multivariate log-t distribution in scale mixtures of multivariate lognormals, the MCMC algorithms are facilitated since the full conditional distributions of the model parameters are simplified and the mixing parameters enable outlier diagnosis. The practicability of the model is demonstrated through the analysis of a bivariate time series of the monthly number of arrests for two illicit drugs use or possession in Sydney. Results in Section 5.5.3 indicate that our proposed model gives the best model fit (smallest DIC) and is more preferable to other three competitive models including the bivariate Poisson model, bivariate Poisson lognormal model and bivariate Poisson lognormal geometric process model because of its nicer properties.

Last but not least, concerning the need in examining the cluster effects which are often observed in multivariate panel count data, the proposed

model can be easily extended to incorporate mixture effects and random effects to allow for heterogeneity in the multiple time series. We believe that the extended mixture model, which can identify subgroups of multivariate time series comprising the population, would be worthy of future research.

Appendix 5.1

Monthly number of arrests for use or possession of amphetamine W_{1t} and narcotics W_{2t} in Sydney LGA during January 1995 - December 2008

month	t	W_{1t}	W_{2t}	month	t	W_{1t}	W_{2t}	month	t	W_{1t}	W_{2t}	month	t	W_{1t}	W_{2t}
Jan 1995	1	14	18	Jul 1998	43	14	23	Jan 2002	85	19	12	Jul 2005	127	33	26
Feb 1995	2	6	12	Aug 1998	44	13	24	Feb 2002	86	16	15	Aug 2005	128	20	10
Mar 1995	3	12	19	Sep 1998	45	9	26	Mar 2002	87	15	7	Sep 2005	129	12	12
Apr 1995	4	3	16	Oct 1998	46	14	41	Apr 2002	88	9	10	Oct 2005	130	28	11
May 1995	5	8	19	Nov 1998	47	7	27	May 2002	89	17	12	Nov 2005	131	24	19
Jun 1995	6	8	19	Dec 1998	48	12	38	Jun 2002	90	26	12	Dec 2005	132	14	7
Jul 1995	7	8	11	Jan 1999	49	6	32	Jul 2002	91	14	11	Jan 2006	133	14	9
Aug 1995	8	8	12	Feb 1999	50	11	38	Aug 2002	92	15	11	Feb 2006	134	14	11
Sep 1995	9	11	17	Mar 1999	51	9	39	Sep 2002	93	19	13	Mar 2006	135	29	17
Oct 1995	10	8	19	Apr 1999	52	15	39	Oct 2002	94	14	21	Apr 2006	136	47	9
Nov 1995	11	5	14	May 1999	53	11	48	Nov 2002	95	15	14	May 2006	137	27	11
Dec 1995	12	8	8	Jun 1999	54	11	25	Dec 2002	96	22	11	Jun 2006	138	19	9
Jan 1996	13	6	17	Jul 1999	55	10	32	Jan 2003	97	21	10	Jul 2006	139	41	7
Feb 1996	14	4	16	Aug 1999	56	17	35	Feb 2003	98	16	12	Aug 2006	140	25	9
Mar 1996	15	14	10	Sep 1999	57	15	16	Mar 2003	99	9	10	Sep 2006	141	28	9
Apr 1996	16	9	14	Oct 1999	58	2	24	Apr 2003	100	9	9	Oct 2006	142	27	14
May 1996	17	9	17	Nov 1999	59	10	32	May 2003	101	22	13	Nov 2006	143	20	17
Jun 1996	18	6	13	Dec 1999	60	17	21	Jun 2003	102	22	13	Dec 2006	144	32	17
Jul 1996	19	4	32	Jan 2000	61	19	46	Jul 2003	103	23	8	Jan 2007	145	29	11
Aug 1996	20	4	21	Feb 2000	62	9	37	Aug 2003	104	22	13	Feb 2007	146	32	11
Sep 1996	21	4	16	Mar 2000	63	14	18	Sep 2003	105	21	12	Mar 2007	147	43	13
Oct 1996	22	6	5	Apr 2000	64	8	28	Oct 2003	106	15	22	Apr 2007	148	23	8
Nov 1996	23	3	17	May 2000	65	5	26	Nov 2003	107	24	12	May 2007	149	25	13
Dec 1996	24	5	15	Jun 2000	66	11	19	Dec 2003	108	18	22	Jun 2007	150	22	8
Jan 1997	25	4	18	Jul 2000	67	18	23	Jan 2004	109	29	22	Jul 2007	151	25	16
Feb 1997	26	7	14	Aug 2000	68	13	27	Feb 2004	110	24	12	Aug 2007	152	32	25
Mar 1997	27	9	11	Sep 2000	69	22	21	Mar 2004	111	24	12	Sep 2007	153	33	16
Apr 1997	28	6	14	Oct 2000	70	9	24	Apr 2004	112	24	27	Oct 2007	154	26	19
May 1997	29	6	13	Nov 2000	71	10	35	May 2004	113	21	24	Nov 2007	155	30	34
Jun 1997	30	7	6	Dec 2000	72	12	28	Jun 2004	114	21	21	Dec 2007	156	45	22
Jul 1997	31	0	13	Jan 2001*	73	8	30	Jul 2004	115	24	13	Jan 2008	157	51	29
Aug 1997	32	12	13	Feb 2001	74	14	17	Aug 2004	116	17	16	Feb 2008	158	50	17
Sep 1997	33	4	15	Mar 2001	75	36	10	Sep 2004	117	12	12	Mar 2008	159	27	16
Oct 1997	34	10	13	Apr 2001	76	17	14	Oct 2004	118	28	20	Apr 2008	160	38	24
Nov 1997	35	8	14	May 2001	77	24	16	Nov 2004	119	27	17	May 2008	161	57	13
Dec 1997	36	2	15	Jun 2001	78	36	16	Dec 2004	120	24	14	Jun 2008	162	38	13
Jan 1998	37	18	21	Jul 2001	79	12	13	Jan 2005	121	26	22	Jul 2008	163	40	25
Feb 1998	38	6	17	Aug 2001	80	14	16	Feb 2005	122	25	18	Aug 2008	164	36	14
Mar 1998	39	7	20	Sep 2001	81	21	8	Mar 2005	123	22	24	Sep 2008	165	41	13
Apr 1998	40	10	19	Oct 2001	82	8	15	Apr 2005	124	17	17	Oct 2008	166	22	17
May 1998	41	16	27	Nov 2001	83	18	8	May 2005	125	37	24	Nov 2008	167	45	27
Jun 1998	42	12	22	Dec 2001	84	24	6	Jun 2005	126	41	14	Dec 2008	168	50	23

* heroin shortage commenced

Appendix 5.2

Tables

Table 5.1: Moments of the joint pmfs for the BGPLTGP model under a set of floating parameters with fixed values of $\sigma_1^2 = 0.07, \sigma_{12} = 0.06, \sigma_2^2 = 0.1, \nu = 20, \beta_{\mu 01} = 2, \beta_{\mu 02} = 2.5, \beta_{a01} = -0.1, \beta_{a02} = 0.1, \lambda_{21} = -0.8, \lambda_{22} = 0.2$

floating	**Using (5.12)***						**Using (5.14)***					
parameter	$E(W_{1t})$	$E(W_{2t})$	$V(W_{1t})$	$V(W_{2t})$	$C(W_{1t},W_{2t})$	$\rho(W_{1t},W_{2t})$	$\widehat{E}(W_{1t})$	$\widehat{E}(W_{2t})$	$\widehat{V}(W_{1t})$	$\widehat{V}(W_{2t})$	$\widehat{C}(W_{1t},W_{2t})$	$\widehat{\rho}(W_{1t},W_{2t})$
$\sigma_{12} = -0.08$	8.497	11.667	8.687	35.001	-8.605	-0.493	8.482	11.670	8.534	35.399	-8.589	-0.494
$\sigma_{12} = -0.02$	8.486	11.646	8.466	34.340	-2.136	-0.125	8.505	11.729	8.434	34.889	-2.149	-0.125
$\sigma_{12} = 0.05$	8.486	11.646	8.454	34.283	5.672	0.333	8.461	11.570	8.449	34.396	5.711	0.335
$\sigma_{12} = 0.08$	8.496	11.665	8.660	34.918	9.568	0.550	8.514	11.701	8.749	35.224	9.726	0.554
$\sigma_{22} = 0.06$	8.491	11.397	8.551	26.892	6.774	0.447	8.511	11.418	8.524	26.979	6.759	0.446
$\sigma_{22} = 0.12$	8.496	11.798	8.669	39.343	7.201	0.390	8.585	11.987	8.885	40.129	7.435	0.394
$\sigma_{22} = 0.20$	8.484	12.300	8.419	58.233	7.279	0.329	8.491	12.336	8.542	57.470	7.275	0.328
$\sigma_{22} = 0.25$	8.490	12.676	8.536	74.908	7.679	0.304	8.508	12.713	8.410	72.170	7.769	0.315
$\nu = 5.0$	8.609	11.895	12.185	48.056	11.527	0.476	8.637	11.863	13.845	45.922	11.699	0.464
$\nu = 7.5$	8.552	11.778	10.197	40.150	8.981	0.444	8.573	11.805	10.099	39.914	8.868	0.442
$\nu = 10$	8.526	11.726	9.454	37.551	8.059	0.428	8.501	11.684	9.451	37.083	7.884	0.421
$\nu = 100$	8.457	11.589	7.804	32.256	6.070	0.383	8.424	11.585	7.686	32.300	5.925	0.376
$\beta_{\mu 02} = 1.6$	8.487	4.735	8.463	10.062	2.787	0.302	8.483	4.735	8.470	10.033	2.763	0.300
$\beta_{\mu 02} = 2.0$	8.486	7.064	8.460	16.962	4.156	0.347	8.483	7.064	8.470	16.901	4.122	0.345
$\beta_{\mu 02} = 2.4$	8.486	10.538	8.459	29.647	6.199	0.391	8.483	10.539	8.470	29.515	6.150	0.389
$\beta_{\mu 02} = 2.8$	8.483	15.713	8.403	53.611	9.161	0.432	8.483	15.722	8.470	53.603	9.175	0.431
$\beta_{a02} = -0.25$	8.497	16.556	8.689	59.674	10.110	0.444	8.497	16.487	8.877	59.850	10.303	0.447
$\beta_{a0} = -0.05$	8.499	13.561	8.748	44.076	8.357	0.426	8.497	13.499	8.879	43.969	8.442	0.427
$\beta_{a0} = 0.3$	8.498	9.554	8.721	26.244	5.864	0.388	8.497	9.512	8.879	26.225	5.949	0.390
$\beta_{a0} = 0.7$	8.498	6.405	8.732	15.102	3.938	0.343	8.497	6.376	8.879	15.068	3.988	0.345
$\lambda_{22} = -0.8$	8.485	11.644	8.433	19.619	6.821	0.530	8.494	11.702	8.389	20.179	6.811	0.523
$\lambda_{22} = -0.2$	8.487	11.647	8.478	24.255	6.875	0.479	8.494	11.701	8.386	24.642	6.798	0.473
$\lambda_{22} = 0.4$	8.486	11.646	8.451	48.425	6.841	0.338	8.493	11.698	8.377	48.828	6.757	0.334
$\lambda_{22} = 0.6$	8.482	11.638	8.371	88.581	6.747	0.248	8.493	11.687	8.372	88.502	6.707	0.246

*Note that $V(W_{it}) = Var(W_{it})$,$C(W_{1t}, W_{2t}) = Cov(W_{1t}, W_{2t})$ and $\rho(W_{1t}, W_{2t}) = Corr(W_{1t}, W_{2t})$

Table 5.2: Parameter estimates, SE and DIC in four fitted models for the amphetamine and narcotics data

			BP model			BPLN model			BPLNGP model			BGPLTGP model		
drug	**shortage**	**type**	**parameter**	**estimate**	SE	**parameter**	**estimate**	SE	**parameter**	**estimate**	SE	**parameter**	**estimate**	SE
AMP	before	mean	β_{011}	2.6430	0.2231	β_{01}	2.6450	0.3220	$\beta_{\mu 01}$	1.8670	0.1019	$\beta_{\mu 01}$	2.0270	0.1057
$i=1$	$p=1$	trend	β_{211}	-0.7488	0.1708	β_{21}	-0.7165	0.2495	β_{a01}	0.0053	0.0063	β_{a01}	0.0353	0.0050
			β_{311}	-0.0180	0.7985	β_{31}	1.0730	0.5498	β_{a11}	-0.0037	0.0014	β_{a11}	-0.0103	0.0010
		var				σ^2_{11}	0.0658	0.0309	σ^2_{11}	0.0725	0.0333	σ^2_{11}	0.0489	0.0354
		cov	β_{012}	-2.6490	0.0574	σ_{121}	0.0152	0.0171	σ_{121}	0.0212	0.0171	σ_{121}	0.0141	0.0167
		disp										λ_{211}	0.1003	0.1933
		df										ν_1	22.99	52.19
	during	mean	β_{111}	-5.8230	2.2460	β_{11}	-2.9910	1.5190	$\beta_{\mu 11}$	0.1899	0.2287	$\beta_{\mu 11}$	2.2450	0.1962
	$p=2$	trend	β_{411}	0.1718	0.0317	β_{41}	0.1628	0.0462	β_{a21}	-0.0124	0.0081	β_{a21}	0.0687	0.0055
			β_{511}	0.2338	0.0813	β_{51}	-0.0779	0.0554	β_{a31}	0.0031	0.0015	β_{a31}	-0.0092	0.0010
		var				σ^2_{12}	0.0661	0.0200	σ^2_{12}	0.0684	0.0197	σ^2_{12}	0.0707	0.0279
		cov	β_{112}	5.3030	0.0406	σ_{122}	0.0178	0.0132	σ_{122}	0.0153	0.0130	σ_{122}	0.0120	0.0115
		disp										λ_{212}	0.0611	0.3476
NAR	before	mean	β_{022}	3.0550	0.1677	β_{02}	3.1220	0.2377	$\beta_{\mu 02}$	2.5470	0.0825	$\beta_{\mu 02}$	2.6220	0.1192
$i=2$	$p=1$	trend	β_{222}	-0.5338	0.1218	β_{22}	-0.5991	0.1781	β_{a02}	-0.0089	0.0067	β_{a02}	0.0014	0.0163
			β_{322}	-0.7184	0.9006	β_{32}	1.6250	0.5007	β_{a12}	-0.0010	0.0015	β_{a12}	-0.0034	0.0036
		var				σ^2_{21}	0.0654	0.0159	σ^2_{21}	0.0612	0.0158	σ^2_{21}	0.0469	0.0239
		disp										λ_{221}	-0.1939	0.3582
		df										ν_2	23.80	56.82
	during	mean	β_{122}	-15.590	3.8330	β_{12}	-3.7140	1.1610	$\beta_{\mu 12}$	-0.1605	0.2123	$\beta_{\mu 12}$	-0.1031	0.4069
	$p=2$	trend	β_{422}	0.1472	0.0219	β_{42}	0.1558	0.0328	β_{a22}	0.0093	0.0074	β_{a22}	0.0083	0.0081
			β_{522}	0.6464	0.1518	β_{52}	-0.2270	0.0632	β_{a32}	0.0004	0.0014	β_{a32}	0.0010	0.0010
		var				σ^2_{22}	0.0713	0.0202	σ^2_{22}	0.0709	0.0207	σ^2_{22}	0.0890	0.0310
		disp										λ_{222}	-0.4167	0.3643
		DIC		2277.19			2073.11			2072.55			**1993.92**	

Remarks: var, cov, disp, df stand for variance, covariance, dispersion and degree of freedom respectively.

Table 5.3: Parameter estimates, SE and DIC in BGPLTGP model after accounting for serial correlation

drug	**shortage**	**type**	**parameter**	**estimate**	SE
AMP	before	mean	$\beta_{\mu 01}$	1.9080	0.1145
$i=1$	$p=1$	AR(1)	$\beta_{\mu 21}$	0.0106	0.0044
		trend	β_{a01}	0.0319	0.0082
			β_{a11}	-0.0087	0.0018
		var	σ^2_{11}	0.0480	0.0362
		cov	σ_{121}	0.0113	0.0146
		disp	λ_{211}	0.1104	0.1945
		df	ν_1	15.070	46.020
	during	mean	$\beta_{\mu 11}$	1.6920	0.1771
	$p=2$	trend	β_{a21}	0.0451	0.0062
			β_{a31}	-0.0062	0.0014
		var	σ^2_{12}	0.0353	0.0208
		cov	σ_{122}	0.0030	0.0099
		disp	λ_{212}	0.1210	0.2825
NAR	before	mean	$\beta_{\mu 02}$	2.2200	0.1005
$i=2$	$p=1$	AR(1)	$\beta_{\mu 22}$	0.0142	0.0040
		AR(2)	$\beta_{\mu 32}$	0.0100	0.0039
		trend	β_{a02}	-0.0176	0.0066
			β_{a12}	0.0026	0.0015
		var	σ^2_{21}	0.0526	0.0227
		disp	λ_{221}	-0.1709	0.3380
		df	ν_2	30.930	58.450
	during	mean	$\beta_{\mu 12}$	0.6510	0.2010
	$p=2$	trend	β_{a22}	0.0586	0.0054
			β_{a32}	-0.0100	0.0011
		var	σ^2_{22}	0.0739	0.0246
		disp	λ_{222}	-0.4732	0.3433
	DIC			1991.23	

Remarks: var, cov, disp, df stand for variance, covariance, dispersion and degree of freedom respectively.

Appendix 5.3

Figures

Figure 5.1: The pmfs of BGPLTGP model with varying parameters

(a) σ_{12} (b) σ_2^2

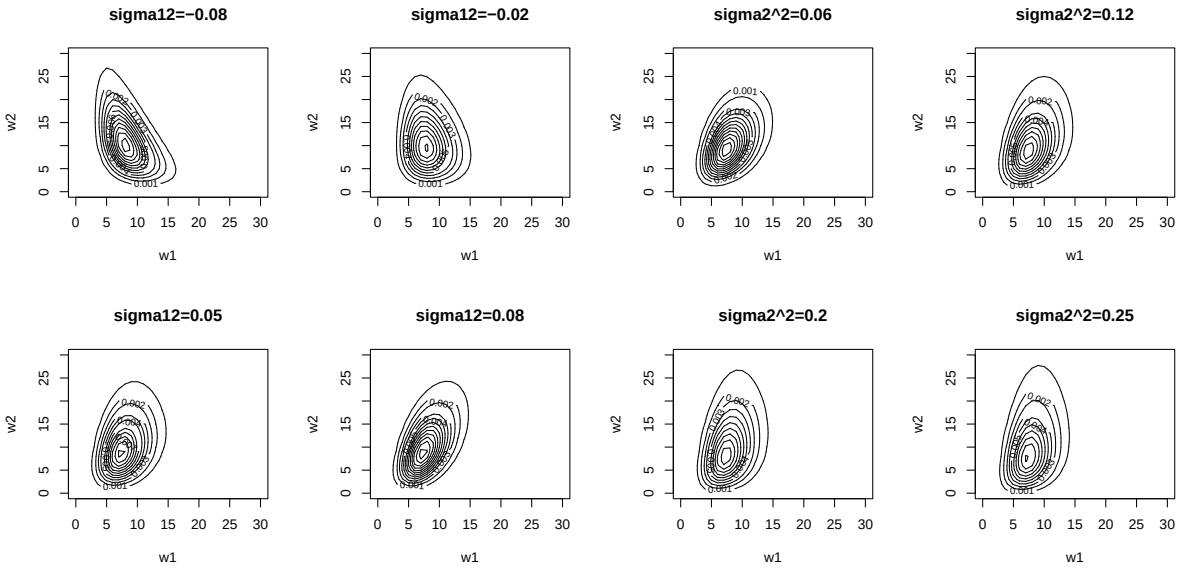

(c) ν (d) $\beta_{\mu 02}$

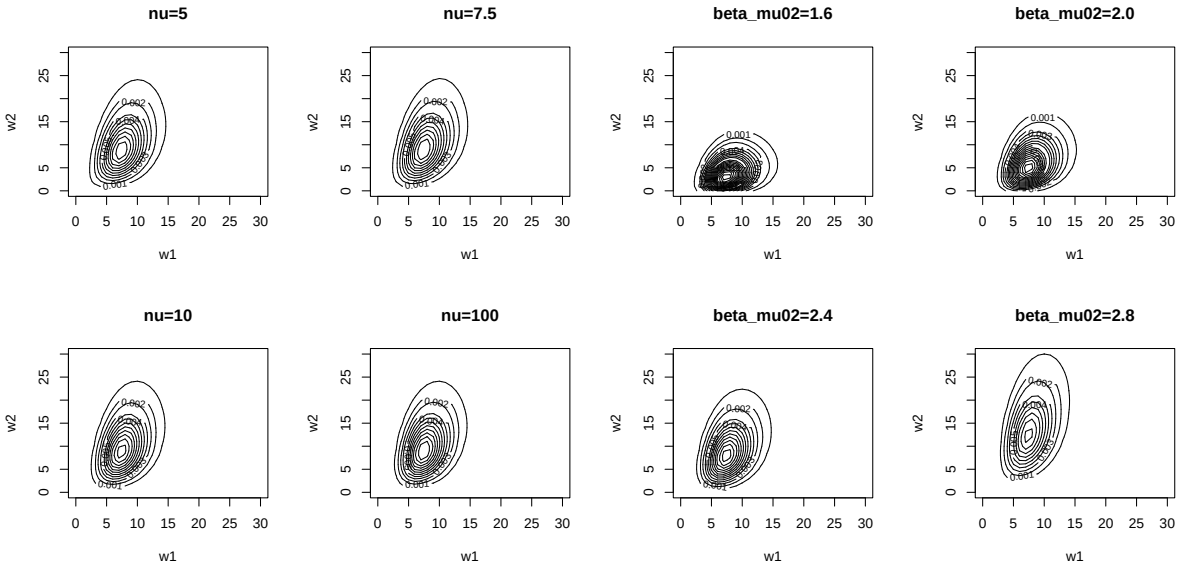

Figure 5.1: The pmfs of BGPLTGP model with varying parameters (continued)

(e) β_{a02} (f) λ_{22}

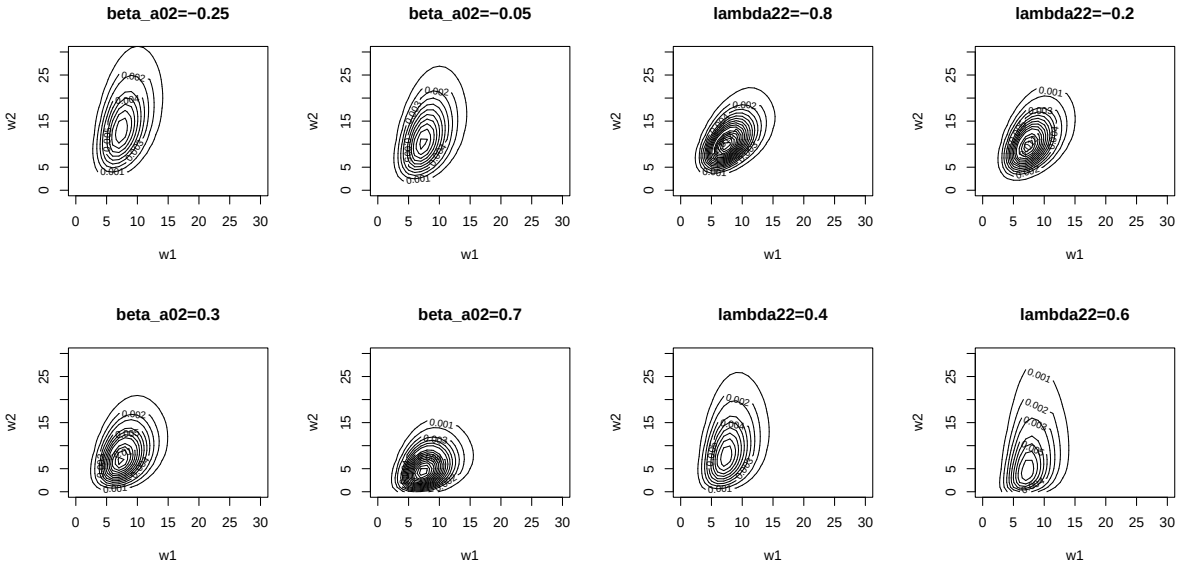

Figure 5.2: Monthly number of arrests for amphetamine (AMP) and narcotics (NAR) use/possession in Sydney during January 1995 - December 2008

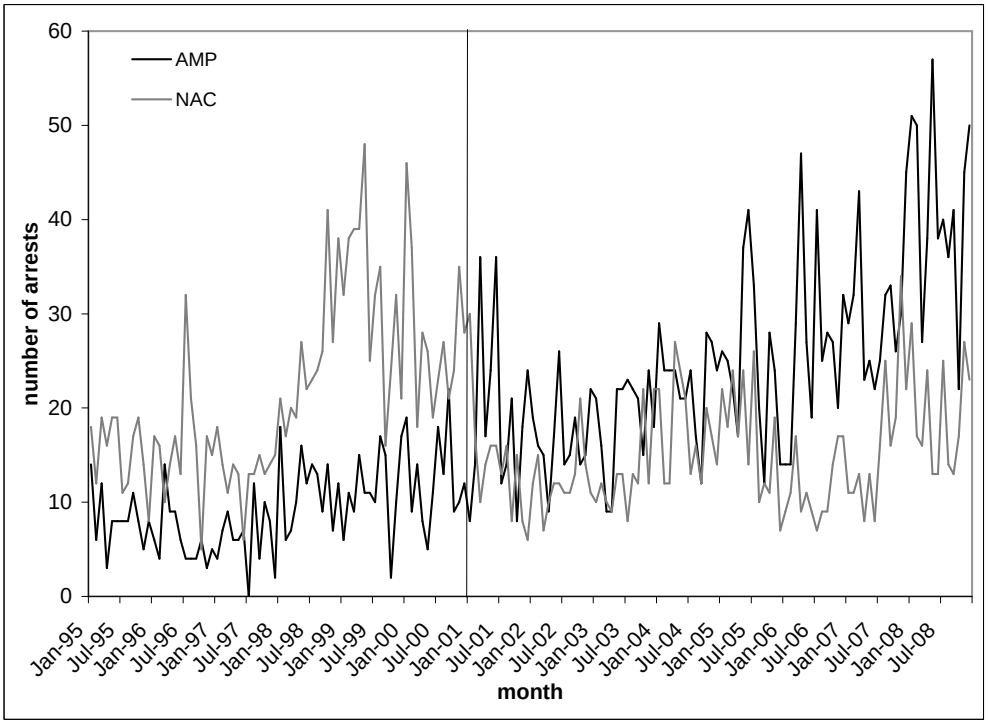

Figure 5.3: Trends of the expected monthly number of arrests for use or possession of two illicit drugs for all fitted models

(a) amphetamine $\left(\widehat{E}(W_{1t})\right)$

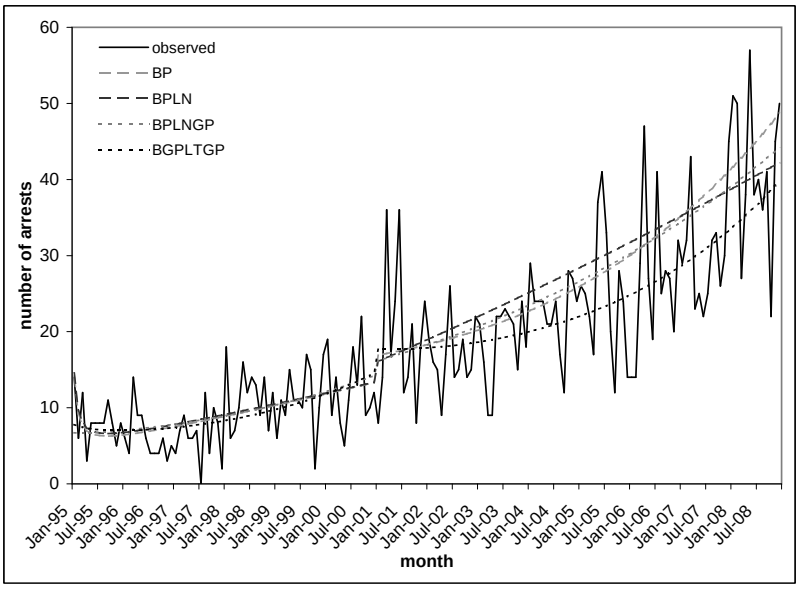

(b) narcotics $\left(\widehat{E}(W_{2t})\right)$

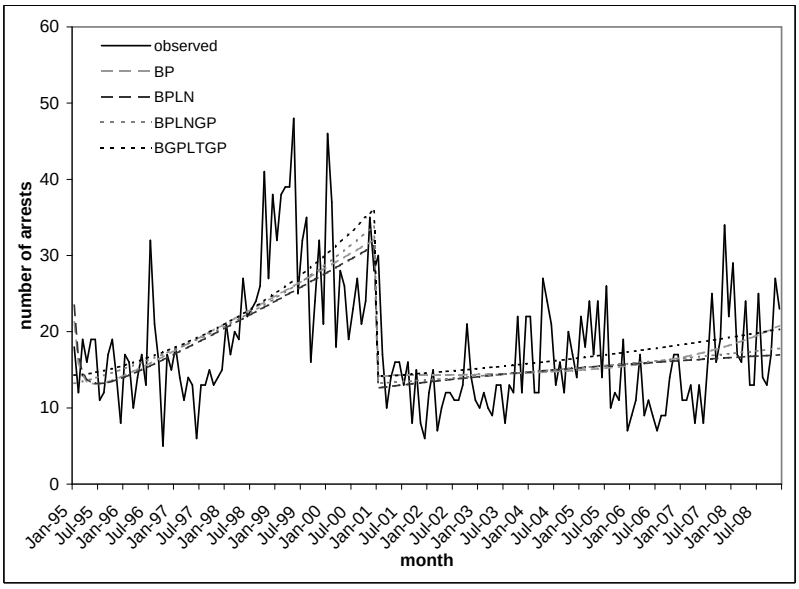

Figure 5.4: Trends of the SE of monthly number of arrests for use or possession of two illicit drugs for all fitted models

(a) amphetamine $\left(\sqrt{\widehat{V}ar(W_{1t})}\right)$

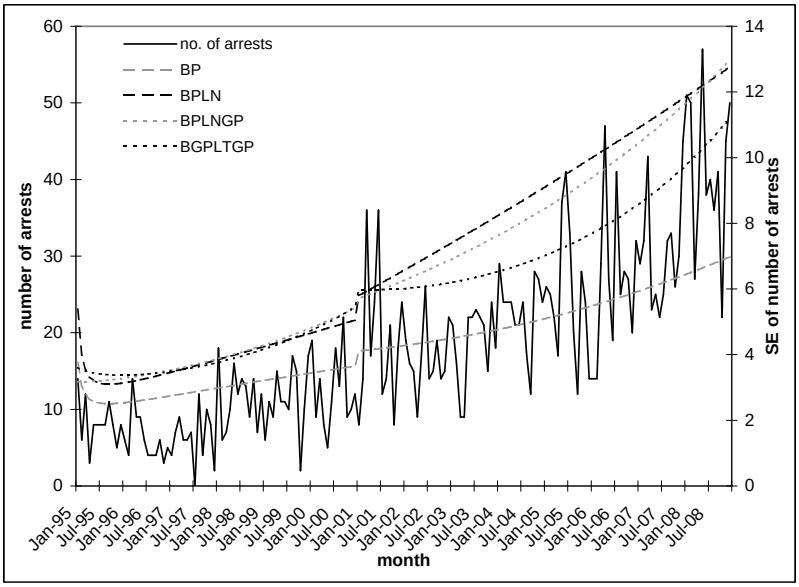

(b) narcotics $\left(\sqrt{\widehat{V}ar(W_{2t})}\right)$

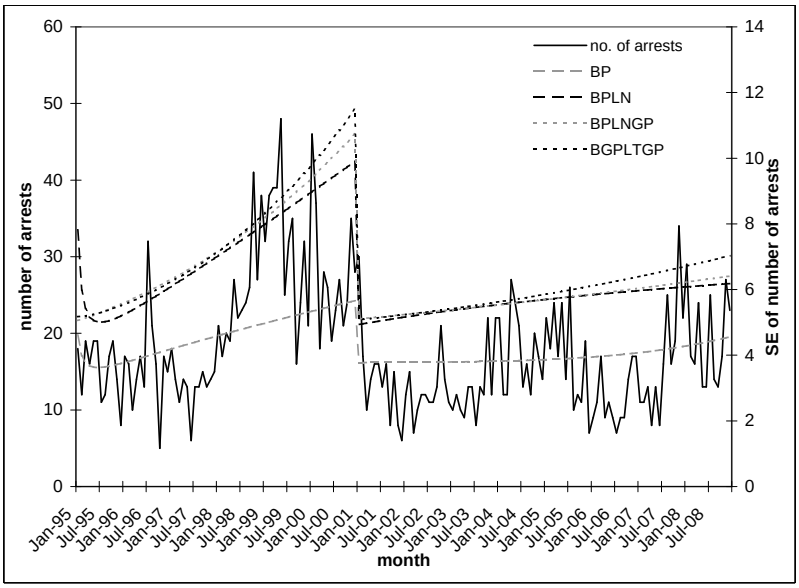

CHAPTER 6

Summary

6.1. Overview

Longitudinal and panel count data appear in every aspect of our lives such as in epidemiology, marketing, engineering and economics. The list of areas in which time series of count data are analyzed is endless. Some common characteristics of time series of counts include non-stationarity, non-monotone trends, time-evolving or time-invariant covariate effects, serial correlation and overdispersion caused by zero-inflation and extreme outliers, and population heterogeneity caused by cluster effects in panel data. Lastly, multiple measurements are sometimes made to each subject at each time point.

To take into account these properties, Wan (2006) introduced the Poisson geometric process (PGP) model to analyze longitudinal and panel count data. However, the PGP models developed in Wan (2006) looked specifically into some aforementioned characteristics and did not address other problems like the serial correlation between observations, overdispersion and underdispersion. So far, the PGP model has been solely applied to univariate analysis of time series of counts, the multivariate area yet remains unexplored.

In light of these, our objective of this research is to extend the PGP model to allow for those characteristics that have not been addressed. As reviewed in Chapter 1, there exist two major categories of models, namely the observation-driven (OD) and parameter-driven (PD) models which specifically allow for serial correlation. In the OD models, the mean of the outcome is expressed explicitly as a function of the past observations in order to construct an autocorrelation structure for accommodating serial correlation. This approach is appealing due to the straightforward prediction and derivation of the likelihood function. However, difficulties arise when we interpret the covariate effects on the outcome. On the contrary, the PD models introduce serial dependence through a latent variable which evolves independently of the past observations in the mean function and thus enables a straightforward interpretation of the covariate effects. However, the parameter estimation of this model is computationally intensive due to the complicated derivation of the likelihood function which involves integration over the latent variables and the forecasting is cumbersome since the model is built on a latent process. Unlike the OD and PD models, the PGP model belongs to the family of the GLMM model and can be classified as a state space model with state variable X_t where $\{X_t, t = 1, \ldots, n\}$ is the latent GP evolving independently of the past outcomes. The main difference between the PGP model and OD/PD models is that the former focuses on modelling the trend of the time series whereas the latter concentrates on investigating the serial correlation structure of the outcomes.

To combine the merits of these models, we extend the PGP model to account for serial correlation between observations using the OD model approach and furthermore to address other characteristics that are prominent in longitudinal and panel count data. As mentioned before, the mixture Poisson geometric process (MPGP) model using exponential distribution as described in Wan (2006) is not adequate to account for excess zeros and substantial overdispersion. Therefore, firstly in Chapter 2, we propose two models namely the zero-altered mixture Poisson geometric process (ZMPGP) model and the mixture Poisson geometric process (MPGP-Ga) model using gamma distribution to cope with zero-inflation. The ZMPGP model is essentially a mixture of zero-degenerated model and a zero-truncated MPGP model via the hurdle approach, while the MPGP-Ga model is a state space model with state variable $E(W_{it}) = X_{it}$ where X_{it} follows a gamma distribution. For model comparison, the analysis of bladder cancer data reveals that the MPGP-Ga model gives a better model fit than the ZMPGP model due to the brevity and flexibility of the model distribution. Nevertheless, both models are capable of modelling zero-inflated count data but do so in a different way and therefore are suitable under different situations.

Secondly, concerning another source of overdispersion, the presence of outlying observations, we pioneer the robust mixture Poisson geometric process (RMPGP) model in Chapter 3 by replacing the gamma distribution of the stochastic process $\{Y_{it}\}$ and assuming the logarithm of the underlying stochastic process $\{Y_{it}^* = \ln Y_{it}\}$ follows some heavy-tailed distributions

including the Student's t- and exponential power (EP) distributions. The resultant models are namely the RPGP-t and RPGP-EP models. Moreover, by expressing the two heavy-tailed distributions in scale mixtures (SM) representation, the model implementation using MCMC algorithms is facilitated and the additional parameter known as the mixing parameter enable us to identify any outliers in the data. For model comparison, the simulation study shows that the performances of the two RPGP models are comparable and satisfactory. In case of data with very heavy tail, the RMPGP-t model seems to fit better since Student's t-distribution allows a much heavier-than-normal tail. On the other hand, the RMPGP-EP model allows more diverse degrees of overdispersion as EP distribution has a more flexible tail which can be either leptokurtic or platykurtic. Therefore, the latter model gives a better fit in the analysis of epilepsy data because the two mixture groups being identified show overdispersion to different extents.

The previous extensions focus on solving the problems related to overdispersion, however the analogous problem, underdispersion, has not received much attention as it is less frequently observed in longitudinal and panel count data. Nevertheless, a comprehensive count model should contain a flexible dispersion structure to accommodate different degrees of dispersion ranging from overdispersion to underdispersion. Therefore, thirdly, we propose the mixture generalized Poisson geometric process (GMPGP) model in Chapter 4 which relaxes the restriction of overdispersion in the previous extended MPGP models. The GMPGP model replaces the Poisson data

distribution with generalized Poisson distribution (GPD) which contains an extra parameter to control the dispersion of the distribution. This unified model is compared with the RPGP-EP model through two simulation experiments and a real data analysis of the cannabis data. The results highlight that while the performances of the two models are comparable and satisfactory in the case of overdispersion, the GMPGP model has a much better performance in handling underdispersed data in which the RMPGP-EP model falls short to do so. Moreover in the real data analysis where the data is overdispersed in the presence of outliers, the GMPGP model still outperforms the RMPGP-EP model as it can accommodate outliers by the heavier tail of the generalized Poisson-gamma mixed distribution.

Last but not least in Chapter 5, we explore a new area for the PGP model on multivariate longitudinal count data by integrating the framework of RMPGP and GMPGP models. The resultant model named as multivariate generalized Poisson log-t geometric process (MGPLTGP) model is essentially a generalized Poisson mixed model within the GP modelling framework and adopting multivariate log-t distribution as the mixing density. Through the real data analysis, we show that the MGPLTGP model has a couple of merits over some traditional multivariate count models including its abilities to handle positive or negative serial, contemporaneous and cross correlations and accommodate different degrees of dispersion, especially serious overdispersion due to outlying observations in multivariate longitudinal count data.

For statistical inference, since the distributions in most of the extended PGP models do not have a closed-form except the ZMPGP and MPGP-Ga models, Markov chain Monte Carlo (MCMC) sampling methods are preferred for parameter estimation to classical approach such as the maximum likelihood (ML) estimation and the expectation-maximization (EM) algorithm as the former avoids the optimization of high-dimensional likelihood functions and can be easily implemented using `WinBUGS`.

In summary, the extended PGP models take into account the serial correlation between observations, overdispersion caused by zero-inflation and outlying observations, different degrees of dispersion and cross and contemporaneous correlations between time series while keeping its old virtue to accommodate non-stationarity, non-monotone trends, covariate and cluster effects. Accompanied by the straightforward model implementation and interpretation, these PGP models, which have been applied extensively in different areas as demonstrated in this research, can undoubtedly compete with other traditional time series models for count data.

6.2. Further research

In spite of the substantial development of PGP models in this thesis, there are still many unattended areas that are worthy of further consideration.

6.2.1. Extension to multivariate panel count data. Since many multivariate longitudinal data comes from panel studies, the presence of population heterogeneity is usually inevitable in the data. Hence, the MGPLTGP model proposed in Chapter 5 which is designed for modelling multivariate longitudinal count data can be further extended to incorporate mixture effect or random effects to allow for the cluster or subject-specific effects amongst multiple time series. We believe that the extended mixture model, which can identify subgroups comprising the population, is useful for all practical purposes.

6.2.2. Comparison of serial dependence structure. In this research, we apply the OD model approach in all extended PGP models to accommodate the serial dependency between observations by adding some past observations as covariates into the mean link function of the stochastic process $\{Y_{it}\}$. On the other hand, we may consider the PD model approach by incorporating some latent serially correlated random effects which are independent of past observations into the mean link function. The model properties of the two diverse approaches can be investigated and compared in terms of model interpretation, parameter estimation and practicability. Moreover, when the time series is long, we can consider some simple but efficient correlation structures to reduce the number of parameters for the random effects model.

6.2.3. Comparison in methodologies of inference. On the whole, we focus on the extensions of PGP models to account for different data properties. Another area that is worthwhile to study is the inference methodology. Though using MCMC algorithm avoids the evaluation of high-dimensional likelihood function, the computation time for this sampling algorithms is sometimes massive if the data size is large and the model is highly complicated.

As an alternative to the ML method in the frequentist approach, the EM method can be considered since the latent variables are evaluated through the E-step. Besides, large sample properties of the estimators can be studied by deriving their large sample distributions. Knowing the asymptotic distributions, we can then construct confidence intervals for and perform hypothesis tests on the model parameters.

6.2.4. Comparisons with traditional time series count models. Last but not least, apart from the model comparison within the extended PGP models, we can compare our proposed models with those benchmarking OD and PD models to justify the pros and cons of adopting the PGP approach in modelling longitudinal and panel count data from different areas. Besides, knowing the shortcomings, the PGP models can be modified accordingly to increase its competence among all existing models.

Bibliography

Akaike, H. (1974). A new look at the statistical model identification. *IEEE Transactions on Automatic Control* **19**, 716-723.

Albrecht, P. (1984). Laplace transforms, Mellin transforms and mixed Poisson processes. *Scandinavian Actuarial Journal* **11**, 58-64.

Al-Osh, M.A. & Alzaid, A.A. (1987). First-order integer-valued autoregressive (INAR(1)) process. *Journal of Time Series Analysis* **8**, 261-275.

Angers, J.F. & Biswas, A. (2003). A Bayesian analysis of zero-inflated generalized Poisson model. *Computational Statistics and Data Analysis* **42**, 37-46.

Aitchinson, J. & Ho, C.H. (1989). The multivariate Poisson-log normal distribution. *Biometrika* **75**, 621-629.

Australian Institute of Health and Welfare. (2008). 2007 National Drug Strategy Household Survey: first results. *Drug Statistics Series number 20*. Cat. no. PHE 98. Canberra: AIHW.

Bae, S., Famoye, F., Wulu, J.T., Bartolucci, A.A. & Singh, K.P. (2005). A rich family of generalized Poisson regression models with applications. *Mathematics and Computers in Simulation* **69**, 4-11.

Baker, J. & Goh, D. (2004). The cannabis cautioning scheme three years on: An implementation and outcome evaluation. *Drug and Alcohol Co-ordination*, NSW Police, Sydney.

Blumer, M.G. (1974). On the fitting the Poisson-lognormal distribution to species abundance data. *Biometrics* **30**, 101-110.

Bohning, D., Dietz, E. & Schlattmann, P. (1999). The zero-inflated Poisson model and the decayed, missing and filled teeth index in dental epidemiology. *Journal of the Royal Statistical Society A* **162**, 195-209.

Box, G.E.P & Tiao, G.C. (1973). Bayesian inference in statistical analysis. Massachusetts: Addison-Wesley.

Brännäs, K. & Johansson, P. (1996). Panel data regression for counts. *Statistical Papers* **37**, 191-213.

Cameron, A.C. & Trivedi, P.K. (1998). Regression Analysis of Count Data. Cambridge: Cambridge University Press.

Celeux, G., Forbes, F., Robert, C.P. & Titterington, D.M. (2006). Deviance information criteria for missing data models. *Bayesian Analysis* **1**, 651-674.

Chan, J.S.K., Choy, S.T.B. & Makov, U.E. (2008). Robust Bayesian analysis of loss reserve data using the generalized-t distribution. *Astin Bulletin* **38**, 207-230.

Chan, J.S.K., Lam, Y. & Leung, D.Y.P. (2004). Statistical inference for geometric processes with gamma distributions. *Computational Statistics and Data Analysis* **47**, 565-581.

Chan, J.S.K., Lam, C.P.Y., Yu, P.L.H. & Choy, S.T.B. (2010a), Bayesian conditional autoregressive geometric process model for range data. Submitted to a journal for publication.

Chan, J.S.K. & Leung, D.Y.P. (2010). Binary geometric process model for the modelling of longitudinal binary data with trend. *Computational Statistics*, DOI 10.1007/s00180-010-0190-8.

Chan, J.S.K., Wan, W.Y., Lee, C.K., Lin, C.K. & Yu, P.L.H. (2010b). Predicting dropout and committed first time whole blood donors: the use of Poisson geometric process model. Submitted to journal.

Chan, J.S.K., Yu, P.L.H., Lam, Y. & Ho, A.P.K. (2006). Modeling SARS data using threshold geometric process. *Statistics in Medicine* **25**, 1826-1839.

Chan, K.S. & Ledolter, J. (1995). Monte Carlo EM estimation for time series models involving counts. *Journal of the American Statistical Association* **90**, 242-251.

Chou, R. (2005). Forecasting financial volatilities with extreme values: The conditional autoregressive range (CARR) model. *Journal of Money Credit and Banking* **37**, 561-582.

Choy, S.T.B. & Chan, C.M. (2003). Scale mixtures distributions in insurance applications. *Astin Bulletin* **33**, 93-104.

Choy, S.T.B. & Smith, A.M.F. (1997). Hierarchical models with scale mixtures of normal distributions. *Test* **6**, 205-221.

Choy, S.T.B. & Walker, S.G. (2003). The extended exponential power distribution and Bayesian robustness. *Statistics and Probability Letters* **65**, 227-232.

Consul, P.C. (1989). Generalized Poisson distributions: Properties and applications. New York: Marcel Dekker Inc.

Consul, P.C. & Famoye, F. (1992). Generalized Poisson regression model. *Communications in Statistics - Theory and Methods* **21**, 81-109.

Consul, P.C. & Jain, G.C. (1973). A Generalization of the Poisson Distribution. *Technometrics* **15**, 791-799.

Conway, R.W. & Maxwell, W.L. (1962). A queuing model with state dependent service rates. *Journal of Industrial Engineering* **12**, 132-136.

Cox, D.R. (1981). Statistical analysis of time series: Some recent developments. *Scandinavian Journal of Statistics* **8**, 93-115.

Davis, R.A., Dunsmuir, W.T.M. & Wang, Y. (1999). Modelling time series of counts. In *Asymptotics, nonparametrics, and time series*, eds S. Ghosh, pp. 63-114. New York: Marcel Dekker.

Davis, R.A., Dunsmuir, W.T.M. & Streett, S.B. (2003). Observation-driven models for Poisson counts. *Biometrika* **90**, 777-790.

Degenhardt, L., Reuter, P., Collins L. & Hall, W. (2005). Evaluating explanations of the Australian 'heroin shortage'. *Addiction* **100**, 459-469.

Dempster, A.P., Laird, N.M. & Rubin, D.B. (1977). Maximum likelihood from incomplete data via the EM algorithm (with discussion). *Journal of the Royal Statistical Society B* **39**, 599-613.

Diggle, P.J. (1988). An approach to the analysis of repeated measurements. *Biometrics* **44**, 959-971.

Dobbie, M.J. & Welsh, A.H. (2001). Modelling correlated zero-inflated count data. *Australian and New Zealand Journal of Statistics* **43**, 431-444.

Efron, B. (1986). Double exponential families and their use in generalized linear regression. *Journal of the American Statistical Association* **81**, 709-721.

Faddy, M.J. (1997). Extended Poisson process modelling and analysis of count data *Biometrical Journal* **39**, 431-440.

Feller, A. (1949). Fluctuation theory of recurrent events. *Transactions of the American Mathematical Society* **67**, 98-119.

Frei, C. & Schär, C. (2001). Detection probability of trends in rare events: Theory and application to heavy precipitation in the Alpine region *Journal of Climate* **14**, 1568-1584.

Freund, D.A., Kniesner, T.J. & LoSasso, A.T. (1999). Dealing with the common econometric problems of count data with excess zeros, endogenous treatment effects, and attrition bias. *Economics Letters* **62**, 7-12.

Gilks, W.R., Richardson, S. & Spiegelhalter, D.J. (1996). *Markov Chain Monte Carlo in Practice*. UK: Chapman and Hall.

Greenwood, M. & Yule, G. (1920). An inquiry into the nature of frequency distributions representative of multiple happenings with particular reference to the occurrence of multiple attacks of Disease or of repeated

accidents. *Journal of the Royal Statistical Society A* **83**, 255-279.

Gupta, R.C. & Ong, S.H. (2005). Analysis of long-tailed count data by Poisson mixtures. *Communications in Statistics - Theory and Methods* **34**, 557-573.

Hand, D.J., Daly, F., Lunn, A.D., McConway, K.J. & Ostrowski, E. (1994). *A Handbook of Small Data Sets*. London: Chapman and Hall.

Hastings, W.K. (1970). Monte Carlo sampling methods using Markov chains and their applications. *Biometrika* **57**, 97-109.

Heinen, A. (2003). Modeling time series count data: an autoregressive conditional Poisson model. *CORE Discussion Paper 2003/62*.

Heinen, A. & Rengifo, E. (2007). Multivariate autoregressive modeling of time series count data using copulas. *Journal of Empirical Finance* **14**, 564-583.

Holla, M. (1966). On a Poisson-inverse Gaussian distribution. *Metrika* **11**, 115-121.

Hur, K., Hedeker, D., Henderson, W., Khuri, S. & Daley, J. (2002). Modeling clustered count data with excess zeros in health care outcomes research. *Health Services and Outcomes Research Methodology* **3**, 5-20.

Jamshidian, M. & Jennrich, R.I. (1997). Acceleration of the EM algorithm by using quasi-Newton methods. *Journal of the Royal Statistical Society B* **59**, 569-587.

Johnson, N.L., Kotz, S. & Balakrishnan, N. (1995). Continuous univariate distributions: Vol. 2. (2nd ed.). New York: Wiley.

Johnson, N., Kotz, S. & Balakrishnan N. (1997). Discrete Multivariate Distributions. New York: Wiley.

Jones, C., Donnelly, N., Swift, W. & Weatherburn, D. (2005). Driving under the influence of cannabis: The problem and potential countermeasures. *Crime and Justice Bulletin* **87**. NSW Bureau of Crime Statistics and Research, Sydney.

Jowaheer, V. & Sutradhar, B.C., 2002. Analysing longitudinal count data with overdispersion. *Biometrika* **89**, 389-399.

Jowaheer, V., Sutradhar, B.C. & Sneddon, E. (2009). On familial Poisson mixed models with multi-dimensional random effects. *Journal of Statistical Computation and Simulation* **79**, 1043-1062.

Jung, R.C. & Liesenfeld, R. (2001). Estimating time series models for count data using efficient importance sampling. *Allgemeines Statistisches Archiv* **85**, 387-407.

Karlis, D. (2003). An EM algorithm for multivariate Poisson distribution and related models. *Journal of Applied Statistics* **30**, 63-77.

Karlis, D. & Meligkotsidou, L. (2005). Multivariate Poisson regression with covariance structure. *Statistics and Computing* **15**, 255-265.

Karlis, D. & Xekalaki, E. (2005). Mixed Poisson distributions. *International Statistical Review* **73**, 35-58.

Karlis, D. & Meligkotsidou, L. (2007). Finite mixtures of multivariate Poisson distributions with application. *Journal of Statistical Planning and Inference* **137**, 1942-1960.

Kocherlakota, S. (1988). On the compounded bivariate Poisson distribution: A unified treatment. *Annals of the Institute of Statistical Mathematics* **40**, 61-76.

Kocherlakota, S. & Kocherlakota, K. (1992). Bivariate Discrete Distributions. New York: Marcel Dekker Inc.

Lam, K.F., Xue, H. & Cheung, Y.B. (2006). Semiparametric analysis of zero-inflated count data. *Biometrics* **62**, 966-1003.

Lam, Y. (1988a). Geometric process and replacement problem. *Acta Mathematicae Applicatae Sinica (English Series)* **4**, 366-377.

Lam, Y. (1988b). A note on the optimal replacement problem. *Advances in Applied Probability* **20**, 479-482.

Lam, Y. (1992a). Optimal geometric process replacement model. *Acta Mathematicae Applicatae Sinica (English Series)* **8**, 73-81.

Lam, Y. (1992b). Nonparametric inference for geometric processes. *Communications in Statistics: Theory and methods* **21**, 2083-2105.

Lam, Y. (1995). Calculating the rate of occurrence of failures for continuous-time Markov chains with application to a two-component parallel system. *Journal of Operational Research Society* **46**, 528-536.

Lam, Y. (1997). The rate of occurrence of failures. *Journal of Applied Probability* **34**, 234-247.

Lam, Y. (2007). The geometric process and its applications. Singapore: World Scientific Publishing Co. Pte. Ltd.

Lam, Y. & Chan, J.S.K. (1998). Statistical inference for geometric processes with lognormal distribution. *Computational Statistics and Data Analysis* **27**, 99-112.

Lam, Y. & Zhang, Y.L. (1996a). Analysis of a two-component series system with a geometric process model. *Naval Research Logistics* **43**, 491-502.

Lam, Y. & Zhang, Y.L. (1996b). Analysis of a parallel system with two different units. *Acta Mathematicae Applicatae Sinica (English Series)* **12**, 408-417.

Lam, Y. & Zhang, Y.L. (2003). A geometric process maintenance model for a deteriorating system under a random environment. *IEEE Transactions on Reliability* **52**, 83-89.

Lam, Y., Zhang, Y.L. & Zheng, Y.H. (2002). A geometric process equivalent model for a multistate degenerative system. *European Journal of Operational Research* **142**, 21-29.

Lam, Y., Zhu, L.X., Chan, J.S.K. & Liu, Q. (2004). Analysis of data from a series of events by a geometric process model. *Acta Mathematica Applicatae Sinica (English Series)* **20**, 263-282.

Lambert, D. (1992). Zero inflated Poisson regression with an application to defects in manufacturing. *Technometrics* **34**, 1-14.

Lee, A.H., Wang, K., Scott, J.A., Yau, K.K.W. & McLachlan, G.J. (2006). Multi-level zero-inflated Poisson regression modelling of correlated count data with excess zeros. *Statistical Methods in Medical Research* **15**, 47-61.

Lee, A.H., Wang, K., Yau, K.K.W., Carrivick, P.J.W. & Stevenson, M.R. (2005). Modelling bivariate count series with excess zeros. *Mathematical Biosciences* **196**, 226-237.

Leppik, I.E., Dreifuss, F.E., Bowman-Cloyd, T., Santilli, N., Jacobs, M., Crosby, C., Cloyd, J., Stockman, J., Graves, N., Sutula, T., Welty, T., Vickery, J., Brundage, R., Gumnit, R. & Guiterres, A. (1985). A double-blind crossover evaluation of progabide in partial seizures. *Neurology* **35**, 285.

Lunn, D.J., Thomas, A., Best, N., & Spiegelhalter, D. (2000). WinBUGS - A Bayesian modelling framework: Concepts, structure, and extensibility. *Statistics and Computing* **10**, 325-337.

Ma, J., Kockelman, K.M. & Damien, P. (2008). A multivariate Poisson-lognormal regression model for prediction of crash counts by severity, using Bayesian methods. *Accident Analysis and Prevention* **40**, 964-975.

Mardia, K.V. (1971). Families of bivariate distributions (Griffin's statistical monograph No. 27). London: Griffin.

McKenzie, E. (2003). Discrete variate time series. In *Handbook of Statistics 21*, eds D.N. Shanbhag, C.R. Rao, pp. 573-606. Amsterdam: Elsevier.

McKetin, R., McLaren, J., Riddell, S. & Robins, L. (2006). The relationship between methamphetamine use and violent behaviour. *Crime and Justice Bulletin No. 97*. NSW Bureau of Crime Statistics and Research, Sydney.

Metropolis, N., Rosenbluth, A.W., Rosenbluth, M.N. & Teller, A.H. (1953). Equations of state calculations by fast computing machines. *Journal of*

Chemical Physics **21**, 1087-1091.

Miaou, S.P. (1994). The relationship between truck accidents and geometric design of road sections: Poisson versus negative binomial regressions. *Accident Analysis and Prevention* **26**, 471-482.

Mullahy, J. (1986). Specification and testing of some modified count data models, *Journal of Econometrics* **33**, 341-365.

Nelder, J. & Wedderburn, R. (1972). Generalized linear models. *Journal of the Royal Statistical Society A* **135**, 370-384.

Qin, Z., Damien, P. & Walker, S. (1998). Uniform scale mixture models with applications to Bayesian inference. *Working paper #98005*, University of Michigan Business School, Michigan.

Quoreshi, A.M.M.S. (2008). A vector integer-valued moving average model for high frequency financial count data. *Economics Letters* **101**, 258-261.

Ridout, M.S. & Besbeas, P. (2004). An empirical model for underdispersed count data. *Statistical Modelling* **4**, 77-89.

Smith, A.F.M. & Roberts, G.O. (1993). Bayesian computation via the Gibbs sampler and related Markov chain Monte Carlo methods. *Journal of the Royal Statistical Society B* **55**, 3-23.

Snowball, L., Moffatt, S., Weatherburn, D. & Burgess, M. (2008). Did the heroin shortage increase amphetamine use? A time series analysis. *Crime and Justice Bulletin No. 114*. NSW Bureau of Crime Statistics and Research, Sydney.

Spiegelhalter, D.J., Best, N.G., Carlin, B.P. & van der Linde, A. (2002). Bayesian measures of model complexity and fit (with discussion). *Journal of the Royal Statistical Society B* **64**, 583-616.

Thall, P.F. & Vail, S.C. (1990). Some covariance models for longitudinal count data with overdispersion. *Biometrics* **46**, 657-671.

Wakefield, J.C., Smith, A.F.M., Racine-Poon, A. & Gelfand, A.E. (1994). Bayesian analysis of linear and non-linear population models by using the Gibbs sampler. *Journal of the Royal Statistical Society C* **43**, 201-221.

Walker, S.G. & Gutiérrez-peña, E. (1999). Robustifying Bayesian procedures. In *Bayesian Statistics 6*, eds J.M. Bernardo, A.P. Dawid, A.F.M. Smith, pp. 685-710. New York: Oxford.

Wan, W.Y. (2006). Analysis of Poisson count data using geometric process model. *M. Phil. Thesis*, University of Hong Kong, Hong Kong.

Wang, K., Lee, A.H., Yau, K.K.W. & Carrivick, P.J.W. (2003). A bivariate zero-inflated Poisson regression model to analyze occupational injuries. *Accident Analysis and Prevention* **35**, 625-629.

Weatherburn, D., Jones, C., Freeman, K. & Makkai, T. (2003). Supply control and harm reduction: lessons from the Australian heroin 'drought'. *Addiction* **98**, 83-91.

Wegman, E.J. (1972). Nonparametric probability density estimation: a comparison of density estimation methods. *Journal of Statistical Computation and Simulation* **1**, 225-245.

Welsh, A.H., Cunningham, R.B., Donnelly, C.F. & Lindenmayer, D.B. (1996). Modelling the abundance of rare species: statistical models for counts with extra zeros. *Ecology Modelling* **88**, 297-308.

Windmeijer, F. (2000). Moment conditions for fixed effects count data models with endogenous regressors. *Economics Letters* **68**, 21-24.

Winkelmann, R. (2008). Econometric analysis of count Data (fifth edition). New York: Springer

Xie, F.C., Wei, B.C. & Lin, J.G. (2009). Score tests for zero-inflated generalized Poisson mixed regression models. *Computational Statistics and Data Analysis* **53**, 3478-3489.

Yau, K.K.W. & Lee, A.H. (2001). Zero-inflated Poisson regression with random effects to evaluate an occupational injury prevention programme. *Statistics in Medicine* **20**, 2907-2920.

Yau, K.K.W., Wang, K. & Lee, A.H. (2003). Zero-inflated negative binomial mixed regression modeling of over-dispersed count data with extra zeros. *Biometrical Journal* **45**, 437-452.

Zeger, S.L. (1988). A regression model for time series of counts. *Biometrika* **75**, 621-629.

Zeger, S.L., Liang, K.Y. & Albert, P.S.(1988). Models for longitudinal data: A generalized estimating equation approach. *Biometrics* **44**, 1049-1060.

Zhang, Y.L. (1999). An optimal geometric process model for a cold standby repairable system. *Reliability Engineering and Systems Safety* **63**, 107-110.

Zhang, Y.L. (2002). A geometric-process repair-model with good-as-new preventive repair. *IEEE Transactions on Reliability* **51**, 223-228.

Zhang, Y.L., Yam, R.C.M. & Zuo, M.J. (2001). Optimal replacement policy for a deteriorating production system with preventive maintenance. *International Journal of Systems Science* **32**, 1193-1198.

Zhang, Y.L., Yam, R.C.M. & Zuo, M.J. (2002). Optimal replacement policy for multistate repairable system. *Journal of Operational Research Society* **53**, 336-341.